NASA
Technical
Paper
2348

September 1984

NASA-TP-2348 19840025308

An Experimental and Theoretical Investigation of Deposition Patterns From an Agricultural Airplane

Dana J. Morris,
Cynthia C. Croom,
Cornelis P. van Dam,
and Bruce J. Holmes

NASA

NASA
Technical
Paper
2348

1984

An Experimental and Theoretical Investigation of Deposition Patterns From an Agricultural Airplane

Dana J. Morris and
Cynthia C. Croom
Langley Research Center
Hampton, Virginia

Cornelis P. van Dam
University of Kansas
Lawrence, Kansas

Bruce J. Holmes
Langley Research Center
Hampton, Virginia

National Aeronautics
and Space Administration

Scientific and Technical
Information Branch

SUMMARY

A flight test program using a representative agricultural airplane has been conducted to provide data for validating a computer program model which predicts aerially applied particle deposition. The data from this test and comparisons of predicted and measured particle deposition are presented. A particular feature of the computer program is that the mean particle trajectory and the variance from the mean resulting from fluid fluctuations are both predicted simultaneously. The comparisons between predicted and measured mean deposition locations showed very good agreement, with crosswind effects accurately accounted for. Deposition pattern spreading, caused by turbulent fluctuations in the wake, however, is underpredicted for most downwind depositions. Both computer predictions and limited tests with winglets support previous model results, in that they demonstrate that the wake characteristics can be tailored to produce desirable effects on deposition and drift characteristics. Applications of the computer program for spray pattern improvement are illustrated.

INTRODUCTION

Since 1976, the National Aeronautics and Space Administration (NASA) has been conducting basic research in aerodynamics relating to aerial applications. During the 1976 to 1978 time period, NASA initiated a specific research program consistent with in-house research capabilities to address the aerial application industry's major technical concerns (ref. 1). Because of increasing chemical costs and environmental concerns, reducing the drift of aerially applied chemicals away from the target area was identified as the industry's most important concern. The control of chemical drift is a complex problem requiring an understanding of spray behavior, airplane wake aerodynamics, and the economic, meteorological, and biological factors involved in aerial applications of agricultural chemicals.

In order to provide some technological assistance in this area, NASA embarked on a research project to develop improved capabilities for integrating airplane wake characteristics with dispersal techniques to produce wider, more uniform deposition patterns with minimum losses due to drift. The initial research efforts required developing the experimental and theoretical research tools necessary to model aerial applications under controlled test conditions. The principal objectives of the early experimental work, conducted at model scale in the Langley Vortex Research Facility and the Langley 30- by 60-Foot Tunnel, were to develop methods to simulate aerial dispersal, to develop a data base to quantify wake and dispersal characteristics, and to examine wake modification as a means of producing favorable changes in deposition characteristics (ref. 2).

Results from the model tests were used in later experimental research centered around full-scale flight tests, which were conducted with an Ayres Thrush Commander-800 airplane, with and without winglets (fig. 1). Simultaneously, theoretical methods to simulate aerial dispersal of particles were developed for predicting the interaction of the dispersed particles with the aircraft wake (refs. 3 to 5). The factors which influence aerially applied particle deposition can be divided into three categories: details related to the particles themselves, aircraft-related parameters, and deposition-site-related variables. The size, shape, and density of the particle affect its viscous drag and terminal velocity, which determine the time the particle remains airborne and how closely the particle follows flow streamlines. If the particle is a liquid, particle evaporation is a concern, since evaporation changes particle size. The pertinent aircraft-related parameters are those which influence the aircraft wake flow field. The details of the distribution of velocity in the wake are primarily dependent on the aircraft load distribution across the wing span. The propeller slipstream has a strong influence on the flow field behind the propeller. At the deposition site, the slope of the terrain and the density of the plant canopy affect both the mean flow field and the turbulence level. Meteorological conditions at the site, such as background atmospheric stability, crosswind level and direction, and relative humidity, also influence both the mean flow field and the turbulence level. Relative humidity also affects the evaporation rate for liquid particles and the size and consistency of dry particles, which may tend to agglomerate at high humidity levels. The theoretical methods attempted to accurately model these factors. The flight test program was designed to measure many of these factors to provide a data base for evaluating the accuracy of the theoretical models. With accurate predictive capability, validated against experimental data, analysis of aircraft configurations and dispersal systems can be made without the necessity of conducting costly experimental tests. Additionally, with accurate modeling of environmental factors (crosswind, terrain, plant canopy), the predictive methods can be used for evaluating alternative operational procedures. This report describes the procedures and presents the results of the flight experiments, summarizes the analytical prediction methods used for the computer model of particle deposition, and provides a comparison of predictions and flight test data.

SYMBOLS AND ABBREVIATIONS

b' distance between vortices, ft

C_L lift coefficient

Flt. flight

GMT Greenwich mean time

h height above collector array, ft

I horizontal distance from array centerline to flight-path-crossing location (positive for locations to right of array centerline), ft

r radial distance from center of vortex, ft

S wing planform area, ft^2

v_r vortex tangential velocity at a given radial distance, ft/sec

V_c calibrated airspeed, knots

w_d vortex descent velocity, ft/sec

W airplane weight for each pass, lb

y	horizontal distance from array centerline (positive for locations to right of array centerline), ft
y'	horizontal distance from flight-path-crossing location, $y' = y - I$, ft
z	altitude above collector array of spray boom at wing root, ft
Γ	circulation strength, ft^2/sec
ρ_o	standard air density at sea level, $lb\text{-}sec^2/ft^4$

TEST APPARATUS AND PROCEDURES

Baseline Airplane

The agricultural airplane used for these tests was an Ayres Thrush Commander-800. A three-view drawing of the basic airplane is shown in figure 2. It is a propeller-driven airplane powered by an 800-horsepower, seven-cylinder, supercharged radial engine. Other characteristics of this airplane are listed in table I. The 9-ft-diameter, three-bladed propeller operates at about 1300 rpm with a cruise propulsive efficiency of about 0.75. A data system on board the airplane recorded parameters for calculating airplane operating conditions. A NASA-modified radar altimeter system was used to provide visual cues to guide the pilot to the target altitude selected for each run.

Modified Airplane

Research in the Langley Vortex Research Facility (ref. 2) has shown that winglets offer some promise of reducing drift problems by displacing the wing-tip vortex upward to near the tip of the winglet, thereby reducing the potential for particles from the spray boom tip to be trapped in the vortex flow-field influence while maintaining the lateral transport, which gives wide swath widths. These potential beneficial effects of winglets were shown to be relatively insensitive to changes in winglet cant angle in the range between 20° outward and 10° inward. On the basis of the promising wake interaction effects caused by winglet configurations, wind-tunnel tests were conducted in the Langley 30- by 60-Foot Tunnel of the full-scale basic configuration airplane equipped with winglets canted outward 20°. These tests (ref. 6) indicated that outwardly canted winglets would provide very unsatisfactory lateral-directional handling qualities for the airplane. Data from subsequent piloted simulator studies (ref. 7), as well as model tests, showed that changing the winglets from an outward to an inward cant of 10° would minimize the unfavorable lateral-directional control response characteristics. As a result of these tests, the airplane flight tests were conducted with winglets canted inward 10° to achieve favorable wake vortex interaction while minimizing the detrimental effects on airplane handling qualities (which still turned out to be marginal) (ref. 8).

The winglets used for the flight tests were constructed with a modified GA(W)-2 (redesignated NASA LS(1)-0413) airfoil section such that the total winglet area was 12 percent of the wing area. These winglet tests were exploratory, and no attempt was made to optimize winglet geometry for maximum aerodynamic or aerial application benefits. The design of winglet configurations which have acceptable handling qualities is possible by using modern computational methods (refs. 8 and 9). A three-view drawing of the airplane with winglets on is shown in figure 3.

Test Site

Particle deposition data were gathered at the Collector Array Test (CAT) Site (see fig. 4) located at NASA Wallops Flight Facility. The CAT Site included three 200-ft-long rows of masonite boards mounted so that the boards were all in a horizontal plane 1 ft above the highest ground elevation. The rows, denoted as row -1, row 0, and row 1, were 50 ft apart. The array was located in a fixed position such that the airplane track normal to the rows was oriented along a path 211° from true north (fig. 5). A tower at the east end of row 0 was instrumented to collect meteorological data. Wind velocity and direction were recorded at 1-sec intervals by cup anemometers located on the tower at positions 10, 20, 30, 40, and 50 ft above the array.

For flow visualization of the airplane wake, a smoke screen was created at row -1. A motor-driven camera set along the airplane flight path photographically recorded the movement of the smoke as it followed the streamlines in the flow. This technique has been used successfully in model facilities (ref. 2).

The NASA Wallops Flight Facility radar/laser tracking system and a laser reflector located on the top of the airplane canopy were used to establish airplane position data. With this system, the airplane lateral and vertical (spray boom height) positions in relation to the particle collector array were determined with an accuracy of ±6 in. in each direction. Accuracy of this order is important for providing confidence in the validation of wake interaction prediction methods. The airplane ground track is presented with the midpoint of the collector array as a reference.

Test Procedure

The test matrix, shown in table II, was designed to provide wake interaction data influenced by dispersal semispan location, flight speed, and particle size. The semispan locations included the influence regions of the propeller slipstream and wing root and tip vortices. The two target airspeeds (90 and 120 knots) represent the lowest and highest application speeds for typical missions. The tests were conducted with a target altitude for the spray boom of 10 ft above the array. For greater reliability in obtaining data, two test runs were made for each condition. The airplane was refueled after each four to eight passes over the test area to maintain approximately the same weight for all flights, and fuel flow was recorded by the data system for accuracy in determination of airplane weight for data reduction. The airplane weight with pilot and load was nominally 6000 lb with winglets off and 6350 lb with winglets on. Therefore, the lift coefficient for the 90-knot passes was approximately 0.70 with winglets off and 0.75 with winglets on, and for the 120-knot passes it was approximately 0.40 with winglets off and 0.42 with winglets on. Actual test conditions resulted in data taken at varying airspeeds and altitudes and in varying crosswinds. Most flights were conducted at night to minimize exposure to high winds. The majority of the tests were made in winds less than 5 knots at the 10-ft-high measurement station. The crosswind, which is the component of the wind perpendicular to the airplane flight path, is derived from the measured wind speed and direction and is specified as positive from the left in table III.

To approximate particle release at discrete locations and to control particle size and density, solid particles were used. Particle dispensers were mounted at specific locations on each spray boom (figs. 1 and 6). This positioned the release location about 1 ft behind and 1.5 ft below the trailing edge of the wing. The pilot remotely triggered the dispenser to release particles as the airplane began each test run. Each dispenser contained enough particles for four data runs between reloadings. Because correlations exist for scaling particles of varying size, shape, and density to a representative sphere (refs. 10 to 12), and scaling laws exist for aerodynamically representing spheres of one diameter and density by another of a different diameter and density (ref. 13), the particles selected for release during the tests were two size ranges of commercially available polystyrene spheres with a specific gravity of 0.65. The 300- to 355-μm-diameter particles scale to represent particle sizes and densities used in insecticide applications. The 600- to 700-μm-diameter particles scale to represent those used in herbicide applications. The CAT Site rows were covered with 4-in-wide paper tape containing a 3-in. strip of adhesive to collect the particles dispensed from the airplane as it passed over the array. Data reduction consisted of counting the number of particles per running foot of the 3-in-wide adhesive strip along each row of the array.

The conditions from the flight tests are contained in the appendix, tables A1 to A83, and summarized in table III. The ground deposition patterns are plotted in figures A1 to A83.

ANALYTICAL PREDICTION METHOD

The analytical prediction method used in this study tracks the path of a particle released from an aircraft as it is influenced by the velocities and the turbulent fluctuations in the plane normal to the aircraft flight path. This is a numerical simulation equivalent to observing a slice across the width of the spray pass. It is assumed that factors in the direction of flight are not changing significantly, and although there are three-dimensional effects in aircraft wakes, two-dimensional effects dominate the aerial application problem. The analytical prediction numerical methods were incorporated in a computer code named "AGDISP." Details of this computer code are covered in reference 4 and are summarized here.

The AGDISP code uses a Lagrangian formulation of the equations of motion, based on a two-component model of atmospheric- and aircraft-generated turbulence in the aircraft wake, to predict the mean trajectory of a particle and the standard deviation about that mean when the particle is released from a specified point in the aircraft wake. The particle location as a function of time is computed to predict the flight path for each particle. The interaction of the particle with the turbulence in the environment creates turbulence correlation functions for the particle position and particle velocity, for particle velocity variance, and for particle position variance. The square root of the position variance gives the standard deviation about the mean position. Particle deposition on the ground is calculated as a Gaussian distribution based on the mean and the standard deviation in the horizontal direction. Particle diameter, density, release location, and initial velocity must be specified. The important forces which act on particles having densities and diameters typically used in aerial applications are viscous drag, the force as a consequence of droplet evaporation, and gravity. The equation used in the code for calculating the drag of the assumed spherical particle comes from the work of Langmuir and Blodgett (ref. 14), where an analytical expression was derived to fit the experimental data. The AGDISP code is applicable to liquid or solid material. Evaporation effects are included in the AGDISP formulation but are not discussed here, since the experimental tests used for comparison were conducted with solid particles.

The AGDISP code has simple flow-field models for the wakes of fixed-wing airplanes and helicopters and is also configured to accept flow fields from experimental data or from other fluid dynamic codes. (See, for example, ref. 15.) The results presented here were calculated by using the model of the fixed-wing aircraft wake contained in the code. The basic feature of this simple flow-field model behind a fixed-wing aircraft is at least one pair of counterrotating vortices which originates near the wing tips. A schematic of such a wake is shown in figure 7. This sketch shows a particle released from a dry spreader. The surface shown rolling up downstream of the wing is a visualization of the vorticity shed from the wing. This sheet of vorticity rolls up into major trailing vortices of circulation strength Γ. There are vortices trailed from the lifting tail surfaces as well, but these are of lesser strength and influence the particle trajectories in only a minor way when the particles are released near the wing. Therefore, these vortices are not included in the model.

The details of the distribution of velocity in the wing-tip vortices are primarily dependent on the aircraft weight distribution across the wing span. The wake model used accepts specification of the load distribution as a function of wing span or specification of rectangular loading as a function of the aircraft weight, wing span, and flight speed. The latter option was selected for the calculations presented here. This models the tangential velocity field as a fully rolled-up vortex with $v_r = \Gamma/2\pi r$ for all r, where r is measured from the center of the vortex. The propeller slipstream is modeled as a swirling jet, as a function of propeller geometry and operating characteristics. The atmospheric crosswind is modeled by a logarithmic velocity profile dependent on a specified crosswind velocity at a height and the surface roughness (generally 1/30 of the physical height of the surface covering). Local background turbulence may be specified by specifying the crosswind velocity, by fixing a constant value (as percent of mean velocity), or by selecting an option for the turbulence field to be computed consistent with the given mean velocity. For the calculations presented here, the turbulence level was specified by the crosswind condition.

The vortex pair does not remain at the altitude of the wing but descends downward with a velocity given by $w_d = \Gamma/2\pi b'$, where b' is the spacing between the vortices. The motion of the vortex pair is further complicated when the pair is near the ground, as is nearly always the rule in aerial applications. The lateral movement of the vortex as it nears the ground increases the size of the swath from an agricultural aircraft by moving particles released into the wake farther outboard. The effect of plant canopy density on the vortex trajectories in the normal plane has been calculated and shows that the tangential velocities and thus the lateral movement of the particles are significantly reduced by the presence of large (in relation to the aircraft wing span) canopies, as in application over forests (ref. 5). This effect is caused by the interference of the canopy with the majority of the vorticity in the wake. This effect is strong when the height of the canopy is of the same order as the wing semispan. The effect of plant canopy is modeled with modifications to surface roughness, turbulence, and particle paths consistent with the specified plant canopy density. Also, either a horizontal or nonhorizontal level surface may be specified. For the experimental data presented in this paper, the height of the ground cover was negligible, and the effects of plant canopy density and surface condition were not evaluated in the comparisons presented here.

RESULTS AND DISCUSSION

The purpose of the present study was to assess the accuracy of the predictions from the theoretical method. For the computations, the measured airplane weight and wing span are input to the computer program along with the airspeed and the wind speed and direction at the time the airplane crossed row 0. The wind speed and direction from the anemometer height closest to the spray boom height for each test run were used to establish the meteorological conditions for that run. The vortex center specified for the computations was determined by means of smoke visualization during flight testing. The collector array height at the centerline is approximately 2 ft; therefore, as previously discussed under the theoretical method description, the surface roughness is specified at 1/30 of this value. The Lagrangian formulation of the computer program tracks the path of a single particle and is therefore restricted to a single-diameter particle. Since no data were available on the percentage of particle diameters within the size range, the particle diameter selected for comparison was the one within the physical size range which resulted in the best agreement with the experimental data. It should be noted that in the experiment, there was no metering of the particles once the pilot had triggered the dispenser to open. In some cases, because of static buildup, the dispenser was still fully loaded when the airplane returned to the hangar. As can be seen by comparing the graphs for the three rows for some flights, there were some runs during which the particles were released at some time other than at the moment the dispenser was triggered.

Comparisons of the measured depositions from the flight test program and the depositions predicted by the computer program for the measured meteorological conditions were made for all the flight test data. In the figures, selected detailed comparisons are presented to illustrate specific points regarding the test matrix, and one summary plot compares all the predicted mean deposition locations to the measured mean deposition locations to illustrate the overall accuracy of the method. Since the smaller particles were influenced more than the larger particles by the flow field, most of the detailed comparisons are for the small-particle cases. In the figures, the right-hand wing (from the pilot's perspective) is shown on the right side. In plots of the predicted trajectory computations, the mean trajectory is shown as a solid line. The dashed lines denote the magnitude of the variance of particle position computed normal to the trajectory. As can be seen in figure 8, the predicted and measured mean locations differ by 10 percent of the span, and the lateral spread differs by 25 percent of the span for the 300- to 355-μm particles released from the 15-percent-semispan location (in the influence field of the propeller slipstream). These particles were released from the basic configuration during flight at 90 knots in a 2.8-knot crosswind. The boom altitude was 11 ft. Improvements in the agreement between predicted and measured mean location and lateral spread might be possible with modeling of the wing-fuselage interference flow field.

For the crosswind levels evaluated, the AGDISP code does a reasonable job of accounting for the crosswind effect on the trajectories. The predicted and measured deposition patterns show generally good agreement for the mean location and the spread, although the lateral spread is underpredicted for the downwind side of the airplane. This is illustrated in figure 9 by a comparison of the AGDISP prediction and the data for the 300- to 355-μm particles released from the basic configuration at 70 percent semispan. These particles were released from a boom altitude of 11 ft during flight at 90 knots in a 2.4-knot crosswind. The strong influence of the crosswind on small particles can be seen in this figure, where the mean deposition from the experiment varies from approximately 28 ft on the right-hand side of the airplane to 58 ft on the left-hand side. For this case, the mean location on the downwind side is predicted within 10 percent of the span, although the lateral spread in ground deposition is twice that predicted. The agreement on the upwind side is closer, with the mean location predicted within 2 percent of the span and the lateral spread within 10 percent of the span.

A comparison of the AGDISP prediction and the data for the 300- to 355-μm particles released from the basic configuration at 80 percent semispan is shown in figure 10. These particles were released from a boom altitude of 9 ft during flight at 120 knots in a 1.5-knot crosswind. The strong influence of even a light (1.5-knot) crosswind on small particles can be seen in this figure, where the mean deposition from the experiment varies from approximately 50 ft on the right-hand side of the airplane to 21 ft on the left-hand side. Also note the multimodal distribution of the data. This is attributed to some of the particles being entrained in the vortex before being deposited on the collector array. It should be noted that the predictive method for ground deposition used in AGDISP provides a Gaussian distribution about the mean based on the computed horizontal variance due to turbulence and thus is not capable of predicting this nonGaussian distribution. For this case, the mean location on the downwind side is predicted within 20 percent of the span, although the spread in ground deposition is three times that predicted. The agreement on the upwind side is again closer, with the mean location predicted within 11 percent of the span and the lateral spread overpredicted by 30 percent of the span.

The accuracy of the AGDISP code in predicting ground deposition of larger particles is shown in figure 11 by a comparison with experimental data from the flight tests. This measured ground deposition is for 600- to 700-μm particles with a specific gravity of 0.65. The particles were released at 80 percent semispan from the basic configuration flying at 90 knots in a 1.8-knot crosswind with a boom altitude of 10 ft. Even these larger particles are affected by a light crosswind, as seen here, where a 1.8-knot crosswind alters the peak deposition location from 30 ft on one side of the airplane to 40 ft on the other. Fewer 600- to 700-μm particles were collected because the dispensers held fewer large spheres. For these large particles, the mean locations are predicted within 2 percent of the span. Spreading of particles due to turbulence on the upwind side is predicted within 5 percent of the span; however, on the downwind side of the airplane, the lateral spread is twice that predicted.

As previously indicated, for all cases, the downwind deposition pattern of the experimental data has more lateral spread than the upwind pattern. This may be caused by the more acute angle which the downwind trajectory makes with the ground plane or by increased turbulence experienced by the downwind particles as a result of "scrubbing" over the ground of the downwind vortex and the vortex "bounce" (rise in altitude after initial descent, see ref. 5). Only the horizontal variance due to turbulence is used when computing the ground deposition. When the particle trajectory makes a more acute angle with the ground, the variance in the vertical direction becomes the more prominent one. Therefore, a different method of calculating ground deposition may improve the agreement in lateral spread.

A flow visualization of the wing-tip wake of the airplane with winglets off and with winglets on is shown in figure 12. Figure 12(a) shows the tightly rolled-up vortex forming at the wing tip of the airplane with winglets off. In figure 12(b), the tip vortex can be seen forming at the tip of the winglet.

The predicted trajectories and the predicted and experimental ground deposition patterns for particles released from the 95-percent-wing-semispan location are shown in figure 13 for the basic configuration and in figure 14 for the configuration with winglets on. Both sets of data were collected from the airplane during flight at 120 knots in a 2.2-knot crosswind. For the basic configuration, the boom altitude was 14 ft and for the configuration with winglets on, the boom altitude was 15 ft. On the downwind side of the airplane, the particles released from the basic configuration are deposited closer to the flight path centerline (than those released from the airplane with winglets on) because of the vortex. With winglets on, in addition to the deposition location being further from the flight path centerline for particles released from this location near the wing tip, more particles were collected. Because of the limited number of runs made with winglets on, further detailed experimental work would be necessary to determine if the increased deposition with winglets on is caused by this lack of entrainment.

A measure of the overall accuracy of the predictions is presented in figure 15, where the predicted mean deposition location versus the experimental mean is plotted for 83 test runs. If the two were in perfect agreement, all the data points would fall along the 45° line. Points within 10 ft (25 percent of the wing span) of this line are considered to be in good agreement. As can be seen in the figure, the agreement for the majority of the test runs was excellent. There are a few points which fall outside this range. One was for the large particles (600 to 700 μm in diameter); the others were for flights which were conducted with the small particles (300 to 355 μm in diameter). In all these cases, particles were released from the airplane at 85-, 90-, or 95-percent-semispan location at altitudes greater than 10 ft. This implies that the particles were in the strong influence of the vortex and that the crosswind, which was not constant, had a relatively long time to act on the particles and to interact with the vortex. A small error in altitude (such as the ±0.5-ft accuracy of the laser tracking system) or in representing the varying crosswind with a single measurement would mean a large difference in the lateral displacement of the deposition.

An AGDISP prediction for the basic configuration with a full-span boom with 10 equally spaced nozzles on each wing is shown in figure 16. The particle trajectory plots aid in determining which nozzle locations to reposition to improve the deposition pattern. For this case, the deposition pattern alone would indicate that repositioning was needed on nozzles near, but not at, the boom tip. The computed trajectories, however, indicate that the two most outboard nozzles are actually the ones causing the high deposition at approximately ±30 ft from the flight centerline. Adding nozzles and adjusting nozzle locations results in the predicted pattern shown in figure 17. The improved pattern is the result of using an 80-percent wing-span boom with 13 nozzles on each side. By overlapping the deposition pattern, the proper distance between adjacent flight paths which should be used to obtain optimum swath width can be determined, as illustrated in figure 18. For this situation, the prediction indicates that the flight path centerline for the second pass should be shifted by 110 ft from the first pass to obtain the cumulative deposition pattern as shown.

The AGDISP prediction for the particle trajectories and deposition pattern for a full-span boom on the winglet-equipped airplane with the nozzles spaced as in figure 16 is shown in figure 19. By comparing the predicted distribution patterns from figures 16 and 19, it is apparent that the displacement of the vortex by the winglet results in a more uniform distribution pattern. However, as pointed out earlier, tests conducted during the flight program indicate that the winglet configuration can have adverse effects on the handling qualities of an airplane. In order to be effective and practical, the winglet configuration must be carefully tailored in terms of its effect on both the wake and the airplane flight characteristics.

CONCLUDING REMARKS

A flight test program using a representative agricultural airplane has been conducted to provide data for validating a computer program model which predicts aerially applied particle deposition. The data from this test are presented here. Comparisons of predicted and measured particle deposition are presented. A particular feature of the computer program is that the mean particle trajectory and the variance from the mean resulting from fluid fluctuations are both predicted simultaneously. The following observations were noted:

1. The comparisons between predicted and measured mean deposition locations showed very good agreement, with crosswind effects accurately accounted for. Deposition pattern spreading, caused by turbulent fluctuations in the wake, however, is underpredicted for the downwind depositions for semispan release locations less than 95 percent.

2. Both computer predictions and limited tests with winglets support previous model results in that they demonstrate that wake characteristics can be tailored to produce desirable effects on deposition and drift characteristics.

3. A nozzle spacing study using the aircraft wake model in the code has illustrated the use of the code for improving deposition patterns.

Langley Research Center
National Aeronautics and Space Administration
Hampton, VA 23665
July 17, 1984

TABLE I.- CHARACTERISTICS OF AYRES THRUSH COMMANDER-800 AIRPLANE

General:	
Overall length, ft	27.38
Height to top of airplane canopy, ft	9.17
Maximum gross weight, lb	7800
Engine	Wright Cyclone R-1300
Wing:	
Type	Full cantilever
Airfoil section	NACA 4412
Dihedral, deg	3.50
Center-of-gravity range:	
Forward limit	22.5 in. aft of wing leading edge
Aft limit	28.0 in. aft of wing leading edge
Span, ft	41.42
Area, ft^2	310.63

TABLE II.- TEST MATRIX

Particle diameter, µm	Target airspeed, knots	Particle release location, percent semispan, of -																					
		15		25		40		50		60		70		75		80		85		90		95	
		Flt. no.	Run no.	Flt. no.	Run no.	Flt. no.	Run no.	Flt. no.	Run no.	Flt. no.	Run no.	Flt. no.	Run no.	Flt. no.	Run no.	Flt. no.	Run no.	Flt. no.	Run no.	Flt. no.	Run no.	Flt. no.	Run no.
300 to 355	90	58 58	2.0 2.9	57	2.6	60	2.1	53 53	2.2 2.3	59 59	4.0 4.1	59 59 67 78	2.0 2.1 2.1 2.0	54 77	2.0 1.5	54 54 74	4.0 4.1 2.4	54 54 74	6.1 6.2 4.0	55 55 56 56	2.1 2.2 2.0 2.1	56 76 76	4.1 2.0 2.1
300 to 355	120	58 58	1.5 1.8	57 57	1.1 1.2	60	1.6	53	1.2	59 59	3.2 3.7	59 67 78	1.3 1.1 1.5	54 54 76 76	1.0 1.1 3.0 3.1	54 54 74	3.0 3.1 1.0	54 54 74	5.0 5.1 3.2	55 56	1.1 1.1	56 56 76 76	3.2 3.4 1.0 1.1
600 to 700	90	51 51	2.1 2.3	47	6.0			47	2.0					47	4.1	49 49	1.0 1.1	49 49	4.1 4.2	49 49	6.2 6.4	50	2.2
600 to 700	120	51	1.2	47 47	5.0 5.1	51	3.3	47	1.1	52	1.0			47 47	3.0 3.1	48 48 49 49	1.0 1.1 2.0 2.1	49 49	3.0 3.1	49 49	5.2 5.4	50	1.1

TABLE III.- RUN SUMMARY

Flight no.	Run no.	Configuration	Particle diameter, μm	Dispenser location, percent semispan	V_c, knots	Spray boom altitude at row 0, ft	Crosswind component, ft/sec
47	1.1	Basic	600 to 700	50	113.2	12	-2.23
47	2.0			50	86.9	12	-3.38
47	3.0			75	113.0	14	-1.64
47	3.1			75	111.3	9	-3.44
47	4.1			75	71.9	12	-1.67
47	5.0			25	118.7	7	-4.46
47	5.1			25	120.8	7	-2.17
47	6.0			25	90.9	11	1.37
48	1.0			80	110.3	9	-3.28
48	1.1				113.3	10	-5.38
49	1.0				90.9	10	-3.25
49	1.1				93.2	10	-2.12
49	2.0				118.1	9	-3.04
49	2.1				114.9	10	-6.79
49	3.0			85	113.6	11	-6.20
49	3.1				117.6	11	-6.23
49	4.1				91.2	10	-6.76
49	4.2				88.7	9	-4.76
49	5.2			90	112.3	13	-4.76
49	5.4				114.4	12	-6.52
49	6.2				87.3	9	-5.48
49	6.4				88.0	8	-5.69
50	1.1			95	118.6	13	-2.72
50	2.2			95	86.7	12	-2.07
51	1.2			15	117.2	8	3.08
51	2.1			15	89.7	6	4.10
51	2.3			15	89.7	9	1.01
51	3.3			40	118.0	13	2.48
52	1.0			60	116.7	11	-5.25
53	1.2		300 to 355	50	123.3	12	-5.84
53	2.2			50	88.5	10	-5.54
53	2.3			50	89.1	10	-5.22
54	1.0			75	115.7	10	5.81
54	1.1			75	117.9	11	2.62
54	2.0			75	86.3	11	2.20
54	3.0			80	115.7	10	2.30
54	3.1				117.4	9	2.47
54	4.0				85.2	2	-2.89
54	4.1				82.9	11	-2.36
54	5.0			85	115.0	12	-3.87
54	5.1				150.3	10	-6.04
54	6.1				86.6	11	-5.50
54	6.2				87.9	10	-4.53

TABLE III.- Concluded

Flight no.	Run no.	Configuration	Particle diameter, μm	Dispenser location, percent semispan	V_c, knots	Spray boom altitude at row 0, ft	Crosswind component, ft/sec
55	1.1	Basic	300 to 355	90	124.7	15	2.40
55	2.1				88.7	6	3.35
55	2.2				87.7	7	5.87
56	1.1				118.3	13	-1.18
56	2.0				86.5	8	-.62
56	2.1				85.6	7	-2.43
56	3.2			95	150.5	16	-5.18
56	3.4			95	119.3	14	-3.73
56	4.1			95	89.4	11	-3.90
57	1.1			25	120.3	19	5.05
57	1.2			25	118.0	17	3.73
57	2.6			25	83.7	8	5.49
58	1.5			15	119.1	12	2.07
58	1.8				121.7	15	-4.72
58	2.0				89.2	11	-4.72
58	2.9				85.1	9	-5.02
59	1.3			70	119.8	13	-4.04
59	2.0			70	87.3	9	-2.65
59	2.1			70	88.2	10	-4.10
59	3.2			60	116.4	12	-3.00
59	3.7				110.5	14	-2.45
59	4.0				82.2	12	-.11
59	4.1				79.1	11	-3.54
60	1.6			40	113.5	11	-3.00
60	2.1			40	80.5	8	-3.40
67	1.1	Winglet		70	118.9	14	4.86
67	2.1			70	81.9	12	2.20
74	1.0			80	121.0	14	-.69
74	2.4			80	81.6	13	-.72
74	3.2			85	118.9	16	1.90
74	4.0			85	83.8	12	1.84
76	1.0			95	120.9	13	-2.10
76	1.1				119.3	15	-3.94
76	2.0				82.1	9	-5.00
76	2.1				83.7	10	-5.58
76	3.0			75	124.3	16	-5.87
76	3.1			75	121.9	16	-5.25
77	1.5			75	84.7	14	10.47
78	1.5			70	121.1	13	-.92
78	2.0			70	81.3	9	-2.49

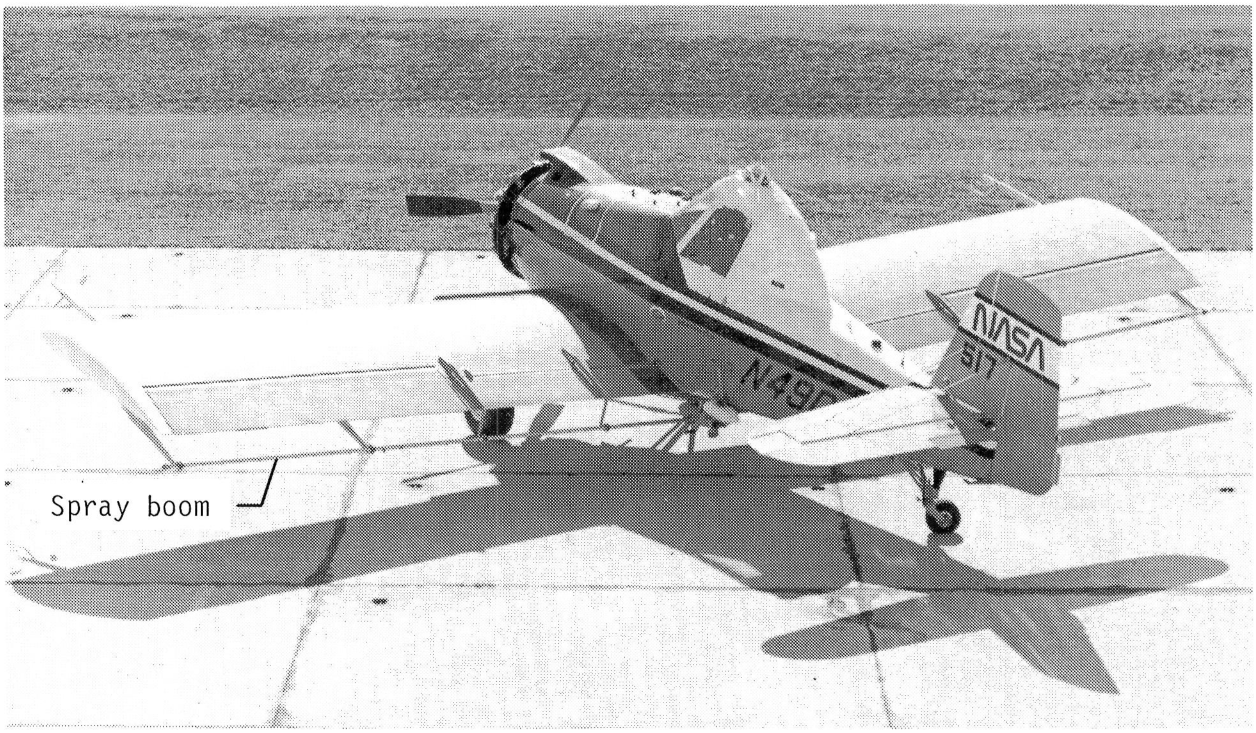

(a) Airplane with winglets off.

(b) Airplane with winglets on.

L-84-96

Figure 1.- Ayres Thrush Commander-800 airplane as modified for aerial application flight tests.

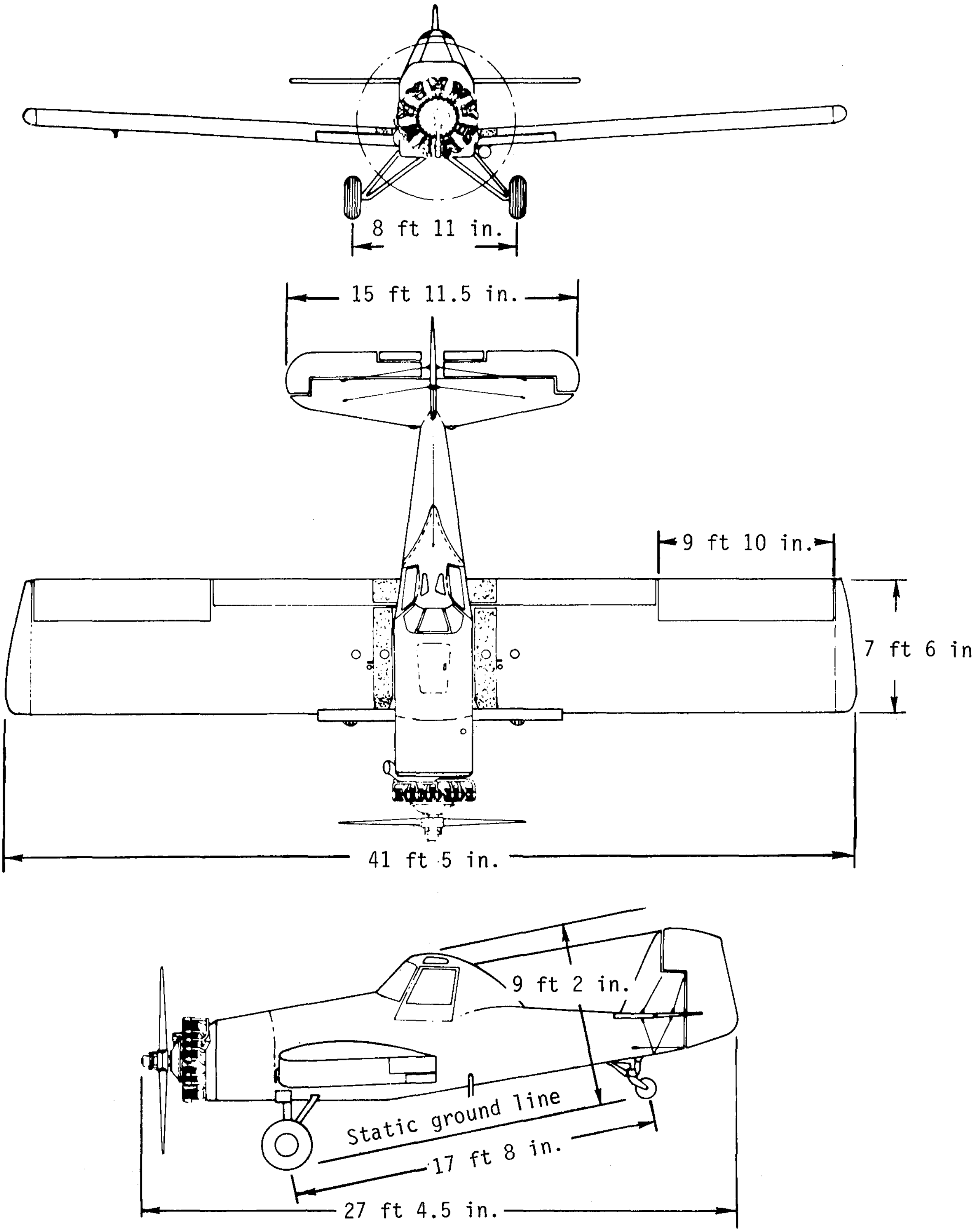

Figure 2.- Ayres Thrush Commander-800 airplane with winglets off.

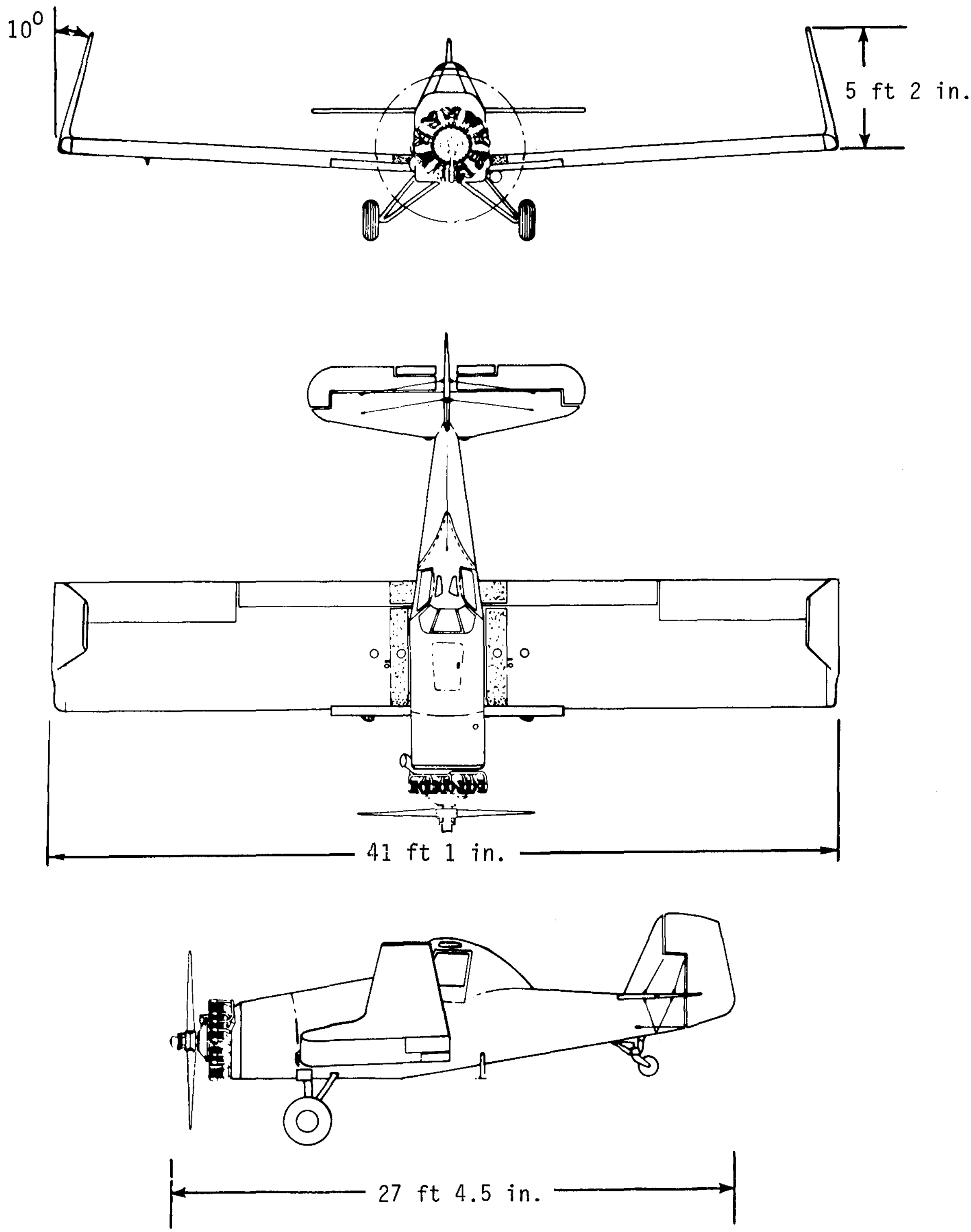

Figure 3.- Ayres Thrush Commander-800 airplane with winglets on.

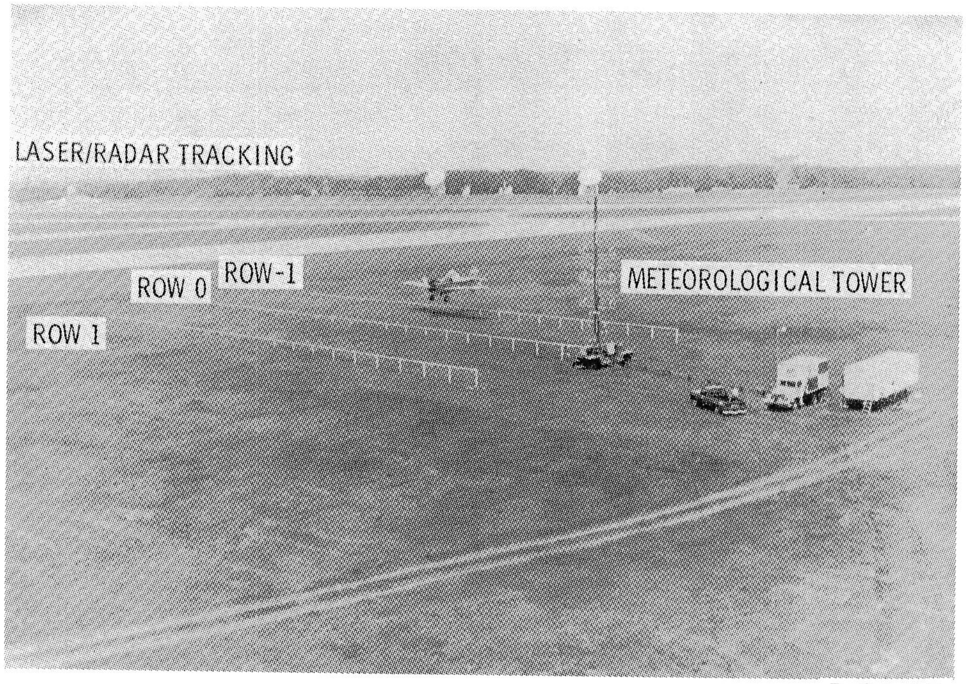

L-84-97

Figure 4.- Collector Array Test Site.

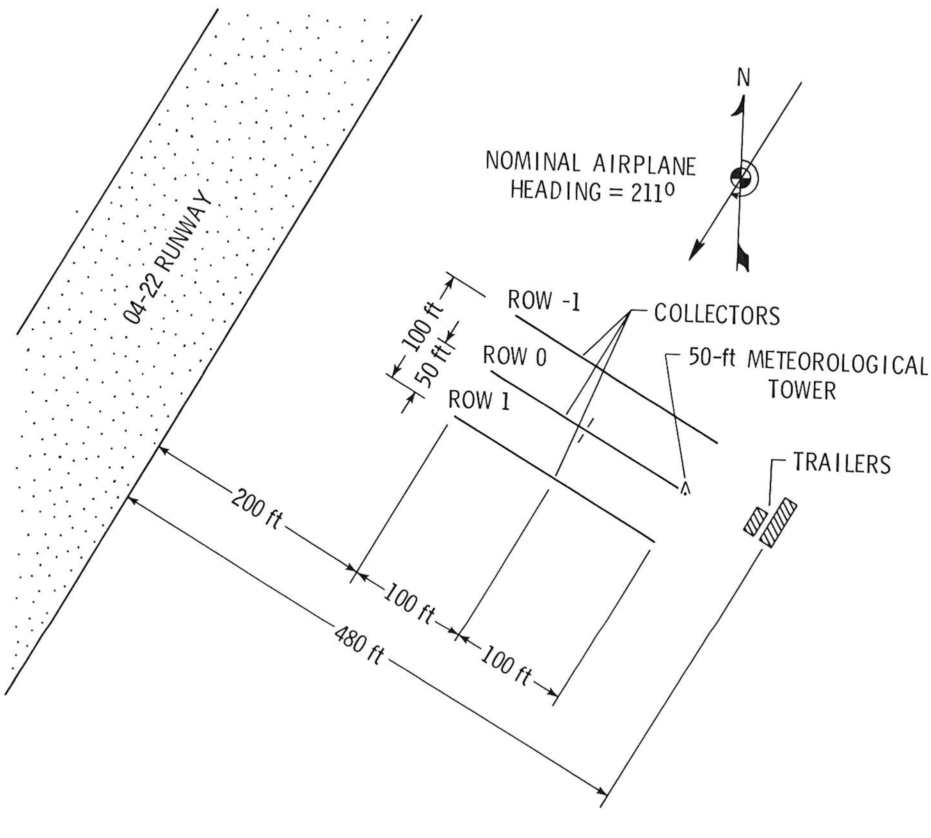

Figure 5.- Planview of Collector Array Test Site.

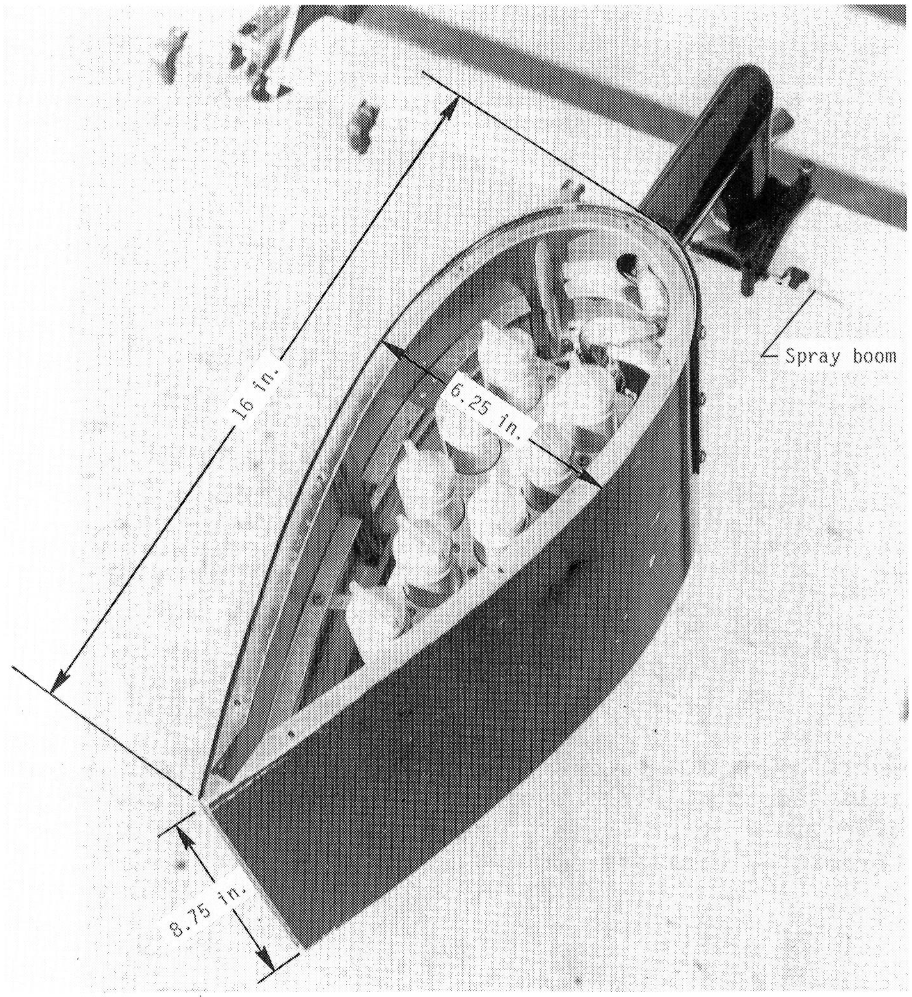

L-84-98

Figure 6.- Particle dispenser mounted on spray boom.

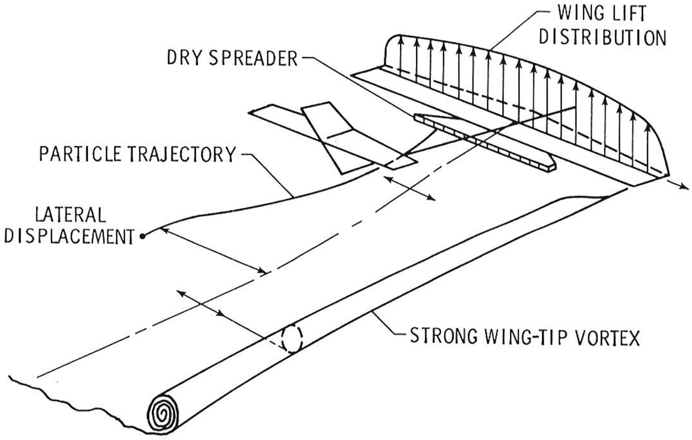

Figure 7.- Schematic of airplane wake.

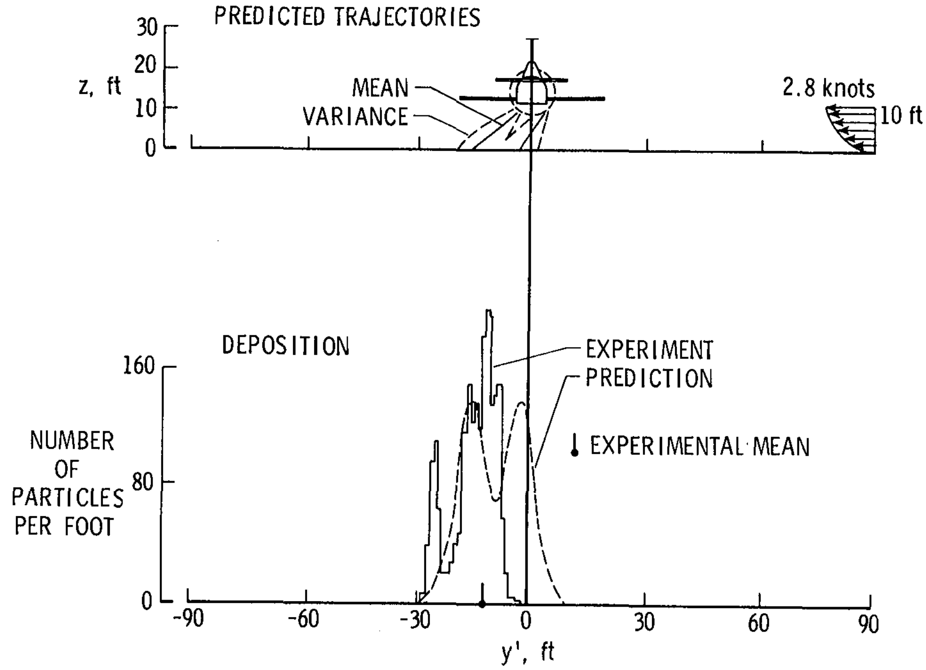

Figure 8.- Comparison of measured and predicted ground deposition patterns for particles released at 15 percent semispan in propeller slipstream during flight at 90 knots in 2.8-knot crosswind. Measured data are for 300- to 355-μm particles; predicted data are for 300-μm particles.

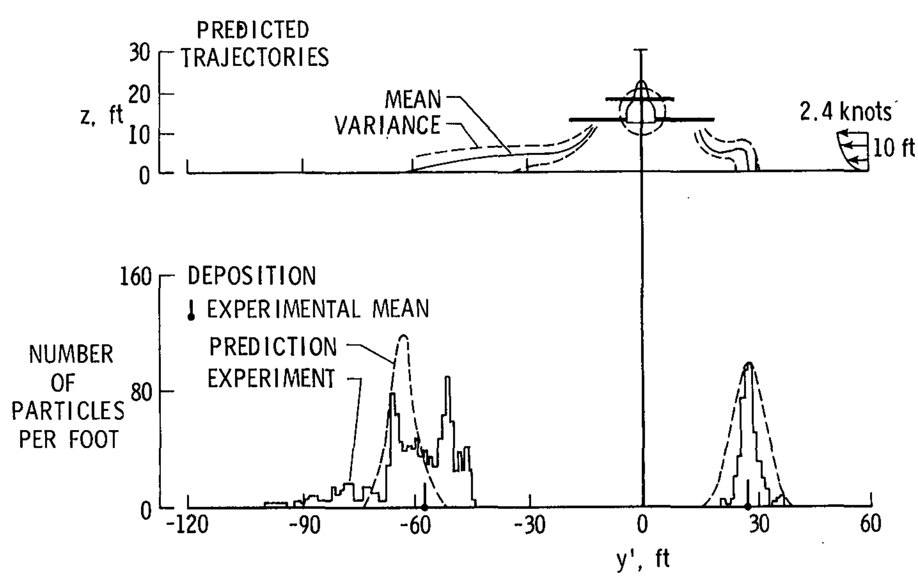

Figure 9.- Comparison of measured and predicted ground deposition patterns for particles released at 70 percent semispan during flight at 90 knots in 2.4-knot crosswind. Measured data are for 300- to 355-μm particles; predicted data are for 300-μm particles.

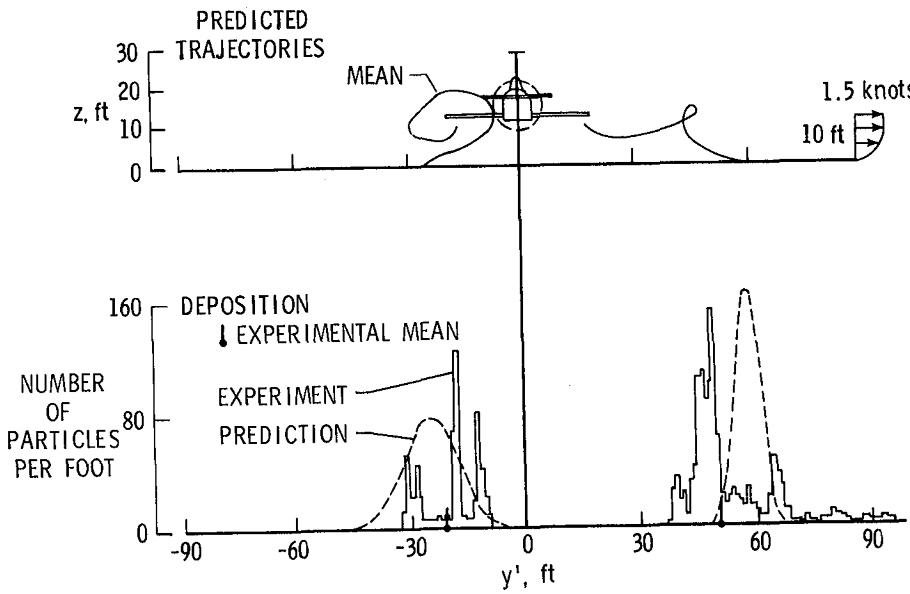

Figure 10.- Comparison of measured and predicted ground deposition patterns for particles released at 80 percent semispan during flight at 120 knots in 1.5-knot crosswind. Measured data are for 300- to 355-μm particles; predicted data are for 300-μm particles.

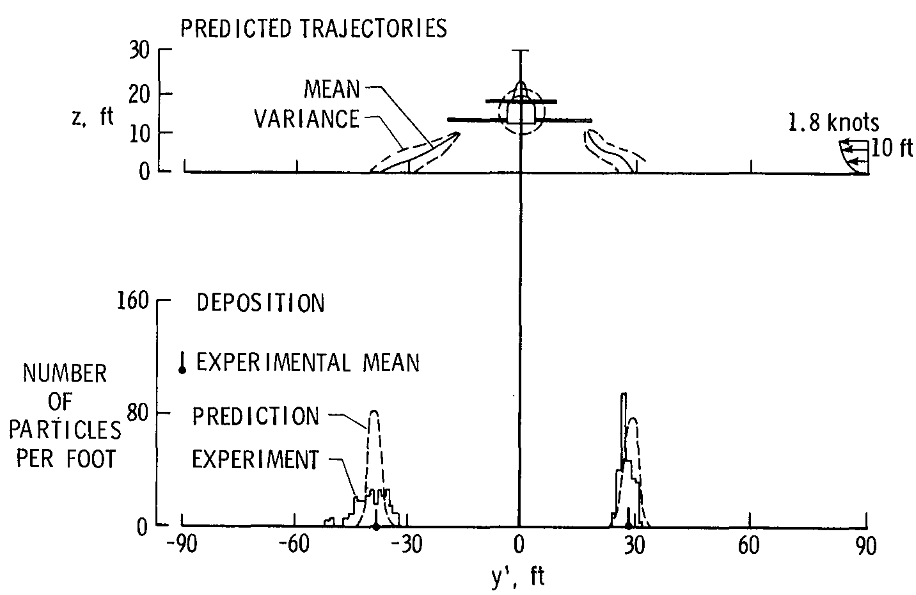

Figure 11.- Comparison of measured and predicted ground deposition patterns for particles released at 80 percent semispan during flight at 90 knots in 1.8-knot crosswind. Measured data are for 600- to 700-μm particles; predicted data are for 600-μm particles.

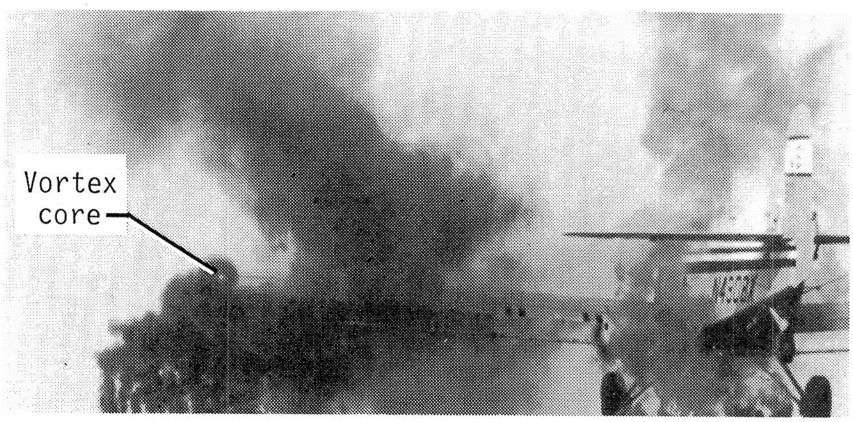

(a) Winglets off.

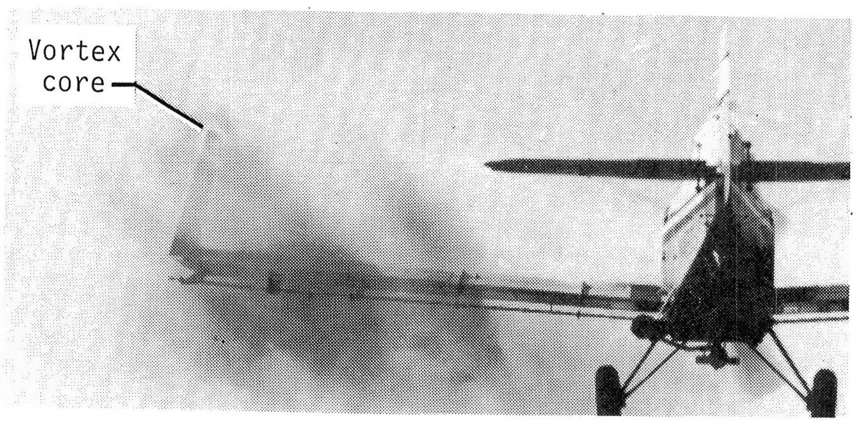

(b) Winglets on.

L-84-99

Figure 12.- Effect of winglets on vortex location.

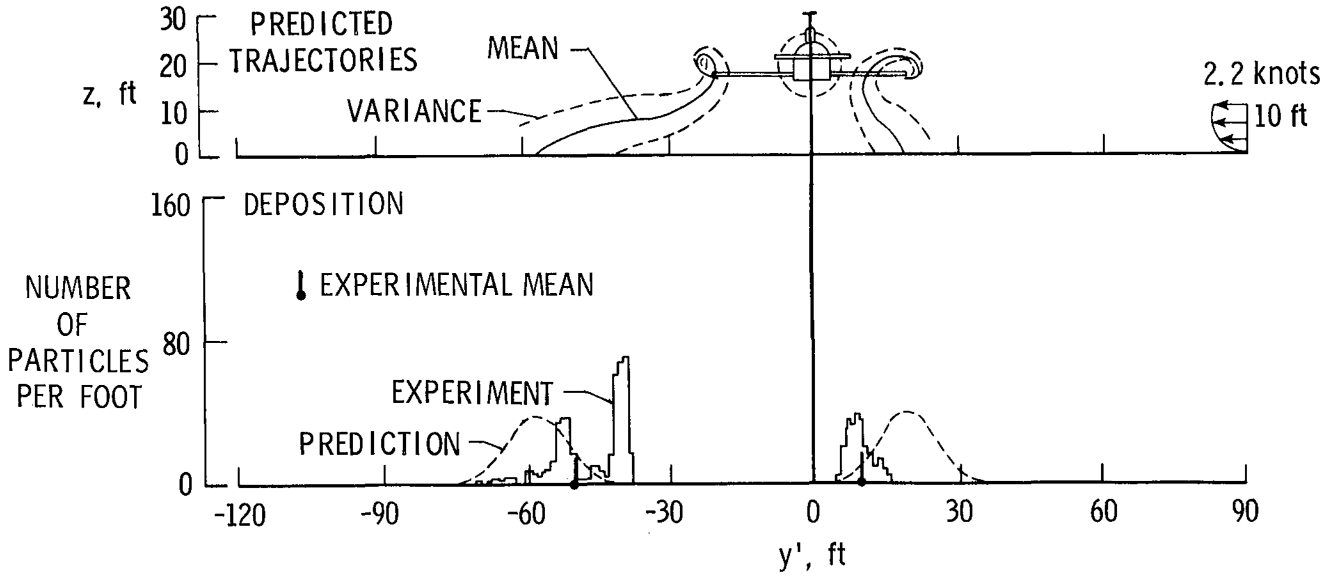

Figure 13.- Measured and predicted ground deposition patterns for particles released at 95 percent semispan from basic configuration during flight at 120 knots in 2.2-knot crosswind. Measured data are for 300- to 355-μm particles; predicted data are for 300-μm particles.

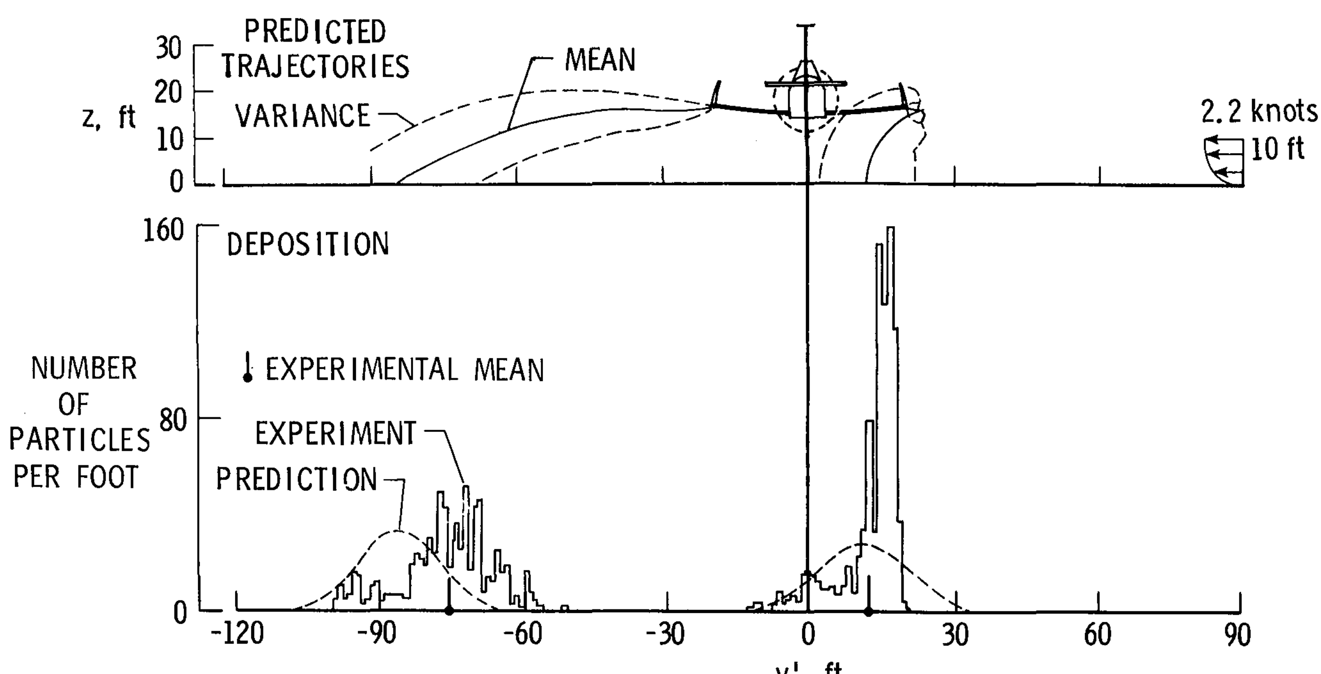

Figure 14.- Measured and predicted ground deposition patterns for particles released at 95 percent semispan from configuration with winglets on during flight at 120 knots in 2.2-knot crosswind. Measured data are for 300- to 355-μm particles; predicted data are for 300-μm particles.

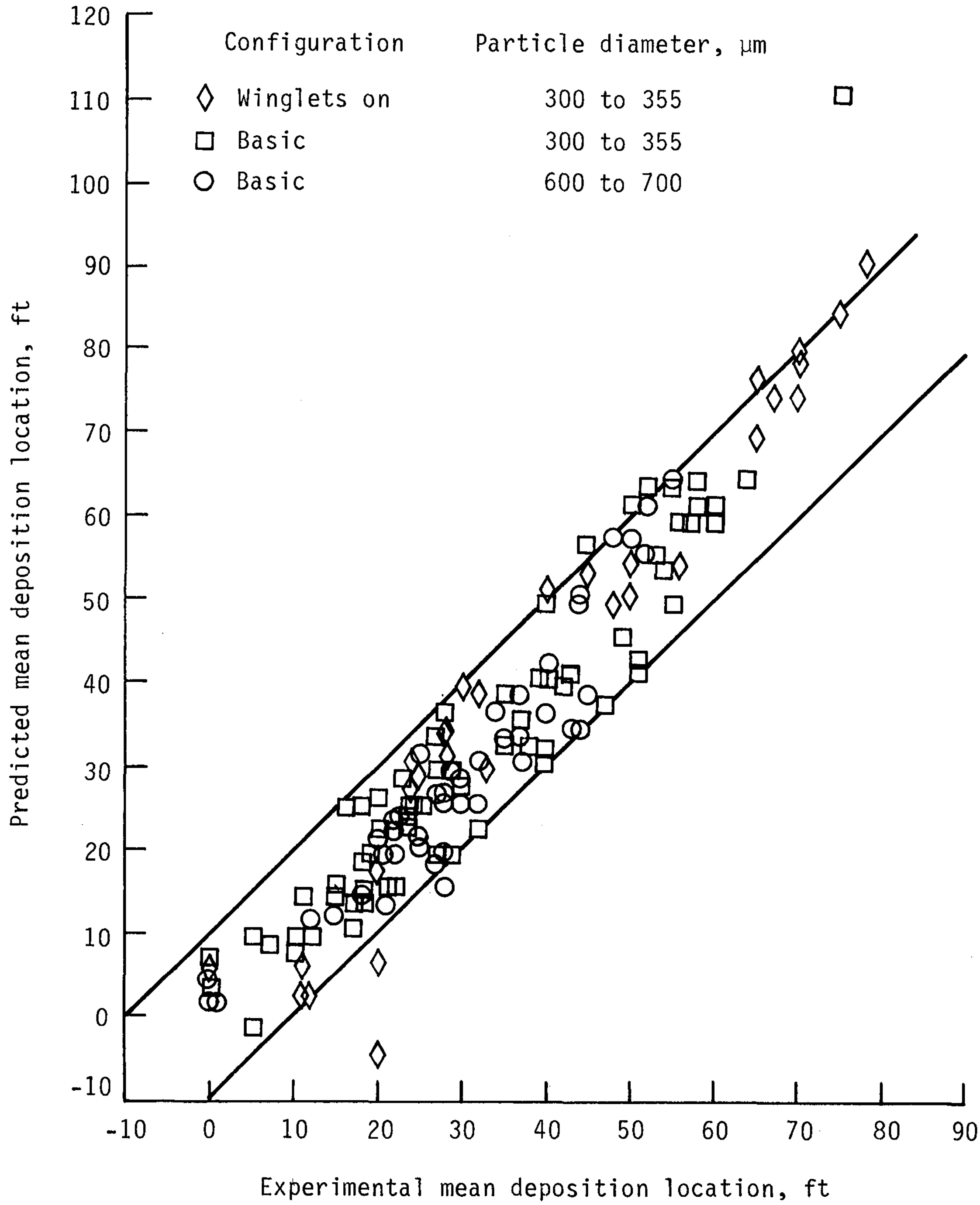

Figure 15.- Comparison of predicted and experimental mean deposition locations.

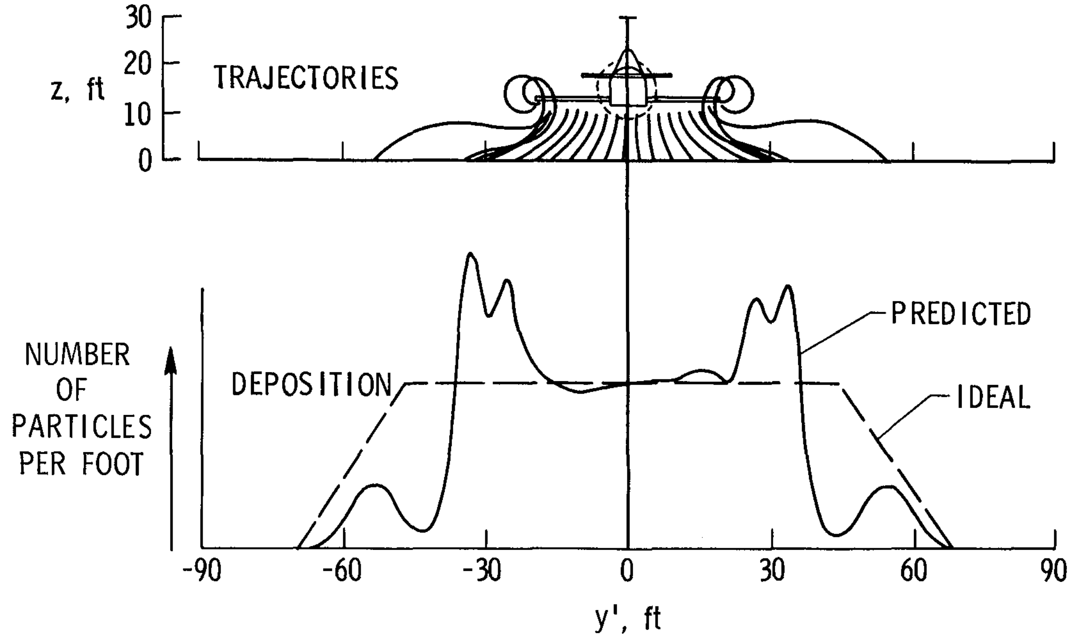

Figure 16.- Predicted trajectories and ground deposition patterns for full-span boom on basic configuration with nozzles equally spaced. Boom altitude = 10 ft; Airpseed = 90 knots; Particle diameter = 300 μm; no wind.

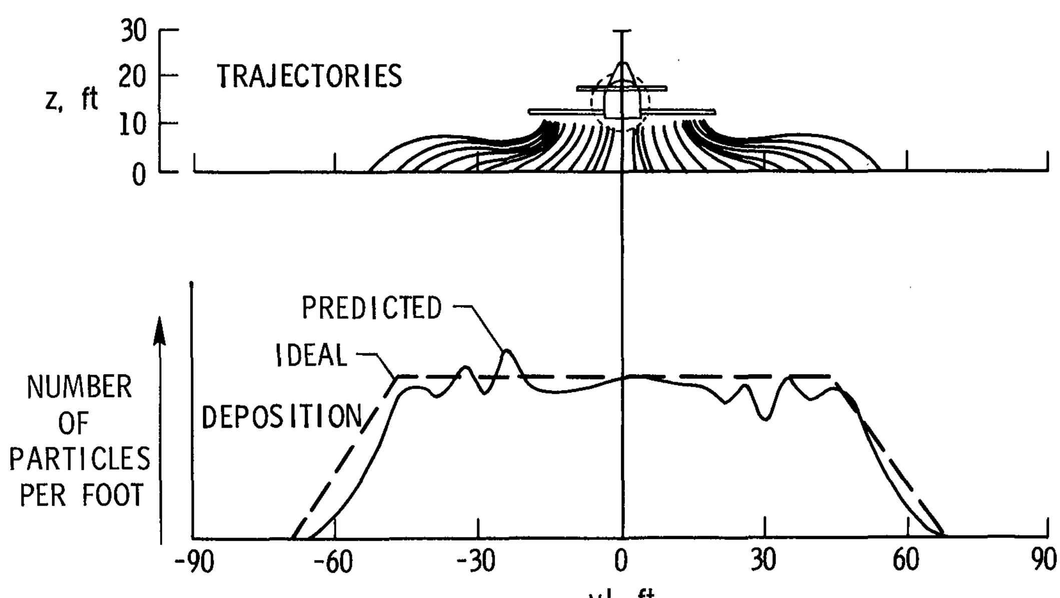

Figure 17.- Predicted trajectories and ground deposition patterns for full-span boom on basic configuration with nozzles added and spacing adjusted to improve ground deposition. Boom altitude = 10 ft; Airspeed = 90 knots; Particle diameter = 300 μm; no wind.

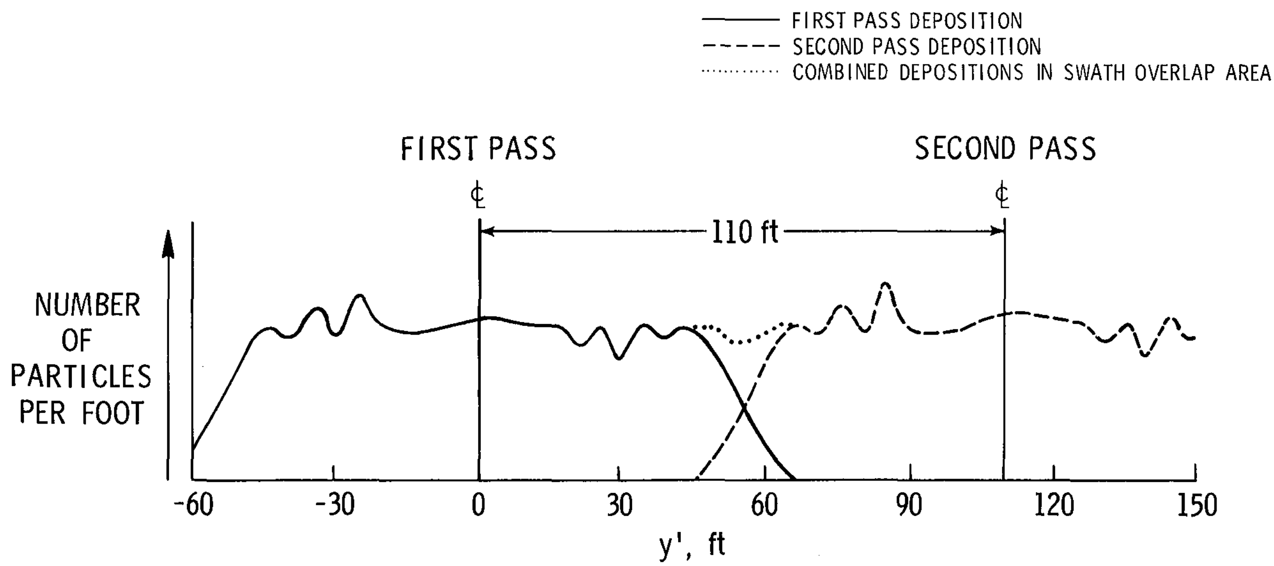

Figure 18.- Overlap of adjacent swath predictions to determine spacing of spray passes.

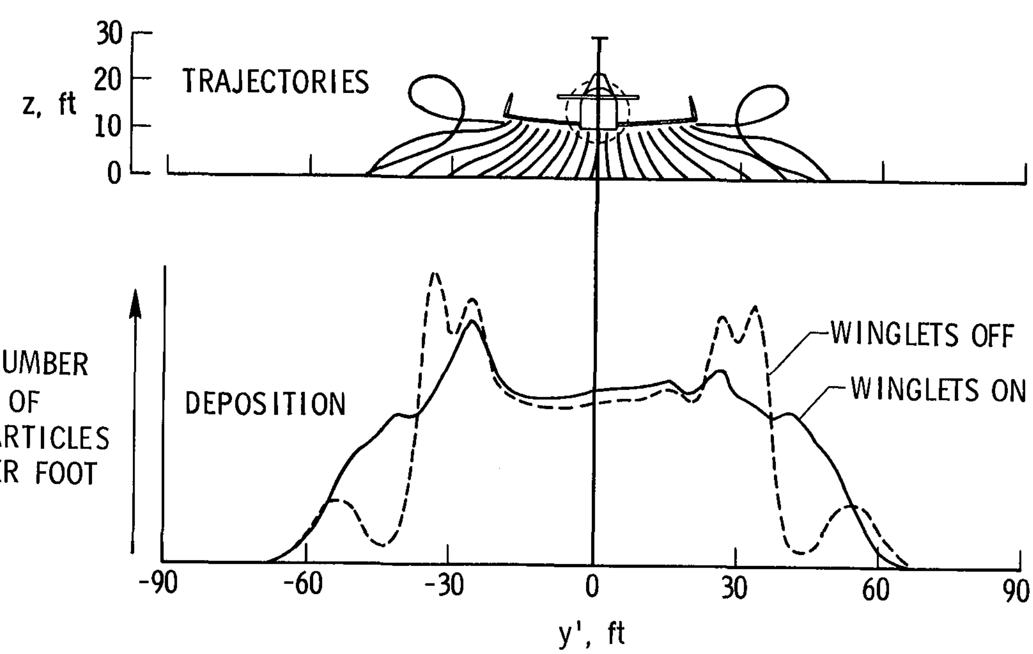

Figure 19.- Predicted effect of winglets on particle trajectories and deposition pattern for full-span boom with nozzles equally spaced. Boom altitude = 10 ft; Airspeed = 90 knots; Particle diameter = 300 μm; no wind.

APPENDIX

FLIGHT TEST CONDITIONS AND MEASURED GROUND DEPOSITIONS

This section lists the data obtained during the wake interaction flight tests at NASA Wallops Flight Facility. Table II contains the test matrix, and table III contains a run summary. In tables A1 to A83, flight conditions, radar/laser data, and meteorological data are described for each test run. The corresponding ground deposition patterns are plotted in figures A1 to A83.

For the particular flight and run number, each table lists the date of the test in addition to the time (Greenwich mean time) the airplane crossed the center row (row 0) of the Collector Array Test Site. Also, airplane configuration, particle dispenser location in percent semispan, and particle diameter are listed.

The radar/laser data are required to accurately know the location of the airplane over the test site. For each row, z indicates the altitude of the spray boom at the wing root above the collector array, and I represents the distance from the array centerline to the point where the airplane track intercepts the indicated row. In addition to the distances z and I, the crossing angle is listed. This is the angle formed by the centerline of the collector array and the track of the airplane.

The meteorological data section lists wind speed, wind direction, and temperature at 10-, 20-, 30-, 40-, and 50-ft altitudes above the array. Also 5-second averages of the data for all five heights above the array (period of data averaging is time that airplane crosses row 0 ± 2.5 seconds) are listed for some flights. Relative humidity at the test site is also shown when available.

For each test run, airplane flight conditions and magnetic heading are listed. The weight of the airplane W has been corrected for the weight of fuel consumed during flight. Calibrated airspeed V_c has been corrected for position error. The lift coefficient is calculated as follows:

$$C_L = \frac{W}{0.5\rho_o V_c^2 S}$$

where ρ_o is the standard sea level air density, S is the wing planform area, and V_c is expressed in ft/sec. Airplane heading angle is provided to indicate the direction of flight in relation to the collector array and the wind direction. In figures A1 to A83, the number of test particles for each row as counted after each run is plotted as a function of y, the distance from the collector array centerline not corrected for airplane track interception.

TABLE A1.- CONDITIONS FOR FLIGHT 47, Run 1.1

Date: 8-7-81
Time: 05:04:59.1 GMT

Dispenser location: 50 percent semispan
Particle diameter: 600 to 700 μm

AIRPLANE CONFIGURATION: Basic

RADAR/LASER DATA:

	Row -1	Row 0	Row 1
z, ft	14	12	12
I, ft	2.0	1.0	0

Crossing angle: 1.25°
Airplane heading: 210°

METEOROLOGICAL DATA:

Relative humidity: 82 percent

h, ft	Wind speed, knots	Wind direction, deg	Temperature, °F
10	1.7	340.3	68.45
20	2.4	336.0	
30	2.7	342.6	
40	2.7	354.8	
50	2.4	350.3	68.14
5-second averages:	2.5	350.3	68.14

FLIGHT CONDITIONS: V_c = 113.2 knots C_L = 0.434 W = 5851 lb

TABLE A2.- CONDITIONS FOR FLIGHT 47, Run 2.0

Date: 8-7-81
Time: 05:47:45.6 GMT

Dispenser location: 50 percent semispan
Particle diameter: 600 to 700 μm

AIRPLANE CONFIGURATION: Basic

RADAR/LASER DATA:

	Row -1	Row 0	Row 1
z, ft	12	12	12
I, ft	1.0	0.3	-0.3

Crossing angle: 0.60°
Airplane heading: 211°

METEOROLOGICAL DATA:

Relative humidity: 82 percent

h, ft	Wind speed, knots	Wind direction, deg	Temperature, °F
10	3.0	350.1	67.24
20	3.3	355.4	
30	3.1	345.9	
40	3.4	347.7	
50	3.3	347.8	66.87
5-second averages:	3.2	348.0	66.87

FLIGHT CONDITIONS: V_c = 86.9 knots C_L = 0.729 W = 5794 lb

TABLE A3.- CONDITIONS FOR FLIGHT 47, Run 3.0

Date: 8-7-81
Time: 07:44:37.2 GMT

Dispenser location: 75 percent semispan
Particle diameter: 600 to 700 μm

AIRPLANE CONFIGURATION: Basic

RADAR/LASER DATA:

	Row -1	Row 0	Row 1
z, ft	14	14	14
I, ft	2.0	1.0	0

Crossing angle: 1.05°
Airplane heading: 211°

METEOROLOGICAL DATA:

Relative humidity: 83 percent

h, ft	Wind speed, knots	Wind direction, deg	Temperature, °F
10	4.2	17.7	65.77
20	4.3	14.8	
30	5.0	8.0	
40	5.3	14.0	
50	5.4	7.9	65.35
5-second averages:	5.2	9.9	65.35

FLIGHT CONDITIONS: V_c = 113.0 knots C_L = 0.458 W = 6166 lb

TABLE A4.- CONDITIONS FOR FLIGHT 47, Run 3.1

Date: 8-7-81
Time: 08:09:15.6 GMT

Dispenser location: 75 percent semispan
Particle diameter: 600 to 700 μm

AIRPLANE CONFIGURATION: Basic

RADAR/LASER DATA:

	Row -1	Row 0	Row 1
z, ft	9	9	9
I, ft	3.9	3.3	2.6

Crossing angle: 0.82°
Airplane heading: 211°

METEOROLOGICAL DATA:

Relative humidity: 78 percent

h, ft	Wind speed, knots	Wind direction, deg	Temperature, °F
10	0.6	11.5	62.58
20	1.2	10.4	
30	1.0	28.1	
40	1.1	8.9	
50	.5	22.9	61.61
5-second averages:	0.7	22.9	61.61

FLIGHT CONDITIONS: V_c = 111.3 knots C_L = 0.469 W = 6118 lb

TABLE A5.- CONDITIONS FOR FLIGHT 47, Run 4.1

Date: 8-7-81
Time: 08:48:41.0 GMT

Dispenser location: 75 percent semispan
Particle diameter: 600 to 700 µm

AIRPLANE CONFIGURATION: Basic

RADAR/LASER DATA:	Row -1	Row 0	Row 1
z, ft	12	12	12
I, ft	1.6	0.7	0

Crossing angle: 1.01°
Airplane heading: 211°

METEOROLOGICAL DATA:

Relative humidity: 78 percent

h, ft	Wind speed, knots	Wind direction, deg	Temperature, °F
10	2.1	2.8	65.55
20	2.5	3.0	
30	2.5	9.7	
40	3.1	14.0	
50	3.3	10.2	65.14
5-second averages:	3.0	11.6	65.16

FLIGHT CONDITIONS: V_c = 71.9 knots C_L = 1.109 W = 6034 lb

TABLE A6.- CONDITIONS FOR FLIGHT 47, Run 5.0

Date: 8-7-81
Time: 10:06:11.50 GMT

Dispenser location: 25 percent semispan
Particle diameter: 600 to 700 µm

AIRPLANE CONFIGURATION: Basic

RADAR/LASER DATA:	Row -1	Row 0	Row 1
z, ft	7	7	7
I, ft	3.9	3.6	3.3

Crossing angle: 0.40°
Airplane heading: 212°

METEOROLOGICAL DATA:

Relative humidity: 69 percent

h, ft	Wind speed, knots	Wind direction, deg	Temperature, °F
10	3.1	333.7	66.29
20	3.3	347.4	
30	3.4	349.5	
40	3.7	354.0	
50	4.2	349.8	65.97
5-second averages:	4.2	349.8	65.97

FLIGHT CONDITIONS: V_c = 118.7 knots C_L = 0.404 W = 5998 lb

TABLE A7.- CONDITIONS FOR FLIGHT 47, Run 5.1

Date: 8-7-81
Time: 10:23:56.6 GMT

Dispenser location: 25 percent semispan
Particle diameter: 600 to 700 μm

AIRPLANE CONFIGURATION: Basic

RADAR/LASER DATA:

	Row -1	Row 0	Row 1
z, ft	7	7	7
I, ft	-0.3	-0.5	0.7

Crossing angle: 0.76°
Airplane heading: 212°

METEOROLOGICAL DATA:

Relative humidity: 69 percent

h, ft	Wind speed, knots	Wind direction, deg	Temperature, °F
10	2.0	353.8	66.8
20	2.3	357.4	
30	2.7	353.3	
40	2.7	350.6	
50	2.4	341.3	66.4
5-second averages:	4.1	341.3	66.4

FLIGHT CONDITIONS: V_c = 120.8 knots C_L = 0.388 W = 5965 lb

TABLE A8.- CONDITIONS FOR FLIGHT 47, Run 6.0

Date: 8-7-81
Time: 10:42:10.40 GMT

Dispenser location: 25 percent semispan
Particle diameter: 600 to 700 μm

AIRPLANE CONFIGURATION: Basic

RADAR/LASER DATA:

	Row -1	Row 0	Row 1
z, ft	11	11	11
I, ft	0.6	0.4	0.3

Crossing angle: 0.54°
Airplane heading: 212°

METEOROLOGICAL DATA:

Relative humidity:

h, ft	Wind speed, knots	Wind direction, deg	Temperature, °F
10	2.2	53.6	67.0
20	2.2	57.0	
30	2.2	50.9	
40	2.9	48.6	
50	3.4	39.8	66.4
5-second averages:			

FLIGHT CONDITIONS: V_c = 90.9 knots C_L = 0.676 W = 6029 lb

TABLE A9.- CONDITIONS FOR FLIGHT 48, Run 1.0

Date: 8-12-81
Time: 4:24:17.30 GMT

Dispenser location: 80 percent semispan
Particle diameter: 600 to 700 μm

AIRPLANE CONFIGURATION: Basic

RADAR/LASER DATA:

	Row -1	Row 0	Row 1
z, ft	9	9	9
I, ft	1.3	1.3	1.3

Crossing angle: -0.003°
Airplane heading: 212°

METEOROLOGICAL DATA:

Relative humidity:

h, ft	Wind speed, knots	Wind direction, deg	Temperature, °F
10	3.4	247.0	70.56
20	3.8	250.8	
30	4.2	244.3	
40	4.9	241.1	
50	5.0	244.8	71.80
5-second averages:	4.6	241.4	71.80

FLIGHT CONDITIONS: V_c = 110.3 knots C_L = 0.488 W = 6247 lb

TABLE A10.- CONDITIONS FOR FLIGHT 48, Run 1.1

Date: 8-12-81
Time: 4:53:49.3 GMT

Dispenser location: 80 percent semispan
Particle diameter: 600 to 700 μm

AIRPLANE CONFIGURATION: Basic

RADAR/LASER DATA:

	Row -1	Row 0	Row 1
z, ft	9	10	10
I, ft	1.6	0.7	0

Crossing angle: 0.94°
Airplane heading: 211°

METEOROLOGICAL DATA:

Relative humidity:

h, ft	Wind speed, knots	Wind direction, deg	Temperature, °F
10	3.1	286.7	70.88
20	3.6	283.0	
30	5.2	287.2	
40	4.7	271.2	
50	4.3	279.4	72.07
5-second averages:	4.4	276.5	72.07

FLIGHT CONDITIONS: V_c = 113.3 knots C_L = 0.457 W = 6176 lb

TABLE A11.- CONDITIONS FOR FLIGHT 49, Run 1.0

Date: 8-13-81
Time: 4:21:6.6 GMT

Dispenser location: 80 percent semispan
Particle diameter: 600 to 700 μm

AIRPLANE CONFIGURATION: Basic

RADAR/LASER DATA:

	Row -1	Row 0	Row 1
z, ft	10	10	10
I, ft	3.3	2.3	1.3

Crossing angle: 1.08°
Airplane heading: 211°

METEOROLOGICAL DATA:

Relative humidity:

h, ft	Wind speed, knots	Wind direction, deg	Temperature, °F
10	2.4	265.0	64.78
20	2.8	276.4	
30	3.0	255.1	
40	3.6	260.0	
50	4.3	260.8	65.21
5-second averages:	3.3	264.7	65.25

FLIGHT CONDITIONS: V_c = 90.9 knots C_L = 0.7168 W = 6235 lb

TABLE A12.- CONDITIONS FOR FLIGHT 49, Run 1.1

Date: 8-13-81
Time: 4:41:37.9 GMT

Dispenser location: 80 percent semispan
Particle diameter: 600 to 700 μm

AIRPLANE CONFIGURATION: Basic

RADAR/LASER DATA:

	Row -1	Row 0	Row 1
z, ft	10	10	10
I, ft	3.9	2.6	1.6

Crossing angle: 1.29°
Airplane heading: 211°

METEOROLOGICAL DATA:

Relative humidity:

h, ft	Wind speed, knots	Wind direction, deg	Temperature, °F
10	1.5	268.0	64.11
20	1.8	270.0	
30	1.8	254.9	
40	2.3	248.5	
50	2.4	251.9	63.64
5-second averages:	1.9	256.4	63.70

FLIGHT CONDITIONS: V_c = 93.2 knots C_L = 0.6767 W = 6188 lb

TABLE A13.- CONDITIONS FOR FLIGHT 49, Run 2.0

Date: 8-13-81
Time: 4:59:46.1 GMT

Dispenser location: 80 percent semispan
Particle diameter: 600 to 700 μm

AIRPLANE CONFIGURATION: Basic

RADAR/LASER DATA:	Row -1	Row 0	Row 1
z, ft	9	9	12
I, ft	0	0	0.3

Crossing angle: -0.17°
Airplane heading: 212°

METEOROLOGICAL DATA:

Relative humidity:

h, ft	Wind speed, knots	Wind direction, deg	Temperature, °F
10	2.5	258.0	63.03
20	3.0	265.8	
30	3.4	267.3	
40	4.3	259.1	
50	4.3	259.7	63.27
5-second averages:	4.3	263.6	63.28

FLIGHT CONDITIONS: V_c = 118.1 knots C_L = 0.419 W = 6147 lb

TABLE A14.- CONDITIONS FOR FLIGHT 49, Run 2.1

Date: 8-13-81
Time: 5:17:58.7 GMT

Dispenser location: 80 percent semispan
Particle diameter: 600 to 700 μm

AIRPLANE CONFIGURATION: Basic

RADAR/LASER DATA:	Row -1	Row 0	Row 1
z, ft	10	10	10
I, ft	0.7	0.3	0

Crossing angle: 0.32°
Airplane heading: 212°

METEOROLOGICAL DATA:

Relative humidity:

h, ft	Wind speed, knots	Wind direction, deg	Temperature, °F
10	4.1	290.5	64.42
20	4.3	288.4	
30	5.0	281.1	
40	5.3	276.7	
50	5.4	274.6	64.42
5-second averages:	5.3	275.1	64.42

FLIGHT CONDITIONS: V_c = 114.9 knots C_L = 0.439 W = 6106 lb

TABLE A15.- CONDITIONS FOR FLIGHT 49, Run 3.0

Date: 8-13-81
Time: 6:33:29.0 GMT

Dispenser location: 85 percent semispan
Particle diameter: 600 to 700 μm

AIRPLANE CONFIGURATION: Basic

RADAR/LASER DATA:

	Row -1	Row 0	Row 1
z, ft	11	11	11
I, ft	-0.7	-1.6	-3.3

Crossing angle: 1.09°
Airplane heading: 211°

METEOROLOGICAL DATA:

Relative humidity: 91 percent

h, ft	Wind speed, knots	Wind direction, deg	Temperature, °F
10	3.7	293.5	64.54
20	4.4	291.0	
30	4.9	278.1	
40	5.4	280.1	
50	5.5	276.9	64.42
5-second averages:	3.5	262.9	62.60

FLIGHT CONDITIONS: V_c = 113.6 knots C_L = 0.455 W = 6178 lb

TABLE A16.- CONDITIONS FOR FLIGHT 49, Run 3.1

Date: 8-13-81
Time: 6:54:45.1 GMT

Dispenser location: 85 percent semispan
Particle diameter: 600 to 700 μm

AIRPLANE CONFIGURATION: Basic

RADAR/LASER DATA:

	Row -1	Row 0	Row 1
z, ft	12	11	11
I, ft	0	0	-0.3

Crossing angle: 0.17°
Airplane heading: 212°

METEOROLOGICAL DATA:

Relative humidity:

h, ft	Wind speed, knots	Wind direction, deg	Temperature, °F
10	3.7	297.5	63.95
20	4.0	295.8	
30	4.8	292.4	
40	5.5	279.7	
50	5.2	281.6	63.88
5-second averages:	4.9	284.1	63.84

FLIGHT CONDITIONS: V_c = 117.7 knots C_L = 0.427 W = 6229 lb

TABLE A17.- CONDITIONS FOR FLIGHT 49, Run 4.1

Date: 8-13-81
Time: 7:15:27.0 GMT

Dispenser location: 85 percent semispan
Particle diameter: 600 to 700 μm

AIRPLANE CONFIGURATION: Basic

RADAR/LASER DATA:

	Row -1	Row 0	Row 1
z, ft	10	10	10
I, ft	6.9	5.6	4.6

Crossing angle: 1.23°
Airplane heading: 211°

METEOROLOGICAL DATA:

Relative humidity:

h, ft	Wind speed, knots	Wind direction, deg	Temperature, °F
10	4.1	288.4	65.28
20	4.7	290.4	
30	5.3	282.9	
40	5.6	284.6	
50	5.9	284.4	65.80
5-second averages:	5.7	282.3	65.80

FLIGHT CONDITIONS: V_c = 91.2 knots C_L = 0.704 W = 6176 lb

TABLE A18.- CONDITIONS FOR FLIGHT 49, Run 4.2

Date: 8-13-81
Time: 7:35:59.8 GMT

Dispenser location: 85 percent semispan
Particle diameter: 600 to 700 μm

AIRPLANE CONFIGURATION: Basic

RADAR/LASER DATA:

	Row -1	Row 0	Row 1
z, ft	9	9	9
I, ft	0.3	-0.3	-1.3

Crossing angle: 0.98°
Airplane heading: 211°

METEOROLOGICAL DATA:

Relative humidity:

h, ft	Wind speed, knots	Wind direction, deg	Temperature, °F
10	2.9	287.6	64.26
20	3.4	292.4	
30	4.0	283.1	
40	4.0	280.6	
50	4.0	276.0	64.44
5-second averages:	4.0	278.6	64.85

FLIGHT CONDITIONS: V_c = 88.7 knots C_L = 0.740 W = 6129 lb

TABLE A19.- CONDITIONS FOR FLIGHT 49, Run 5.2

Date: 8-13-81
Time: 8:57:51.8 GMT

Dispenser location: 90 percent semispan
Particle diameter: 600 to 700 μm

AIRPLANE CONFIGURATION: Basic

RADAR/LASER DATA:	Row -1	Row 0	Row 1
z, ft	13	13	13
I, ft	1.0	0	-0.7

Crossing angle: 0.83°
Airplane heading: 211°

METEOROLOGICAL DATA:

Relative humidity:

h, ft	Wind speed, knots	Wind direction, deg	Temperature, °F
10	4.2	276.2	65.37
20	4.7	260.0	
30	4.2	266.6	
40	5.6	269.7	
50	5.5	265.1	65.70
5-second averages:	5.2	261.7	65.70

FLIGHT CONDITIONS: V_c = 112.3 knots C_L = 0.469 W = 6235 lb

TABLE A20.- CONDITIONS FOR FLIGHT 49, Run 5.4

Date: 8-13-81
Time: 9:22:17.1 GMT

Dispenser location: 90 percent semispan
Particle diameter: 600 to 700 μm

AIRPLANE CONFIGURATION: Basic

RADAR/LASER DATA:	Row -1	Row 0	Row 1
z, ft	10	12	12
I, ft	0	-0.3	-1.0

Crossing angle: 0.56°
Airplane heading: 212°

METEOROLOGICAL DATA:

Relative humidity:

h, ft	Wind speed, knots	Wind direction, deg	Temperature, °F
10	4.0	286.7	65.86
20	4.6	279.8	
30	5.3	272.3	
40	6.5	265.9	
50	6.2	278.5	66.81
5-second averages:	5.6	276.2	66.85

FLIGHT CONDITIONS: V_c = 114.4 knots C_L = 0.448 W = 6165 lb

TABLE A21.- CONDITIONS FOR FLIGHT 49, Run 6.2

Date: 8-13-81
Time: 10:05:53.8 GMT

Dispenser location: 90 percent semispan
Particle diameter: 600 to 700 μm

AIRPLANE CONFIGURATION: Basic

RADAR/LASER DATA:

	Row -1	Row 0	Row 1
z, ft	9	9	9
I, ft	1.6	1.3	1.0

Crossing angle: 0.28°
Airplane heading: 212°

METEOROLOGICAL DATA:

Relative humidity:

h, ft	Wind speed, knots	Wind direction, deg	Temperature, °F
10	3.6	276.2	65.43
20	4.0	282.4	
30	4.2	278.7	
40	6.1	268.3	
50	6.0	270.3	66.22
5-second averages:	6.0	272.8	66.22

FLIGHT CONDITIONS: V_c = 87.3 knots C_L = 0.757 W = 6079 lb

TABLE A22.- CONDITIONS FOR FLIGHT 49, Run 6.4

Date: 8-13-81
Time: 10:29:57.1 GMT

Dispenser location: 90 percent semispan
Particle diameter: 600 to 700 μm

AIRPLANE CONFIGURATION: Basic

RADAR/LASER DATA:

	Row -1	Row 0	Row 1
z, ft	9	8	8
I, ft	0.7	0.7	0.7

Crossing angle: -0.16°
Airplane heading: 212°

METEOROLOGICAL DATA:

Relative humidity: 62 percent

h, ft	Wind speed, knots	Wind direction, deg	Temperature, °F
10	3.8	274.5	66.27
20	4.6	280.0	
30	4.9	276.0	
40	4.9	274.3	
50	5.9	267.5	67.24
5-second averages:	5.4	270.8	67.24

FLIGHT CONDITIONS: V_c = 88.0 knots C_L = 0.740 W = 6026 lb

TABLE A23.- CONDITIONS FOR FLIGHT 50, Run 1.1

Date: 8-14-81
Time: 04:22:15.2 GMT

Dispenser location: 95 percent semispan
Particle diameter: 600 to 700 μm

AIRPLANE CONFIGURATION: Basic

RADAR/LASER DATA:

	Row -1	Row 0	Row 1
z, ft	13	13	13
I, ft	3.3	2.6	2.0

Crossing angle: 0.90°
Airplane heading: 211°

METEOROLOGICAL DATA:

Relative humidity: 83 percent

h, ft	Wind speed, knots	Wind direction, deg	Temperature, °F
10	3.0	243.5	65.34
20	3.4	237.4	
30	3.7	235.6	
40	4.1	232.0	
50	4.8	230.6	65.25
5-second averages:	4.8	230.9	65.25

FLIGHT CONDITIONS: V_c = 118.6 knots C_L = 0.413   W = 6115 lb

TABLE A24.- CONDITIONS FOR FLIGHT 50, Run 2.2

Date: 8-14-81
Time: 04:59:17.6 GMT

Dispenser location: 95 percent semispan
Particle diameter: 600 to 700 μm

AIRPLANE CONFIGURATION: Basic

RADAR/LASER DATA:

	Row -1	Row 0	Row 1
z, ft	12	12	12
I, ft	5.3	4.9	4.9

Crossing angle: 0.08°
Airplane heading: 212°

METEOROLOGICAL DATA:

Relative humidity: 83 percent

h, ft	Wind speed, knots	Wind direction, deg	Temperature, °F
10	3.4	233.1	65.64
20	3.3	243.4	
30	3.1	237.4	
40	3.4	235.8	
50	3.5	235.6	65.17
5-second averages:	3.498	235.50	65.19

FLIGHT CONDITIONS: V_c = 86.7 knots C_L = 0.761   W = 6019 lb

TABLE A25.- CONDITIONS FOR FLIGHT 51, Run 1.2

Date: 8-19-81
Time: 4:24:05.0 GMT

Dispenser location: 15 percent semispan
Particle diameter: 600 to 700 μm

AIRPLANE CONFIGURATION: Basic

RADAR/LASER DATA:

	Row -1	Row 0	Row 1
z, ft	8	8	8
I, ft	6.2	5.6	4.6

Crossing angle: 0.94°
Airplane heading: 211°

METEOROLOGICAL DATA:

Relative humidity:

h, ft	Wind speed, knots	Wind direction, deg	Temperature, °F
10	2.8	72.4	66.43
20	3.3	85.0	
30	3.0	101.9	
40	4.0	84.8	
50	4.1	70.5	67.1
5-second averages:	3.7	80.3	67.1

FLIGHT CONDITIONS: V_c = 117.2 knots C_L = 0.430 W = 6273 lb

TABLE A26.- CONDITIONS FOR FLIGHT 51, Run 2.1

Date: 8-19-81
Time: 5:11:54.4 GMT

Dispenser location: 15 percent semispan
Particle diameter: 600 to 700 μm

AIRPLANE CONFIGURATION: Basic

RADAR/LASER DATA:

	Row -1	Row 0	Row 1
z, ft	6	6	6
I, ft	4.6	3.3	2.0

Crossing angle: 1.49°
Airplane heading: 211°

METEOROLOGICAL DATA:

Relative humidity:

h, ft	Wind speed, knots	Wind direction, deg	Temperature, °F
10	3.4	89.7	65.70
20	3.8	85.4	
30	3.4	82.5	
40	4.0	53.0	
50	4.2	66.0	67.62
5-second averages:	3.8	78.8	67.62

FLIGHT CONDITIONS: V_c = 89.7 knots C_L = 0.719 W = 6099 lb

TABLE A27.- CONDITIONS FOR FLIGHT 51, Run 2.3

Date: 8-19-81
Time: 5:34:25.1 GMT

Dispenser location: 15 percent semispan
Particle diameter: 600 to 700 μm

AIRPLANE CONFIGURATION: Basic

RADAR/LASER DATA:	Row -1	Row 0	Row 1
z, ft	9	9	9
I, ft	5.6	4.6	3.9

Crossing angle: 1.11°
Airplane heading: 211°

METEOROLOGICAL DATA:

Relative humidity:

h, ft	Wind speed, knots	Wind direction, deg	Temperature, °F
10	2.0	48.9	65.53
20	2.0	78.0	
30	2.7	85.9	
40	2.7	76.9	
50	3.3	97.4	67.06
5-second averages:	3.1	92.1	67.1

FLIGHT CONDITIONS: V_c = 89.7 knots C_L = 0.713 W = 6050 lb

TABLE A28.- CONDITIONS FOR FLIGHT 51, Run 3.3

Date: 8-19-81
Time: 7:13:07.2 GMT

Dispenser location: 40 percent semispan
Particle diameter: 600 to 700 μm

AIRPLANE CONFIGURATION: Basic

RADAR/LASER DATA:	Row -1	Row 0	Row 1
z, ft	13	13	13
I, ft	4.9	3.9	3.0

Crossing angle: 1.25°
Airplane heading: 211°

METEOROLOGICAL DATA:

Relative humidity:

h, ft	Wind speed, knots	Wind direction, deg	Temperature, °F
10	3.4	60.3	66.45
20	3.5	53.8	
30	3.3	68.7	
40	5.2	63.9	
50	5.3	66.7	67.82
5-second averages:	4.0	69.1	67.82

FLIGHT CONDITIONS: V_c = 118.0 knots C_L = 0.423 W = 6212 lb

TABLE A29.- CONDITIONS FOR FLIGHT 52, Run 1.0

Date: 8-25-81
Time: 4:50:37.6 GMT

Dispenser location: 60 percent semispan
Particle diameter: 600 to 700 μm

AIRPLANE CONFIGURATION: Basic

RADAR/LASER DATA:

	Row -1	Row 0	Row 1
z, ft	11	11	11
I, ft	0	-0.3	-1.0

Crossing angle: 0.68°
Airplane heading: 212°

METEOROLOGICAL DATA:

Relative humidity: 86 percent

h, ft	Wind speed, knots	Wind direction, deg	Temperature, °F
10	3.1	302.6	70.92
20	3.5	308.4	
30	3.6	306.1	
40	3.7	301.5	
50	4.1	302.9	69.51
5-second averages:	4.1	302.9	69.54

FLIGHT CONDITIONS: V_c = 116.7 knots C_L = 0.429 W = 6148 lb

TABLE A30.- CONDITIONS FOR FLIGHT 53, Run 1.2

Date: 8-26-81
Time: 8:12:27.6 GMT

Dispenser location: 50 percent semispan
Particle diameter: 300 to 355 μm

AIRPLANE CONFIGURATION: Basic

RADAR/LASER DATA:

	Row -1	Row 0	Row 1
z, ft	12	12	12
I, ft	4.6	3.9	4.0

Crossing angle: 1.02°
Airplane heading: 211°

METEOROLOGICAL DATA:

Relative humidity:

h, ft	Wind speed, knots	Wind direction, deg	Temperature, °F
10	3.4	307.7	59.27
20	4.4	310.8	
30	4.6	311.7	
40	4.4	319.6	
50	4.3	324.7	57.27
5-second averages:	4.4	319.8	57.27

FLIGHT CONDITIONS: V_c = 123.3 knots C_L = 0.389 W = 6235 lb

TABLE A31.- CONDITIONS FOR FLIGHT 53, Run 2.2

Date: 8-26-81
Time: 8:59:52.1 GMT

Dispenser location: 50 percent semispan
Particle diameter: 300 to 355 μm

AIRPLANE CONFIGURATION: Basic

RADAR/LASER DATA:	Row -1	Row 0	Row 1
z, ft	13	10	10
I, ft	3.9	2.6	1.3

Crossing angle: 1.57°
Airplane heading: 211°

METEOROLOGICAL DATA:

Relative humidity:

h, ft	Wind speed, knots	Wind direction, deg	Temperature, °F
10	3.4	303.1	58.64
20	3.7	316.8	
30	4.1	323.7	
40	4.4	331.5	
50	4.4	327.7	56.55
5-second averages:	4.4	329.8	56.55

FLIGHT CONDITIONS: V_c = 88.5 knots C_L = 0.739 W = 6094 lb

TABLE A32.- CONDITIONS FOR FLIGHT 53, Run 2.3

Date: 8-26-81
Time: 09:13:49.4 GMT

Dispenser location: 50 percent semispan
Particle diameter: 300 to 355 μm

AIRPLANE CONFIGURATION: Basic

RADAR/LASER DATA:	Row -1	Row 0	Row 1
z, ft	10	10	10
I, ft	5.6	5.3	4.9

Crossing angle: 0.30°
Airplane heading: 212°

METEOROLOGICAL DATA:

Relative humidity: 70 percent

h, ft	Wind speed, knots	Wind direction, deg	Temperature, °F
10	3.1	307.1	58.44
20	3.4	323.4	
30	4.0	324.0	
40	4.3	330.9	
50	4.6	330.3	56.30
5-second averages:	4.6	334.0	56.30

FLIGHT CONDITIONS: V_c = 89.1 knots C_L = 0.712 W = 5956 lb

TABLE A33.- CONDITIONS FOR FLIGHT 54, Run 1.0

Date: 8-27-81
Time: 04:13:22.2 GMT

Dispenser location: 75 percent semispan
Particle diameter: 300 to 355 μm

AIRPLANE CONFIGURATION: Basic

RADAR/LASER DATA:	Row -1	Row 0	Row 1
z, ft	8	10	10
I, ft	1.3	0.7	0.3

Crossing angle: 0.57°
Airplane heading: 212°

METEOROLOGICAL DATA:

Relative humidity: 83 percent

h, ft	Wind speed, knots	Wind direction, deg	Temperature, °F
10	4.0	177.3	61.90
20	4.0	172.4	
30	4.7	174.6	
40	4.9	168.2	
50	4.8	173.6	58.28
5-second averages:	4.4	173.9	58.28

FLIGHT CONDITIONS: V_c = 115.7 knots C_L = 0.437 W = 6154 lb

TABLE A34.- CONDITIONS FOR FLIGHT 54, Run 1.1

Date: 8-27-81
Time: 04:27:35.2 GMT

Dispenser location: 75 percent semispan
Particle diameter: 300 to 355 μm

AIRPLANE CONFIGURATION: Basic

RADAR/LASER DATA:	Row -1	Row 0	Row 1
z, ft	12	11	11
I, ft	-1.6	-2.0	-2.3

Crossing angle: 0.44°
Airplane heading: 212°

METEOROLOGICAL DATA:

Relative humidity: 83 percent

h, ft	Wind speed, knots	Wind direction, deg	Temperature, °F
10	2.9	179.4	60.89
20	3.1	182.8	
30	3.4	172.4	
40	4.3	171.0	
50	4.3	181.2	58.80
5-second averages:	4.6	177.5	58.78

FLIGHT CONDITIONS: V_c = 117.9 knots C_L = 0.418 W = 6115 lb

TABLE A35.- CONDITIONS FOR FLIGHT 54, Run 2.0

Date: 8-27-81
Time: 04:40:47.0 GMT

Dispenser location: 75 percent semispan
Particle diameter: 300 to 355 μm

AIRPLANE CONFIGURATION: Basic

RADAR/LASER DATA:

	Row -1	Row 0	Row 1
z, ft	11	11	9
I, ft	1.3	1.0	0.7

Crossing angle: 0.43°
Airplane heading: 212°

METEOROLOGICAL DATA:

Relative humidity:

h, ft	Wind speed, knots	Wind direction, deg	Temperature, °F
10	2.7	183.4	61.50
20	3.4	173.4	
30	3.7	174.0	
40	3.5	179.8	
50	4.3	184.9	59.38
5-second averages:	4.4	189.8	59.38

FLIGHT CONDITIONS: V_c = 86.3 knots C_L = 0.776 W = 6079 lb

TABLE A36.- CONDITIONS FOR FLIGHT 54, Run 3.0

Date: 8-27-81
Time: 06:00:33.1 GMT

Dispenser location: 80 percent semispan
Particle diameter: 300 to 355 μm

AIRPLANE CONFIGURATION: Basic

RADAR/LASER DATA:

	Row -1	Row 0	Row 1
z, ft	10	10	10
I, ft	-1.6	-1.6	-1.3

Crossing angle: -0.23°
Airplane heading: 212°

METEOROLOGICAL DATA:

Relative humidity: 88 percent

h, ft	Wind speed, knots	Wind direction, deg	Temperature, °F
10	2.9	184.0	60.58
20	3.5	185.8	
30	4.0	182.5	
40	4.3	186.9	
50	4.6	190.5	59.72
5-second averages:	4.6	189.9	59.74

FLIGHT CONDITIONS: V_c = 115.7 knots C_L = 0.439 W = 6181 lb

TABLE A37.- CONDITIONS FOR FLIGHT 54, Run 3.1

Date: 8-27-81
Time: 06:17:10.4 GMT

Dispenser location: 80 percent semispan
Particle diameter: 300 to 355 μm

AIRPLANE CONFIGURATION: Basic

RADAR/LASER DATA:

	Row -1	Row 0	Row 1
z, ft	9	9	9
I, ft	-3.0	-3.0	-3.0

Crossing angle: 0.15°
Airplane heading: 212°

METEOROLOGICAL DATA:

Relative humidity: 88 percent

h, ft	Wind speed, knots	Wind direction, deg	Temperature, °F
10	3.1	183.9	61.09
20	3.5	187.0	
30	4.4	178.6	
40	5.0	174.9	
50	5.3	184.8	58.95
5-second averages:	5.4	185.4	58.96

FLIGHT CONDITIONS: V_c = 117.4 knots C_L = 0.423 W = 6139 lb

TABLE A38.- CONDITIONS FOR FLIGHT 54, Run 4.0

Date: 8-27-81
Time: 06:50:32.8 GMT

Dispenser location: 80 percent semispan
Particle diameter: 300 to 355 μm

AIRPLANE CONFIGURATION: Basic

RADAR/LASER DATA:

	Row -1	Row 0	Row 1
z, ft	2	2	2
I, ft	-8.9	-9.5	-10.5

Crossing angle: 1.07°
Airplane heading: 211°

METEOROLOGICAL DATA:

Relative humidity: 88 percent

h, ft	Wind speed, knots	Wind direction, deg	Temperature, °F
10	2.7	250.4	60.81
20	2.9	232.4	
30	3.1	224.4	
40	4.1	214.5	
50	4.0	215.7	57.56
5-second averages:	4.1	214.9	57.56

FLIGHT CONDITIONS: V_c = 85.2 knots C_L = 0.790 W = 6043 lb

TABLE A39.- CONDITIONS FOR FLIGHT 54, Run 4.1

Date: 8-27-81
Time: 07:05:00.1 GMT

Dispenser location: 80 percent semispan
Particle diameter: 300 to 355 μm

AIRPLANE CONFIGURATION: Basic

RADAR/LASER DATA:	Row -1	Row 0	Row 1
z, ft	11	11	11
I, ft	-1.3	-1.3	-1.3

Crossing angle: -0.06°
Airplane heading: 212°

METEOROLOGICAL DATA:

Relative humidity: 89 percent

h, ft	Wind speed, knots	Wind direction, deg	Temperature, °F
10	1.8	262.7	59.32
20	2.3	251.8	
30	2.4	229.5	
40	3.3	213.9	
50	3.3	213.4	56.97
5-second averages:	3.1	213.9	56.98

FLIGHT CONDITIONS: V_c = 82.9 knots C_L = 0.831 W = 6007 lb

TABLE A40.- CONDITIONS FOR FLIGHT 54, Run 5.0

Date: 8-27-81
Time: 08:07:17.9 GMT

Dispenser location: 85 percent semispan
Particle diameter: 300 to 355 μm

AIRPLANE CONFIGURATION: Basic

RADAR/LASER DATA:	Row -1	Row 0	Row 1
z, ft	12	12	12
I, ft	-1.0	-1.3	-2.0

Crossing angle: 0.60°
Airplane heading: 212°

METEOROLOGICAL DATA:

Relative humidity: 74 percent

h, ft	Wind speed, knots	Wind direction, deg	Temperature, °F
10	2.5	278.0	58.68
20	2.5	277.8	
30	3.4	239.6	
40	4.2	232.6	
50	4.4	230.1	56.46
5-second averages:	4.6	228.2	56.46

FLIGHT CONDITIONS: V_c = 115.1 knots C_L = 0.443 W = 6178 lb

TABLE A41.- CONDITIONS FOR FLIGHT 54, Run 5.1

Date: 8-27-81
Time: 08:19:17.4 GMT

Dispenser location: 85 percent semispan
Particle diameter: 300 to 355 μm

AIRPLANE CONFIGURATION: Basic

RADAR/LASER DATA:	Row -1	Row 0	Row 1
z, ft	10	10	10
I, ft	-1.6	-2.3	-2.6

Crossing angle: 0.60°
Airplane heading: 212°

METEOROLOGICAL DATA:

Relative humidity: 74 percent

h, ft	Wind speed, knots	Wind direction, deg	Temperature, °F
10	3.6	295.4	58.41
20	3.5	289.4	
30	3.4	269.0	
40	3.3	254.9	
50	3.7	249.7	56.68
5-second averages:	3.8	250.4	56.68

FLIGHT CONDITIONS: V_c = 150.3 knots C_L = 0.258 W = 6142 lb

TABLE A42.- CONDITIONS FOR FLIGHT 54, Run 6.1

Date: 8-27-81
Time: 08:45:18.3 GMT

Dispenser location: 85 percent semispan
Particle diameter: 300 to 355 μm

AIRPLANE CONFIGURATION: Basic

RADAR/LASER DATA:	Row -1	Row 0	Row 1
z, ft	11	11	11
I, ft	2.0	2.0	2.0

Crossing angle: -0.04°
Airplane heading: 212°

METEOROLOGICAL DATA:

Relative humidity: 74 percent

h, ft	Wind speed, knots	Wind direction, deg	Temperature, °F
10	3.3	298.4	57.78
20	4.0	294.8	
30	4.1	286.9	
40	4.4	284.8	
50	4.8	278.9	56.17
5-second averages:	4.9	278.8	56.17

FLIGHT CONDITIONS: V_c = 86.6 knots C_L = 0.770 W = 6070 lb

TABLE A43.- CONDITIONS FOR FLIGHT 54, Run 6.2

Date: 8-27-81
Time: 08:58:52.4 GMT

Dispenser location: 85 percent semispan
Particle diameter: 300 to 355 μm

AIRPLANE CONFIGURATION: Basic

RADAR/LASER DATA:	Row -1	Row 0	Row 1
z, ft	10	10	10
I, ft	3.9	4.6	5.6

Crossing angle: -1.13°
Airplane heading: 213°

METEOROLOGICAL DATA:

Relative humidity: 74 percent

h, ft	Wind speed, knots	Wind direction, deg	Temperature, °F
10	2.7	295.7	57.61
20	3.1	299.0	
30	3.4	282.7	
40	3.6	278.9	
50	3.6	272.6	55.81
5-second averages:	3.7	270.8	55.81

FLIGHT CONDITIONS: V_c = 87.9 knots C_L = 0.742 W = 6034 lb

TABLE A44.- CONDITIONS FOR FLIGHT 55, Run 1.1

Date: 8-31-81
Time: 10:21:13.3 GMT

Dispenser location: 90 percent semispan
Particle diameter: 300 to 355 μm

AIRPLANE CONFIGURATION: Basic

RADAR/LASER DATA:	Row -1	Row 0	Row 1
z, ft	15	15	15
I, ft	10.2	9.8	9.2

Crossing angle: 0.66°
Airplane heading: 212°

METEOROLOGICAL DATA:

Relative humidity: 68 percent

h, ft	Wind speed, knots	Wind direction, deg	Temperature, °F
10	2.5	59.8	65.48
20	3.0	60.0	
30	3.4	58.3	
40	3.8	55.7	
50	4.3	69.2	62.13
5-second averages:	4.1	65.1	62.13

FLIGHT CONDITIONS: V_c = 124.7 knots C_L = 0.376 W = 6157 lb

TABLE A45.- CONDITIONS FOR FLIGHT 55, Run 2.1

Date: 8-31-81
Time: 11:14:16.5 GMT

Dispenser location: 90 percent semispan
Particle diameter: 300 to 355 μm

AIRPLANE CONFIGURATION: Basic

RADAR/LASER DATA:	Row -1	Row 0	Row 1
z, ft	6	6	6
I, ft	4.9	4.6	4.6

Crossing angle: 0.26°
Airplane heading: 212°

METEOROLOGICAL DATA:

Relative humidity: 68 percent

h, ft	Wind speed, knots	Wind direction, deg	Temperature, °F
10	3.6	65.5	70.39
20	4.6	58.8	
30	4.3	63.1	
40	5.6	43.9	
50	5.0	56.2	69.91
5-second averages:	6.0	77.2	69.91

FLIGHT CONDITIONS: V_c = 88.7 knots C_L = 0.725 W = 6009 lb

TABLE A46.- CONDITIONS FOR FLIGHT 55, Run 2.2

Date: 8-31-81
Time: 11:44:45.0 GMT

Dispenser location: 90 percent semispan
Particle diameter: 300 to 355 μm

AIRPLANE CONFIGURATION: Basic

RADAR/LASER DATA:	Row -1	Row 0	Row 1
z, ft	7	7	7
I, ft	2.6	2.0	1.3

Crossing angle: 0.76°
Airplane heading: 211°

METEOROLOGICAL DATA:

Relative humidity: 68 percent

h, ft	Wind speed, knots	Wind direction, deg	Temperature, °F
10	6.6	63.8	71.37
20	7.5	66.4	
30	7.2	49.5	
40	6.5	59.1	
50	6.6	58.2	71.06
5-second averages:	6.4	58.7	71.08

FLIGHT CONDITIONS: V_c = 87.7 knots C_L = 0.734 W = 5950 lb

TABLE A47.- CONDITIONS FOR FLIGHT 56, Run 1.1

Date: 9-1-81
Time: 10:01:54.9 GMT

Dispenser location: 90 percent semispan
Particle diameter: 300 to 355 μm

AIRPLANE CONFIGURATION: Basic

RADAR/LASER DATA:

	Row -1	Row 0	Row 1
z, ft	13	13	13
I, ft	13.5	13.1	12.8

Crossing angle: 0.38°
Airplane heading: 212°

METEOROLOGICAL DATA:

Relative humidity: 70 percent

h, ft	Wind speed, knots	Wind direction, deg	Temperature, °F
10	2.1	339.5	68.13
20	2.0	340.8	
30	2.2	350.9	
40	2.0	2.1	
50	2.2	3.4	66.90
5-second averages:	2.3	10.1	66.90

FLIGHT CONDITIONS: V_c = 118.3 knots C_L = 0.414 W = 6100 lb

TABLE A48.- CONDITIONS FOR FLIGHT 56, Run 2.0

Date: 9-1-81
Time: 10:25:28.60 GMT

Dispenser location: 90 percent semispan
Particle diameter: 300 to 355 μm

AIRPLANE CONFIGURATION: Basic

RADAR/LASER DATA:

	Row -1	Row 0	Row 1
z, ft	8	8	8
I, ft	5.6	4.3	3.3

Crossing angle: 1.29°
Airplane heading: 211°

METEOROLOGICAL DATA:

Relative humidity: 70 percent

h, ft	Wind speed, knots	Wind direction, deg	Temperature, °F
10	1.6	17.6	67.89
20	1.7	29.0	
30	2.1	30.5	
40	2.1	29.7	
50	2.3	28.9	62.82
5-second averages:	2.2	32.1	65.84

FLIGHT CONDITIONS: V_c = 86.5 knots C_L = 0.765 W = 6028 lb

TABLE A49.- CONDITIONS FOR FLIGHT 56, Run 2.1

Date: 9-1-81
Time: 10:42:35.60 GMT

Dispenser location: 90 percent semispan
Particle diameter: 300 to 355 μm

AIRPLANE CONFIGURATION: Basic

RADAR/LASER DATA:

	Row -1	Row 0	Row 1
z, ft	7	7	7
I, ft	0	-0.7	-0.9

Crossing angle: 0.61°
Airplane heading: 212°

METEOROLOGICAL DATA:

Relative humidity: 70 percent

h, ft	Wind speed, knots	Wind direction, deg	Temperature, °F
10	3.6	8.6	67.23
20	3.4	5.0	
30	3.6	10.2	
40	3.5	4.4	
50	3.7	13.5	66.49
5-second averages:	3.4	22.9	66.49

FLIGHT CONDITIONS: V_c = 85.6 knots C_L = 0.777 W = 5998 lb

TABLE A50.- CONDITIONS FOR FLIGHT 56, Run 3.2

Date: 9-1-81
Time: 12:13:50.60 GMT

Dispenser location: 95 percent semispan
Particle diameter: 300 to 355 μm

AIRPLANE CONFIGURATION: Basic

RADAR/LASER DATA:

	Row -1	Row 0	Row 1
z, ft	16	16	16
I, ft	0.3	-0.3	-0.7

Crossing angle: 0.65°
Airplane heading: 212°

METEOROLOGICAL DATA:

Relative humidity: 72 percent

h, ft	Wind speed, knots	Wind direction, deg	Temperature, °F
10	3.5	330.5	71.28
20	3.6	330.8	
30	3.8	325.7	
40	3.7	321.7	
50	3.8	319.5	70.86
5-second averages:	4.0	332.0	70.70

FLIGHT CONDITIONS: V_c = 150.5 knots C_L = 0.258 W = 6148 lb

TABLE A51.- CONDITIONS FOR FLIGHT 56, Run 3.4

Date: 9-1-81
Time: 12:29:52.20 GMT

Dispenser location: 95 percent semispan
Particle diameter: 300 to 355 μm

AIRPLANE CONFIGURATION: Basic

RADAR/LASER DATA:	Row -1	Row 0	Row 1
z, ft	14	14	14
I, ft	-0.3	-1.3	-2.0

Crossing angle: 0.88°
Airplane heading: 211°

METEOROLOGICAL DATA:

Relative humidity: 72 percent

h, ft	Wind speed, knots	Wind direction, deg	Temperature, °F
10	3.1	346.1	73.15
20	2.3	354.0	
30	2.7	359.4	
40	2.3	5.6	
50	2.5	6.2	72.77
5-second averages:	2.4	352.6	72.75

FLIGHT CONDITIONS: V_c = 119.3 knots C_L = 0.408 W = 6112 lb

TABLE A52.- CONDITIONS FOR FLIGHT 56, Run 4.1

Date: 9-1-81
Time: 12:47:22.80 GMT

Dispenser location: 95 percent semispan
Particle diameter: 300 to 355 μm

AIRPLANE CONFIGURATION: Basic

RADAR/LASER DATA:	Row -1	Row 0	Row 1
z, ft	11	11	11
I, ft	10.5	16.1	21.7

Crossing angle: -6.59°
Airplane heading: 219°

METEOROLOGICAL DATA:

Relative humidity: 72 percent

h, ft	Wind speed, knots	Wind direction, deg	Temperature, °F
10	3.5	357.4	74.71
20	3.4	354.0	
30	2.9	358.2	
40	3.7	10.4	
50	3.7	12.1	74.57
5-second averages:	3.3	9.0	74.57

FLIGHT CONDITIONS: V_c = 89.4 knots C_L = 0.721 W = 6070 lb

TABLE A53.- CONDITIONS FOR FLIGHT 57, Run 1.1

Date: 9-2-81
Time: 10:00:37.7 GMT

Dispenser location: 25 percent semispan
Particle diameter: 300 to 355 µm

AIRPLANE CONFIGURATION: Basic

RADAR/LASER DATA:

	Row -1	Row 0	Row 1
z, ft	19	19	19
I, ft	4.9	4.3	3.9

Crossing angle: 0.61°
Airplane heading: 212°

METEOROLOGICAL DATA:

Relative humidity:

h, ft	Wind speed, knots	Wind direction, deg	Temperature, °F
10	3.4	91.9	69.66
20	3.7	83.4	
30	5.2	95.8	
40	4.7	90.5	
50	5.9	87.1	69.06
5-second averages:	4.4	85.9	69.06

FLIGHT CONDITIONS: V_c = 120.3 knots C_L = 0.408 W = 6218 lb

TABLE A54.- CONDITIONS FOR FLIGHT 57, Run 1.2

Date: 9-2-81
Time: 10:15:30.9 GMT

Dispenser location: 25 percent semispan
Particle diameter: 300 to 355 µm

AIRPLANE CONFIGURATION: Basic

RADAR/LASER DATA:

	Row -1	Row 0	Row 1
z, ft	17	17	17
I, ft	13.1	13.8	14.4

Crossing angle: -0.70°
Airplane heading: 213°

METEOROLOGICAL DATA:

Relative humidity:

h, ft	Wind speed, knots	Wind direction, deg	Temperature, °F
10	2.5	61.5	69.42
20	2.9	75.0	
30	3.3	54.0	
40	3.4	81.3	
50	4.8	83.5	69.13
5-second averages:	4.3	95.7	69.13

FLIGHT CONDITIONS: V_c = 118.0 knots C_L = 0.422 W = 6182 lb

TABLE A55.- CONDITIONS FOR FLIGHT 57, Run 2.6

Date: 9-2-81
Time: 10:44:46.9 GMT

Dispenser location: 25 percent semispan
Particle diameter: 300 to 355 μm

AIRPLANE CONFIGURATION: Basic

RADAR/LASER DATA:	Row -1	Row 0	Row 1
z, ft	8	8	8
I, ft	4.3	3.0	1.3

Crossing angle: 1.66°
Airplane heading: 211°

METEOROLOGICAL DATA:

Relative humidity:

h, ft	Wind speed, knots	Wind direction, deg	Temperature, °F
10	3.1	106.0	70.02
20	3.4	122.0	
30	4.7	98.9	
40	5.2	76.1	
50	5.4	62.7	69.66
5-second averages:	4.4	108.3	69.66

FLIGHT CONDITIONS: V_c = 83.7 knots C_L = 0.825 W = 6088 lb

TABLE A56.- CONDITIONS FOR FLIGHT 58, Run 1.5

Date: 9-3-81
Time: 10:22:44.2 GMT

Dispenser location: 15 percent semispan
Particle diameter: 300 to 355 μm

AIRPLANE CONFIGURATION: Basic

RADAR/LASER DATA:	Row -1	Row 0	Row 1
z, ft	12	12	12
I, ft	3.0	2.6	2.6

Crossing angle: 0.26°
Airplane heading: 212°

METEOROLOGICAL DATA:

Relative humidity:

h, ft	Wind speed, knots	Wind direction, deg	Temperature, °F
10	3.8	50.8	69.75
20	4.6	59.4	
30	5.3	64.0	
40	5.3	54.1	
50	4.9	78.1	69.13
5-second averages:	5.5	60.3	69.13

FLIGHT CONDITIONS: V_c = 119.1 knots C_L = 0.403 W = 6016 lb

TABLE A57.- CONDITIONS FOR FLIGHT 58, Run 1.8

Date: 9-3-81
Time: 10:49:59.0 GMT

Dispenser location: 15 percent semispan
Particle diameter: 300 to 355 μm

AIRPLANE CONFIGURATION: Basic

RADAR/LASER DATA:	Row -1	Row 0	Row 1
z, ft	15	15	16
I, ft	1.0	-0.3	-1.3

Crossing angle: 1.29°
Airplane heading: 211°

METEOROLOGICAL DATA:

Relative humidity:

h, ft	Wind speed, knots	Wind direction, deg	Temperature, °F
10	3.4	335.1	67.89
20	3.6	336.4	
30	3.7	330.4	
40	3.7	335.8	
50	3.7	333.5	67.89
5-second averages:	3.2	358.3	67.91

FLIGHT CONDITIONS: V_c = 121.7 knots C_L = 0.379 W = 5902 lb

TABLE A58.- CONDITIONS FOR FLIGHT 58, Run 2.0

Date: 9-3-81
Time: 11:02:58.1 GMT

Dispenser location: 15 percent semispan
Particle diameter: 300 to 355 μm

AIRPLANE CONFIGURATION: Basic

RADAR/LASER DATA:	Row -1	Row 0	Row 1
z, ft	8	11	11
I, ft	3.9	5.6	6.9

Crossing angle: -1.72°
Airplane heading: 214°

METEOROLOGICAL DATA:

Relative humidity:

h, ft	Wind speed, knots	Wind direction, deg	Temperature, °F
10	3.0	325.6	66.61
20	3.7	328.0	
30	4.2	335.6	
40	4.4	337.4	
50	4.6	350.5	66.15
5-second averages:	4.42	344.17	66.16

FLIGHT CONDITIONS: V_c = 89.2 knots C_L = 0.702 W = 5878 lb

TABLE A59.- CONDITIONS FOR FLIGHT 58, Run 2.9

Date: 9-3-81
Time: 11:27:17.30 GMT

Dispenser location: 15 percent semispan
Particle diameter: 300 to 355 μm

AIRPLANE CONFIGURATION: Basic

RADAR/LASER DATA:	Row -1	Row 0	Row 1
z, ft	8	9	9
I, ft	2.6	2.6	2.6

Crossing angle: -0.38°
Airplane heading: 212°

METEOROLOGICAL DATA:

Relative humidity:

h, ft	Wind speed, knots	Wind direction, deg	Temperature, °F
10	4.0	343.9	66.58
20	4.0	343.8	
30	4.0	343.4	
40	4.3	346.7	
50	4.3	353.3	66.13
5-second averages:	4.7	352.1	66.13

FLIGHT CONDITIONS: V_c = 85.1 knots C_L = 0.760 W = 5800 lb

TABLE A60.- CONDITIONS FOR FLIGHT 59, Run 1.3

Date: 9-10-81
Time: 11:44:16.5 GMT

Dispenser location: 70 percent semispan
Particle diameter: 300 to 355 μm

AIRPLANE CONFIGURATION: Basic

RADAR/LASER DATA:	Row -1	Row 0	Row 1
z, ft	13	13	13
I, ft	-0.3	-1.0	-1.3

Crossing angle: 0.61°
Airplane heading: 212°

METEOROLOGICAL DATA:

Relative humidity:

h, ft	Wind speed, knots	Wind direction, deg	Temperature, °F
10	3.3	345.4	58.89
20	3.1	3.8	
30	3.6	1.8	
40	3.8	4.6	
50	4.2	5.5	57.45
5-second averages:	3.6	6.4	57.42

FLIGHT CONDITIONS: V_c = 119.8 knots C_L = 0.409 W = 6176 lb

TABLE A61.- CONDITIONS FOR FLIGHT 59, Run 2.0

Date: 9-10-81
Time: 11:58:10.4 GMT

Dispenser location: 70 percent semispan
Particle diameter: 300 to 355 μm

AIRPLANE CONFIGURATION: Basic

RADAR/LASER DATA:

	Row -1	Row 0	Row 1
z, ft	9	9	9
I, ft	1.0	2.0	3.0

Crossing angle: 1.24°
Airplane heading: 211°

METEOROLOGICAL DATA:

Relative humidity:

h, ft	Wind speed, knots	Wind direction, deg	Temperature, °F
10	3.6	5.2	61.41
20	3.8	11.0	
30	3.8	17.2	
40	3.7	14.3	
50	3.8	24.2	60.49
5-second averages:	4.3	18.9	60.49

FLIGHT CONDITIONS: V_c = 87.3 knots C_L = 0.746 W = 5982 lb

TABLE A62.- CONDITIONS FOR FLIGHT 59, Run 2.1

Date: 9-10-81
Time: 12:11:44.3 GMT

Dispenser location: 70 percent semispan
Particle diameter: 300 to 355 μm

AIRPLANE CONFIGURATION: Basic

RADAR/LASER DATA:

	Row -1	Row 0	Row 1
z, ft	10	10	10
I, ft	-2.0	-3.3	-4.6

Crossing angle: 1.43°
Airplane heading: 211°

METEOROLOGICAL DATA:

Relative humidity:

h, ft	Wind speed, knots	Wind direction, deg	Temperature, °F
10	2.9	334.0	62.96
20	2.9	353.0	
30	3.4	0.1	
40	3.8	358.9	
50	3.7	353.9	62.24
5-second averages:	3.2	2.0	62.22

FLIGHT CONDITIONS: V_c = 88.2 knots C_L = 0.747 W = 6117 lb

TABLE A63.- CONDITIONS FOR FLIGHT 59, Run 3.2

Date: 9-10-81
Time: 13:23:44.3 GMT

Dispenser location: 60 percent semispan
Particle diameter: 300 to 355 μm

AIRPLANE CONFIGURATION: Basic

RADAR/LASER DATA:	Row -1	Row 0	Row 1
z, ft	12	12	12
I, ft	-7.6	-8.5	-9.5

Crossing angle: 1.20°
Airplane heading: 211°

METEOROLOGICAL DATA:

Relative humidity:

h, ft	Wind speed, knots	Wind direction, deg	Temperature, °F
10	2.5	346.2	69.39
20	2.8	335.0	
30	2.8	346.9	
40	2.7	347.7	
50	3.8	334.9	69.46
5-second averages:	3.2	329.2	69.44

FLIGHT CONDITIONS: V_c = 116.4 knots C_L = 0.416 W = 5929 lb

TABLE A64.- CONDITIONS FOR FLIGHT 59, Run 3.7

Date: 9-10-81
Time: 13:44:51.8 GMT

Dispenser location: 60 percent semispan
Particle diameter: 300 to 355 μm

AIRPLANE CONFIGURATION: Basic

RADAR/LASER DATA:	Row -1	Row 0	Row 1
z, ft	14	14	14
I, ft	2.3	1.3	0.3

Crossing angle: 1.15°
Airplane heading: 211°

METEOROLOGICAL DATA:

Relative humidity:

h, ft	Wind speed, knots	Wind direction, deg	Temperature, °F
10	2.9	1.3	71.1
20	3.0	353.4	
30	2.9	348.0	
40	2.1	347.3	
50	3.0	344.0	70.50
5-second averages:	3.2	340.2	70.50

FLIGHT CONDITIONS: V_c = 110.5 knots C_L = 0.482 W = 6206 lb

TABLE A65.- CONDITIONS FOR FLIGHT 59, Run 4.0

Date: 9-10-81
Time: 14:01:01 GMT

Dispenser location: 60 percent semispan
Particle diameter: 300 to 355 μm

AIRPLANE CONFIGURATION: Basic

RADAR/LASER DATA:	Row -1	Row 0	Row 1
z, ft	12	12	12
I, ft	0.3	1.0	2.0

Crossing angle: 1.04°
Airplane heading: 211°

METEOROLOGICAL DATA:

Relative humidity:

h, ft	Wind speed, knots	Wind direction, deg	Temperature, °F
10	3.5	29.9	72.68
20	3.5	18.4	
30	3.4	18.7	
40	2.7	15.7	
50	3.4	15.8	72.34
5-second averages:	3.4	15.8	72.36

FLIGHT CONDITIONS: V_c = 82.2 knots C_L = 0.867 W = 6173 lb

TABLE A66.- CONDITIONS FOR FLIGHT 59, Run 4.1

Date: 9-10-81
Time: 14:19:4.2 GMT

Dispenser location: 60 percent semispan
Particle diameter: 300 to 355 μm

AIRPLANE CONFIGURATION: Basic

RADAR/LASER DATA:	Row -1	Row 0	Row 1
z, ft	7	11	11
I, ft	2.3	3.3	4.6

Crossing angle: 1.33°
Airplane heading: 211°

METEOROLOGICAL DATA:

Relative humidity:

h, ft	Wind speed, knots	Wind direction, deg	Temperature, °F
10	3.6	355.4	73.98
20	3.5	343.0	
30	3.4	352.8	
40	2.4	353.8	
50	3.4	338.5	73.58
5-second averages:	3.3	338.0	73.62

FLIGHT CONDITIONS: V_c = 79.1 knots C_L = 0.934 W = 6147 lb

TABLE A67.- CONDITIONS FOR FLIGHT 60, Run 1.6

Date: 9-11-81
Time: 10:30:56.20 GMT

Dispenser location: 40 percent semispan
Particle diameter: 300 to 355 μm

AIRPLANE CONFIGURATION: Basic

RADAR/LASER DATA:

	Row -1	Row 0	Row 1
z, ft	11	11	11
I, ft	0.7	-0.3	-1.6

Crossing angle: 1.27°
Airplane heading: 211°

METEOROLOGICAL DATA:

Relative humidity:

h, ft	Wind speed, knots	Wind direction, deg	Temperature, °F
10	3.0	247.2	62.65
20	3.4	240.4	
30	4.3	253.7	
40	4.4	247.8	
50	4.7	249.1	61.72
5-second averages:	4.5	254.1	61.71

FLIGHT CONDITIONS: V_c = 113.5 knots C_L = 0.454   W = 6150 lb

TABLE A68.- CONDITIONS FOR FLIGHT 60, Run 2.1

Date: 9-11-81
Time: 10:56:51.9 GMT

Dispenser location: 40 percent semispan
Particle diameter: 300 to 355 μm

AIRPLANE CONFIGURATION: Basic

RADAR/LASER DATA:

	Row -1	Row 0	Row 1
z, ft	8	8	8
I, ft	1.0	0	0.7

Crossing angle: 0.88°
Airplane heading: 211°

METEOROLOGICAL DATA:

Relative humidity:

h, ft	Wind speed, knots	Wind direction, deg	Temperature, °F
10	2.2	277.0	62.18
20	2.8	272.4	
30	2.5	275.4	
40	2.1	272.8	
50	2.8	266.9	61.12
5-second averages:	3.0	274.2	61.14

FLIGHT CONDITIONS: V_c = 80.5 knots C_L = 0.892   W = 6094 lb

TABLE A69.- CONDITIONS FOR FLIGHT 67, Run 1.1

Date: 12-4-81
Time: 13:02:32.3 GMT

Dispenser location: 70 percent semispan
Particle diameter: 300 to 355 μm

AIRPLANE CONFIGURATION: Winglets on

RADAR/LASER DATA:

	Row -1	Row 0	Row 1
z, ft	14	14	14
I, ft	7.5	7.5	7.5

Crossing angle: 0.44°
Airplane heading: 212°

METEOROLOGICAL DATA:

Relative humidity:

h, ft	Wind speed, knots	Wind direction, deg	Temperature, °F
10	2.9	164.2	45.2
20	3.3	151.4	
30	3.4	178.1	
40	4.0	171.2	
50	4.1	160.6	45.0
5-second averages:	4.6	175.4	45.0

FLIGHT CONDITIONS: V_c = 118.9 knots C_L = 0.434 W = 6414 lb

TABLE A70.- CONDITIONS FOR FLIGHT 67, Run 2.1

Date: 12-4-81
Time: 13:47:31.3 GMT

Dispenser location: 70 percent semispan
Particle diameter: 300 to 355 μm

AIRPLANE CONFIGURATION: Winglets on

RADAR/LASER DATA:

	Row -1	Row 0	Row 1
z, ft	12	12	12
I, ft	3.9	3.9	3.6

Crossing angle: 0.38°
Airplane heading: 212°

METEOROLOGICAL DATA:

Relative humidity:

h, ft	Wind speed, knots	Wind direction, deg	Temperature, °F
10	3.3	188.5	49.7
20	3.5	164.4	
30	4.3	160.8	
40	5.0	159.4	
50	5.3	158.9	49.0
5-second averages:	6.1	161.2	49.0

FLIGHT CONDITIONS: V_c = 81.9 knots C_L = 0.904 W = 6342 lb

TABLE A71.- CONDITIONS FOR FLIGHT 74, Run 1.0

Date: 2-8-82
Time: 23:29:03.8 GMT

Dispenser location: 80 percent semispan
Particle diameter: 300 to 355 μm

AIRPLANE CONFIGURATION: Winglets on

RADAR/LASER DATA:

	Row -1	Row 0	Row 1
z, ft	14	14	14
I, ft	3.3	2.6	2.0

Crossing angle: 0.73°
Airplane heading: 211°

METEOROLOGICAL DATA:

Relative humidity:

h, ft	Wind speed, knots	Wind direction, deg	Temperature, °F
10	3.3	204.1	31.9
20	3.5	204.8	
30	3.8	202.8	
40	3.5	201.0	
50	3.6	196.2	29.7

5-second averages:

FLIGHT CONDITIONS: V_c = 121.0 knots C_L = 0.422 W = 6447 lb

TABLE A72.- CONDITIONS FOR FLIGHT 74, Run 2.4

Date: 2-8-82
Time: 01:38:22.1 GMT

Dispenser location: 80 percent semispan
Particle diameter: 300 to 355 μm

AIRPLANE CONFIGURATION: Winglets on

RADAR/LASER DATA:

	Row -1	Row 0	Row 1
z, ft	13	13	13
I, ft			

Crossing angle: 0.17°
Airplane heading: 212°

METEOROLOGICAL DATA:

Relative humidity:

h, ft	Wind speed, knots	Wind direction, deg	Temperature, °F
10	2.2	223.7	33.2
20	2.5	220.8	
30	2.7	213.6	
40	2.9	207.9	
50	2.8	204.0	27.7
5-second averages:	2.9	204.2	27.7

FLIGHT CONDITIONS: V_c = 81.6 knots C_L = 0.895 W = 6216 lb

TABLE A73.- CONDITIONS FOR FLIGHT 74, Run 3.2

Date: 2-8-82
Time: 03:22:51.3 GMT

Dispenser location: 85 percent semispan
Particle diameter: 300 to 355 μm

AIRPLANE CONFIGURATION: Winglets on

RADAR/LASER DATA:

	Row -1	Row 0	Row 1
z, ft	16	16	16
I, ft	4.3	3.6	2.6

Crossing angle: 0.90°
Airplane heading: 211°

METEOROLOGICAL DATA:

Relative humidity:

h, ft	Wind speed, knots	Wind direction, deg	Temperature, °F
10	2.0	170.8	35.7
20	1.2	140.8	
30	2.0	152.3	
40	2.0	137.5	
50	2.1	148.0	35.9
5-second averages:	2.3	140.6	35.9

FLIGHT CONDITIONS: V_c = 118.9 knots C_L = 0.434 W = 6414 lb

TABLE A74.- CONDITIONS FOR FLIGHT 74, Run 4.0

Date: 2-8-82
Time: 03:43:55.6 GMT

Dispenser location: 85 percent semispan
Particle diameter: 300 to 355 μm

AIRPLANE CONFIGURATION: Winglets on

RADAR/LASER DATA:

	Row -1	Row 0	Row 1
z, ft	12	12	12
I, ft	-1.0	-1.6	-2.0

Crossing angle: 0.57°
Airplane heading: 212°

METEOROLOGICAL DATA:

Relative humidity:

h, ft	Wind speed, knots	Wind direction, deg	Temperature, °F
10	2.0	178.5	35.5
20	2.3	164.8	
30	2.7	170.5	
40	2.7	165.3	
50	3.0	160.4	35.8
5-second averages:	3.3	164.5	35.8

FLIGHT CONDITIONS: V_c = 83.8 knots C_L = 0.871 W = 6378 lb

TABLE A75.- CONDITIONS FOR FLIGHT 76, Run 1.0

Date: 2-26-82
Time: 05:07:15.8 GMT

Dispenser location: 95 percent semispan
Particle diameter: 300 to 355 µm

AIRPLANE CONFIGURATION: Winglets on

RADAR/LASER DATA:

	Row -1	Row 0	Row 1
z, ft	13	13	13
I, ft	4.3	3.6	2.6

Crossing angle: 0.97°
Airplane heading: 211°

METEOROLOGICAL DATA:

Relative humidity:

h, ft	Wind speed, knots	Wind direction, deg	Temperature, °F
10	3.3	8.9	20.3
20	3.5	357.0	
30	3.7	356.9	
40	4.2	352.7	
50	4.0	5.1	16.6
5-second averages:	3.8	349.8	16.2

FLIGHT CONDITIONS: V_c = 120.9 knots C_L = 0.424 W = 6474 lb

TABLE A76.- CONDITIONS FOR FLIGHT 76, Run 1.1

Date: 2-26-82
Time: 05:37:39.5 GMT

Dispenser location: 95 percent semispan
Particle diameter: 300 to 355 µm

AIRPLANE CONFIGURATION: Winglets on

RADAR/LASER DATA:

	Row -1	Row 0	Row 1
z, ft	15	15	15
I, ft	0	-1.0	-1.6

Crossing angle: 1.09°
Airplane heading: 211°

METEOROLOGICAL DATA:

Relative humidity:

h, ft	Wind speed, knots	Wind direction, deg	Temperature, °F
10	2.9	337.4	19.2
20	3.6	342.0	
30	3.8	349.7	
40	4.2	349.0	
50	4.4	349.0	16.0
5-second averages:	4.5	348.3	16.0

FLIGHT CONDITIONS: V_c = 119.3 knots C_L = 0.432 W = 6426 lb

TABLE A77.- CONDITIONS FOR FLIGHT 76, Run 2.0

Date: 2-26-82
Time: 06:06:57.5 GMT

Dispenser location: 95 percent semispan
Particle diameter: 300 to 355 μm

AIRPLANE CONFIGURATION: Winglets on

RADAR/LASER DATA:

	Row -1	Row 0	Row 1
z, ft	9	9	9
I, ft	5.0	4.0	3.0

Crossing angle: 0.96°
Airplane heading: 211°

METEOROLOGICAL DATA:

Relative humidity:

h, ft	Wind speed, knots	Wind direction, deg	Temperature, °F
10	3.0	313.0	18.4
20	3.1	317.4	
30	3.4	332.3	
40	3.8	332.0	
50	3.6	332.0	14.6
5-second averages:	3.8	332.7	14.6

FLIGHT CONDITIONS: V_c = 82.1 knots C_L = 0.906 W = 6378 lb

TABLE A78.- CONDITIONS FOR FLIGHT 76, Run 2.1

Date: 2-26-82
Time: 06:35:35.2 GMT

Dispenser location: 95 percent semispan
Particle diameter: 300 to 355 μm

AIRPLANE CONFIGURATION: Winglets on

RADAR/LASER DATA:

	Row -1	Row 0	Row 1
z, ft	11	10	10
I, ft	5.6	4.9	4.2

Crossing angle: 0.74°
Airplane heading: 211°

METEOROLOGICAL DATA:

Relative humidity:

h, ft	Wind speed, knots	Wind direction, deg	Temperature, °F
10	3.3	305.3	17.4
20	3.3	309.0	
30	3.4	319.7	
40	3.7	315.8	
50	4.0	319.0	14.7
5-second averages:	3.9	319.2	14.7

FLIGHT CONDITIONS: V_c = 83.7 knots C_L = 0.865 W = 6330 lb

TABLE A79.- CONDITIONS FOR FLIGHT 76, Run 3.0

Date: 2-26-82
Time: 08:32:49.1 GMT

Dispenser location: 75 percent semispan
Particle diameter: 300 to 355 μm

AIRPLANE CONFIGURATION: Winglets on

RADAR/LASER DATA:

	Row -1	Row 0	Row 1
z, ft	14	16	16
I, ft	6.8	6.6	5.9

Crossing angle: 0.57°
Airplane heading: 212°

METEOROLOGICAL DATA:

Relative humidity:

h, ft	Wind speed, knots	Wind direction, deg	Temperature, °F
10	3.3	312.0	15.4
20	3.5	309.0	
30	3.6	313.5	
40	4.3	311.1	
50	4.6	312.9	12.7
5-second averages:	4.5	312.5	12.7

FLIGHT CONDITIONS: V_c = 124.3 knots C_L = 0.401 W = 6477 lb

TABLE A80.- CONDITIONS FOR FLIGHT 76, Run 3.1

Date: 2-26-82
Time: 09:06:11.8 GMT

Dispenser location: 75 percent semispan
Particle diameter: 300 to 355 μm

AIRPLANE CONFIGURATION: Winglets on

RADAR/LASER DATA:

	Row -1	Row 0	Row 1
z, ft	16	16	16
I, ft	6.2	5.5	4.9

Crossing angle: 0.94°
Airplane heading: 211°

METEOROLOGICAL DATA:

Relative humidity:

h, ft	Wind speed, knots	Wind direction, deg	Temperature, °F
10	3.1	299.6	15.4
20	3.5	295.0	
30	3.5	305.3	
40	3.5	306.1	
50	3.8	308.6	12.8
5-second averages:	3.8	308.9	12.8

FLIGHT CONDITIONS: V_c = 121.9 knots C_L = 0.414 W = 6429 lb

TABLE A81.- CONDITIONS FOR FLIGHT 77, Run 1.5

Date: 3-9-82
Time: 06:08:50.9 GMT

Dispenser location: 75 percent semispan
Particle diameter: 300 to 355 μm

AIRPLANE CONFIGURATION: Winglets on

RADAR/LASER DATA:

	Row -1	Row 0	Row 1
z, ft	14	14	14
I, ft	8.5	7.9	7.2

Crossing angle: 0.76°
Airplane heading: 211°

METEOROLOGICAL DATA:

Relative humidity:

h, ft	Wind speed, knots	Wind direction, deg	Temperature, °F
10	6.0	140.0	15.5
20	6.4	136.5	
30	7.2	142.8	
40	6.8	144.5	
50	8.2	146.0	13.6
5-second averages:	6.9	143.2	13.6

FLIGHT CONDITIONS: V_c = 84.7 knots C_L = 0.845 W = 6324 lb

TABLE A82.- CONDITIONS FOR FLIGHT 78, Run 1.5

Date: 3-12-82
Time: 12:11:19.5 GMT

Dispenser location: 70 percent semispan
Particle diameter: 300 to 355 μm

AIRPLANE CONFIGURATION: Winglets on

RADAR/LASER DATA:

	Row -1	Row 0	Row 1
z, ft	13	13	13
I, ft	0.6	0	-0.6

Crossing angle: 0.80°
Airplane heading: 211°

METEOROLOGICAL DATA:

Relative humidity:

h, ft	Wind speed, knots	Wind direction, deg	Temperature, °F
10	5.2	217.3	48.1
20	5.9	222.8	
30	6.1	225.4	
40	5.9	229.2	
50	5.9	231.0	48.0
5-second averages:	5.9	230.3	48.0

FLIGHT CONDITIONS: V_c = 121.1 knots C_L = 0.410 W = 6288 lb

TABLE A83.- CONDITIONS FOR FLIGHT 78, Run 2.0

Date: 3-12-82
Time: 12:43:18.2 GMT

Dispenser location: 70 percent semispan
Particle diameter: 300 to 355 μm

AIRPLANE CONFIGURATION: Winglets on

RADAR/LASER DATA:

	Row -1	Row 0	Row 1
z, ft	10	9	9
I, ft	-2.3	-3.0	-3.6

Crossing angle: 0.84°
Airplane heading: 211°

METEOROLOGICAL DATA:

Relative humidity:

h, ft	Wind speed, knots	Wind direction, deg	Temperature, °F
10	3.3	237.9	52.5
20	4.2	260.0	
30	4.4	246.0	
40	4.6	242.3	
50	5.4	241.9	52.3
5-second averages:	5.5	239.3	52.3

FLIGHT CONDITIONS: V_c = 81.3 knots C_L = 0.904 W = 6240 lb

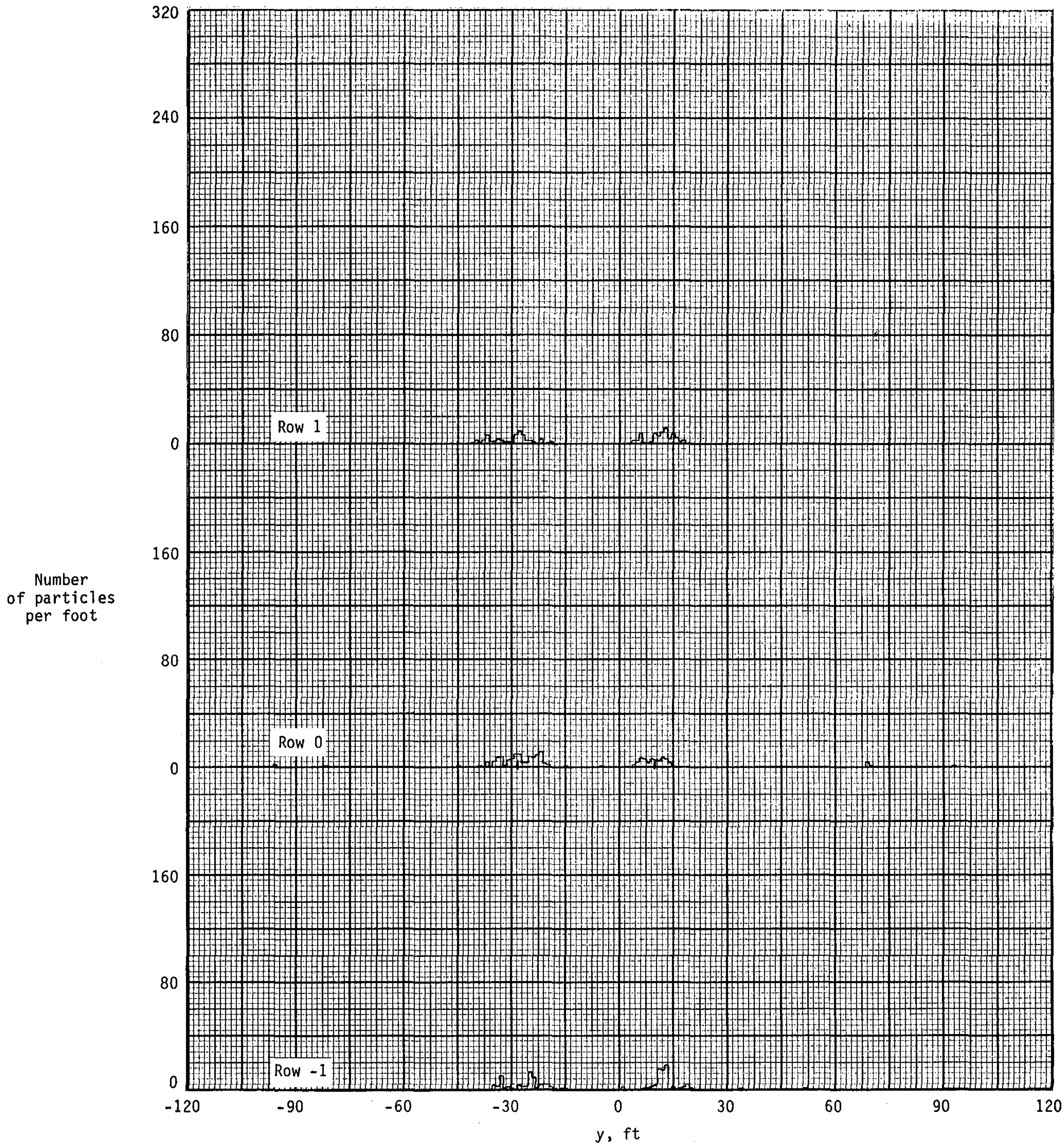

Figure A1.- Ground deposition patterns for flight 47, run 1.1.

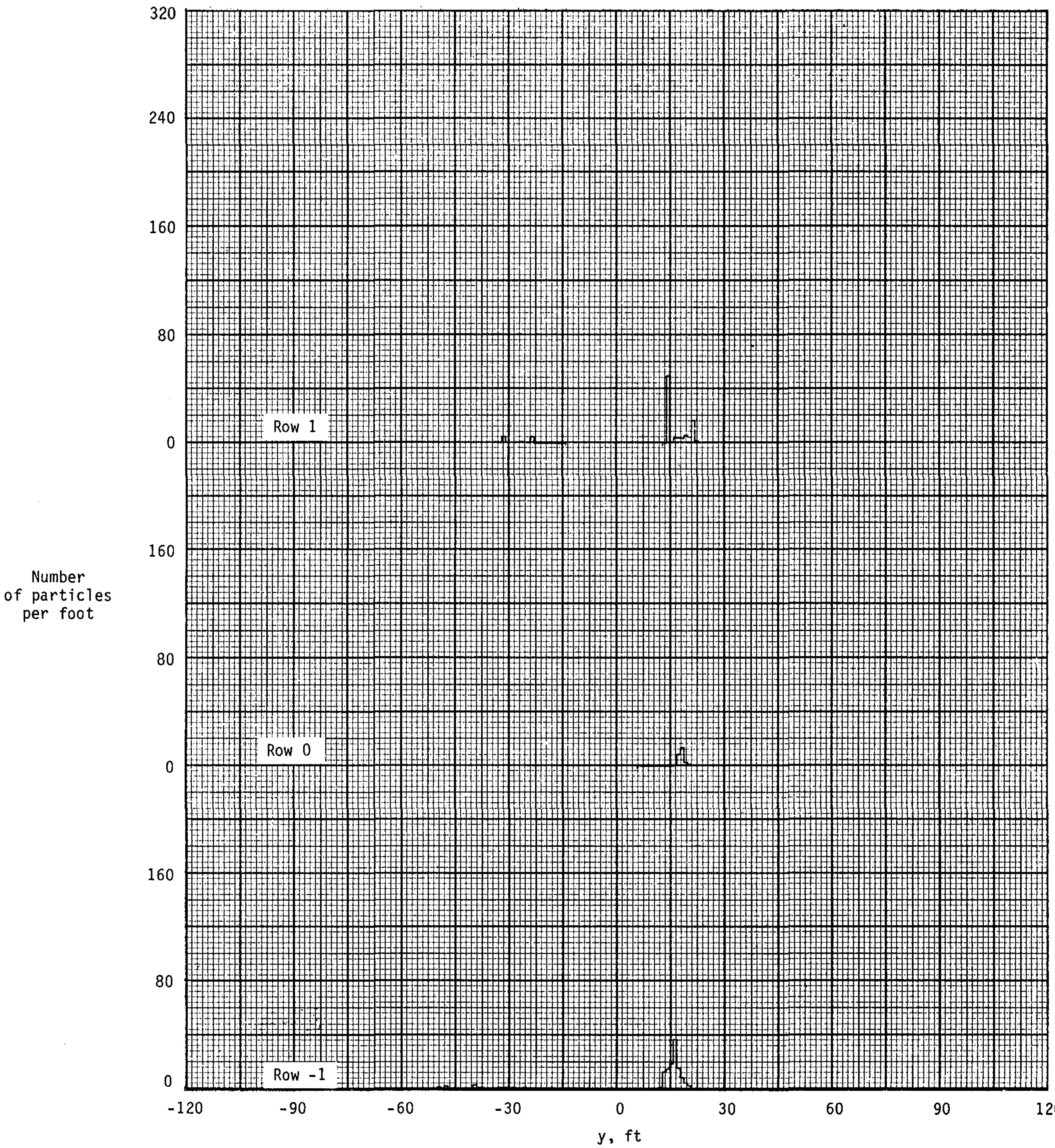

Figure A2.- Ground deposition patterns for flight 47, run 2.0.

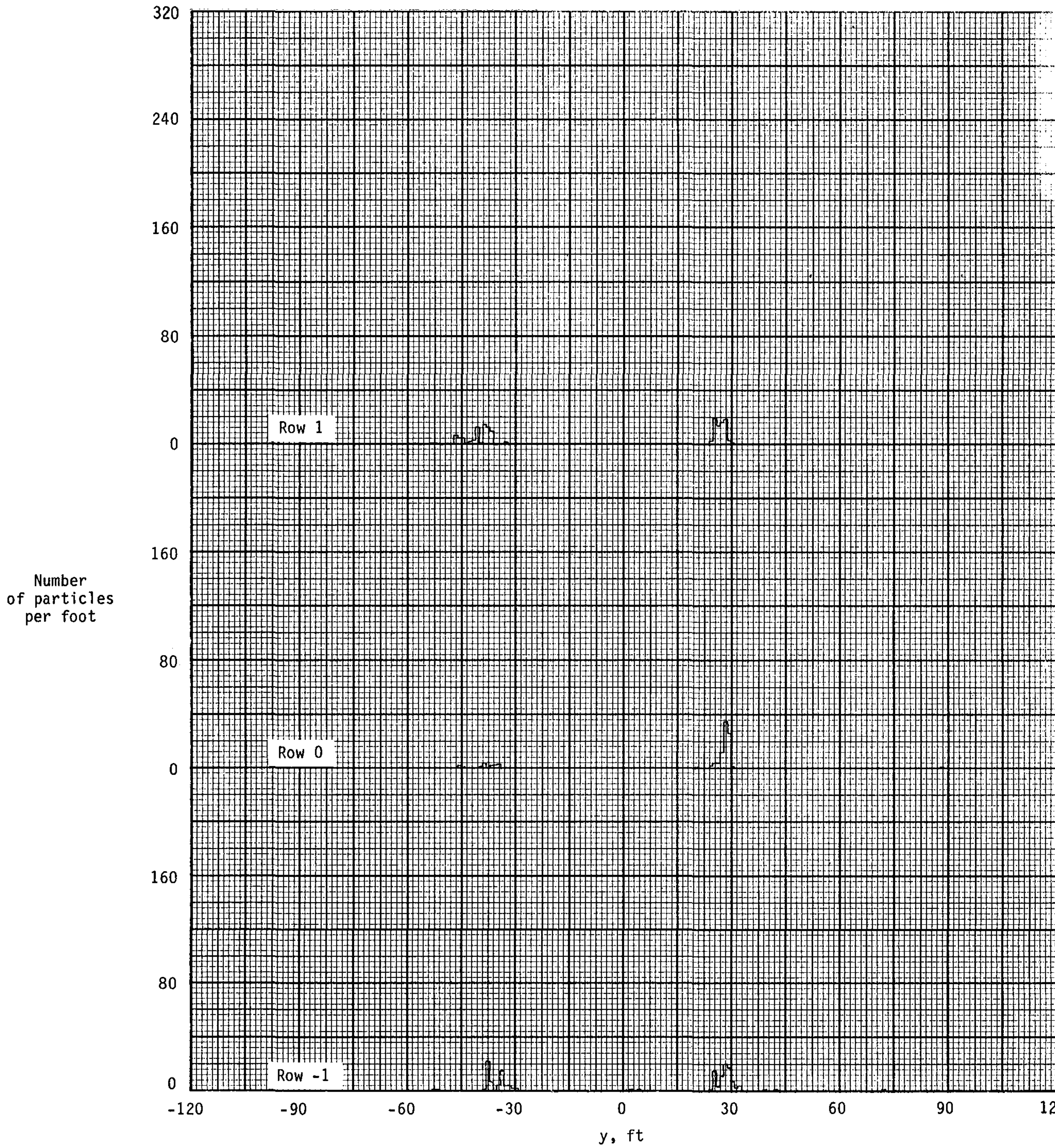

Figure A3.- Ground deposition patterns for flight 47, run 3.0.

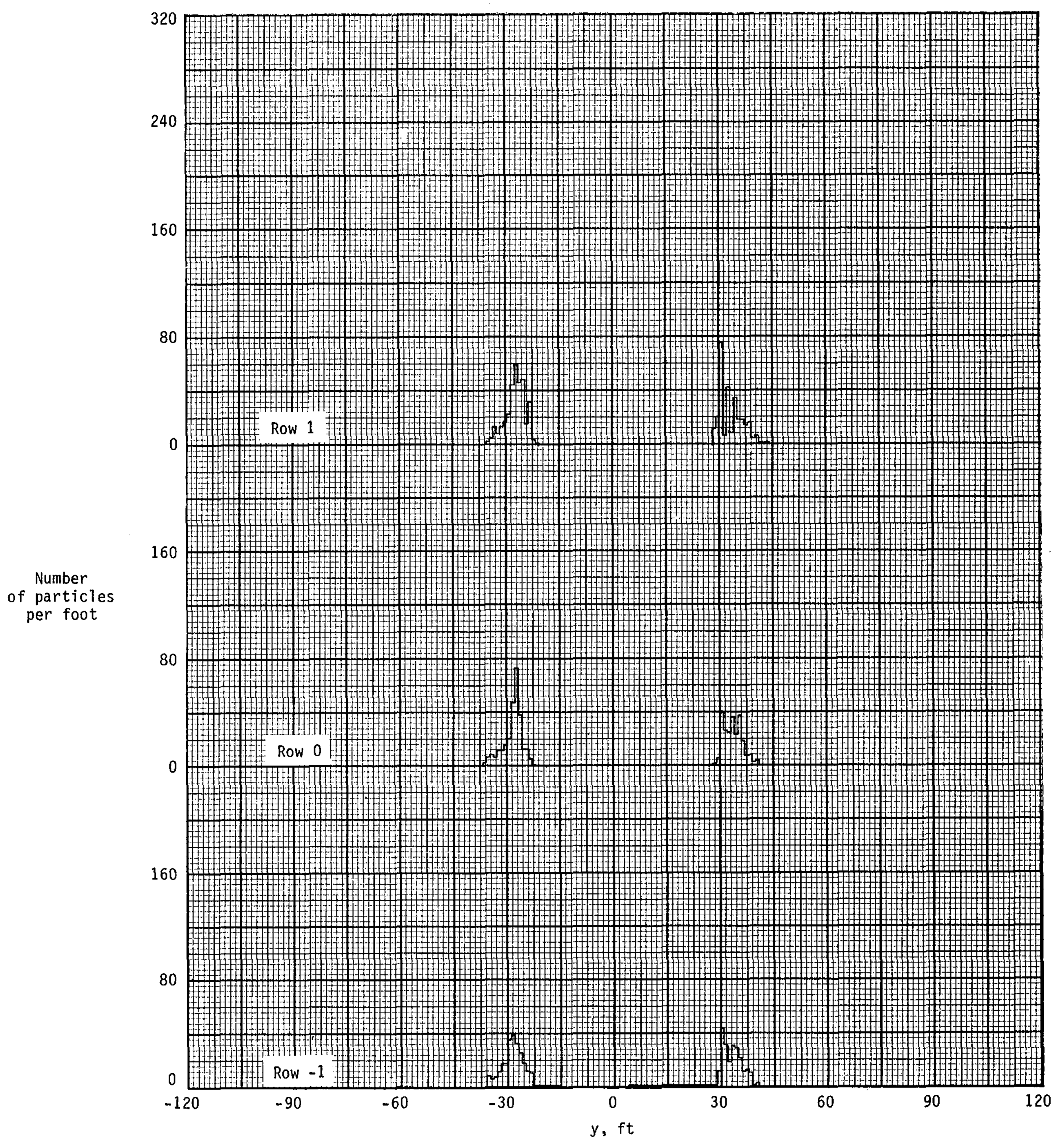

Figure A4.- Ground deposition patterns for flight 47, run 3.1.

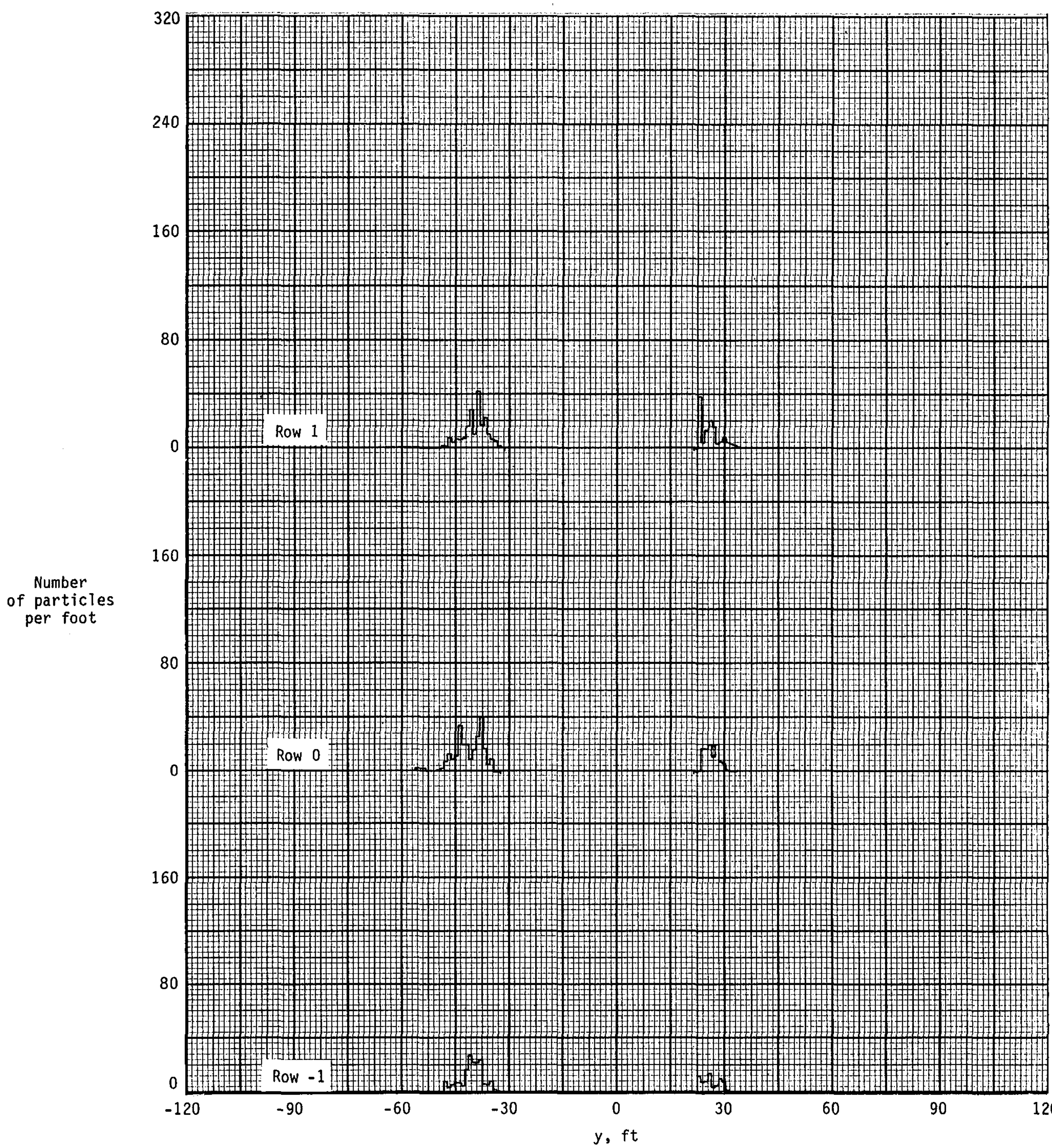

Figure A5.- Ground deposition patterns for flight 47, run 4.1.

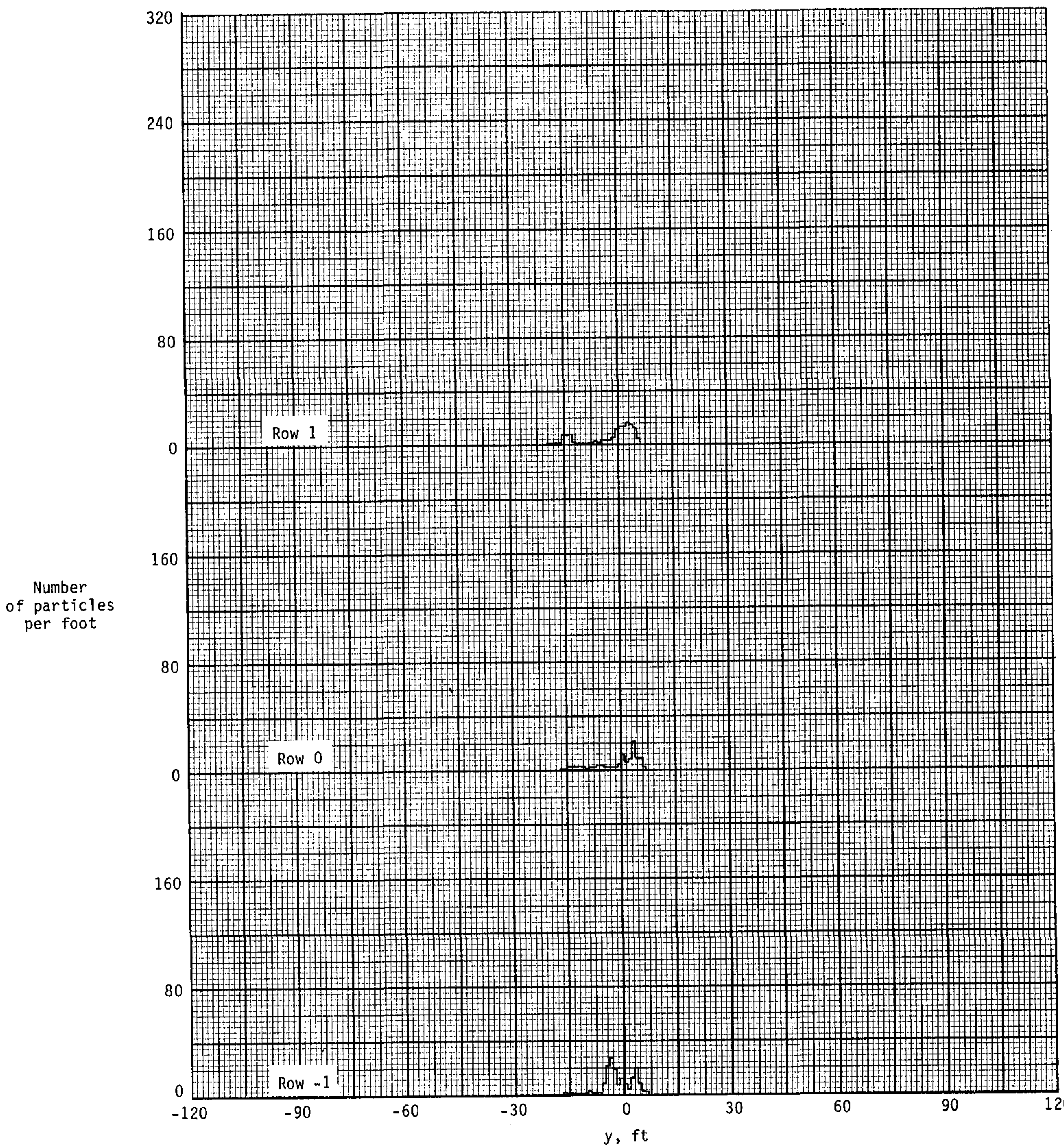

Figure A6.- Ground deposition patterns for flight 47, run 5.0.

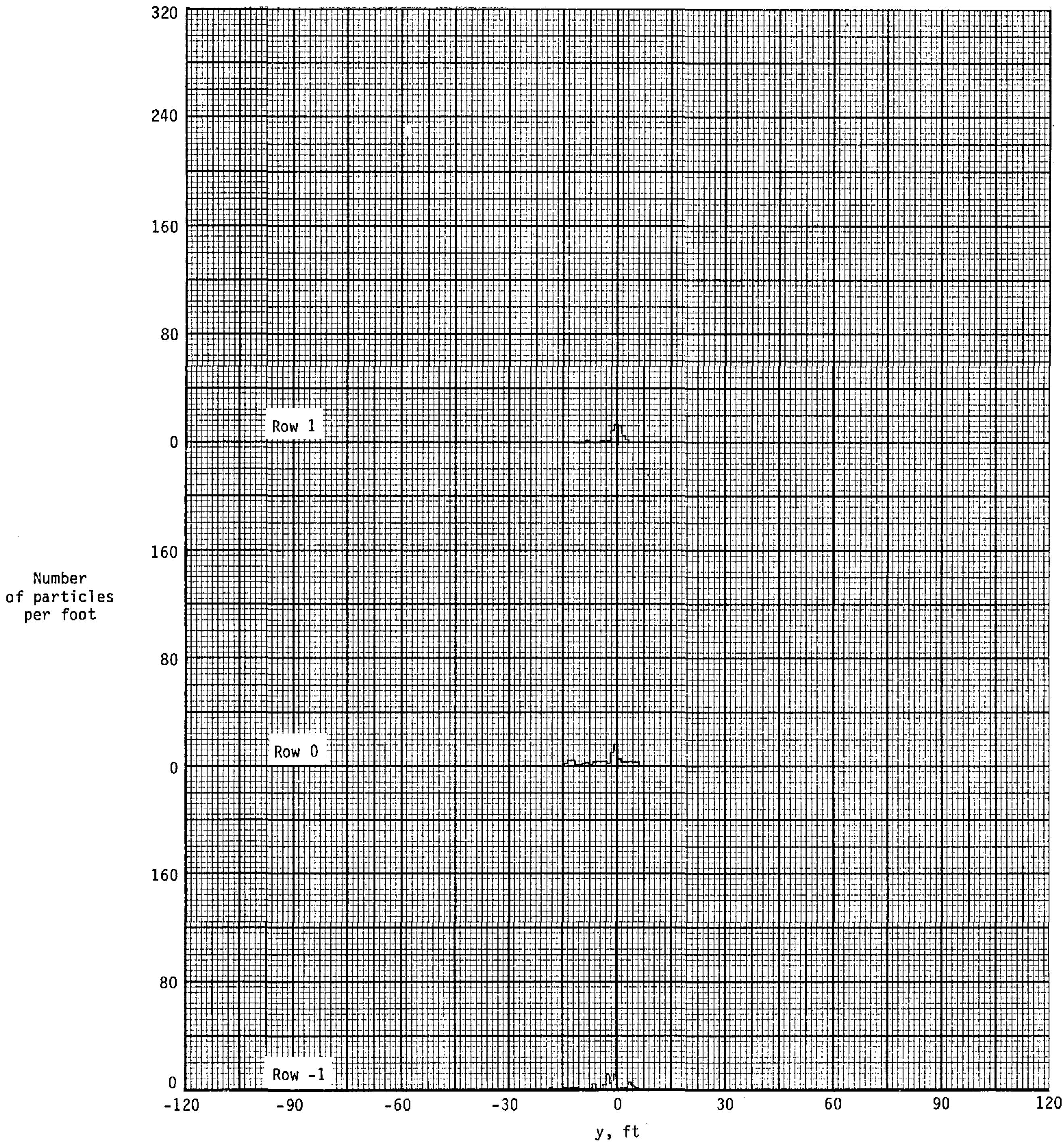

Figure A7.- Ground deposition patterns for flight 47, run 5.1.

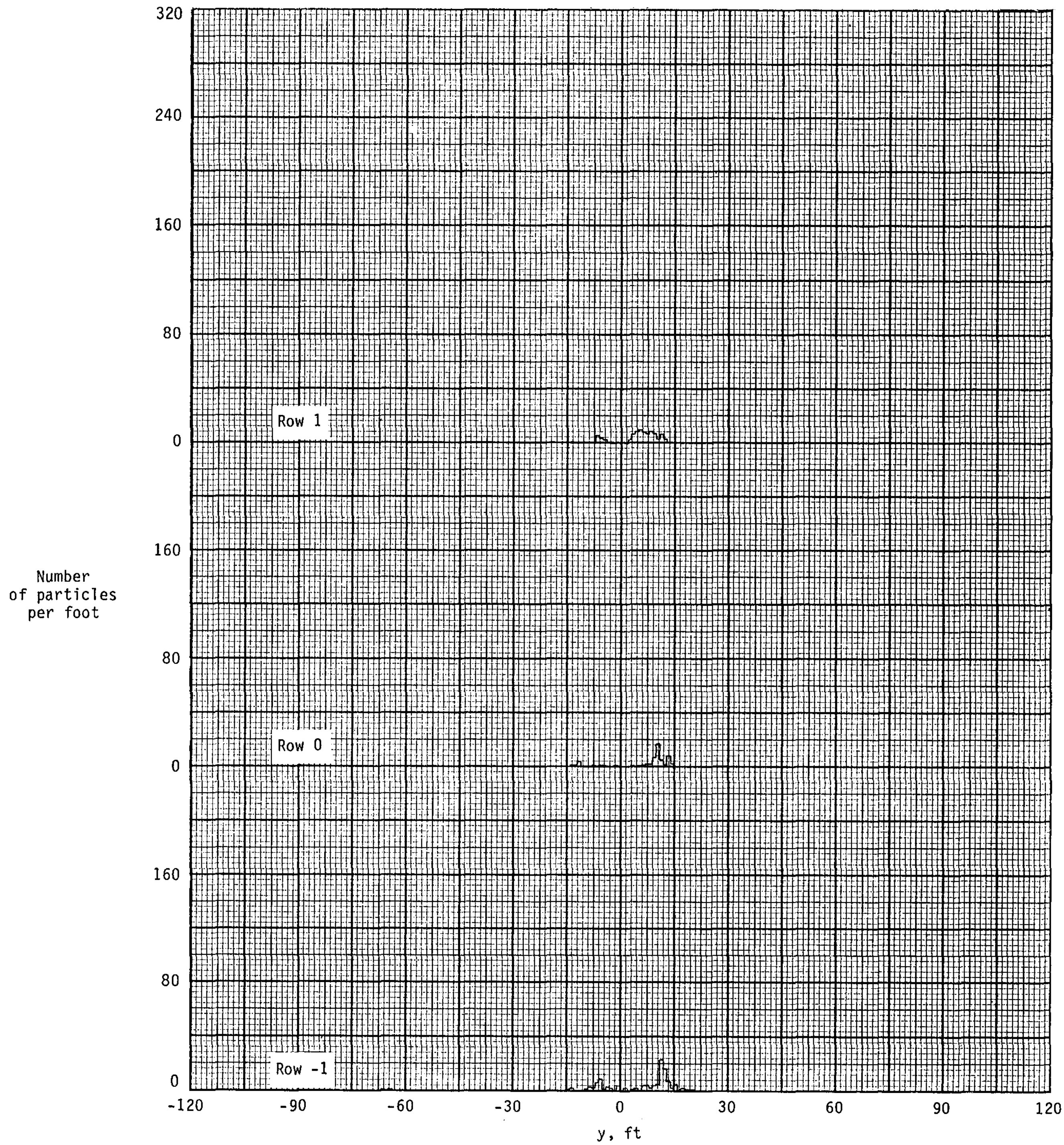

Figure A8.- Ground deposition patterns for flight 47, run 6.0.

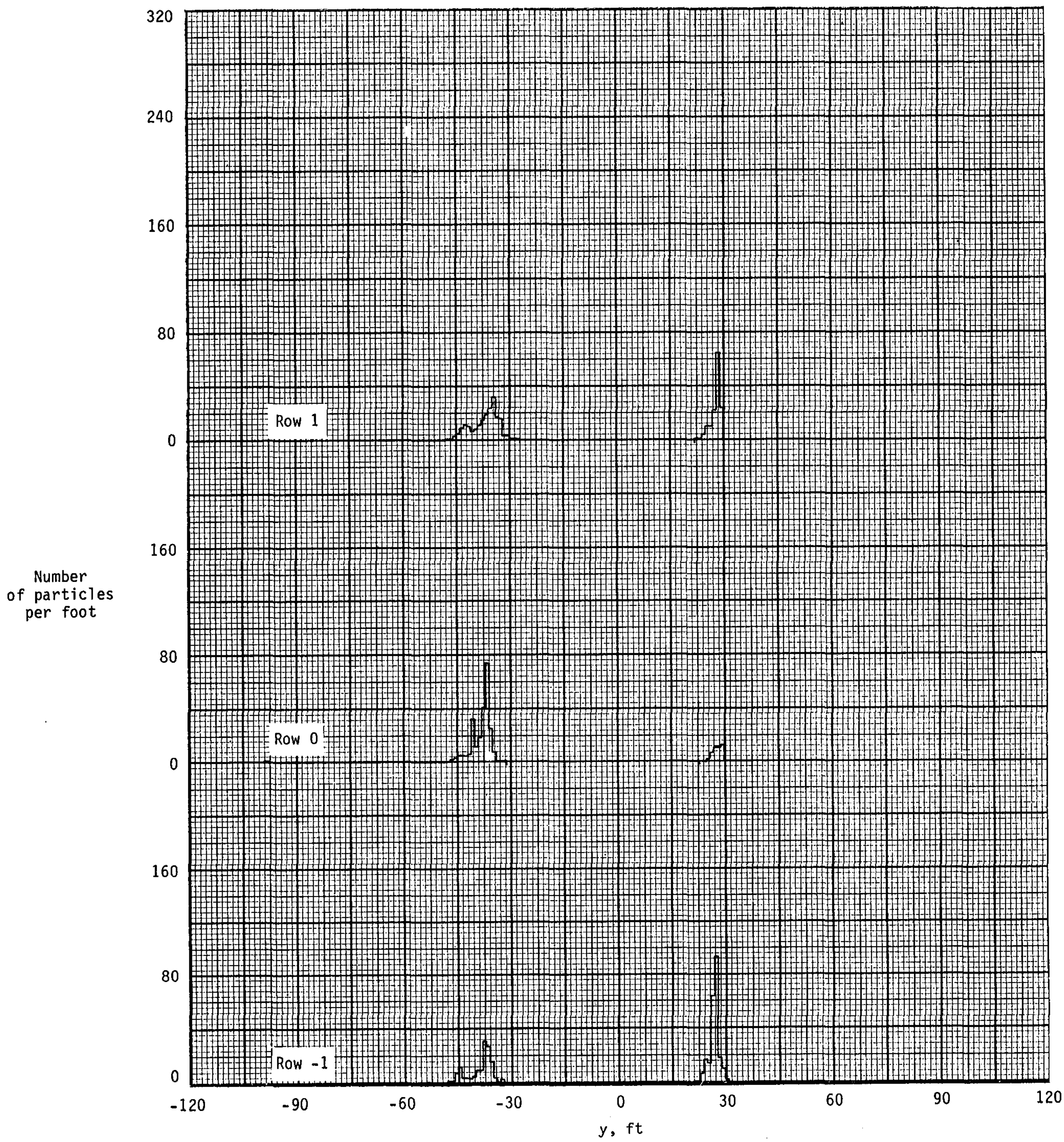

Figure A9.- Ground deposition patterns for flight 48, run 1.0.

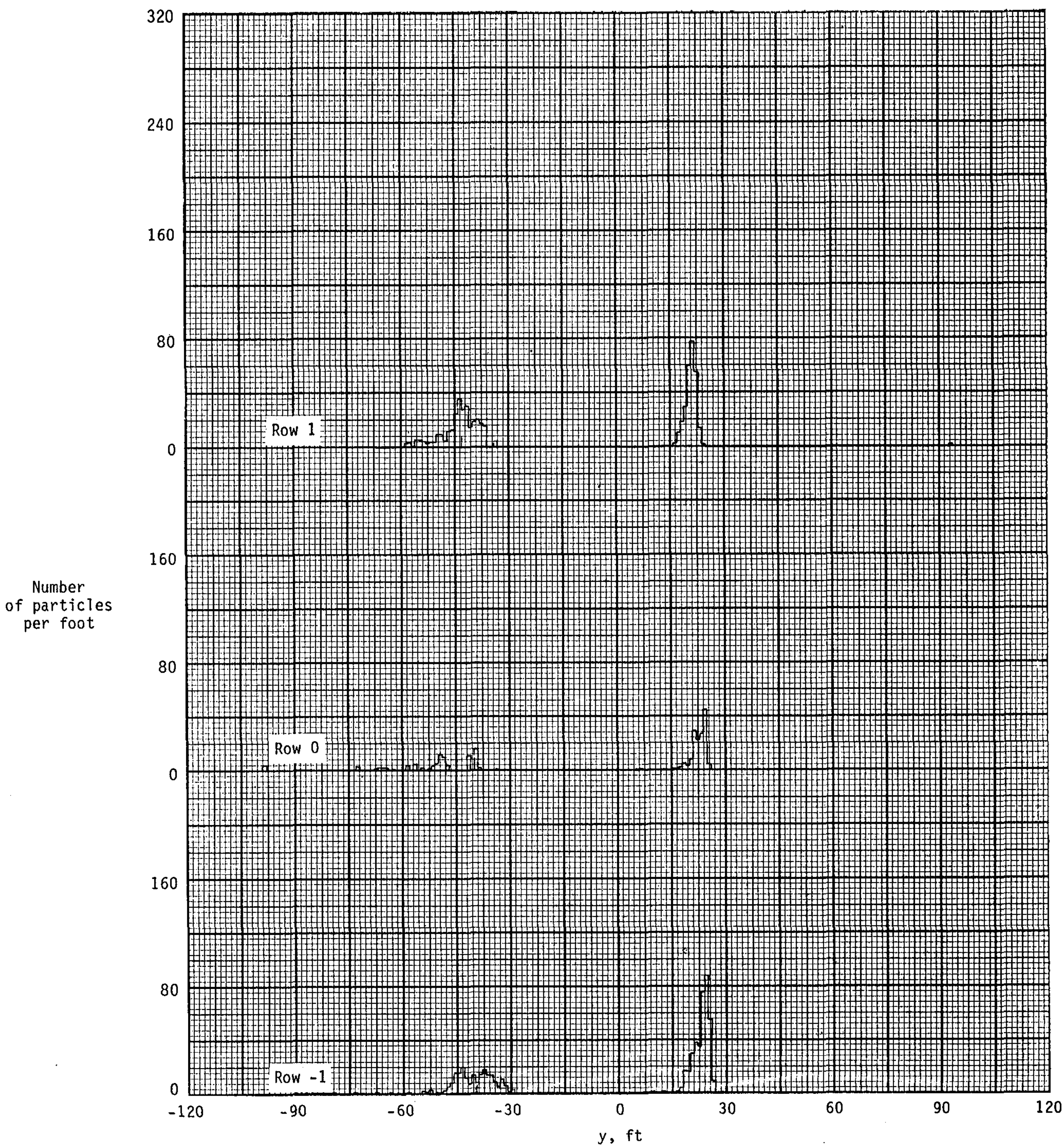

Figure A10.- Ground deposition patterns for flight 48, run 1.1.

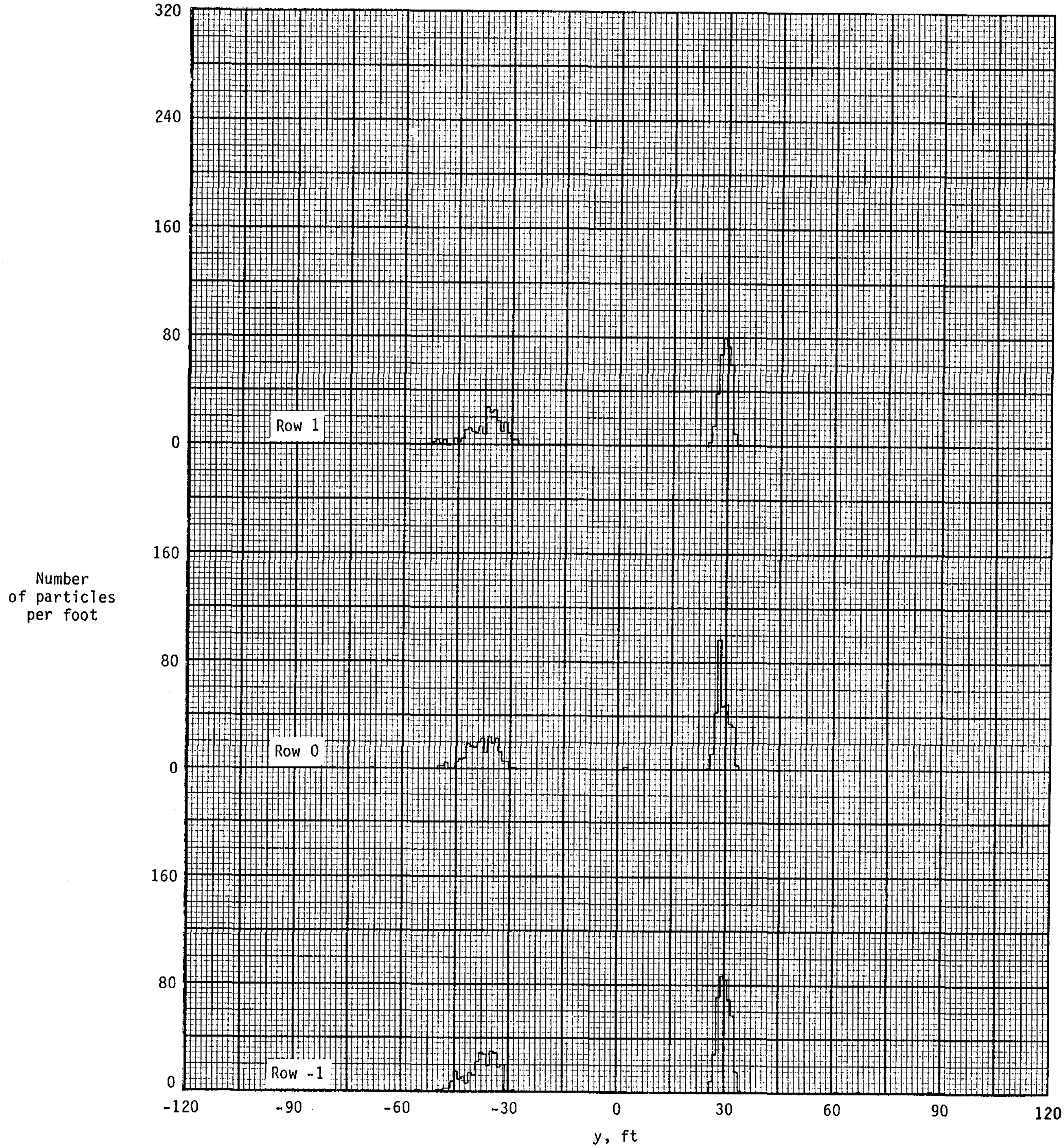

Figure A11.- Ground deposition patterns for flight 49, run 1.0.

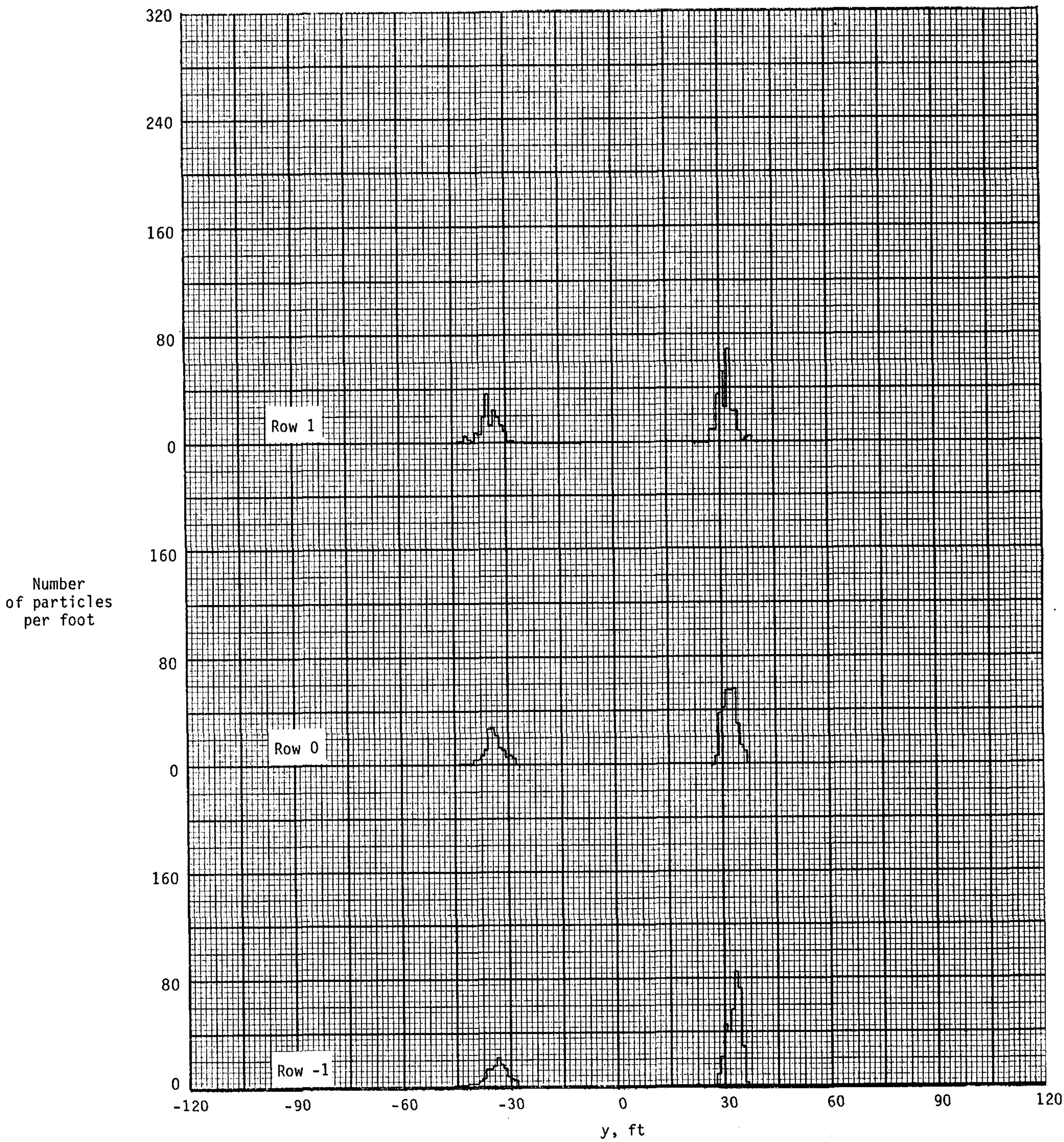

Figure A12.- Ground deposition patterns for flight 49, run 1.1.

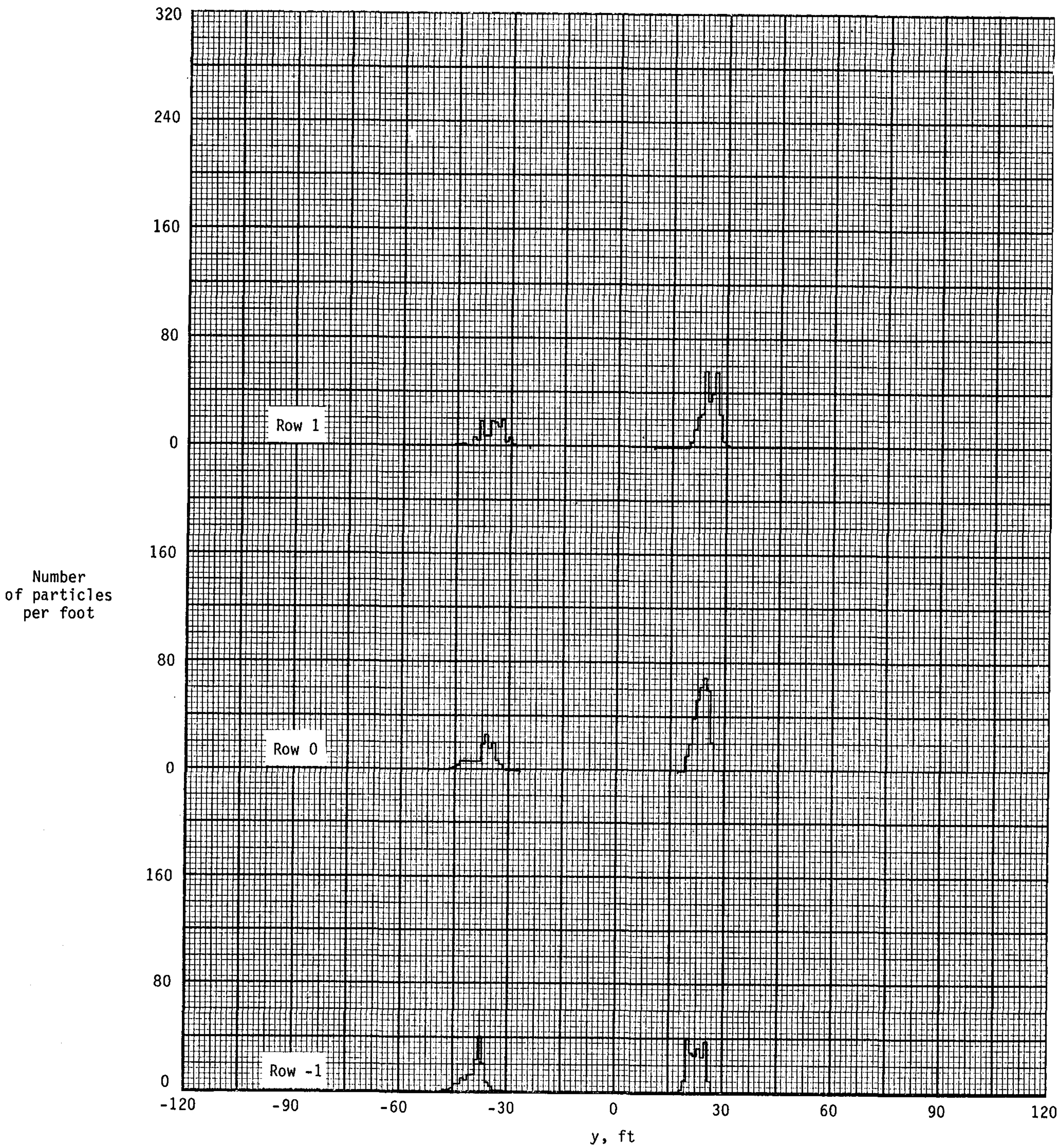

Figure A13.- Ground deposition patterns for flight 49, run 2.0.

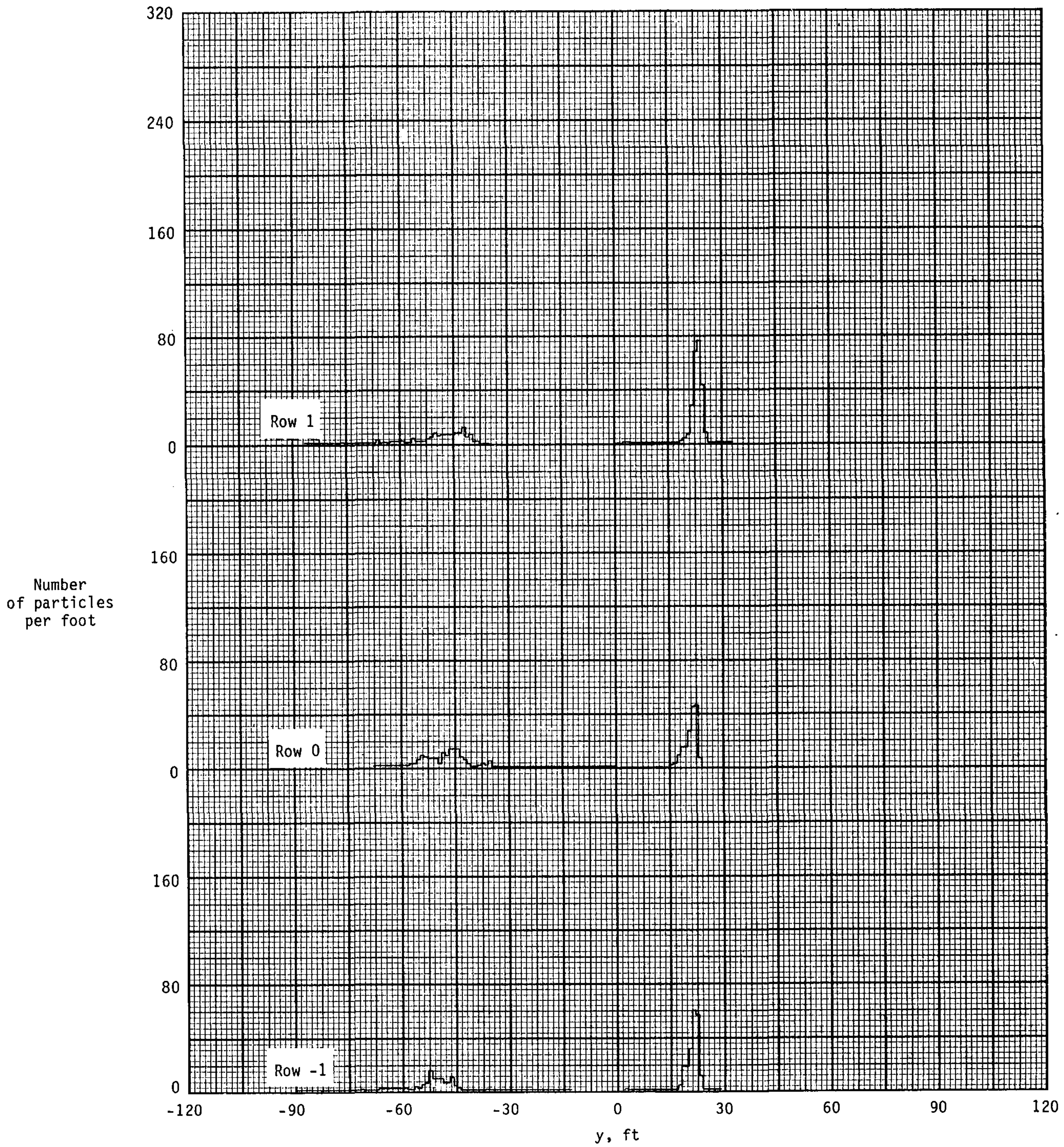

Figure A14.- Ground deposition patterns for flight 49, run 2.1.

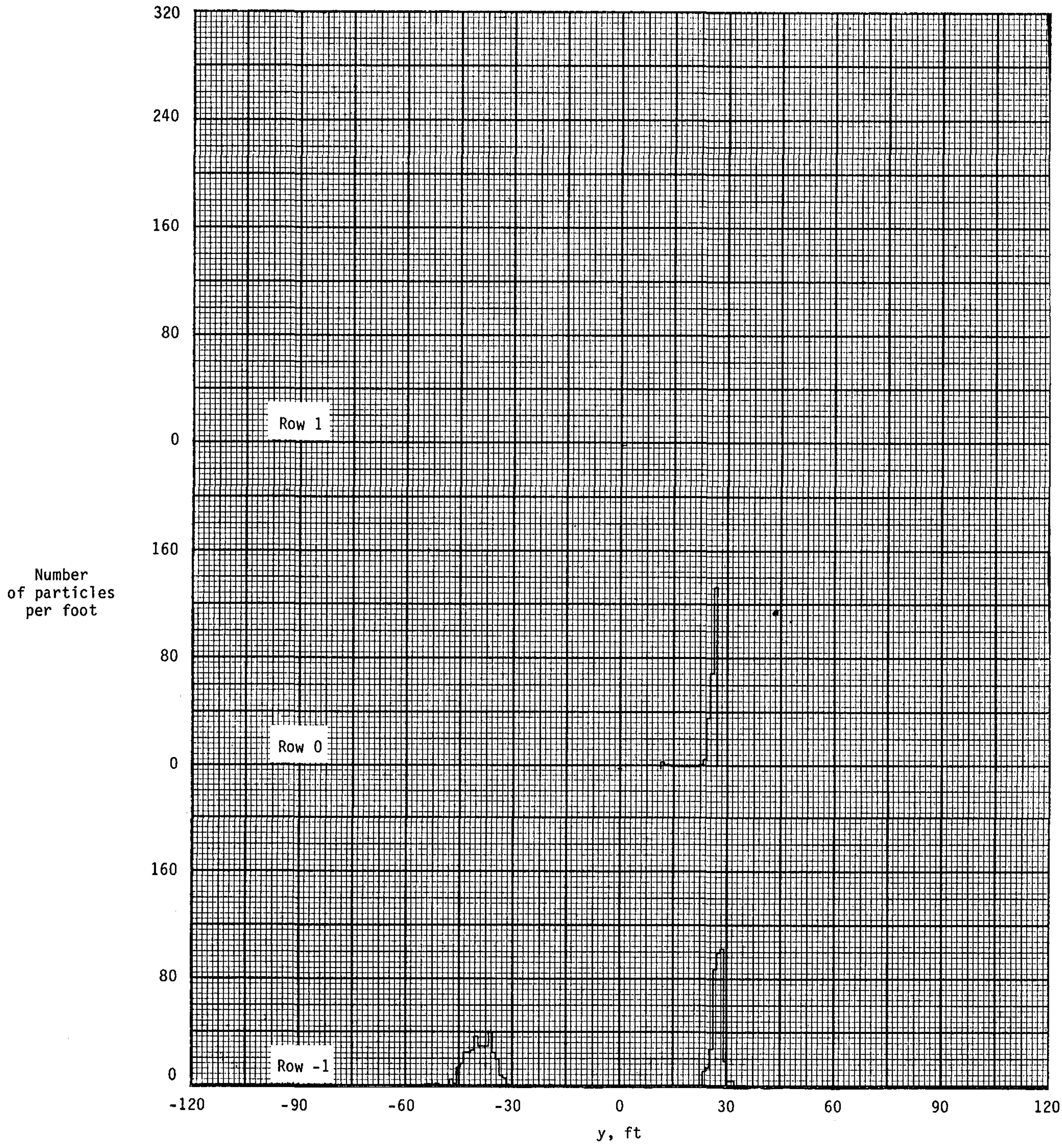

Figure A15.- Ground deposition patterns for flight 49, run 3.0.

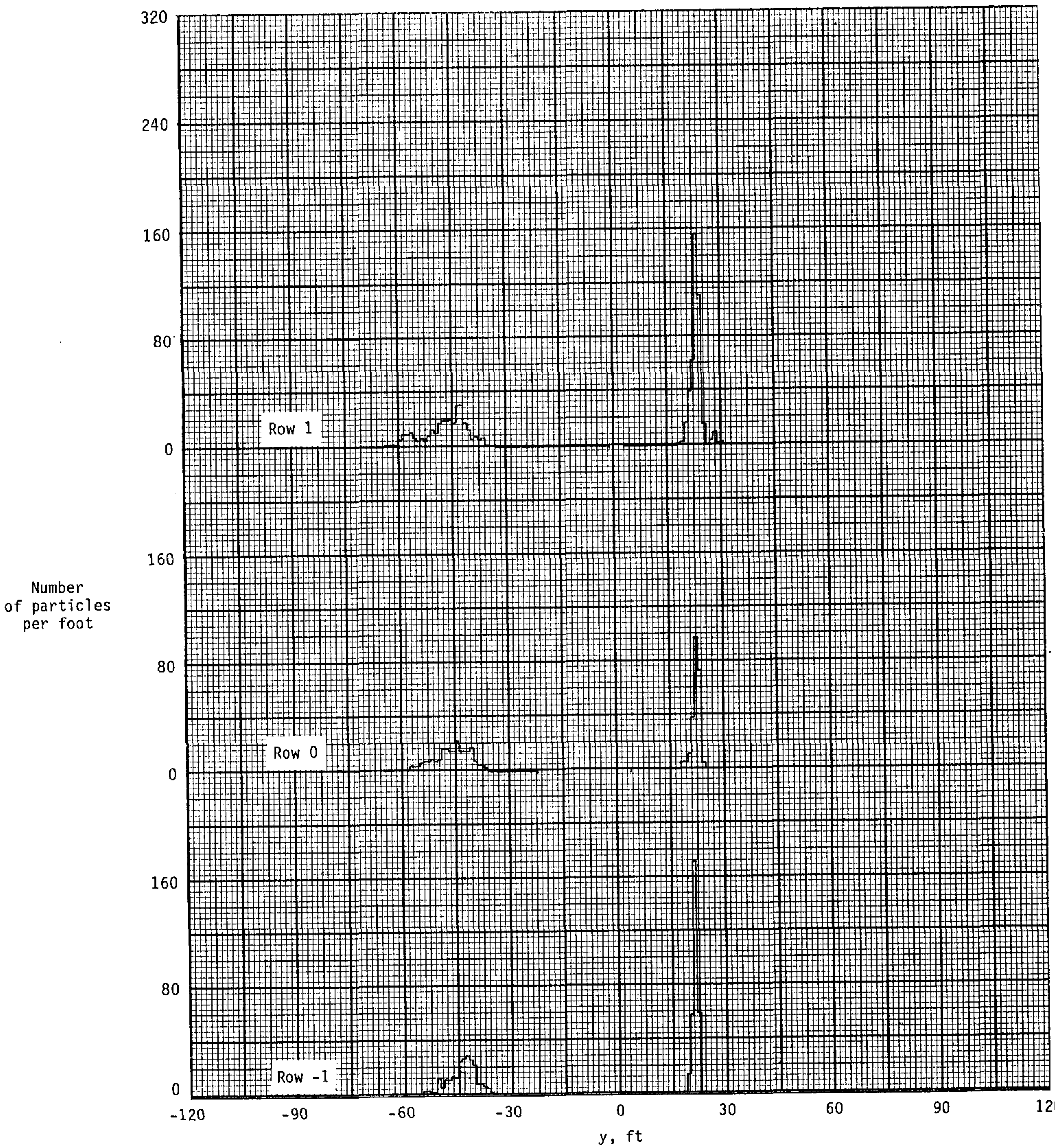

Figure A16.- Ground deposition patterns for flight 49, run 3.1.

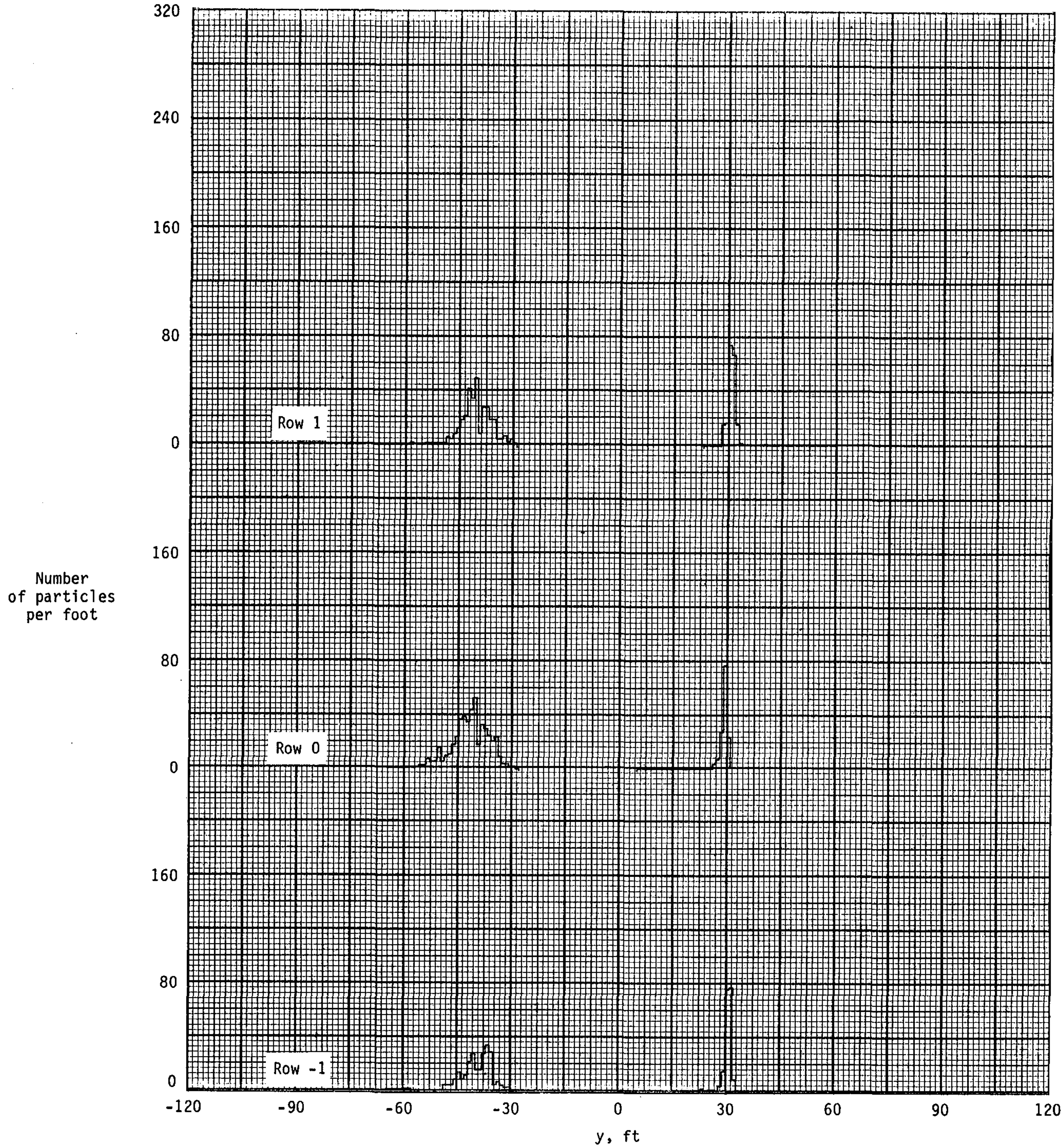

Figure A17.- Ground deposition patterns for flight 49, run 4.1.

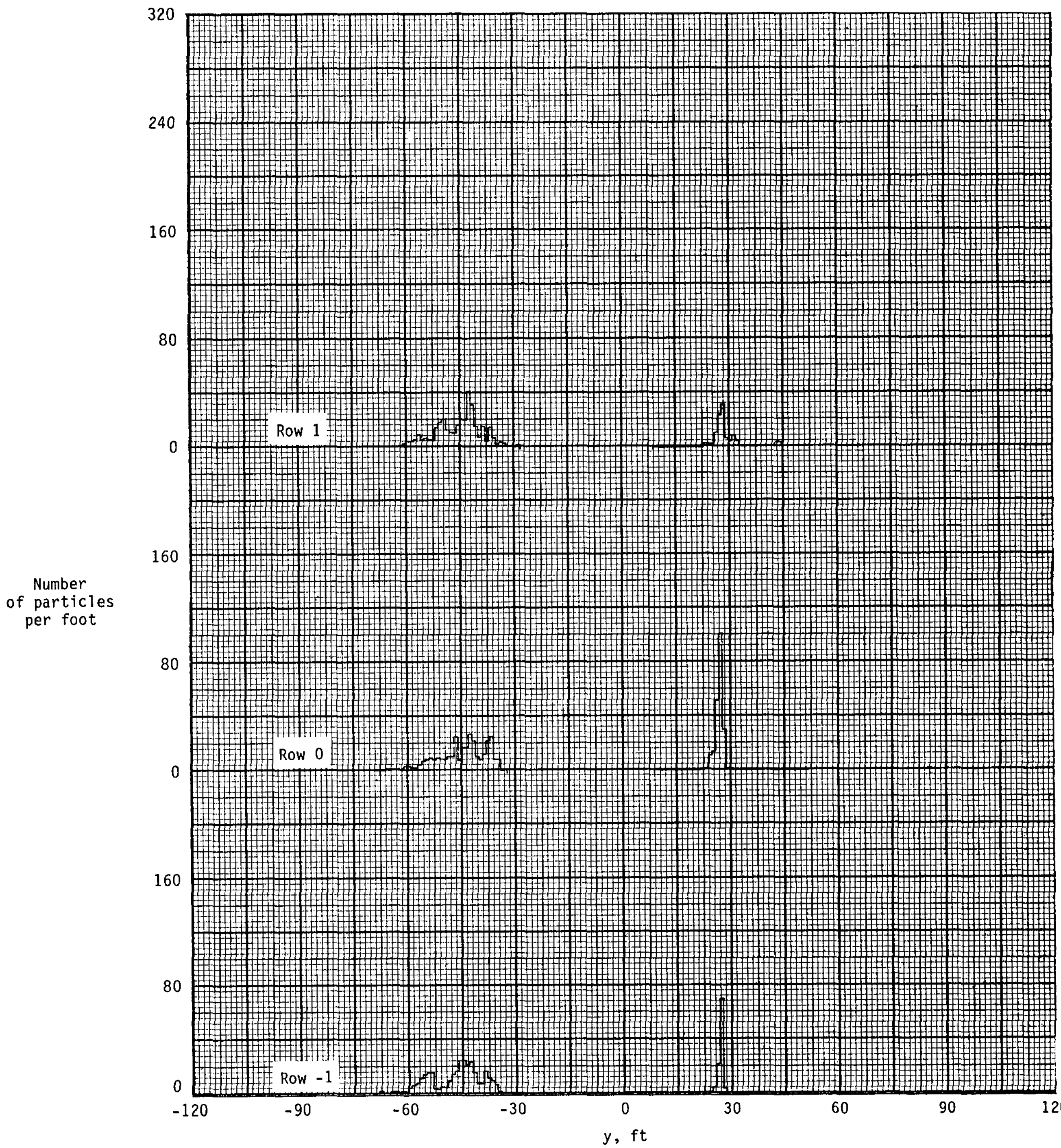

Figure A18.- Ground deposition patterns for flight 49, run 4.2.

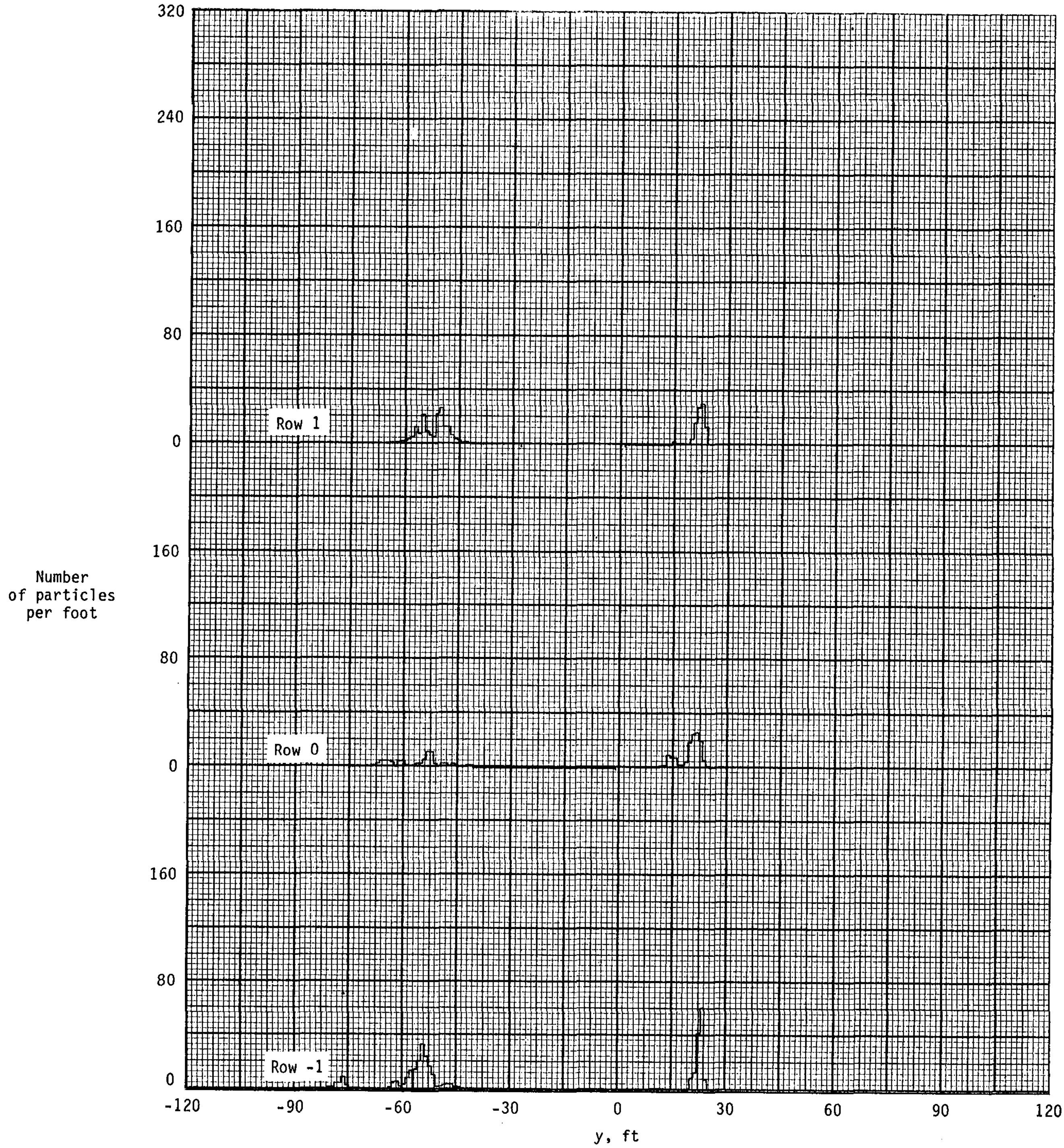

Figure A19.- Ground deposition patterns for flight 49, run 5.2.

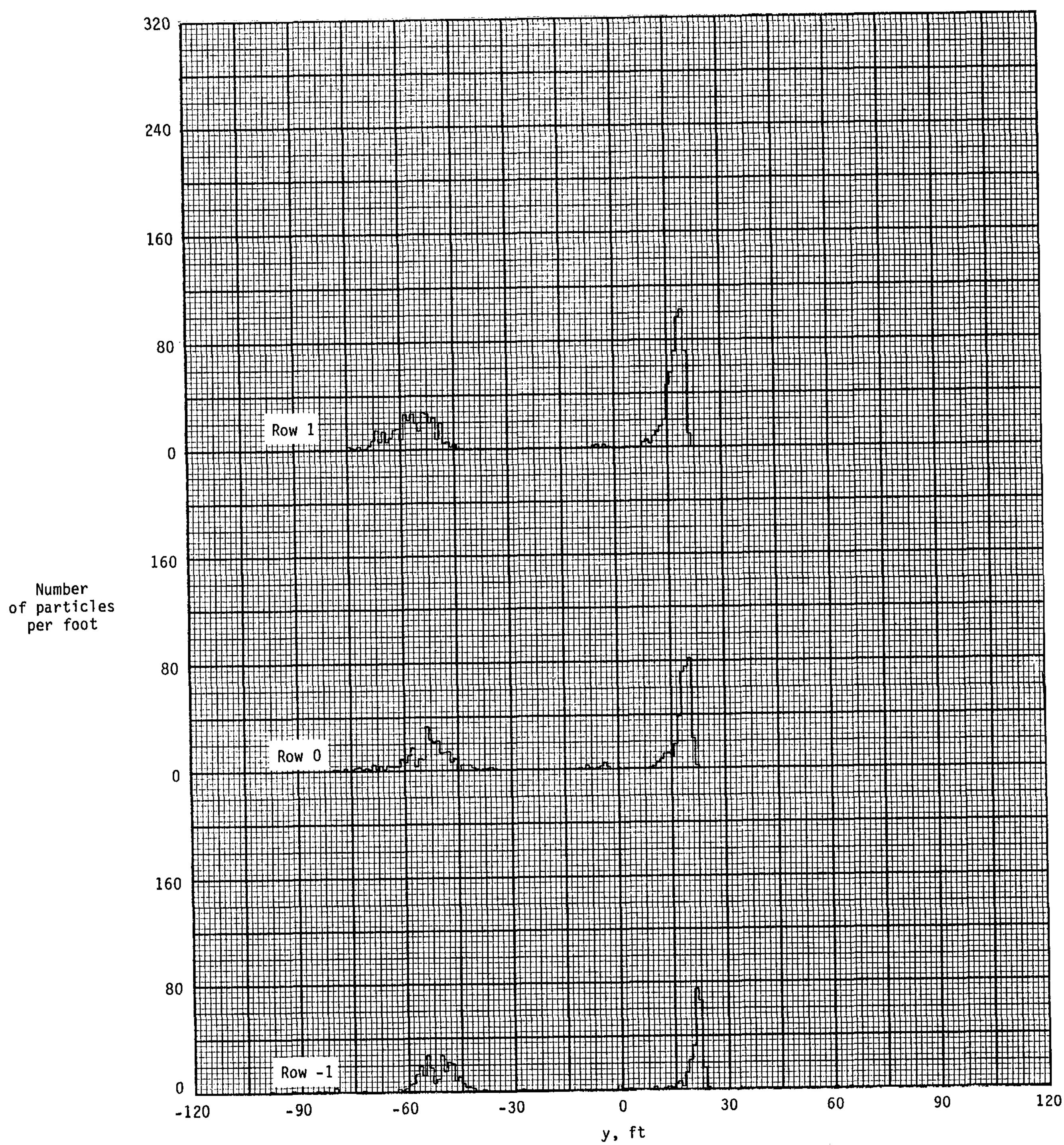

Figure A20.- Ground deposition patterns for flight 49, run 5.4.

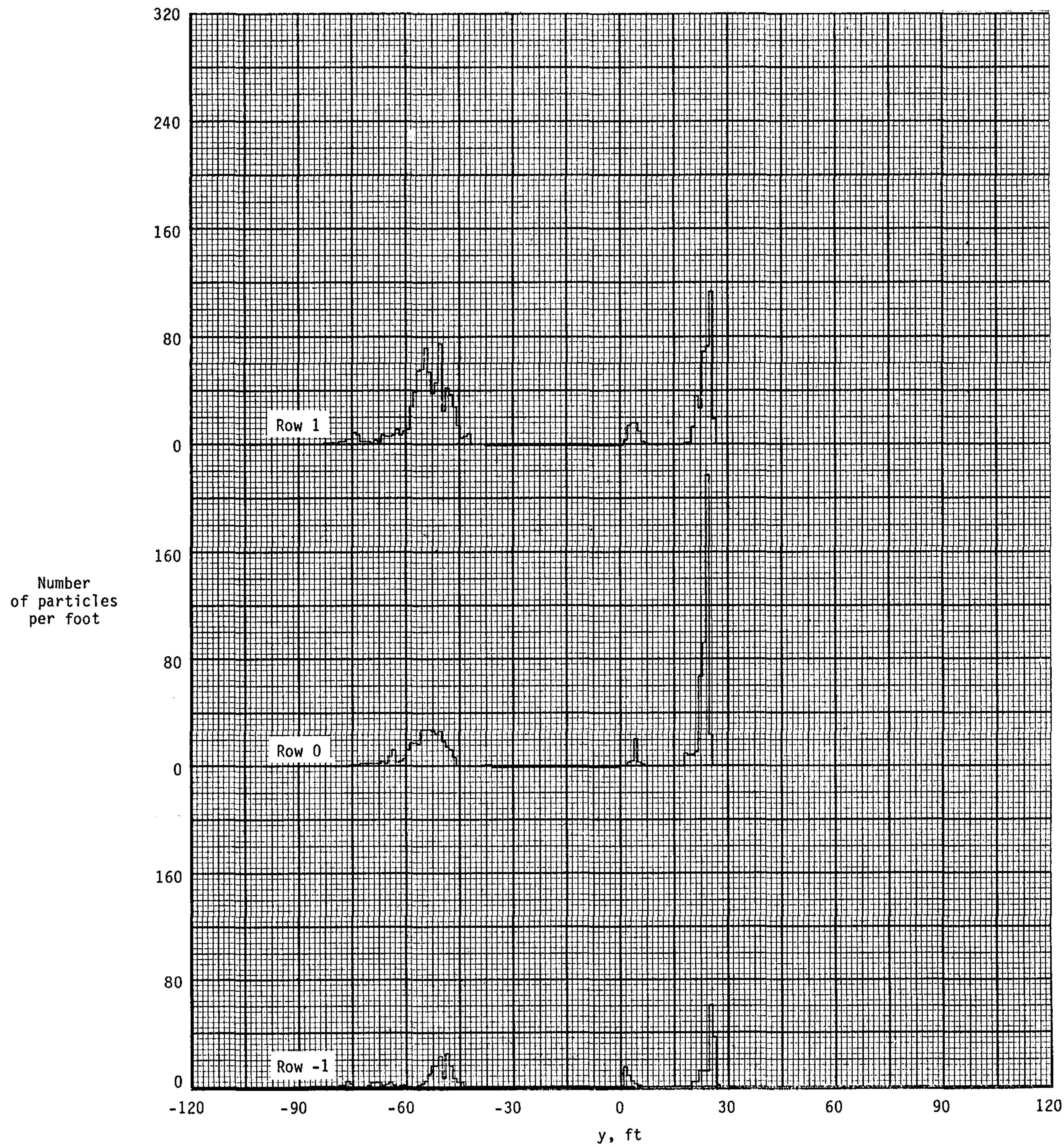

Figure A21.- Ground deposition patterns for flight 49, run 6.2.

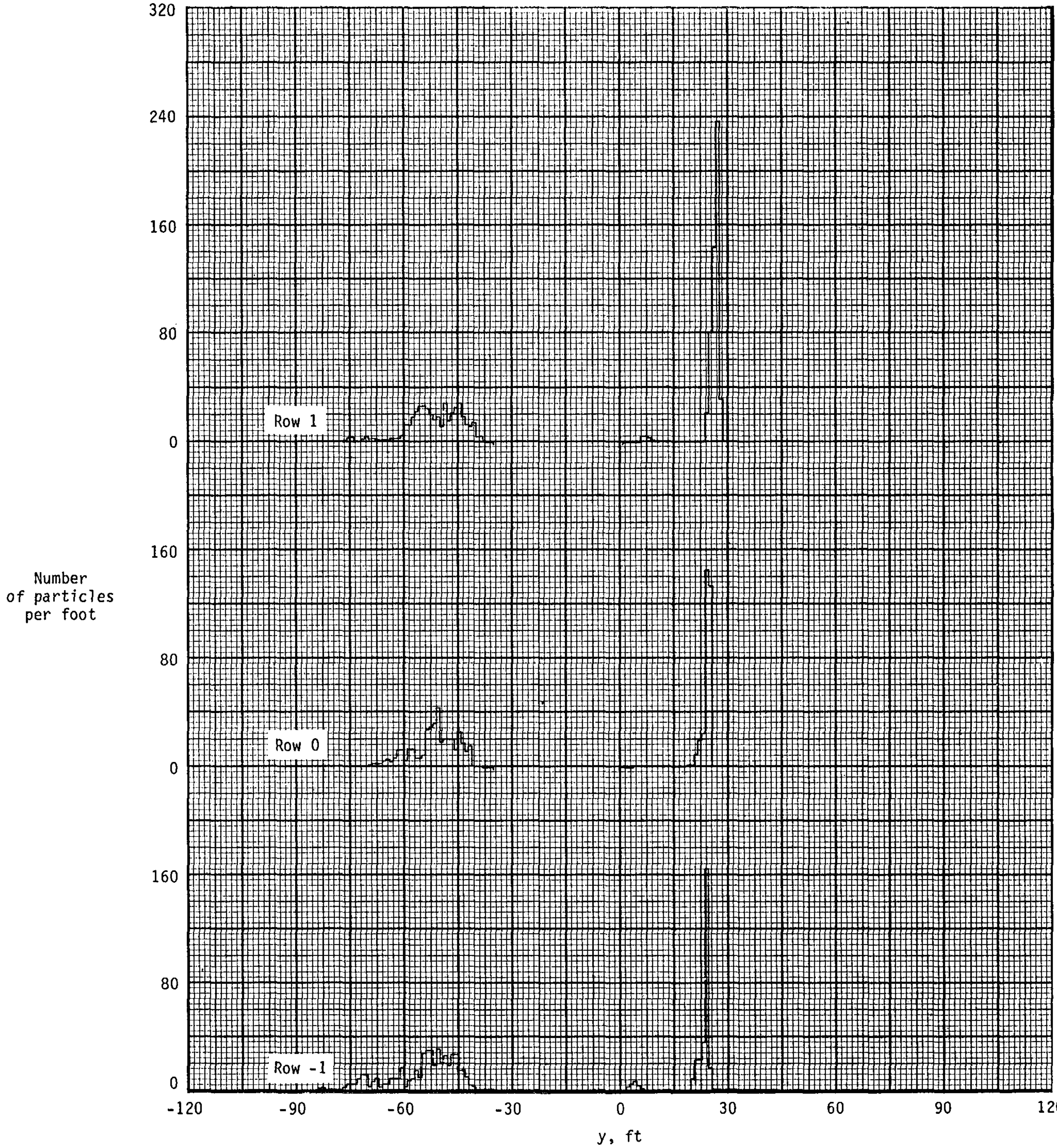

Figure A22.- Ground deposition patterns for flight 49, run 6.4.

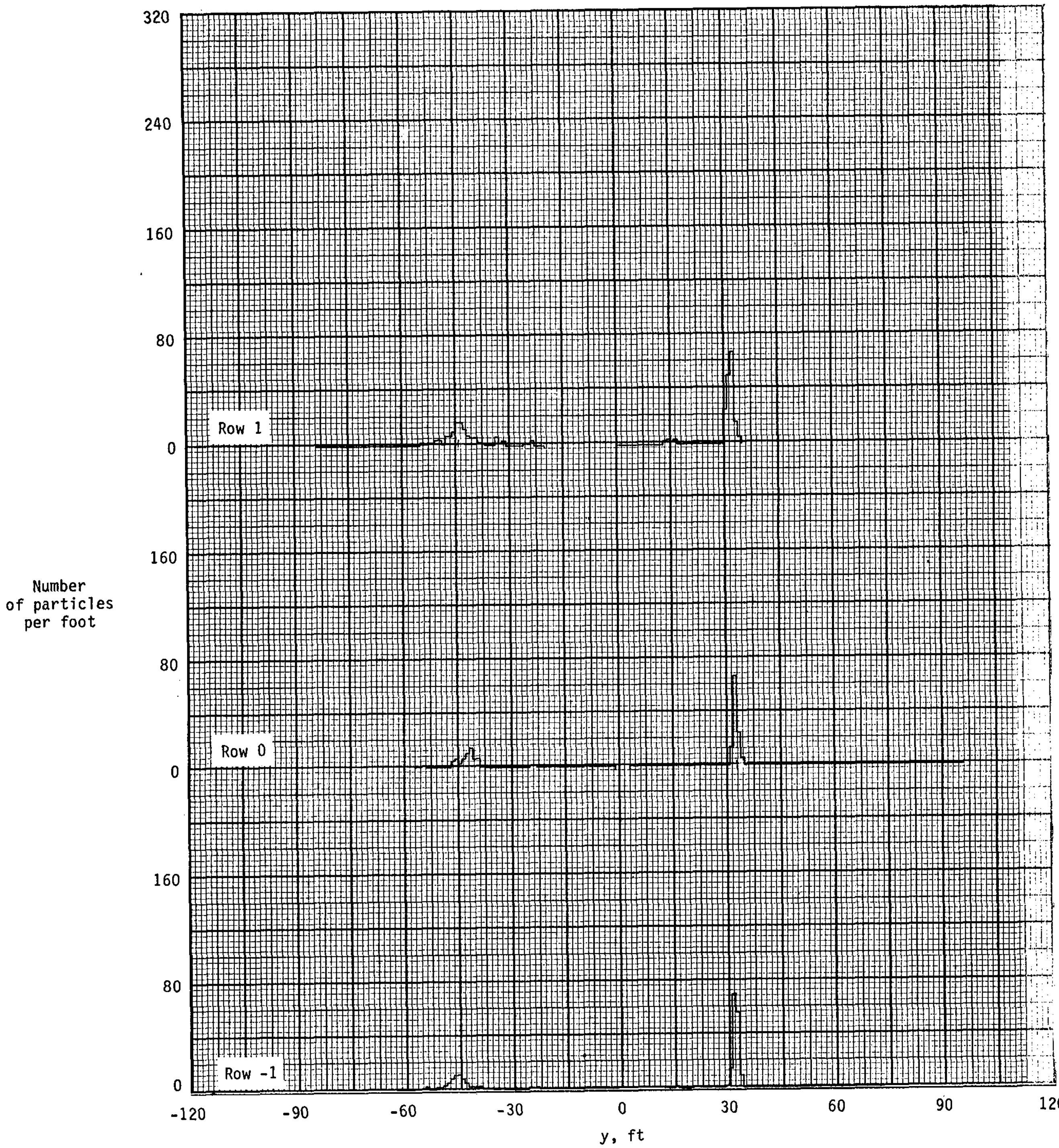

Figure A23.- Ground deposition patterns for flight 50, run 1.1.

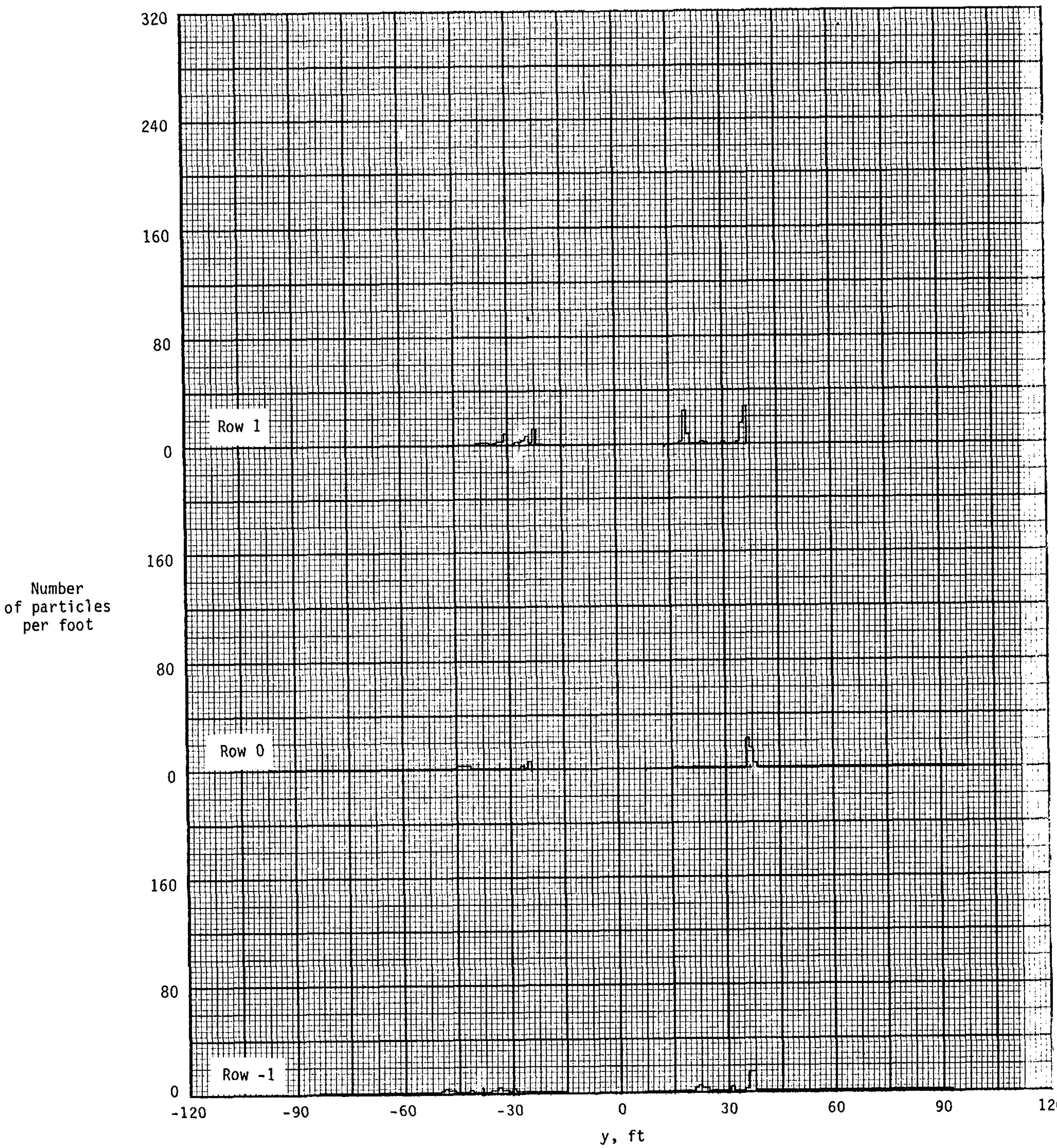

Figure A24.- Ground deposition patterns for flight 50, run 2.2.

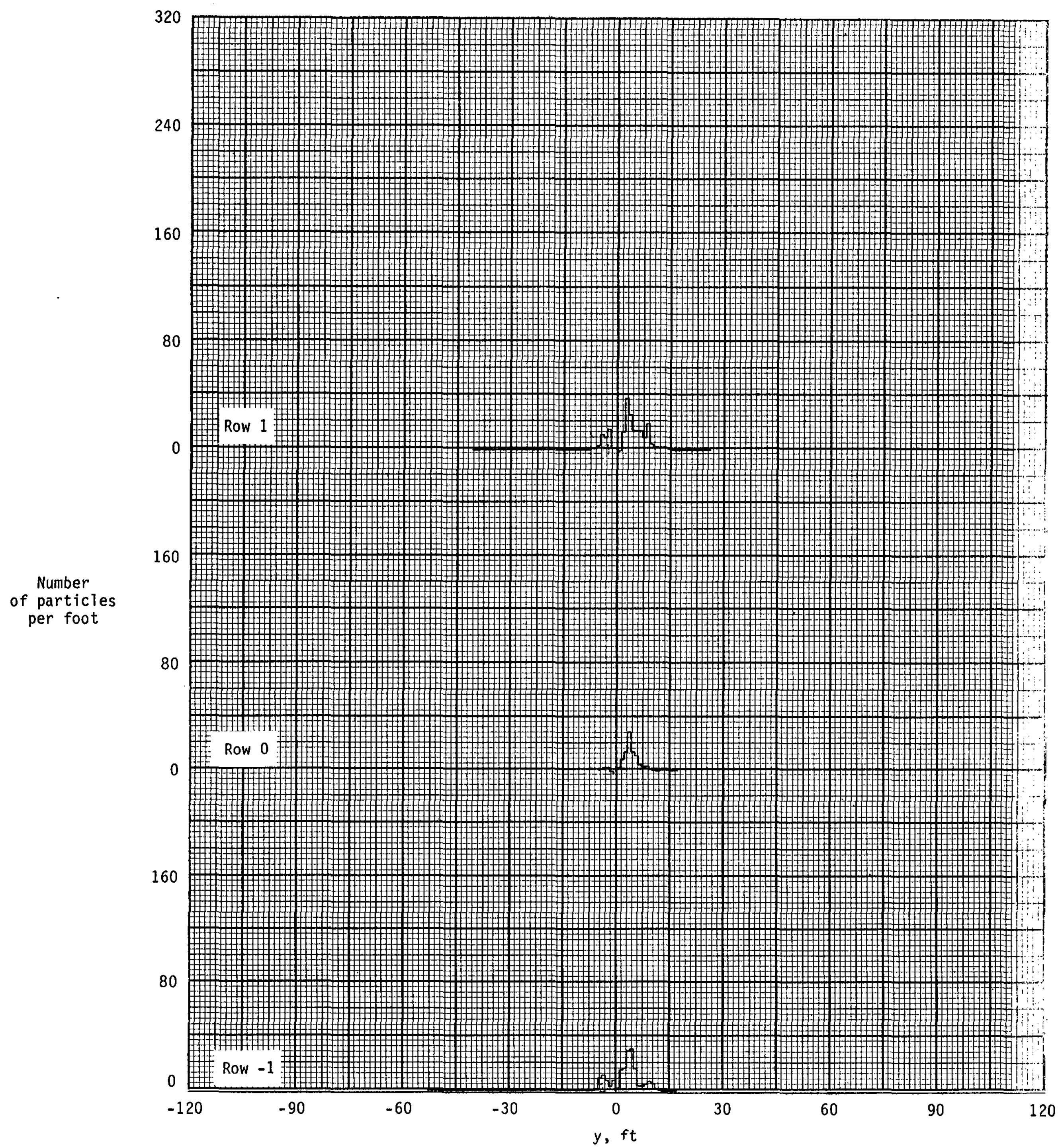

Figure A25.- Ground deposition patterns for flight 51, run 1.2.

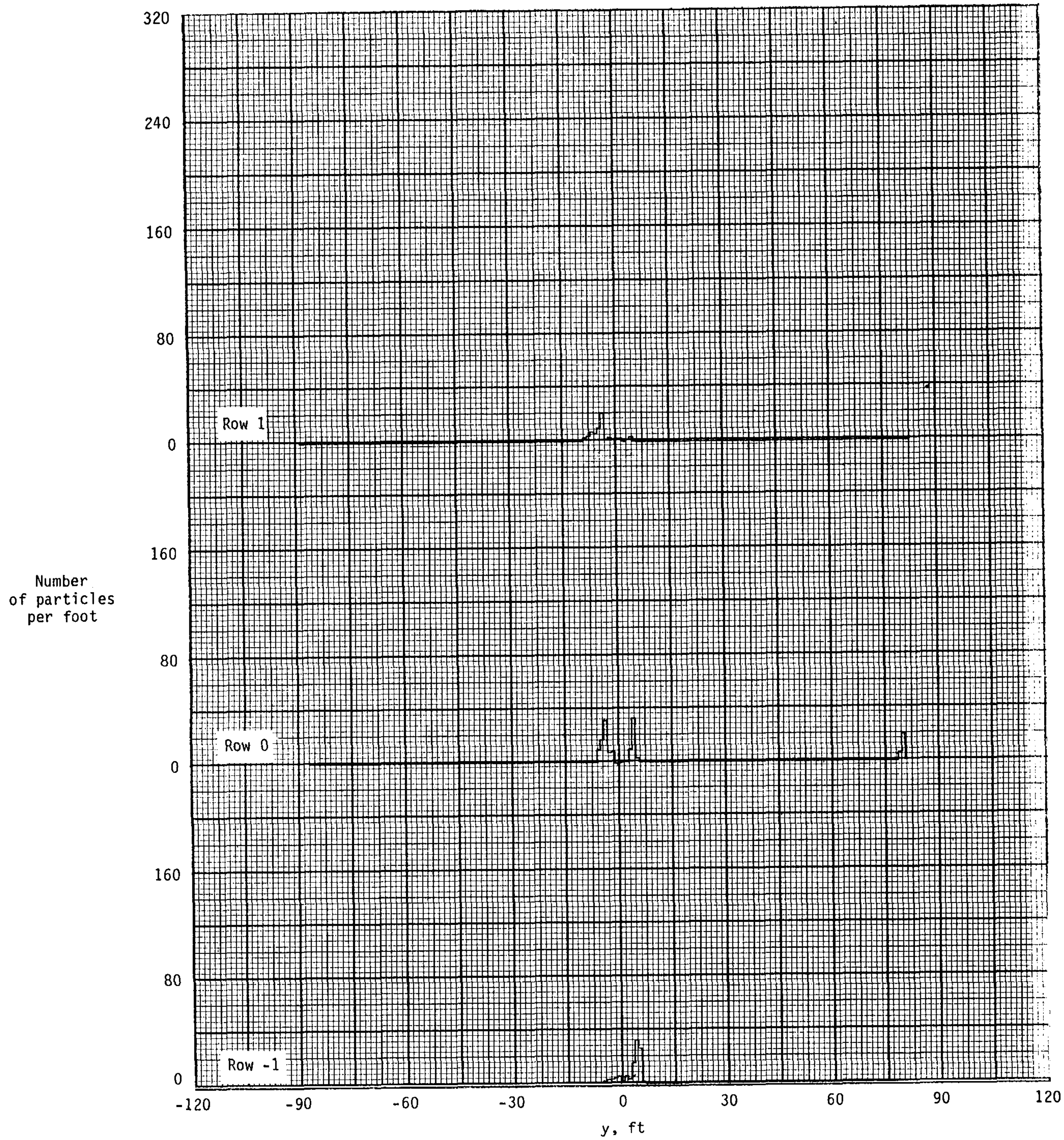

Figure A26.- Ground deposition patterns for flight 51, run 2.1.

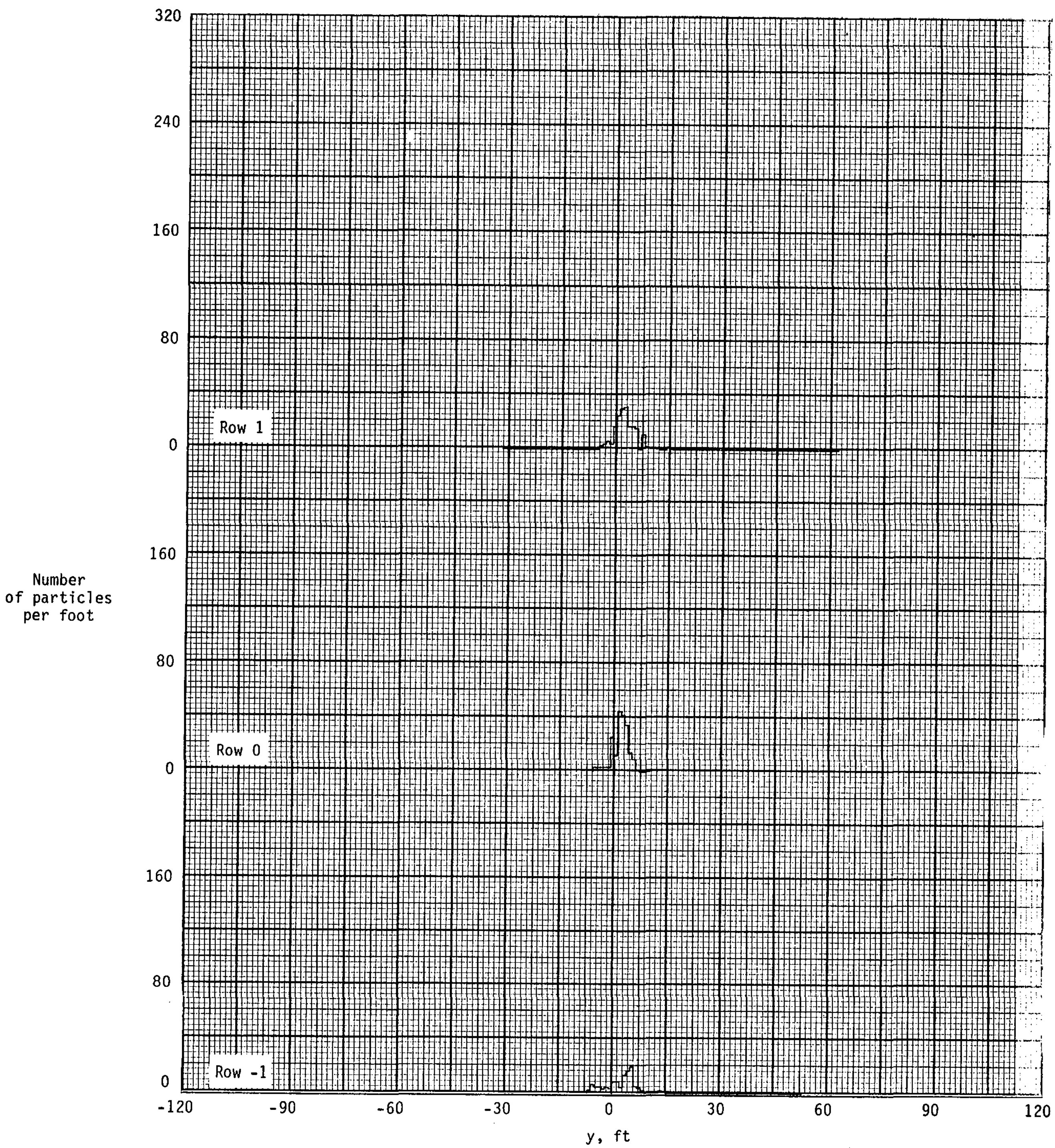

Figure A27.- Ground deposition patterns for flight 51, run 2.3.

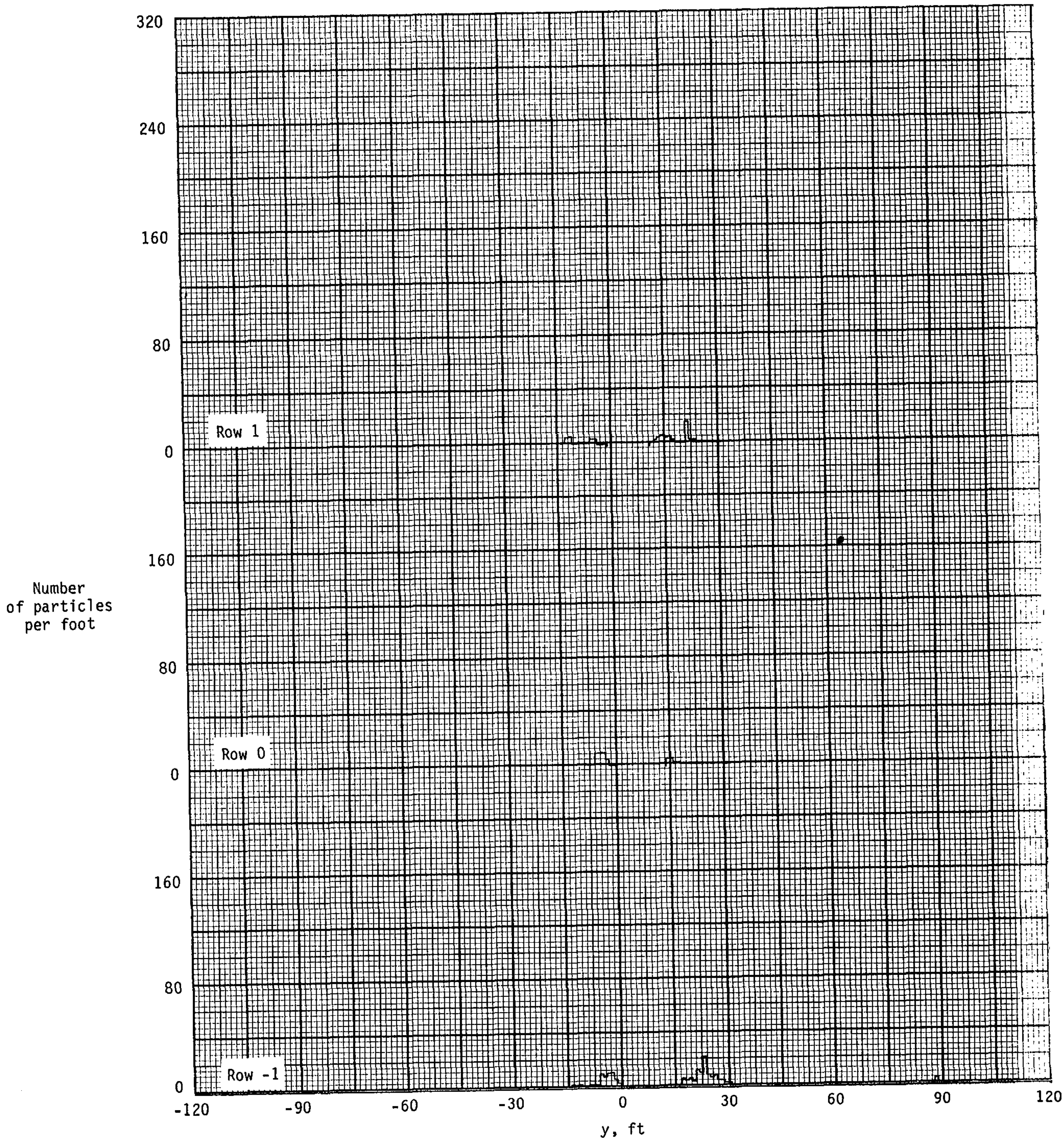

Figure A28.- Ground deposition patterns for flight 51, run 3.3.

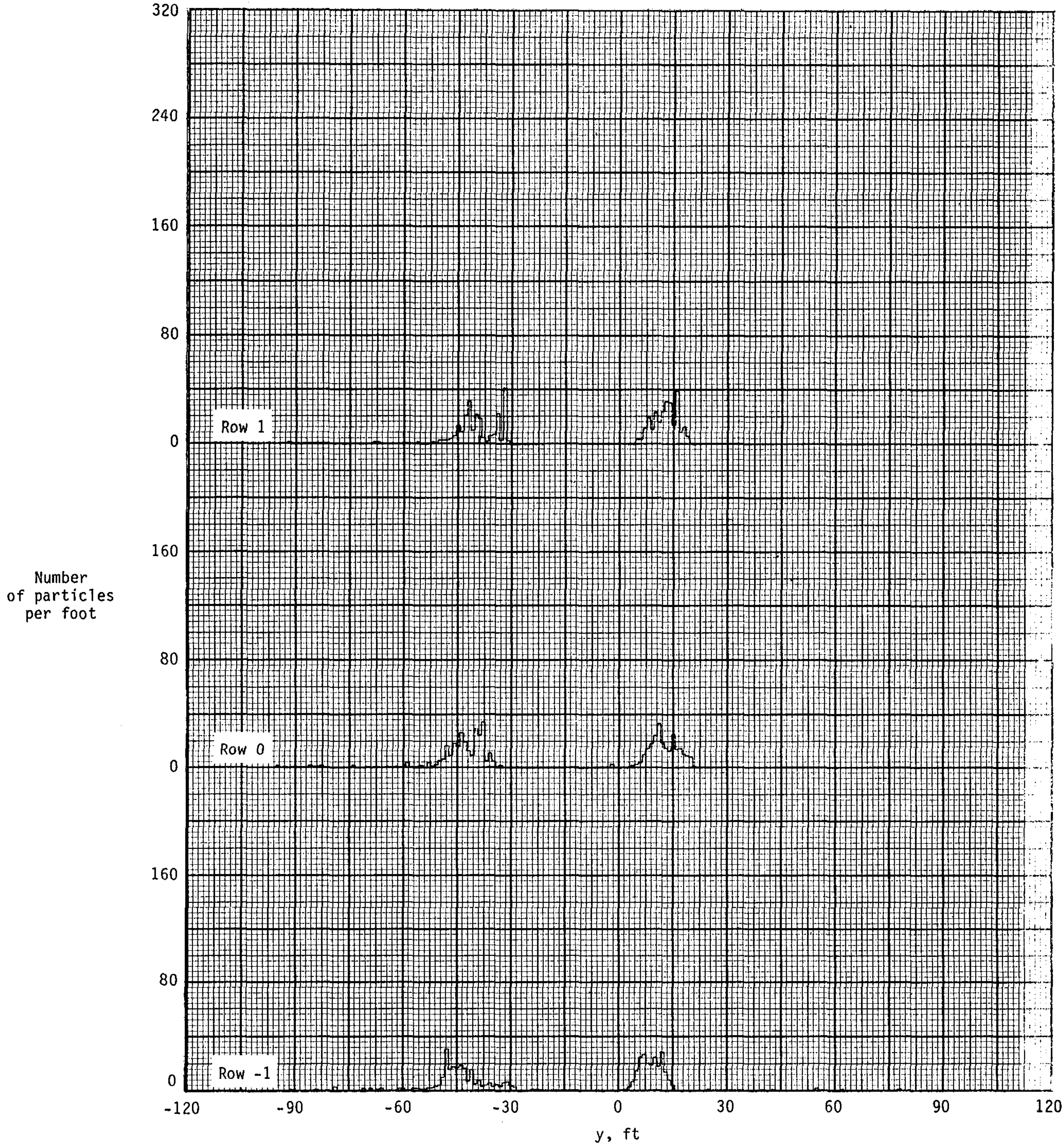

Figure A29.- Ground deposition patterns for flight 52, run 1.0.

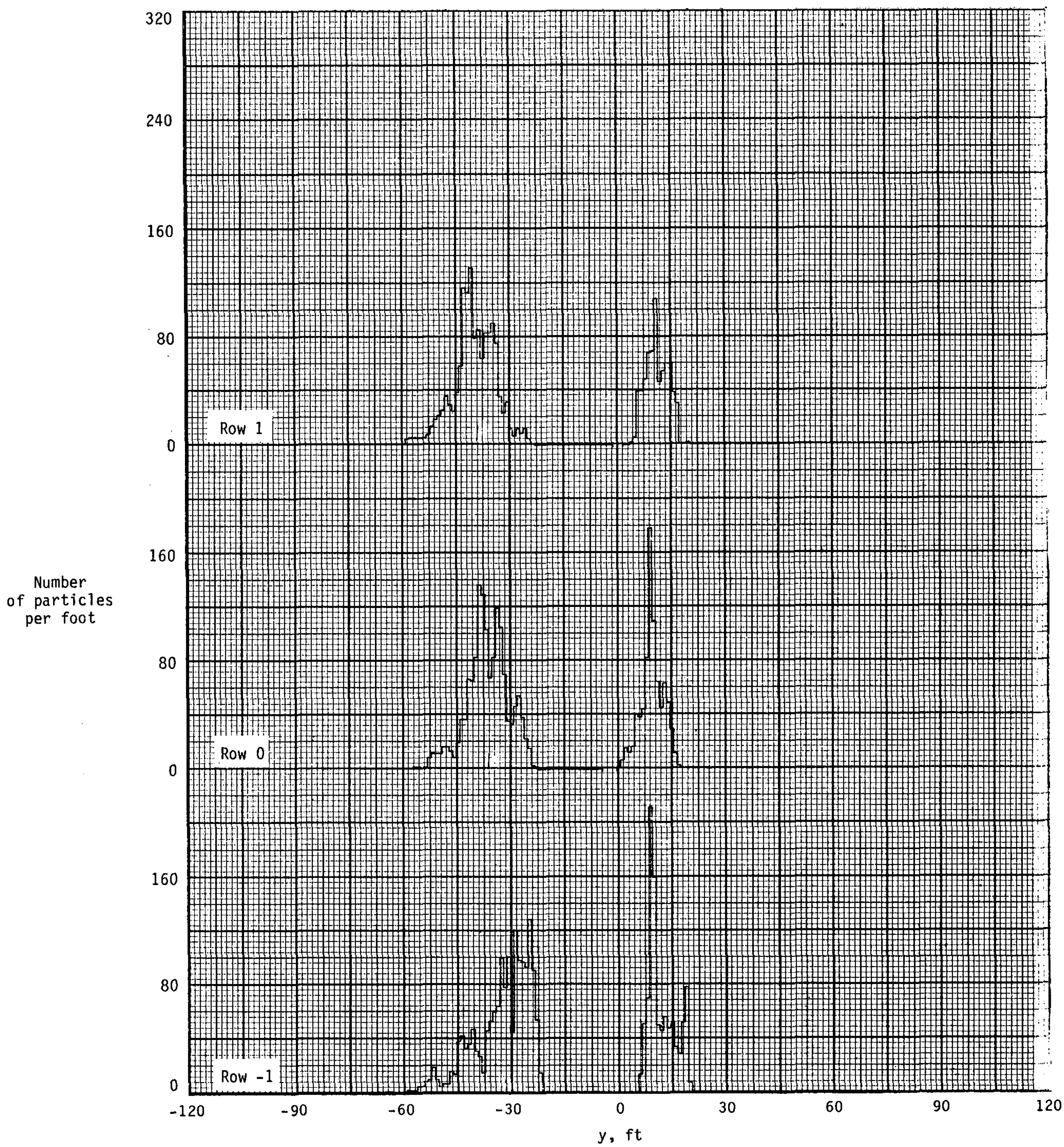

Figure A30.- Ground deposition patterns for flight 53, run 1.2.

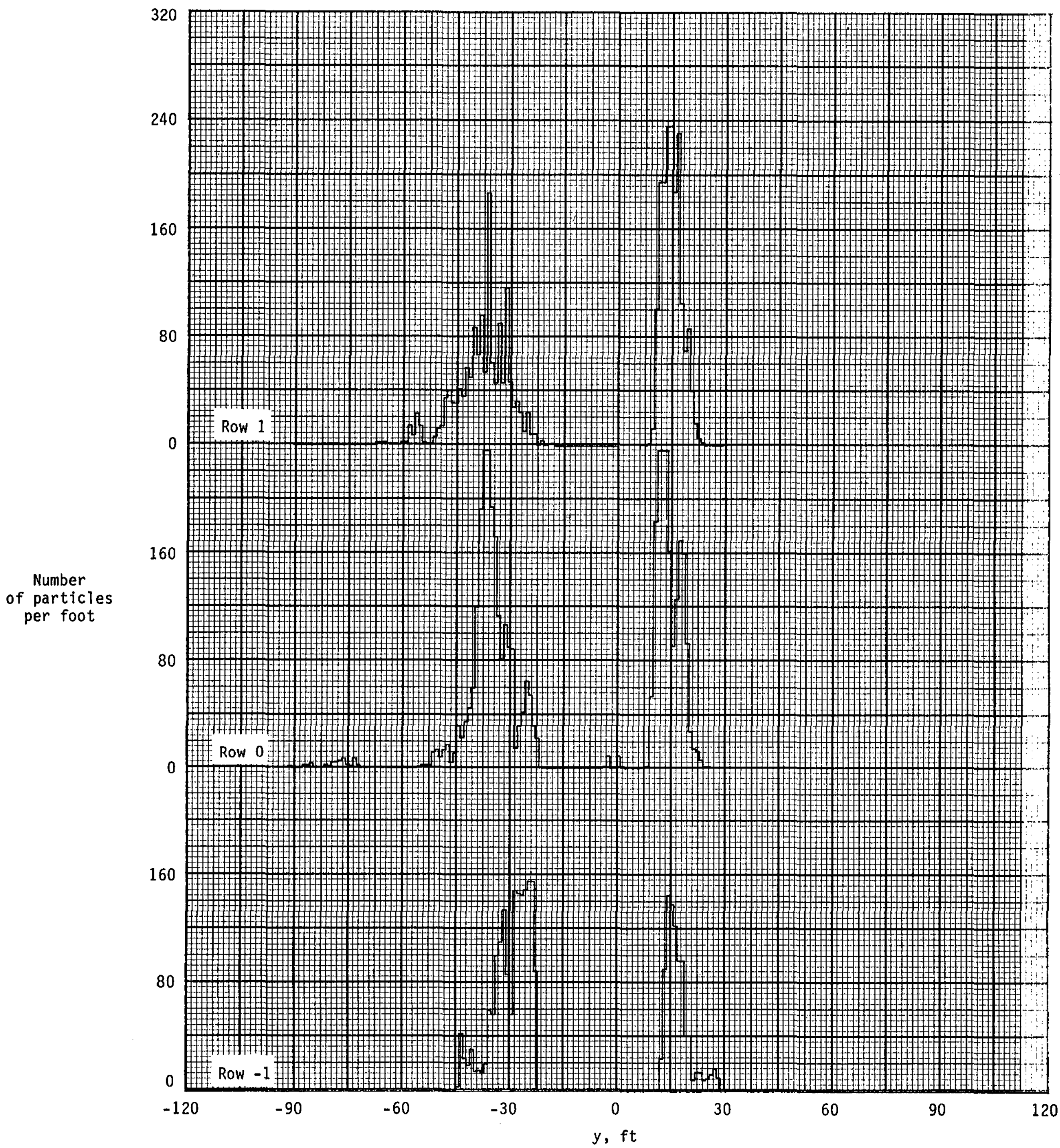

Figure A31.- Ground deposition patterns for flight 53, run 2.2.

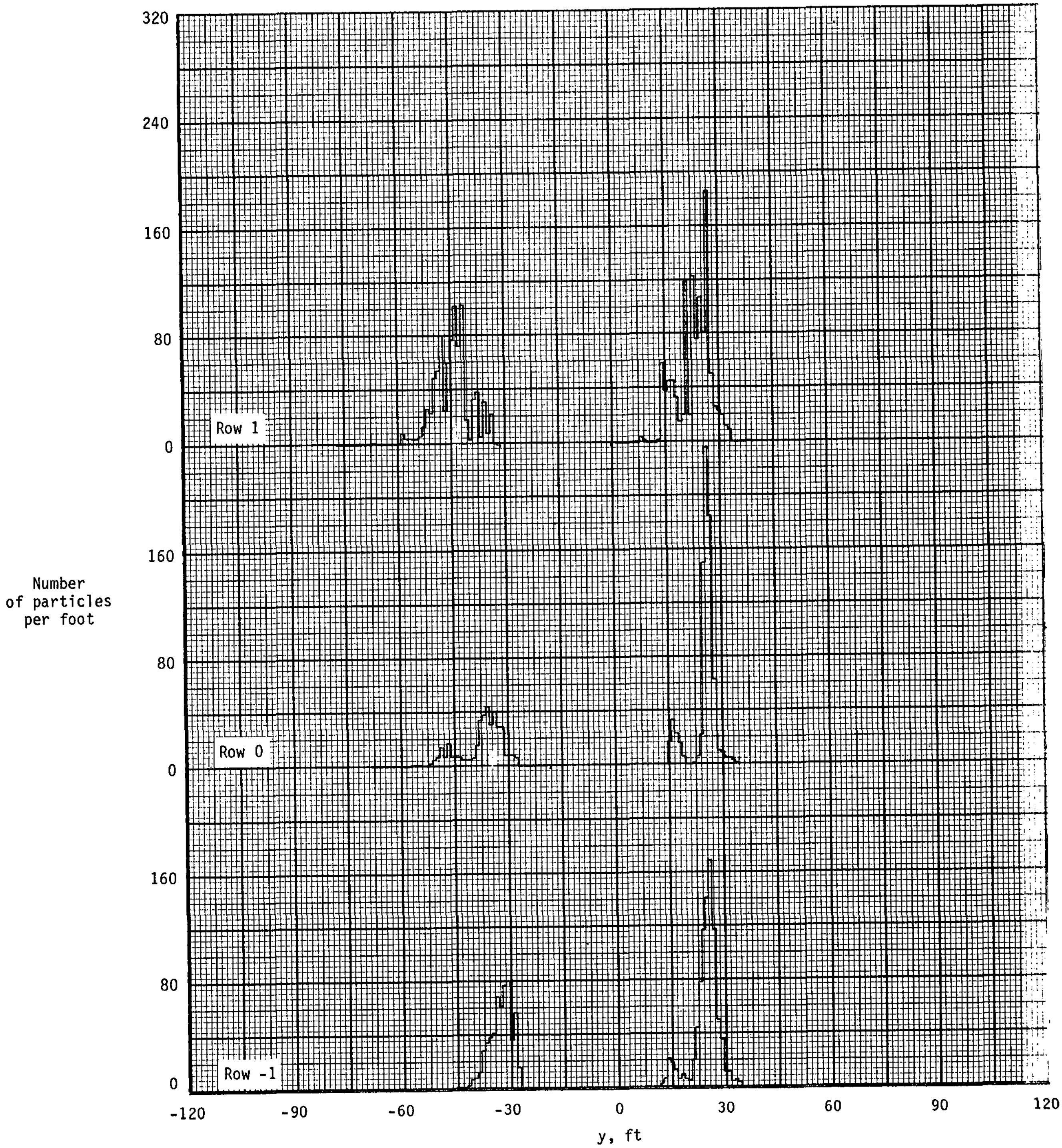

Figure A32.- Ground deposition patterns for flight 53, run 2.3.

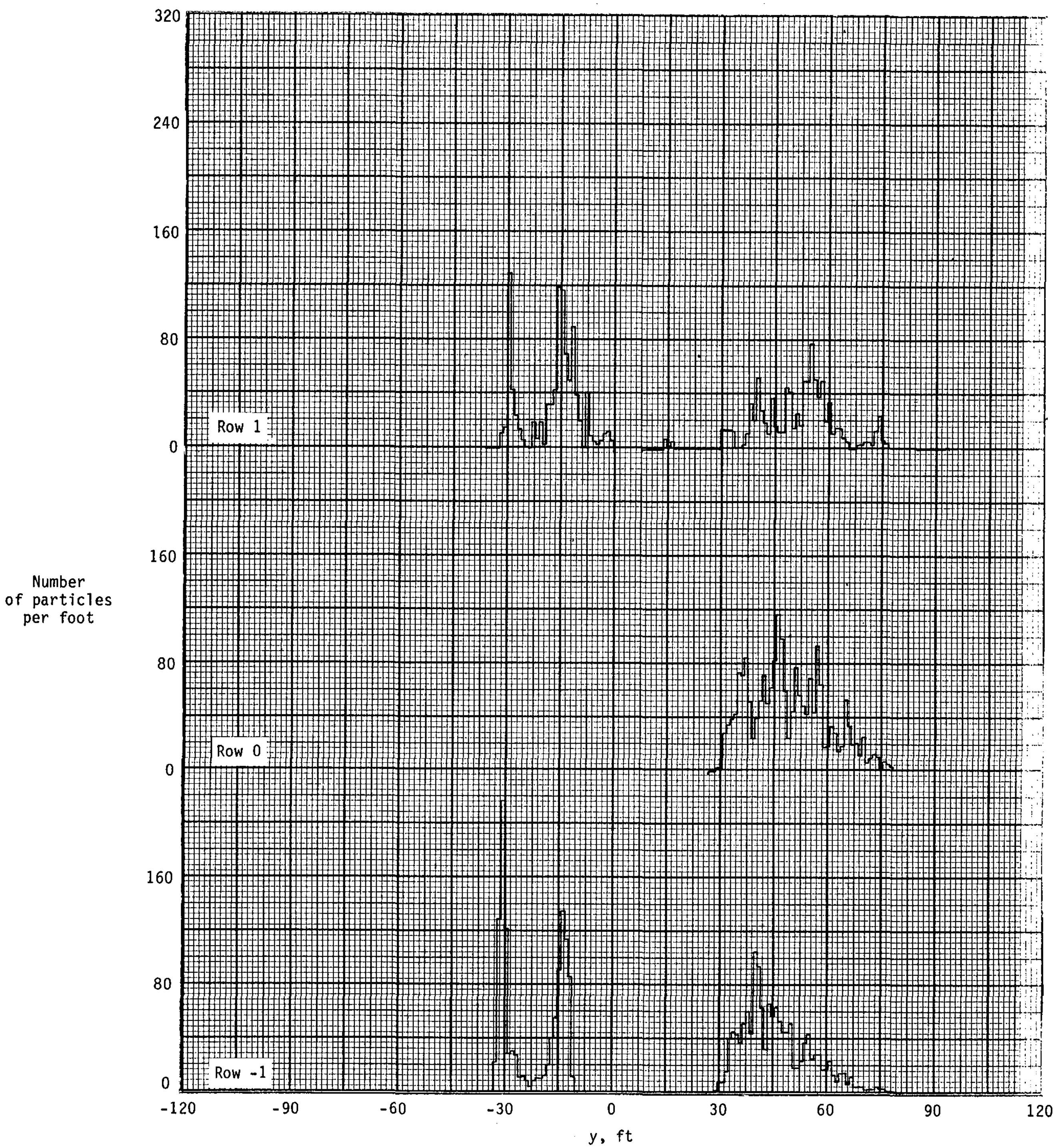

Figure A33.- Ground deposition patterns for flight 54, run 1.0.

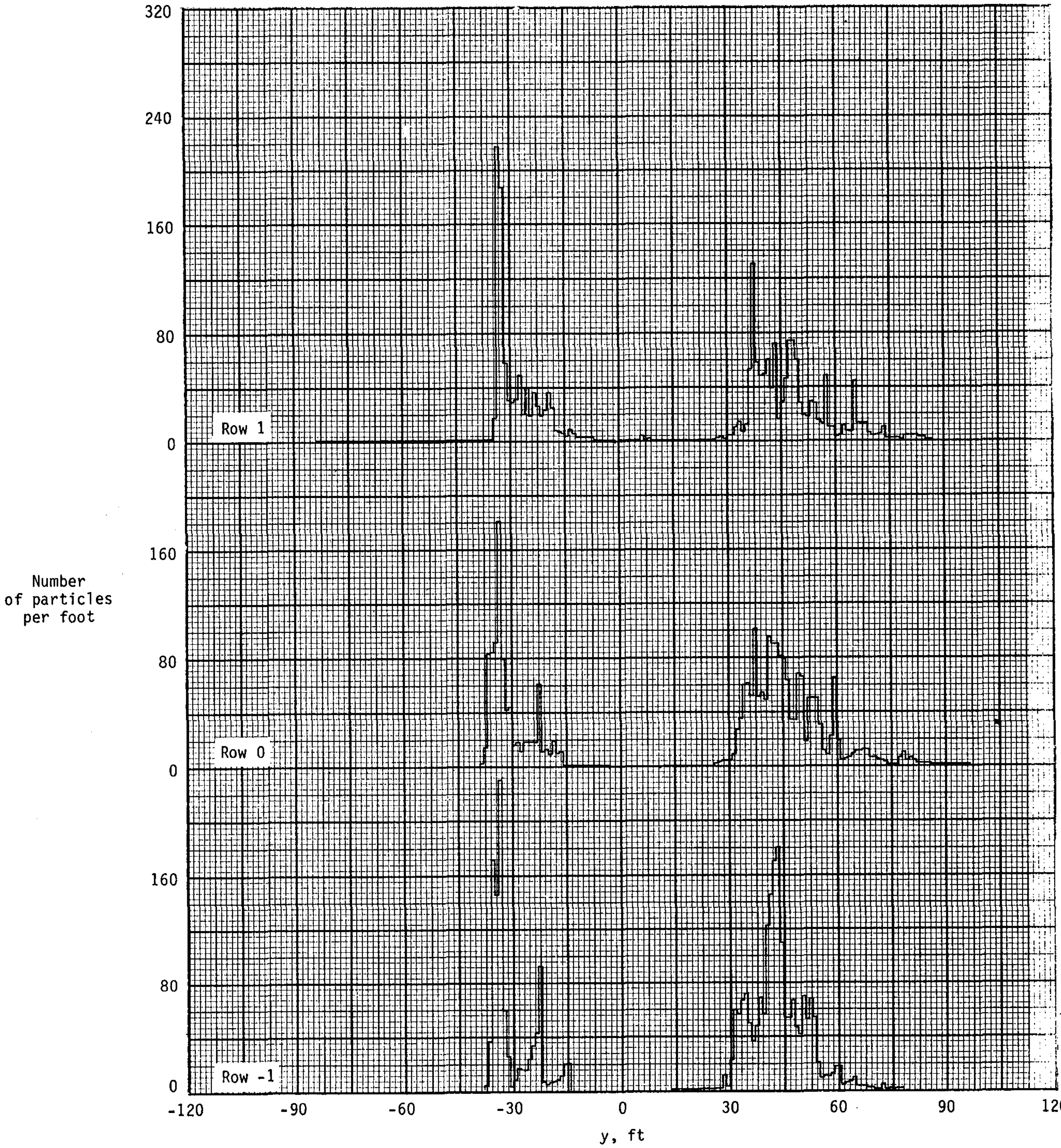

Figure A34.- Ground deposition patterns for flight 54, run 1.1.

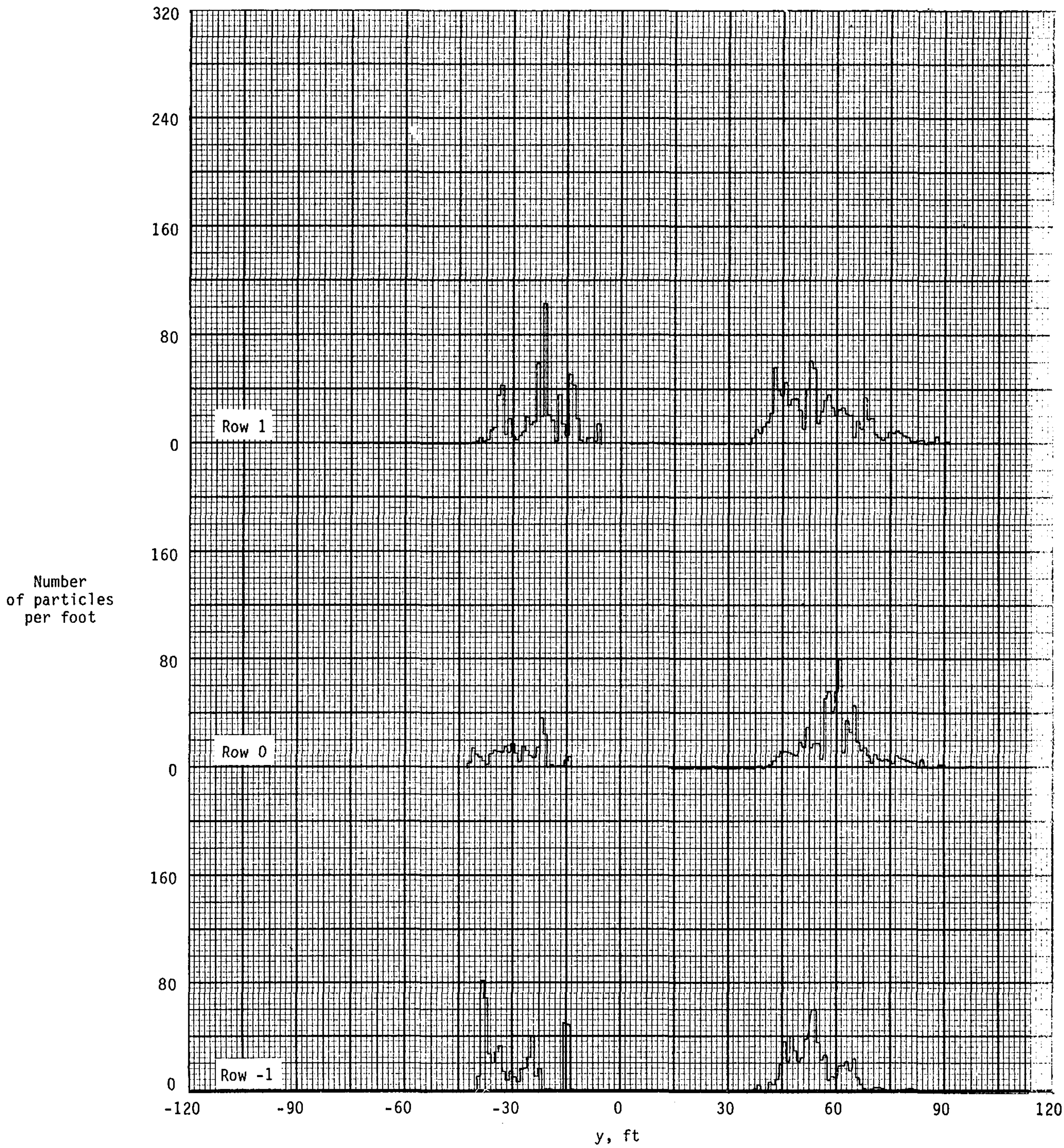

Figure A35.- Ground deposition patterns for flight 54, run 2.0.

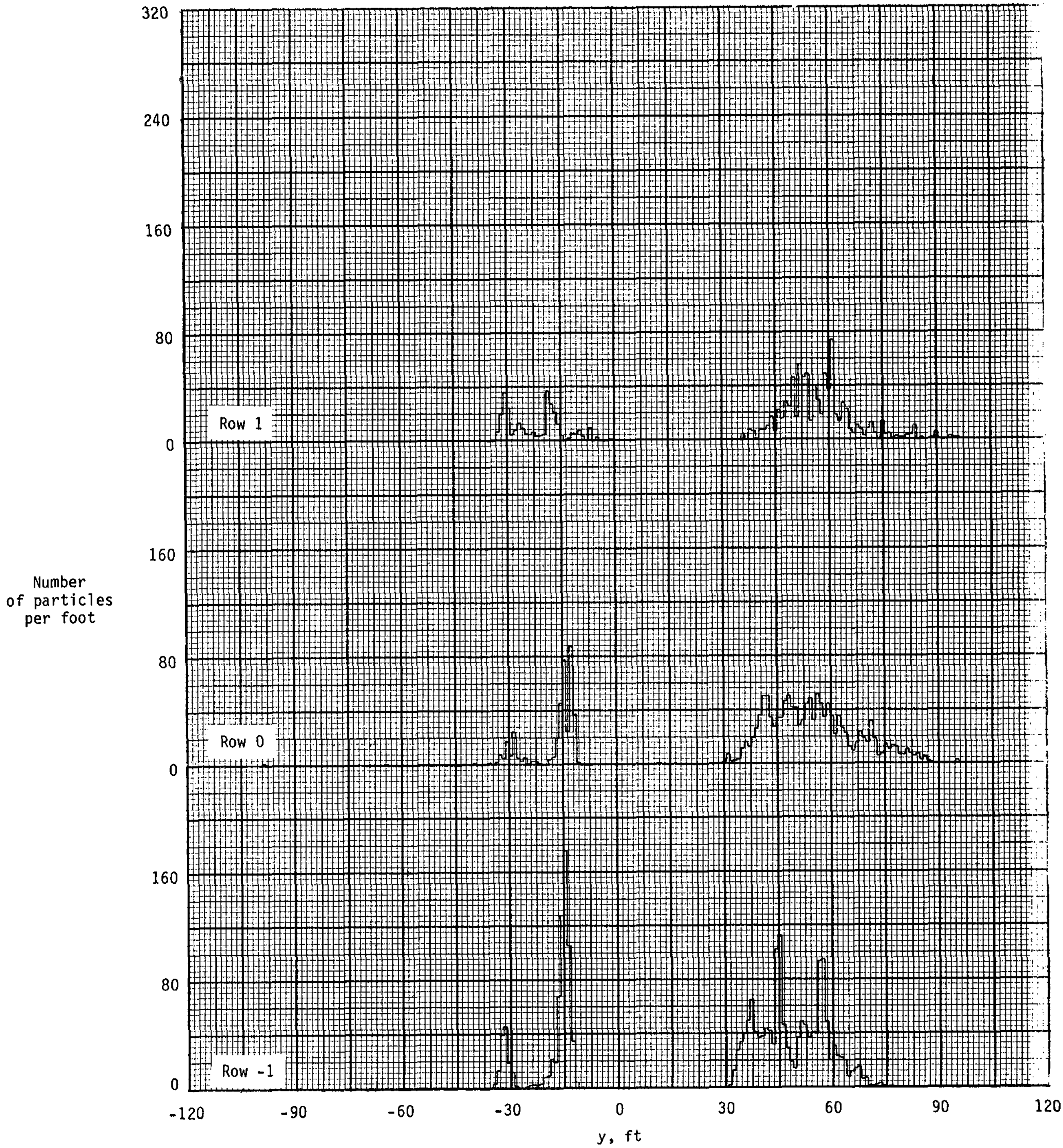

Figure A36.- Ground deposition patterns for flight 54, run 3.0.

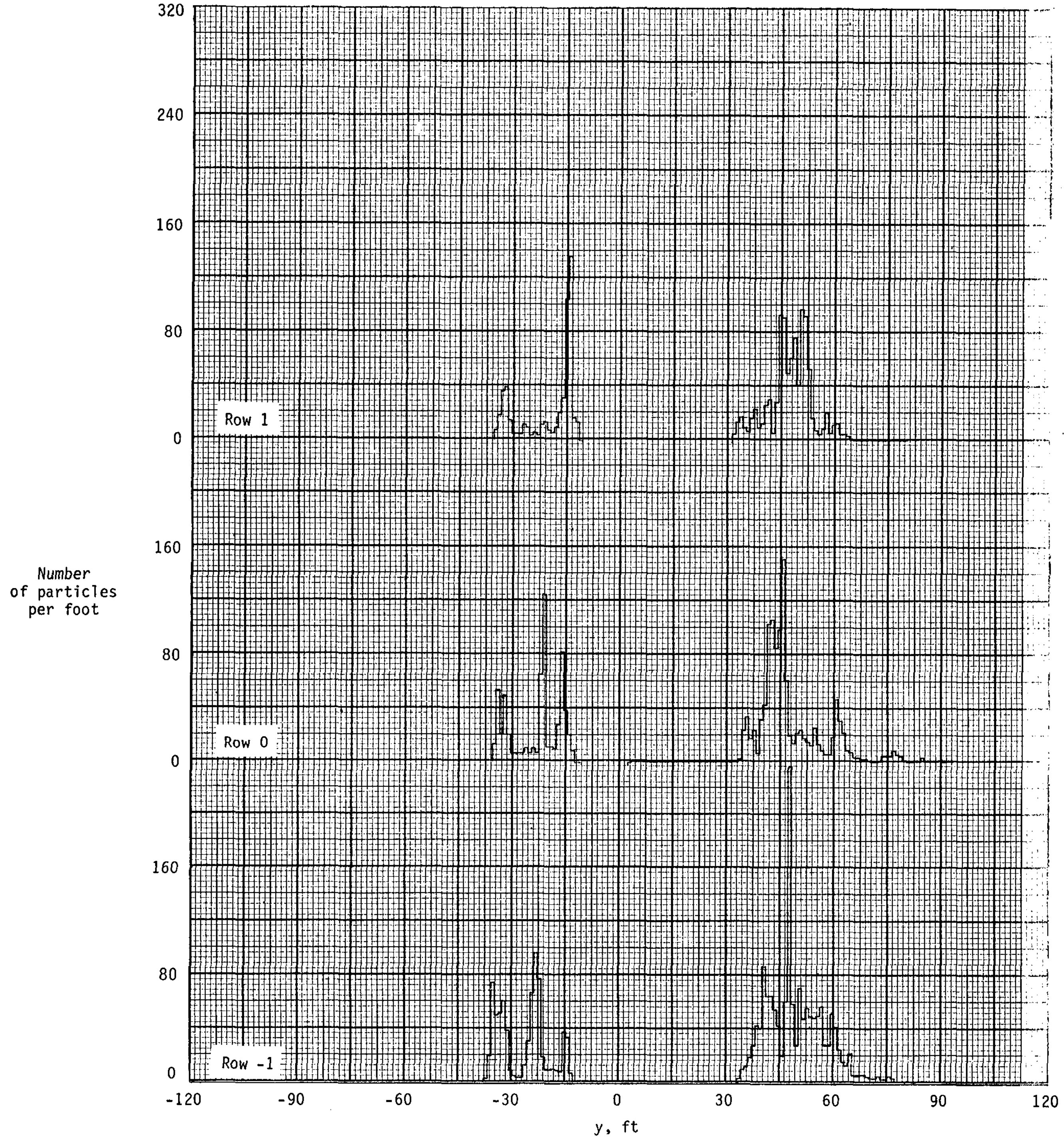

Figure A37.- Ground deposition patterns for flight 54, run 3.1.

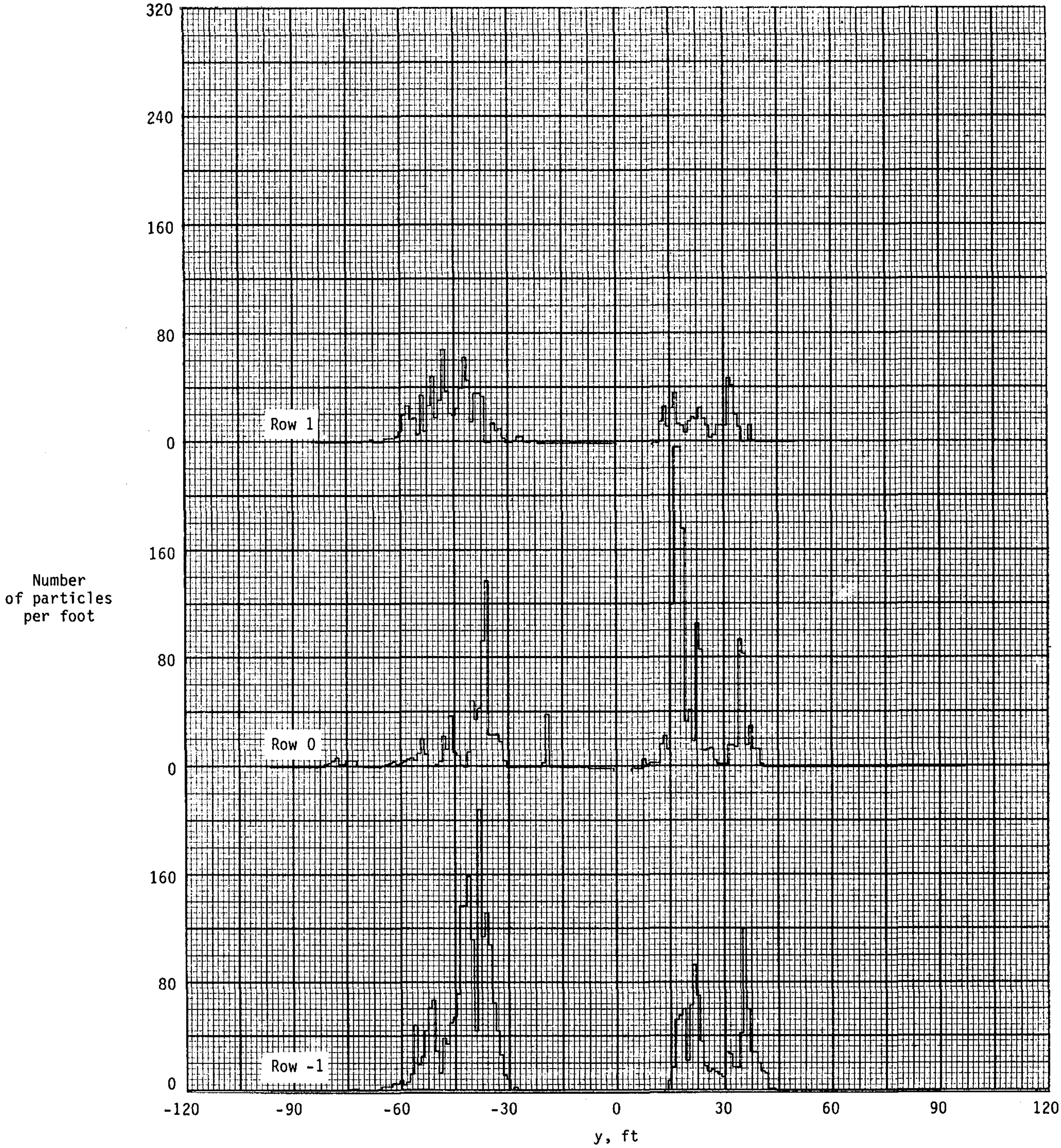

Figure A38.- Ground deposition patterns for flight 54, run 4.0.

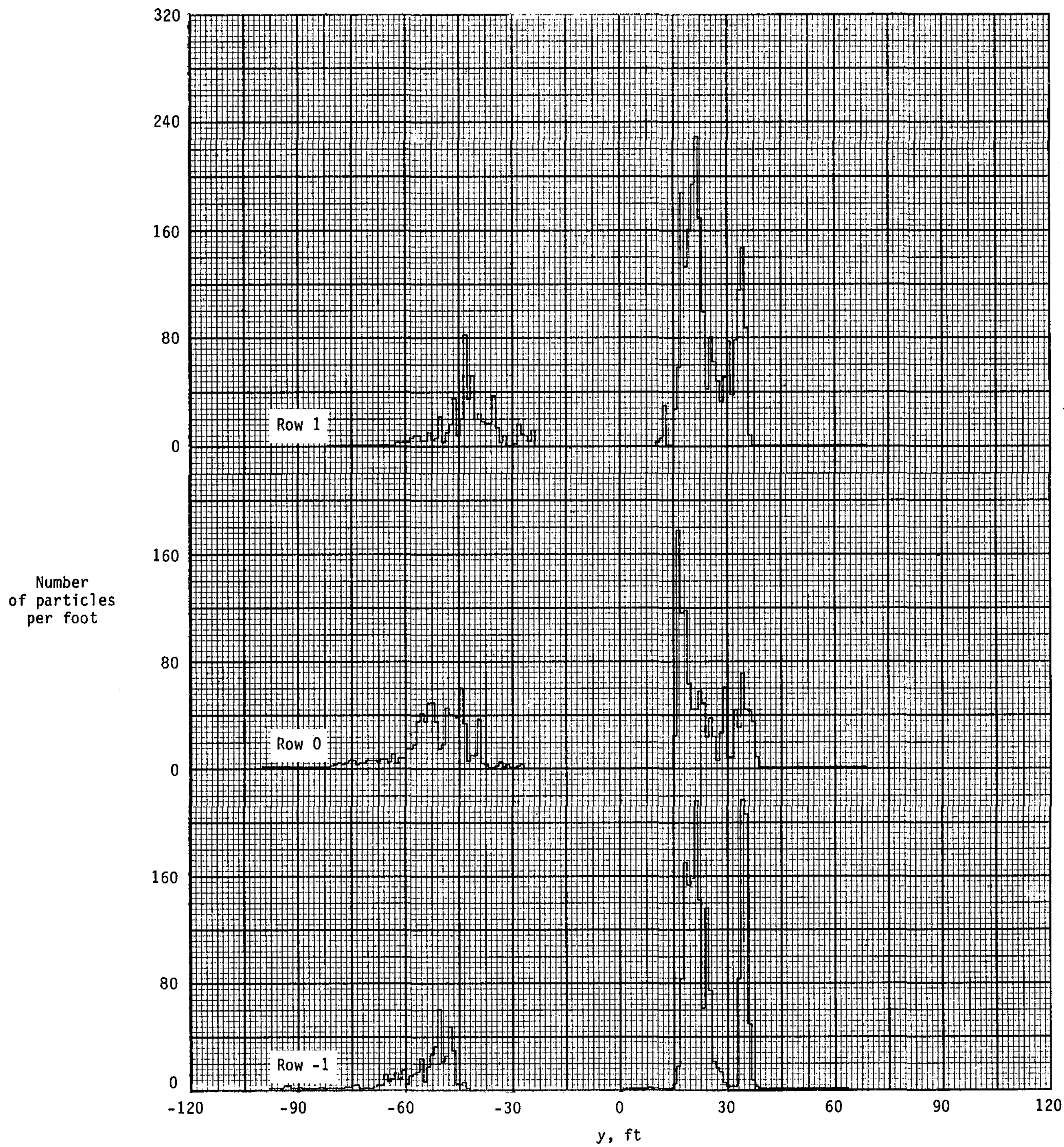

Figure A39.- Ground deposition patterns for flight 54, run 4.1.

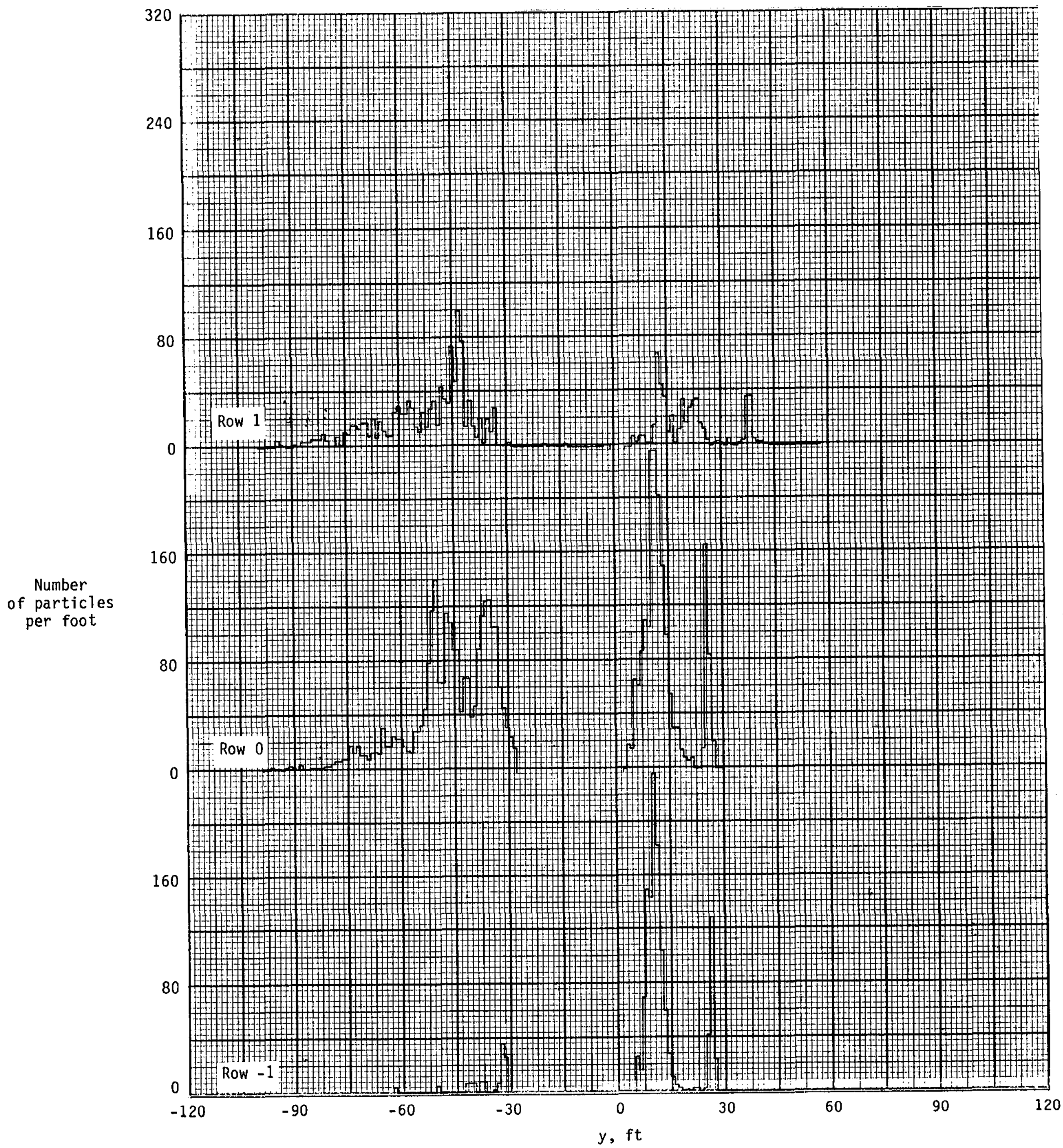

Figure A40.- Ground deposition patterns for flight 54, run 5.0.

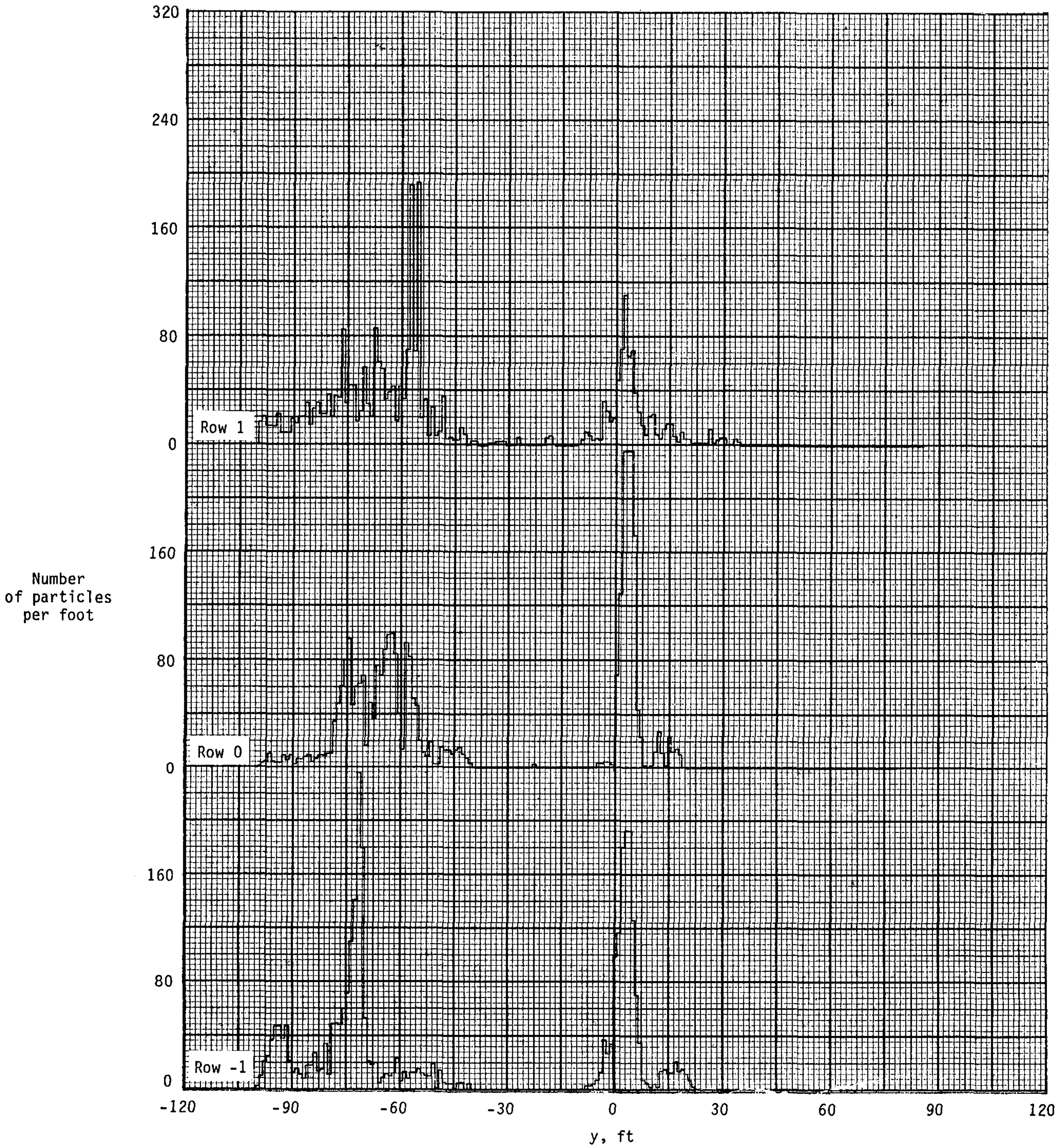

Figure A41.- Ground deposition patterns for flight 54, run 5.1.

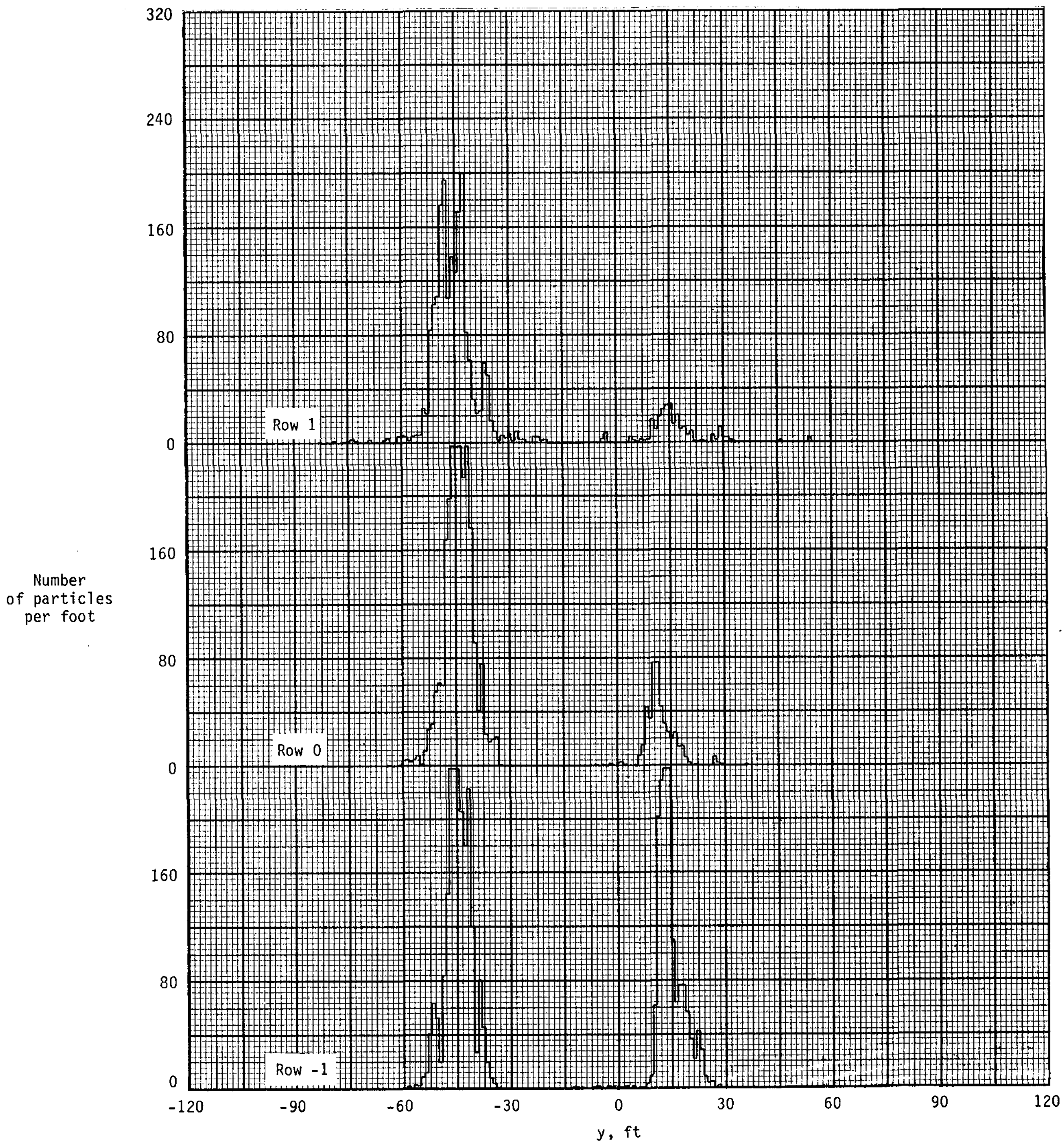

Figure A42.- Ground deposition patterns for flight 54, run 6.1.

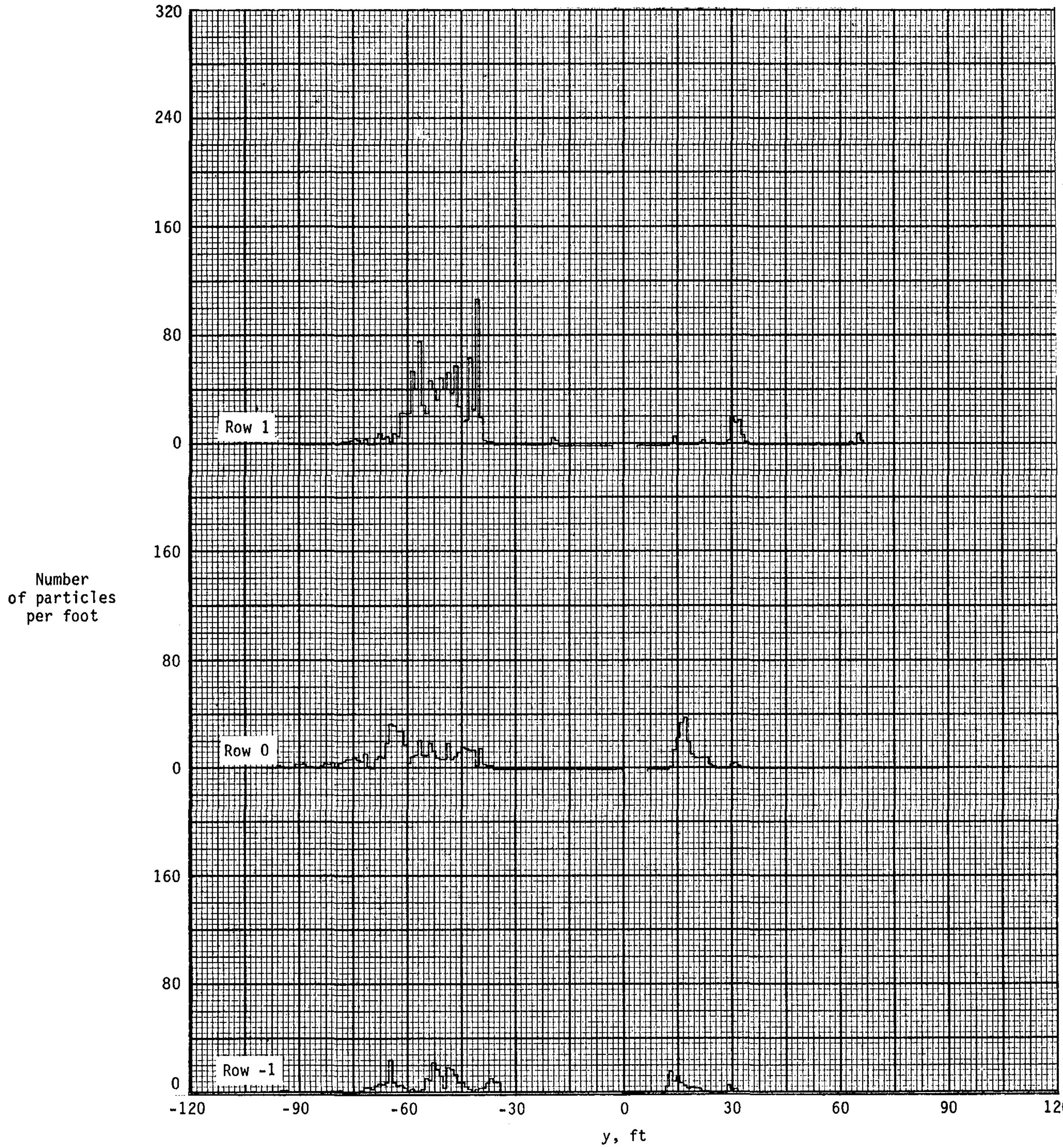

Figure A43.- Ground deposition patterns for flight 54, run 6.2.

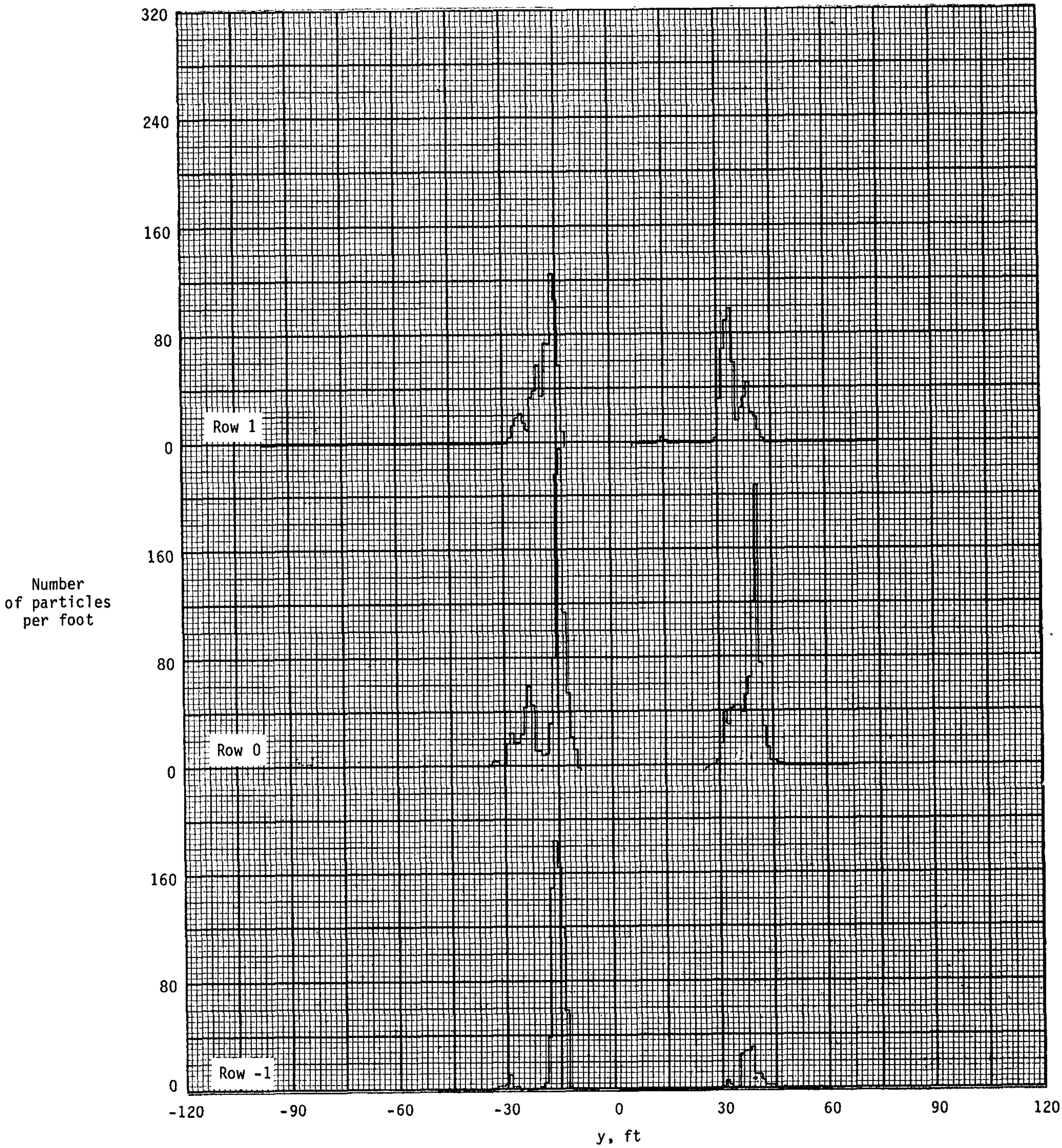

Figure A44.- Ground deposition patterns for flight 55, run 1.1.

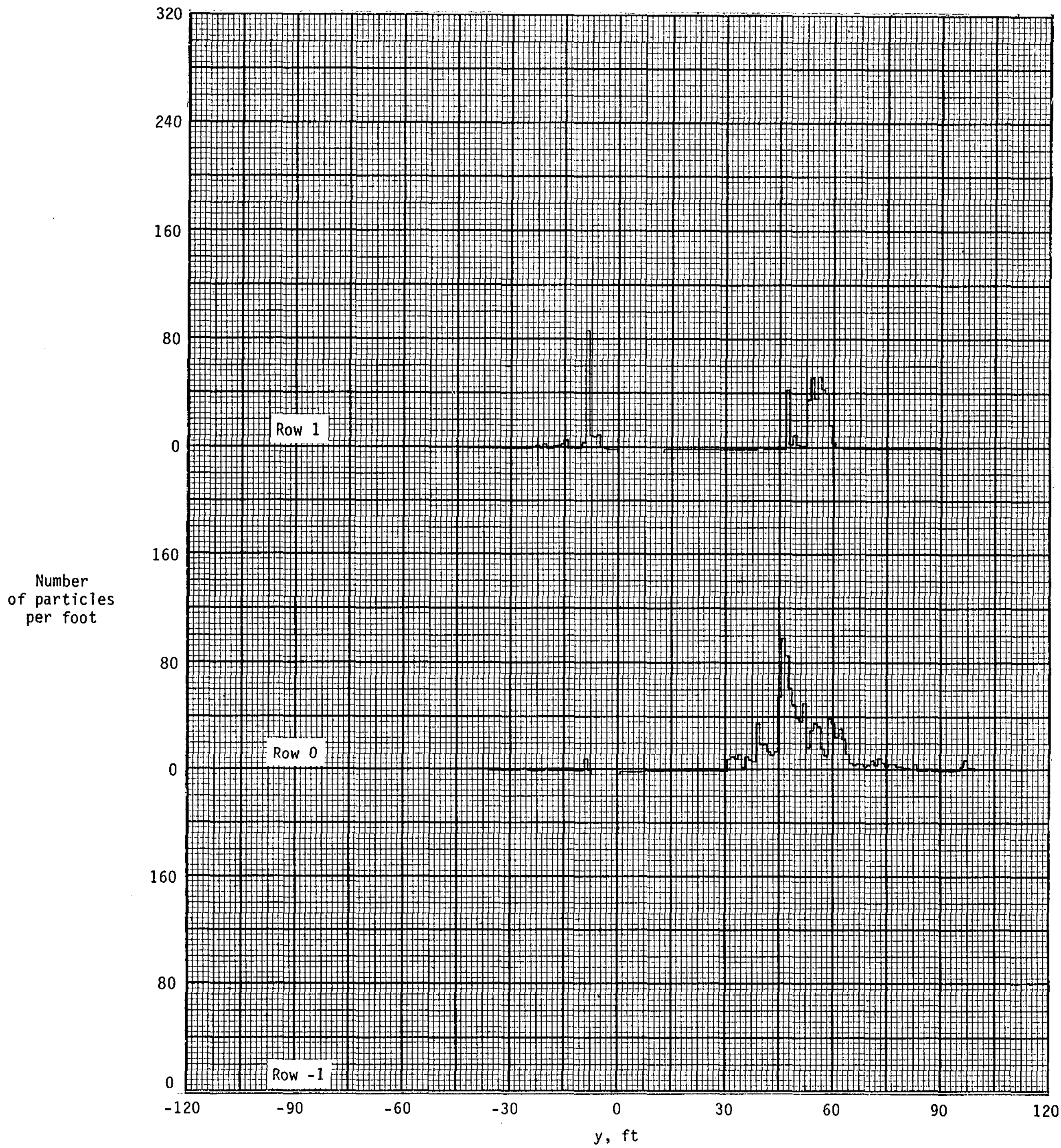

Figure A45.- Ground deposition patterns for flight 55, run 2.1.

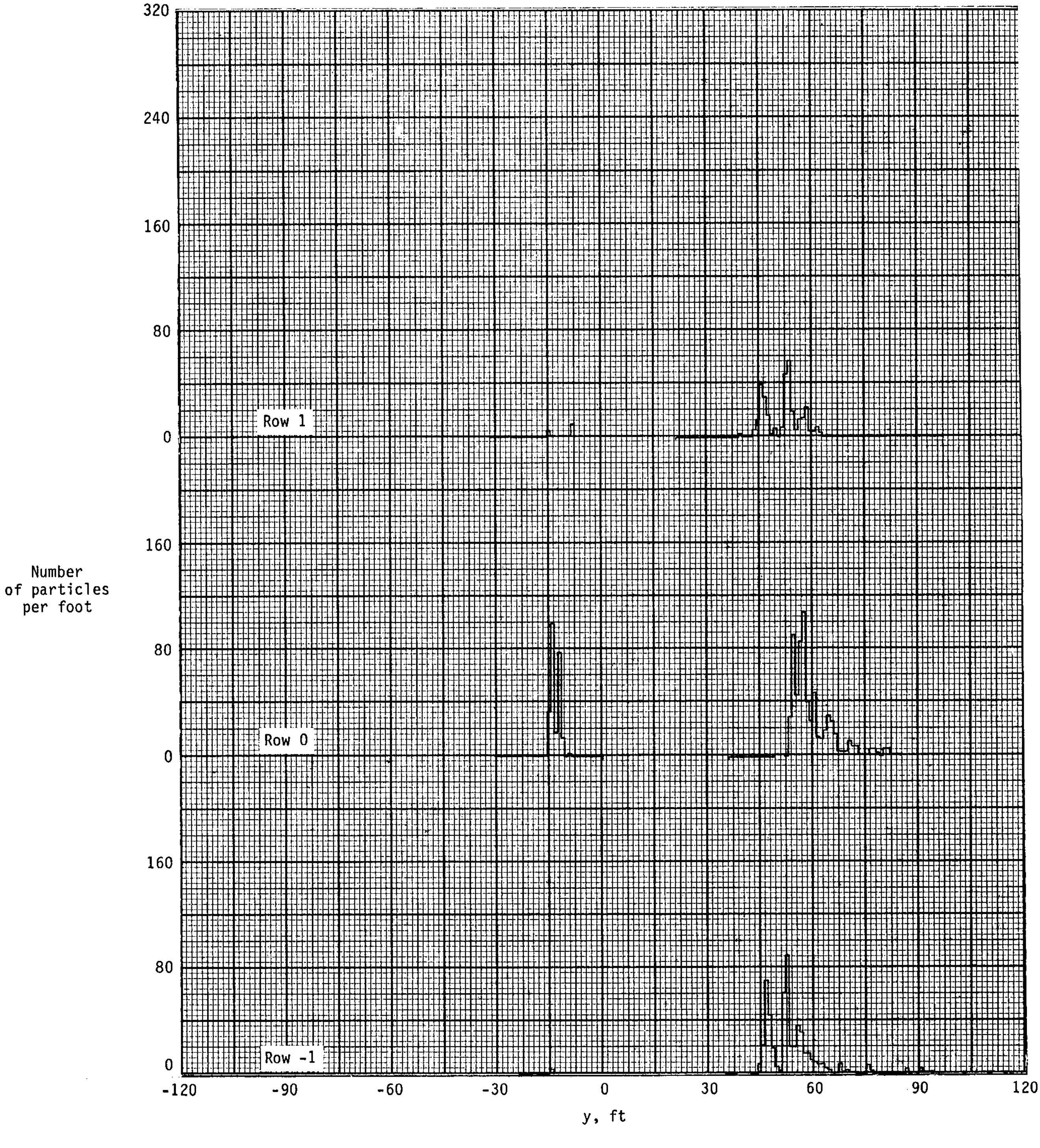

Figure A46.- Ground deposition patterns for flight 55, run 2.2.

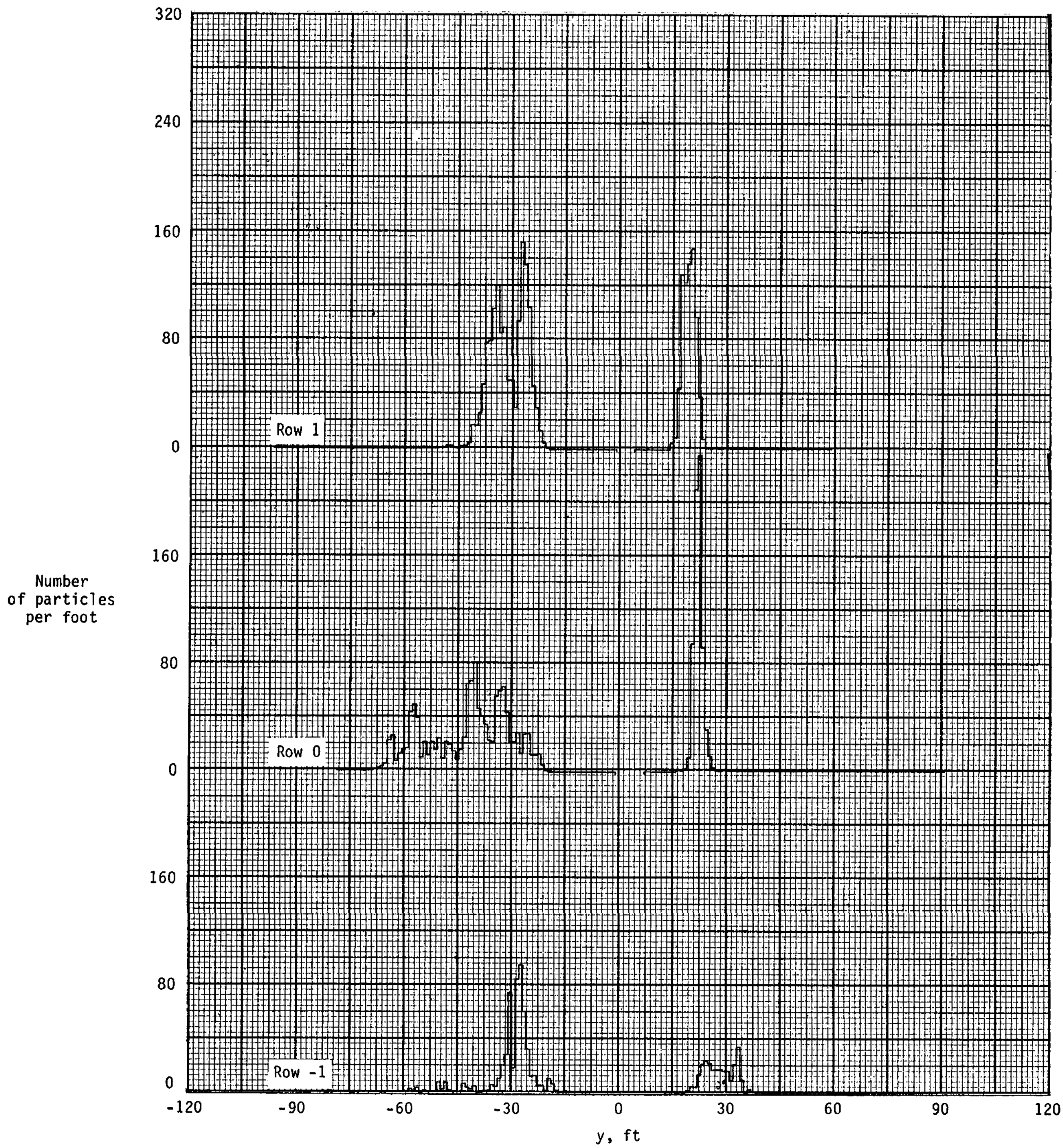

Figure A47.- Ground deposition patterns for flight 56, run 1.1.

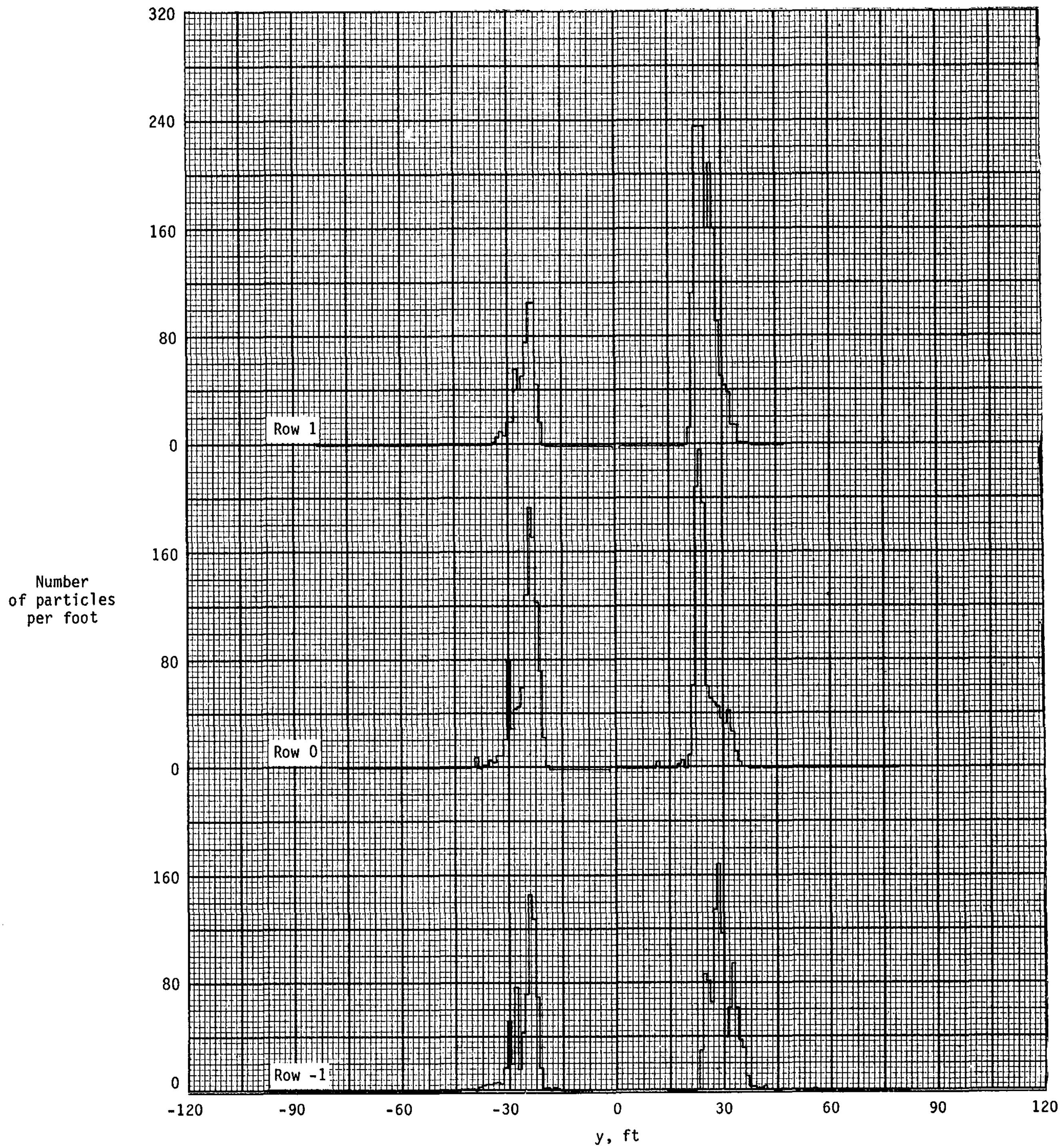

Figure A48.- Ground deposition patterns for flight 56, run 2.0.

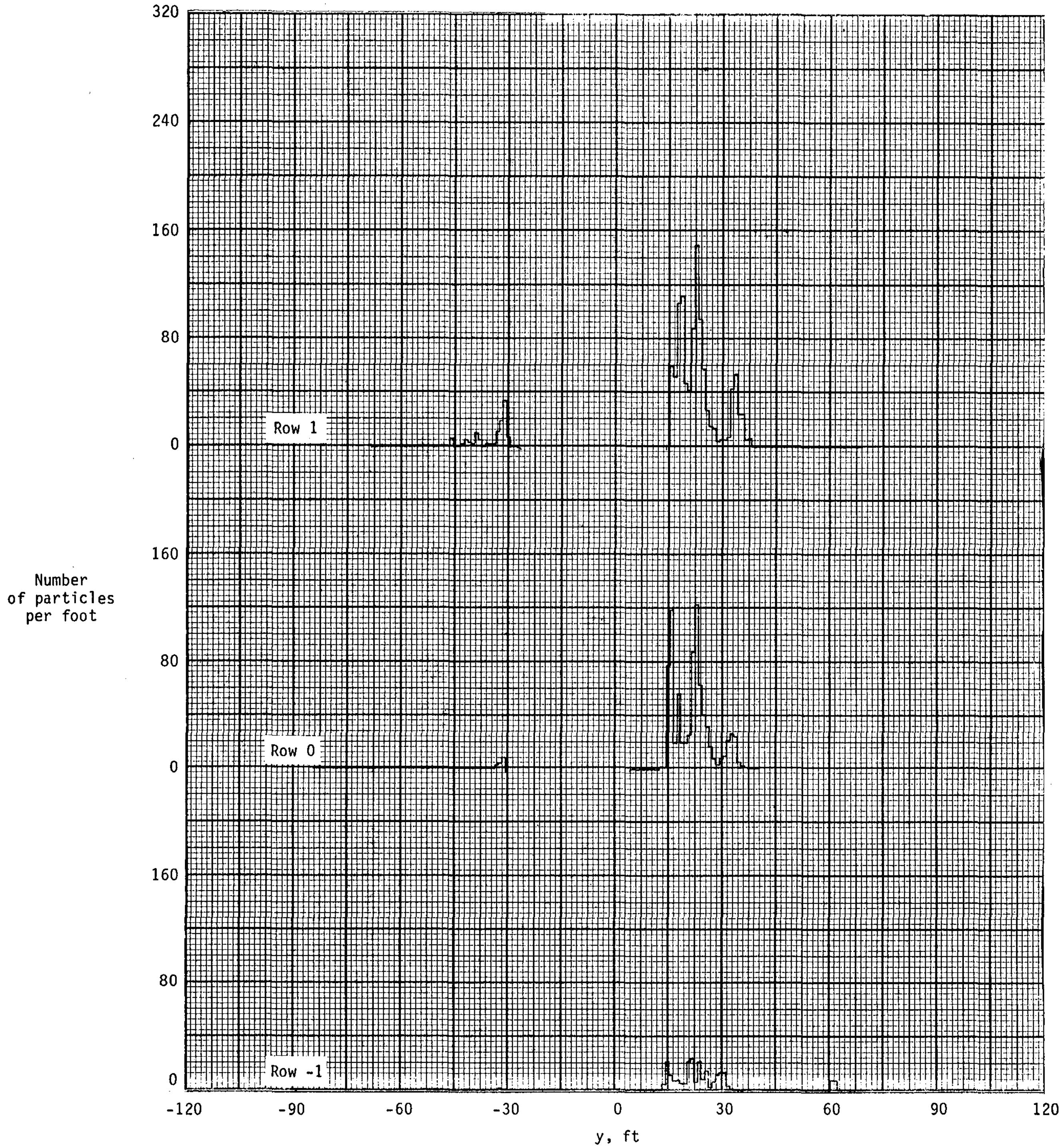

Figure A49.- Ground deposition patterns for flight 56, run 2.1.

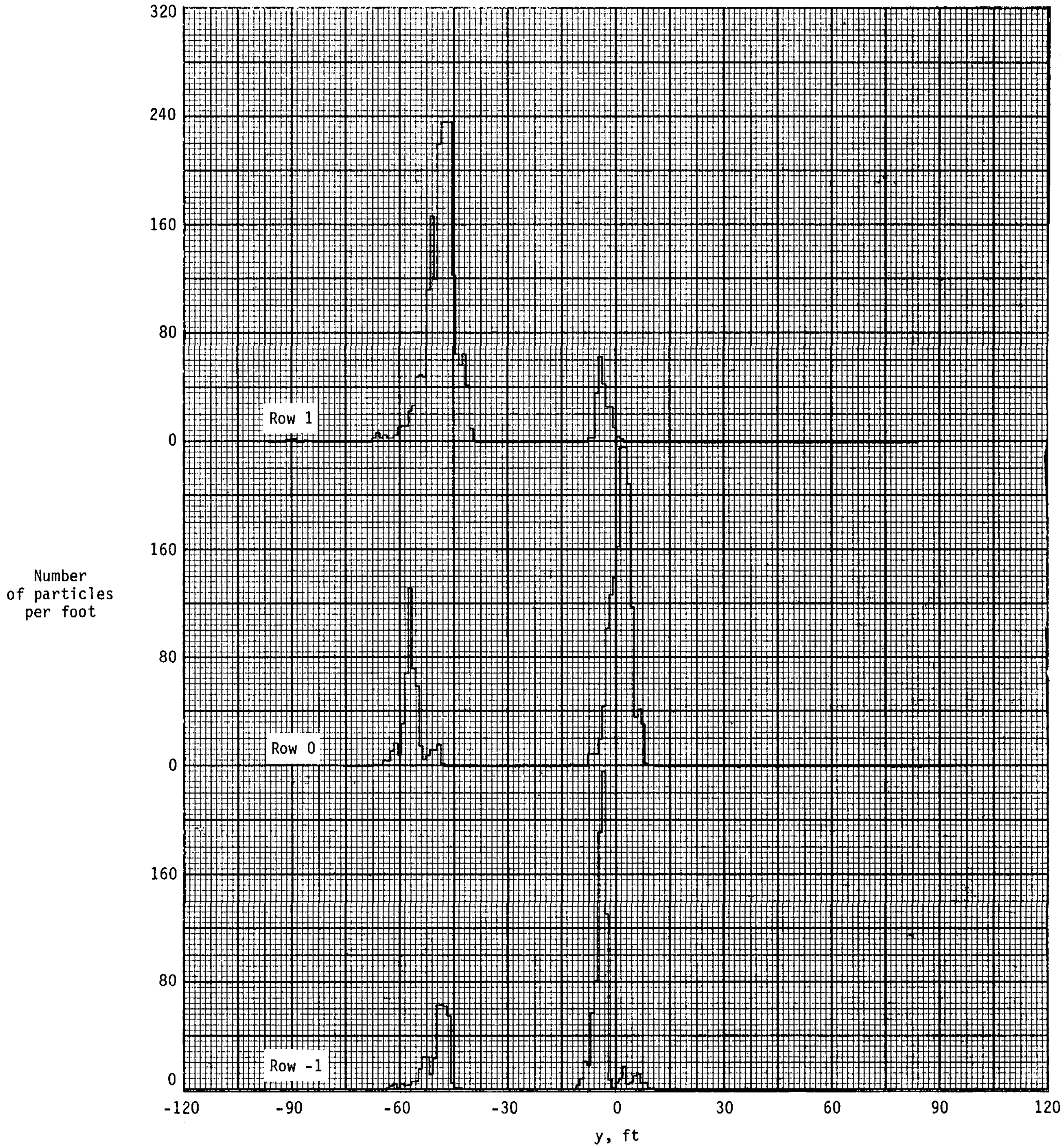

Figure A50.- Ground deposition patterns for flight 56, run 3.2.

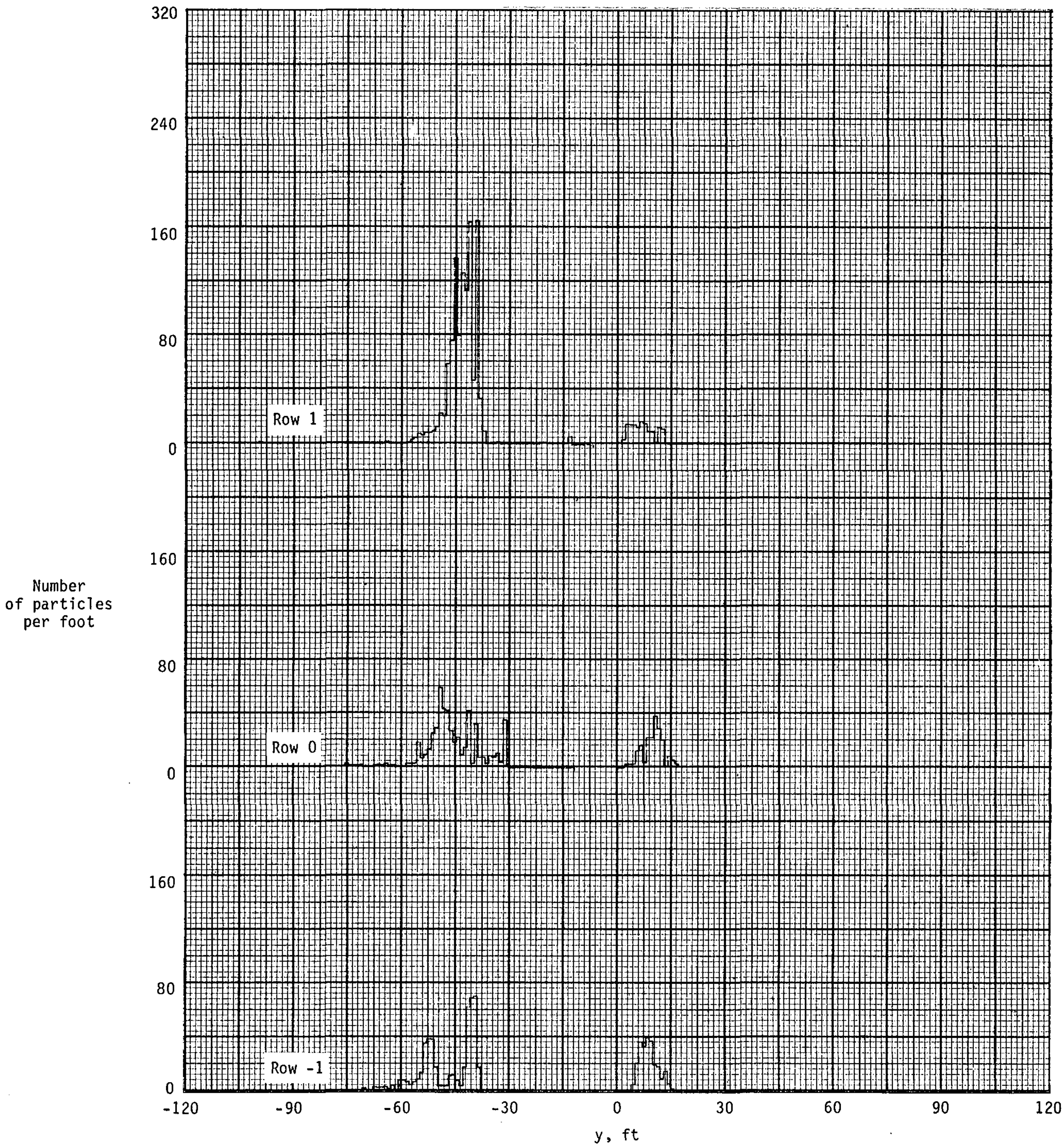

Figure A51.- Ground deposition patterns for flight 56, run 3.4.

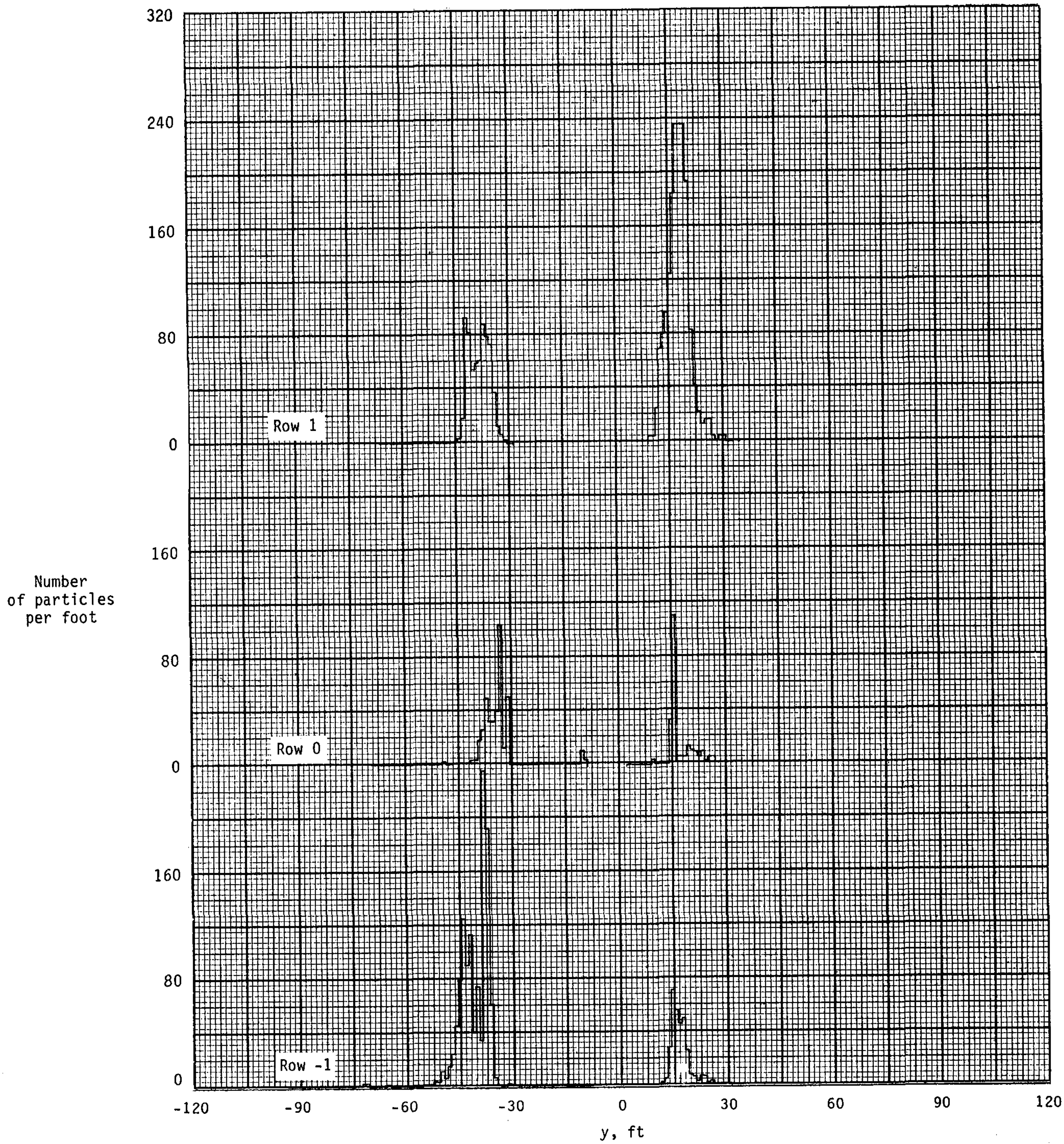

Figure A52.- Ground deposition patterns for flight 56, run 4.1.

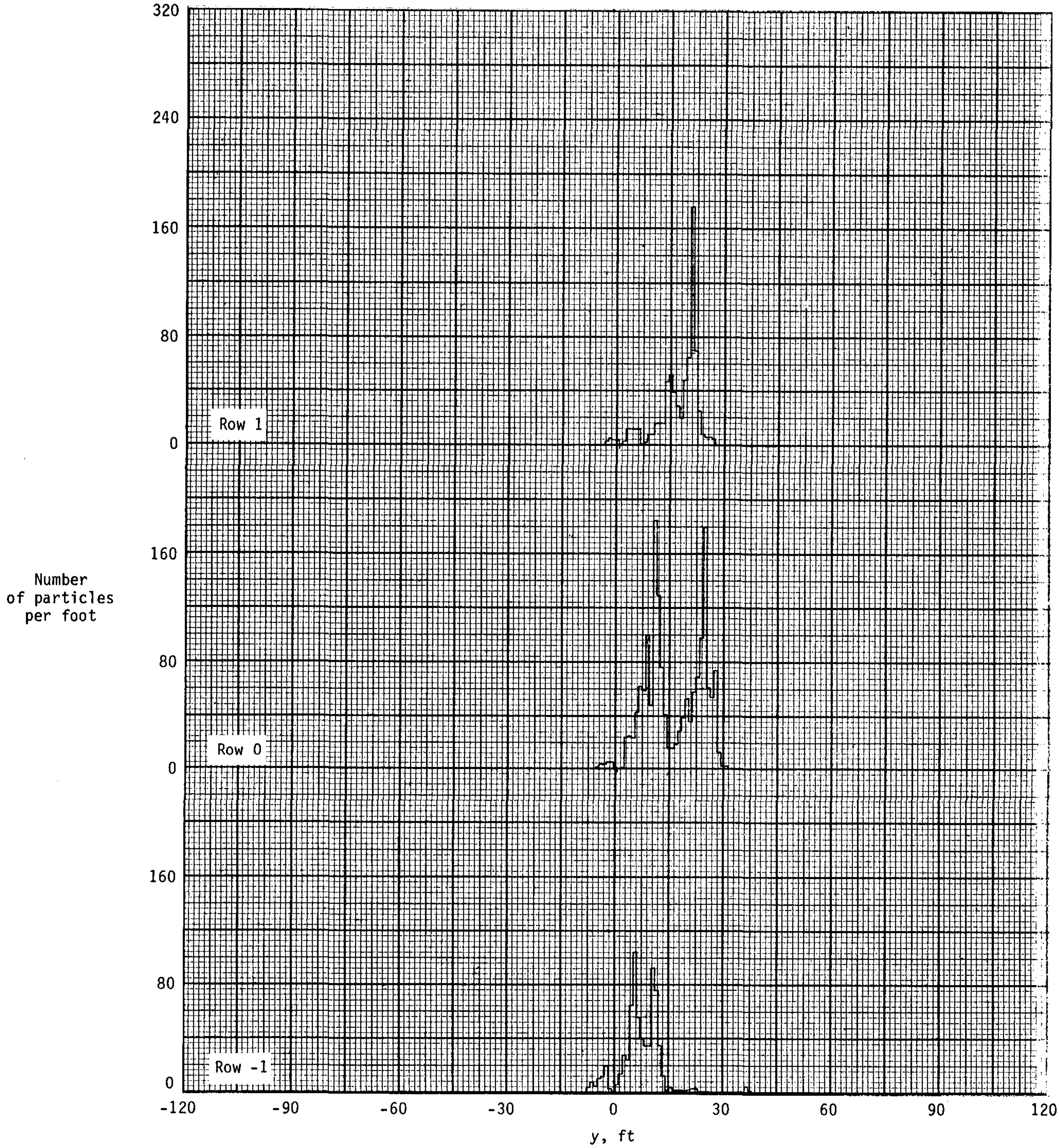

Figure A53.- Ground deposition patterns for flight 57, run 1.1.

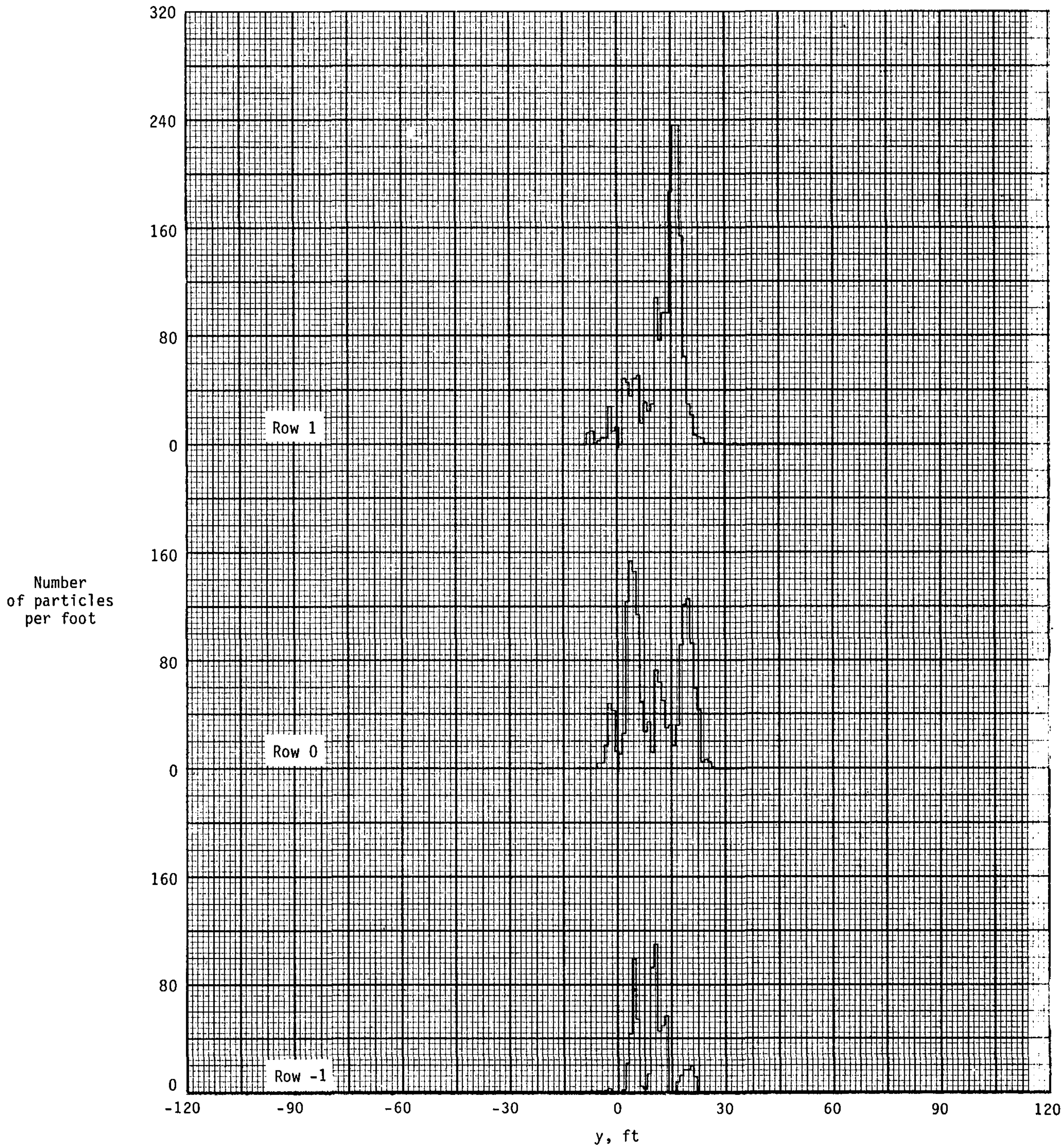

Figure A54.- Ground deposition patterns for flight 57, run 1.2.

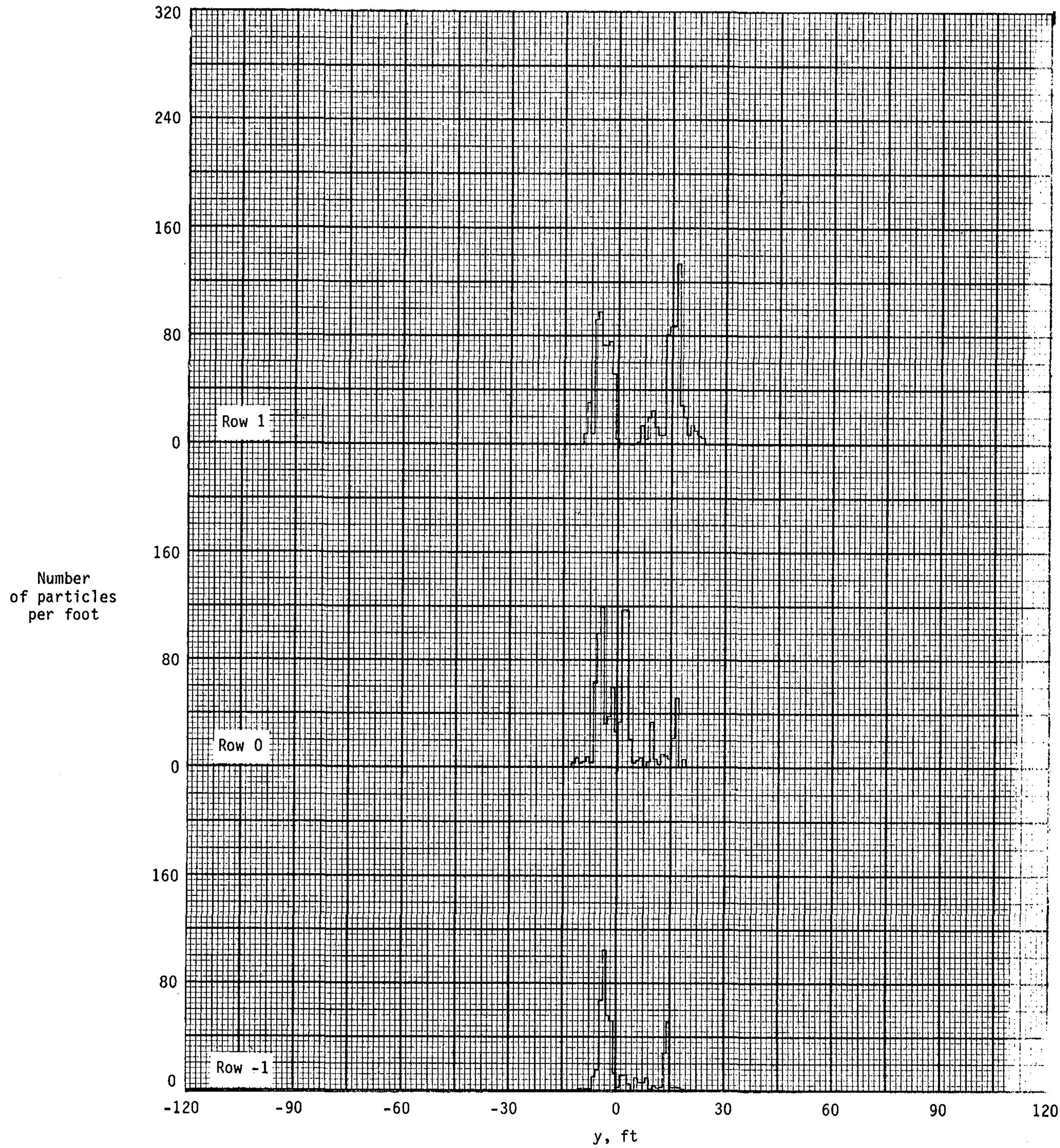

Figure A55.- Ground deposition patterns for flight 57, run 2.6.

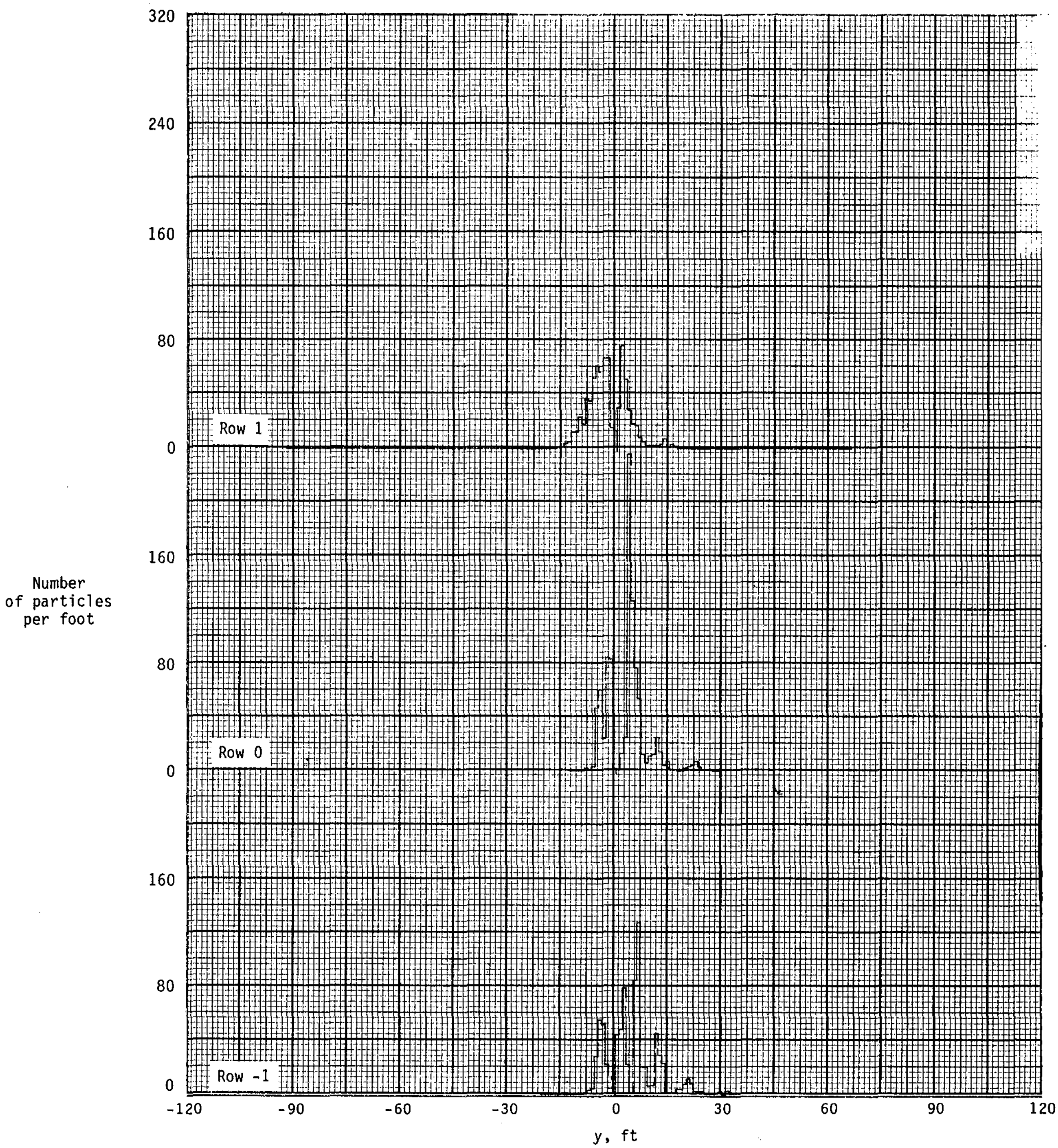

Figure A56.- Ground deposition patterns for flight 58, run 1.5.

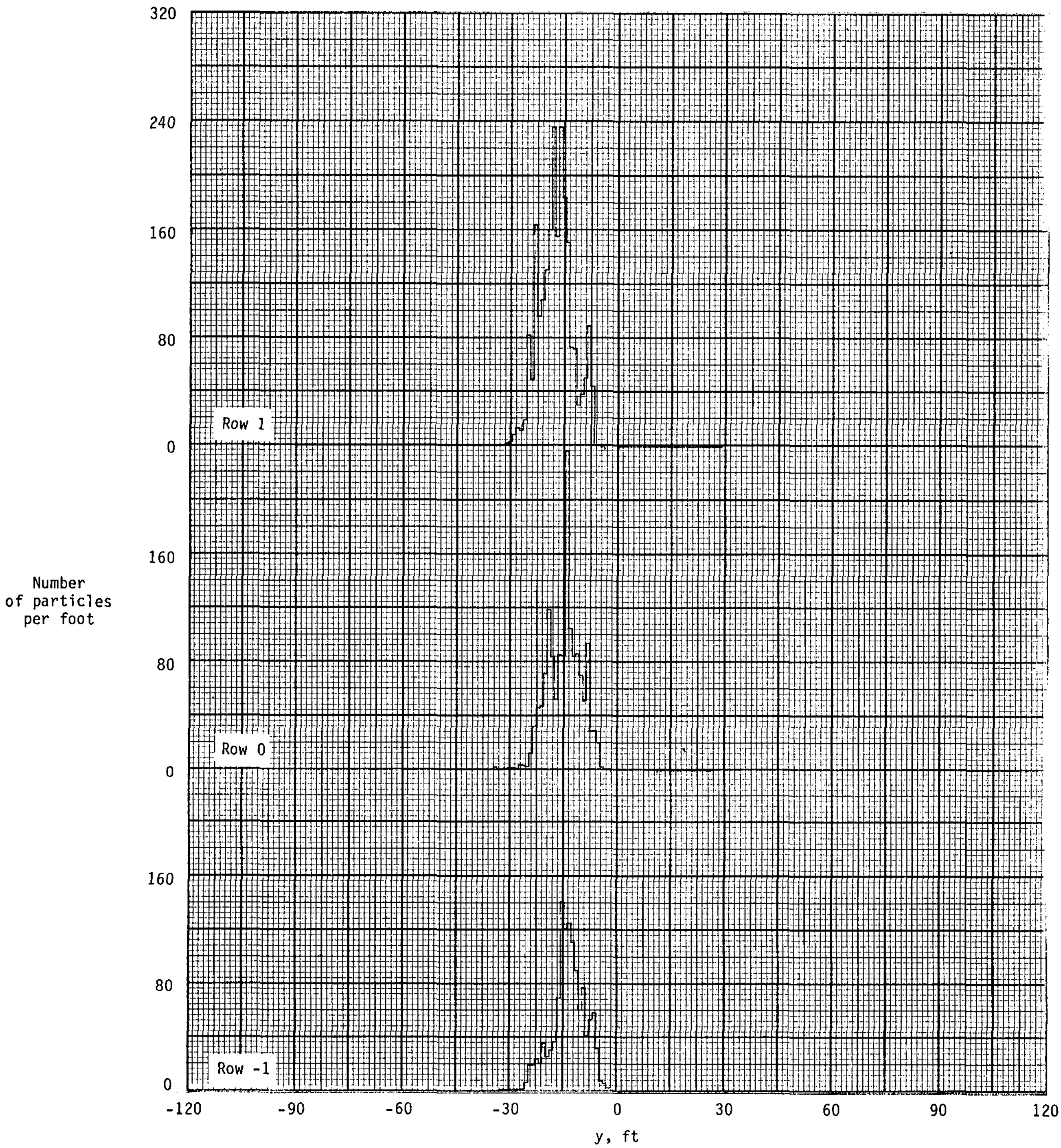

Figure A57.- Ground deposition patterns for flight 58, run 1.8.

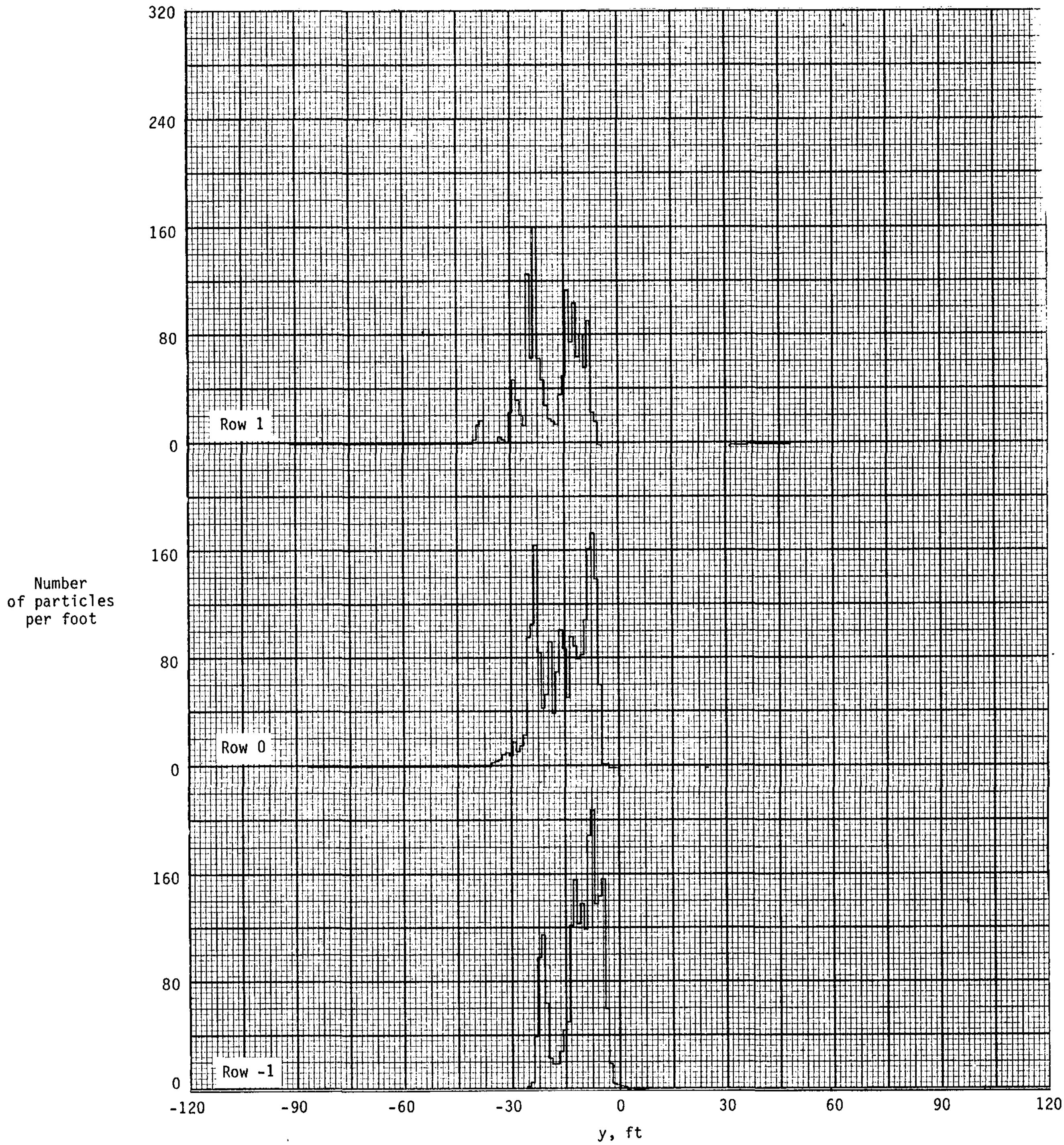

Figure A58.- Ground deposition patterns for flight 58, run 2.0.

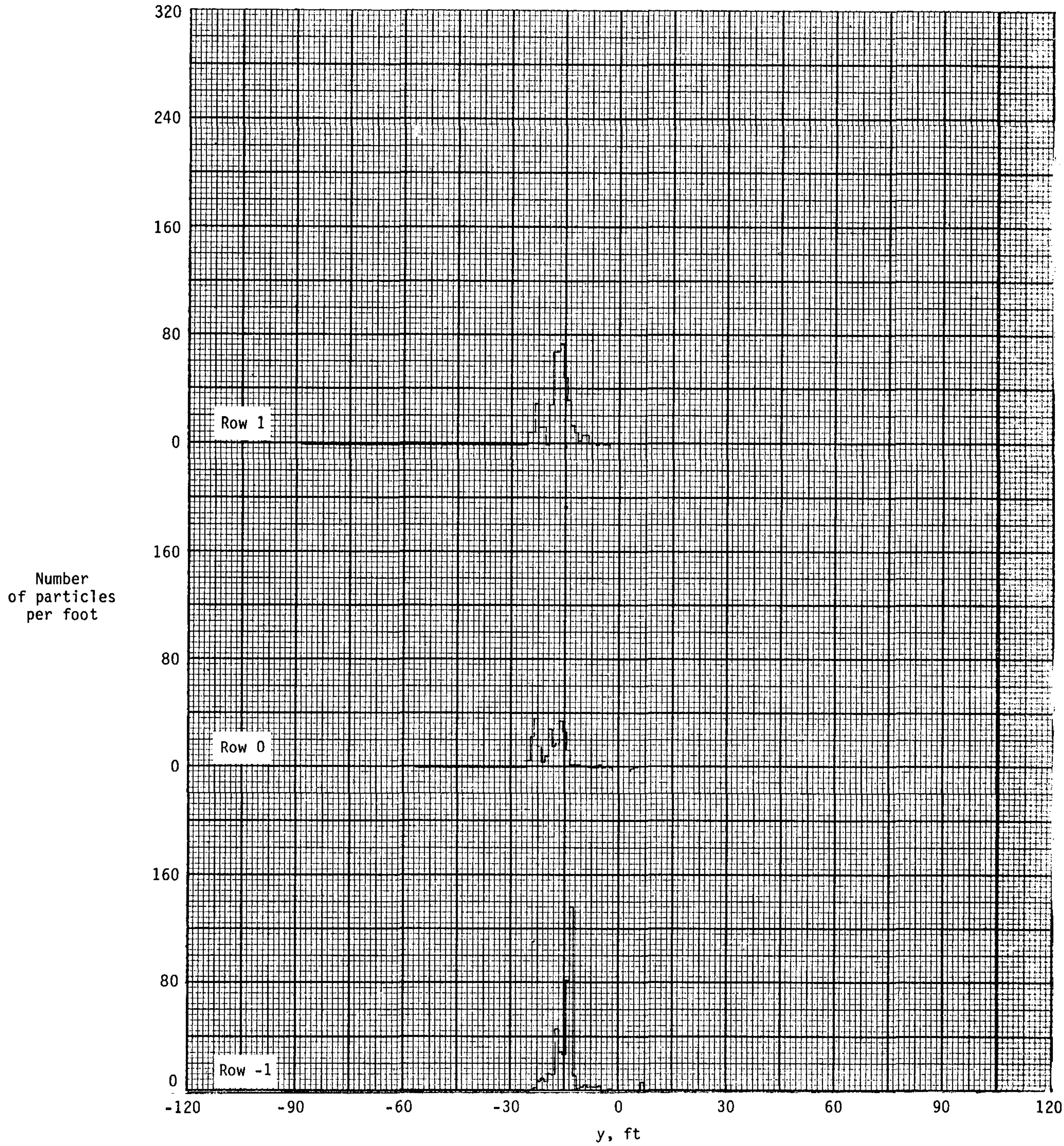

Figure A59.- Ground deposition patterns for flight 58, run 2.9.

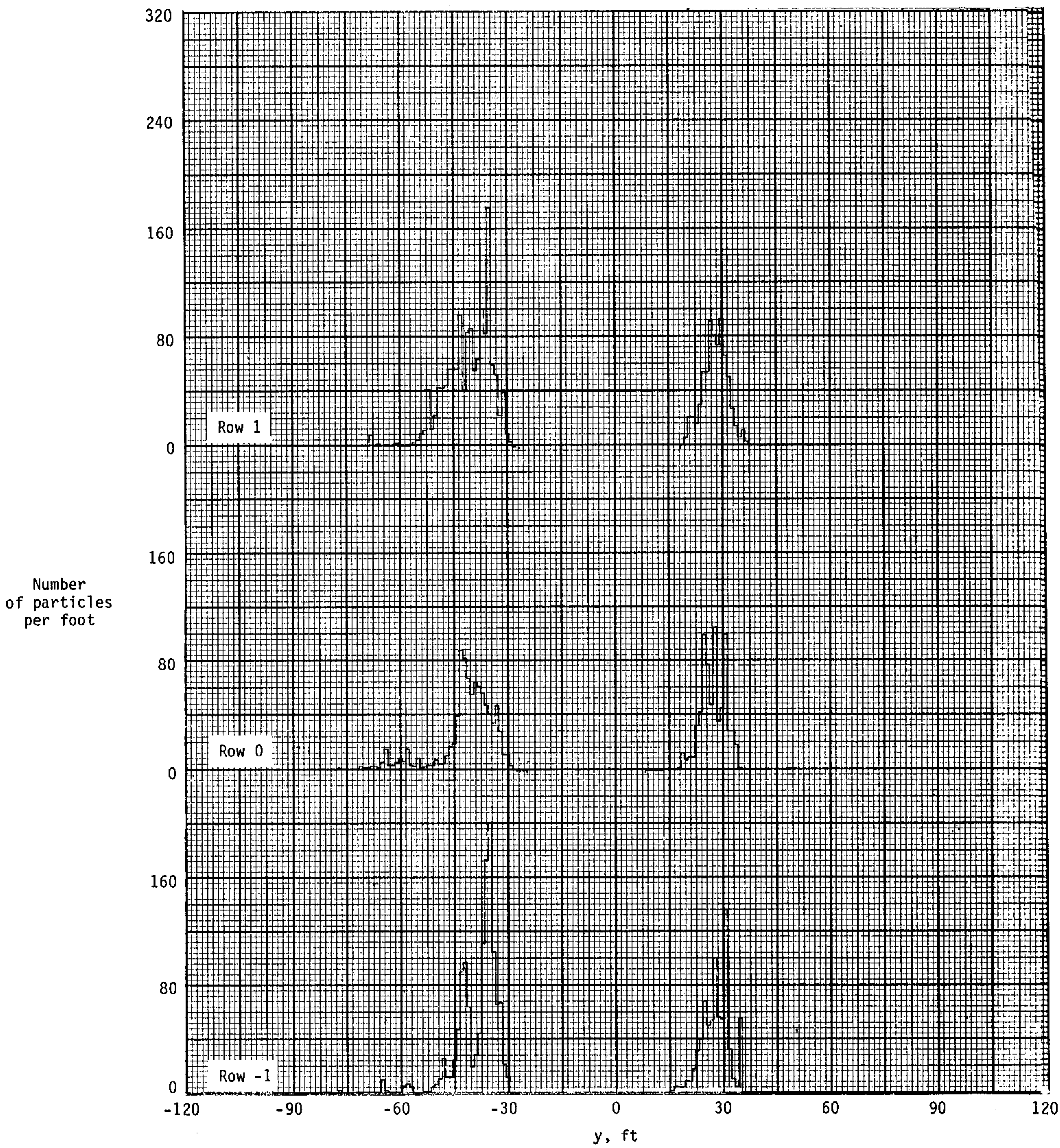

Figure A60.- Ground deposition patterns for flight 59, run 1.3.

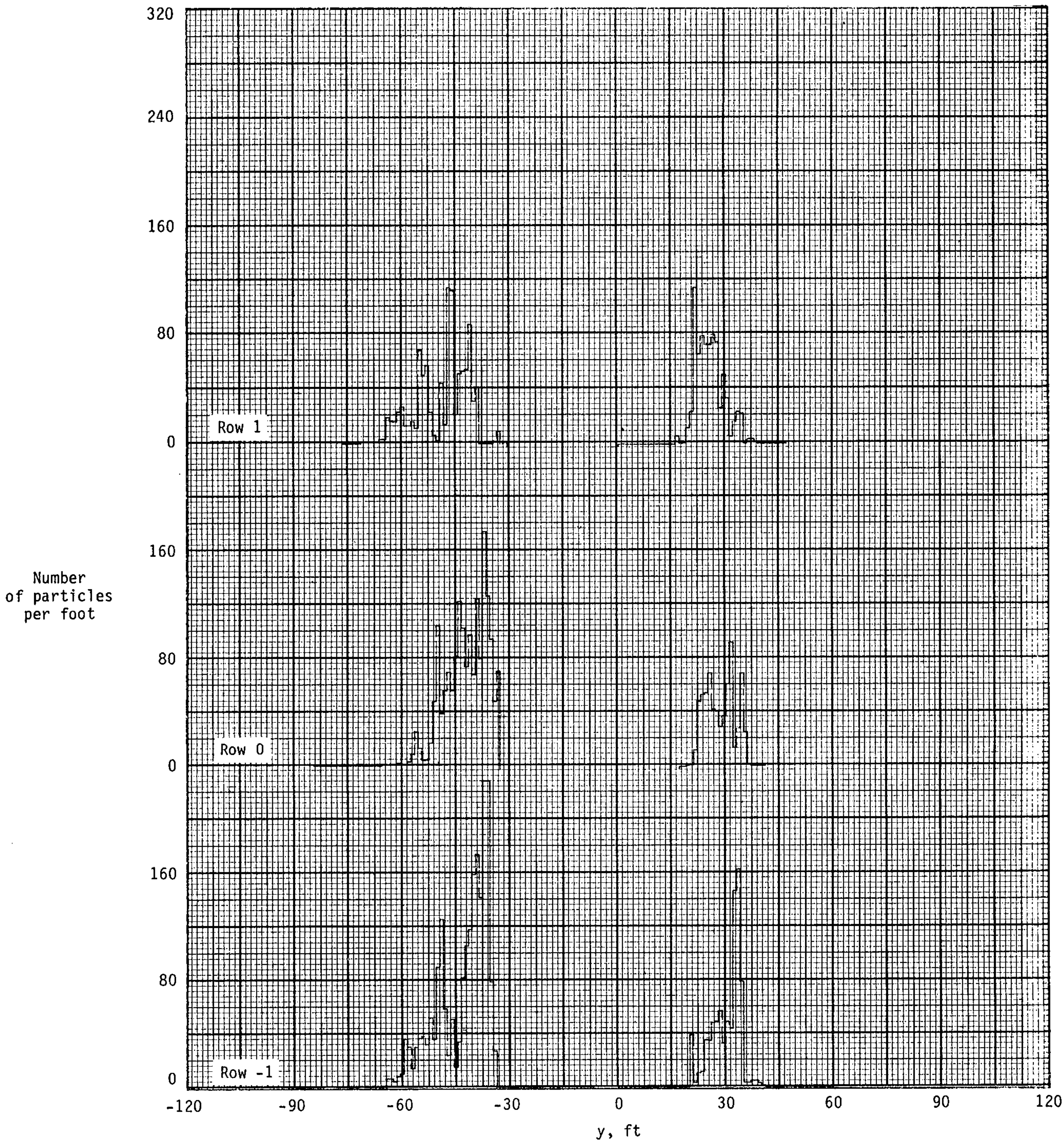

Figure A61.- Ground deposition patterns for flight 59, run 2.0.

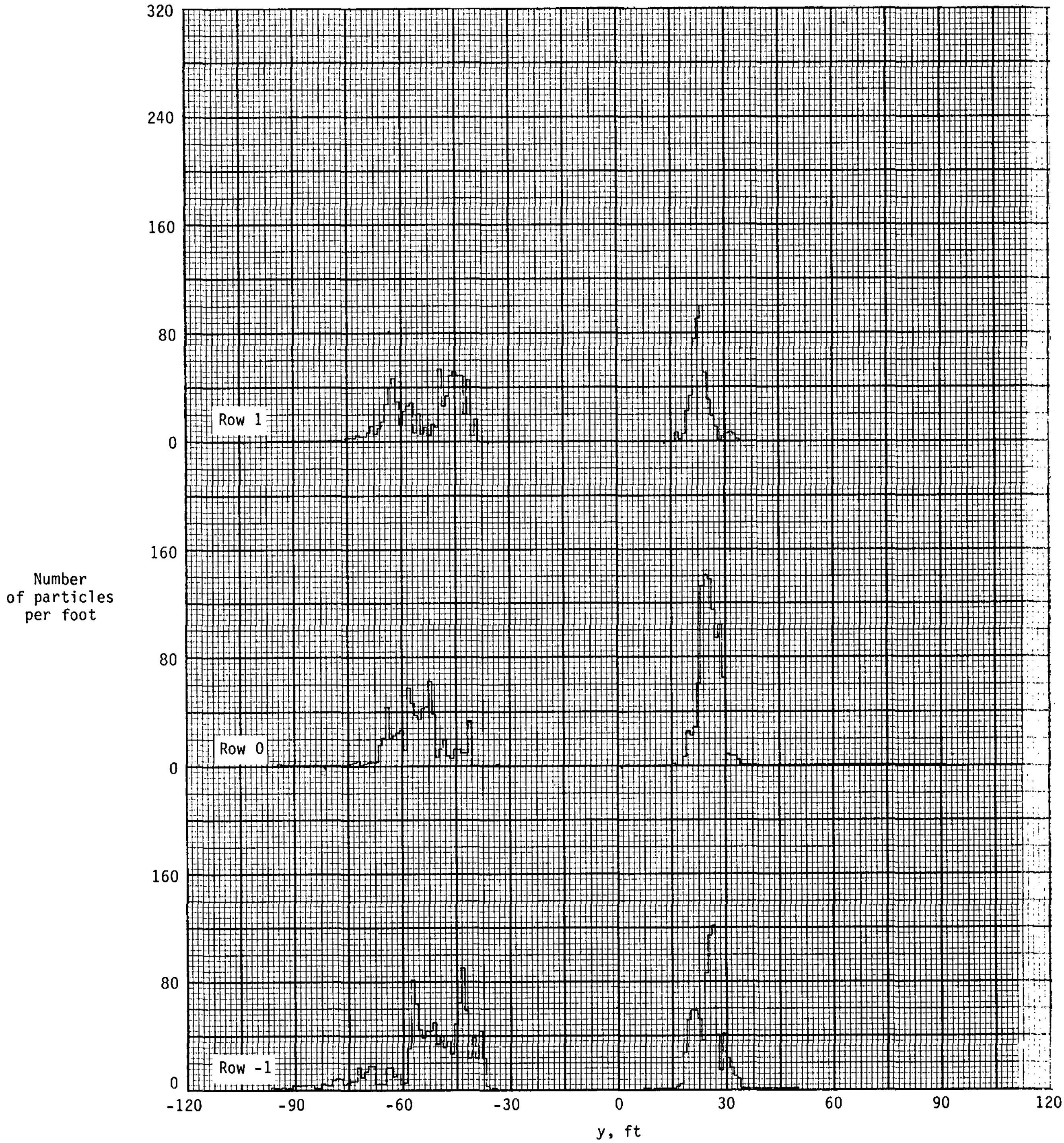

Figure A62.- Ground deposition patterns for flight 59, run 2.1.

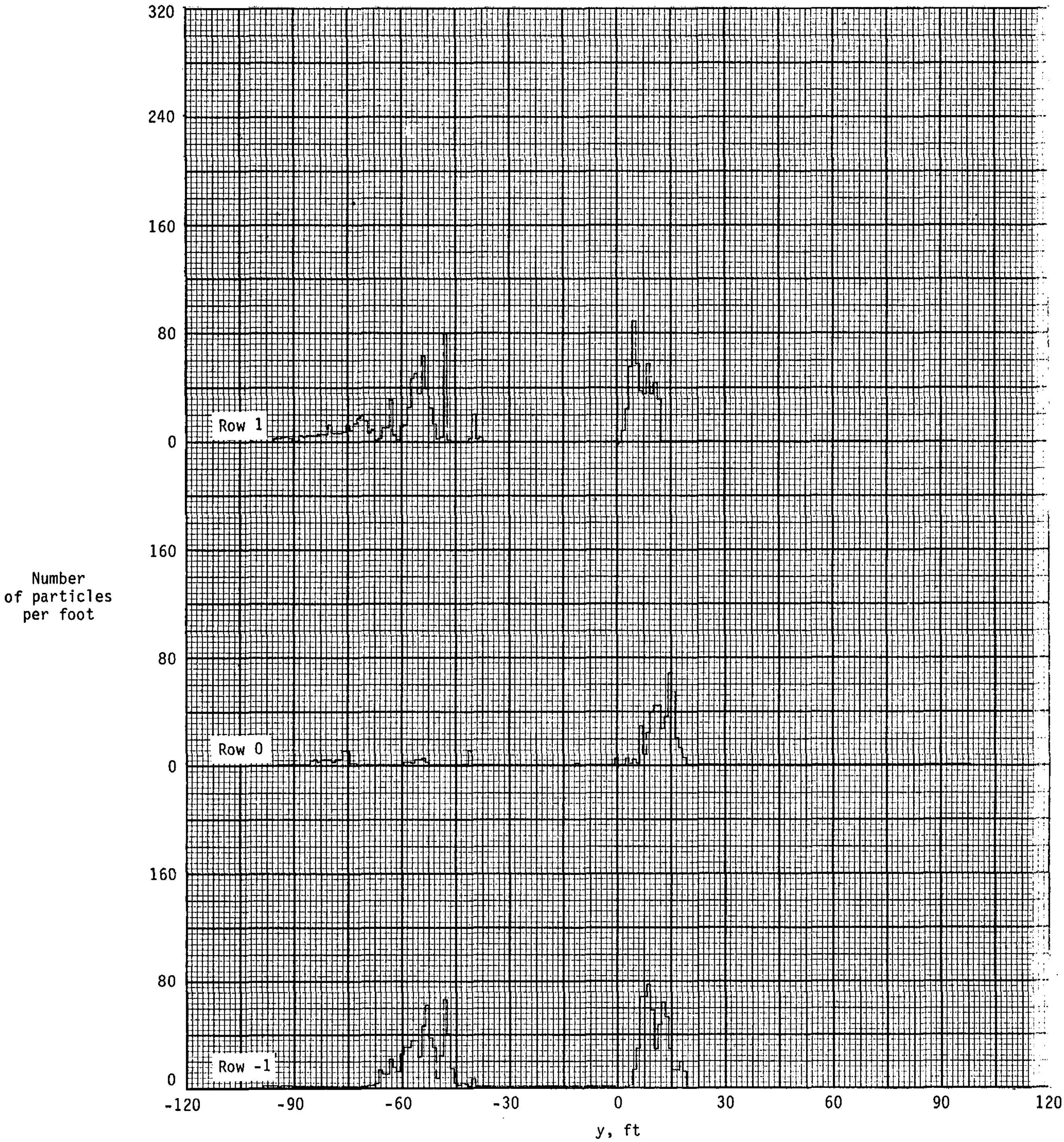

Figure A63.- Ground deposition patterns for flight 59, run 3.2.

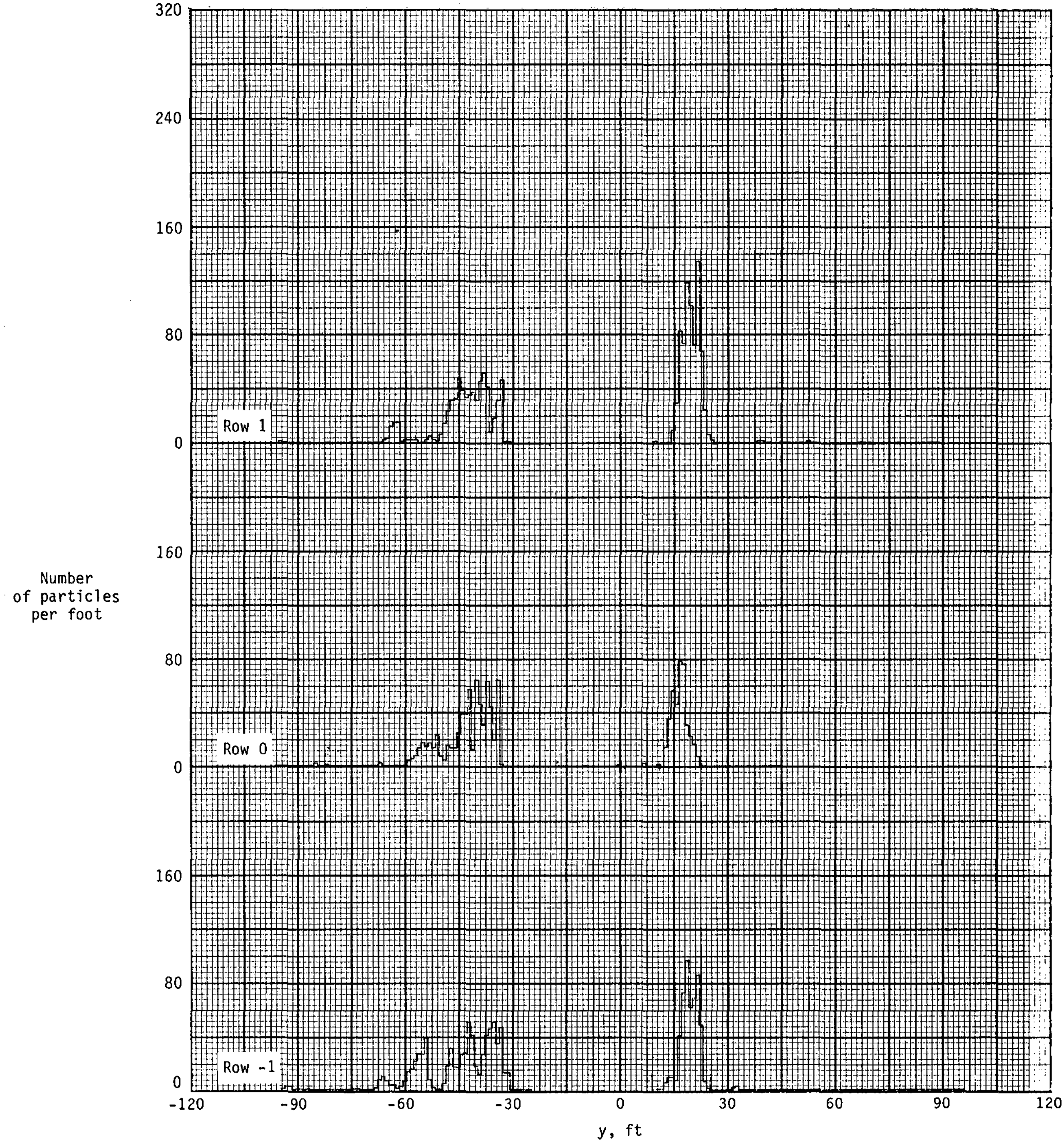

Figure A64.- Ground deposition patterns for flight 59, run 3.7.

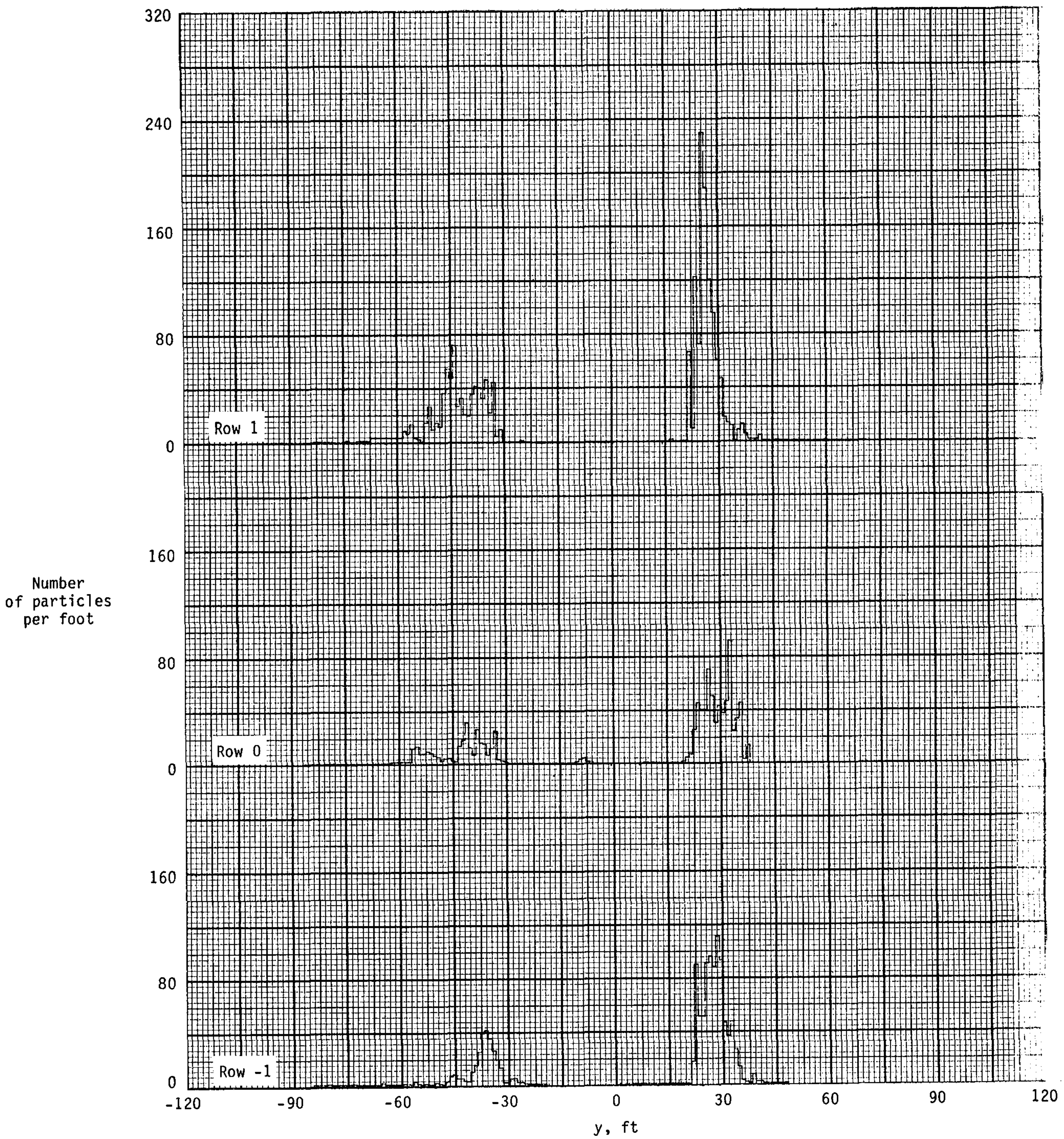

Figure A65.- Ground deposition patterns for flight 59, run 4.0.

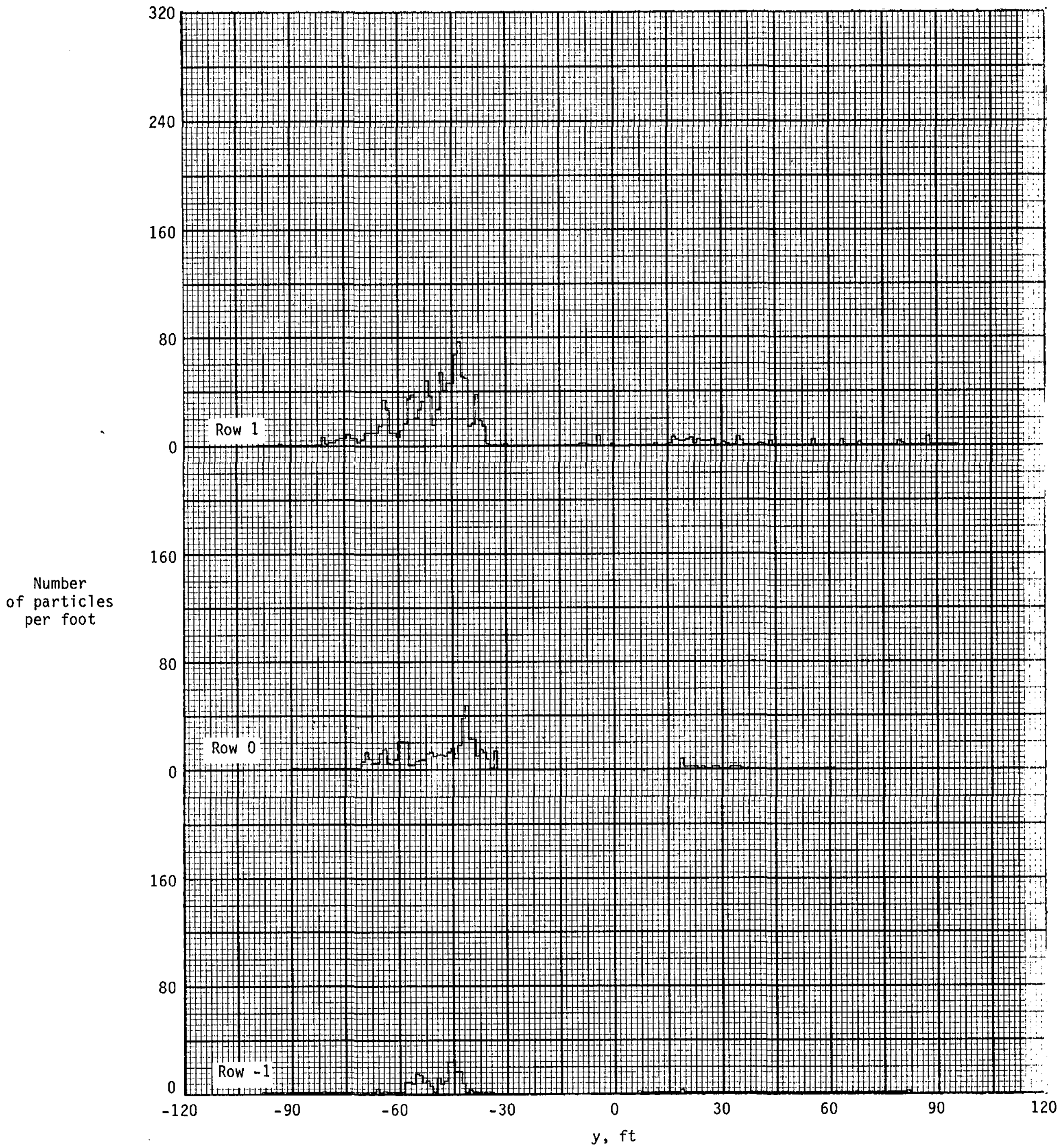

Figure A66.- Ground deposition patterns for flight 59, run 4.1.

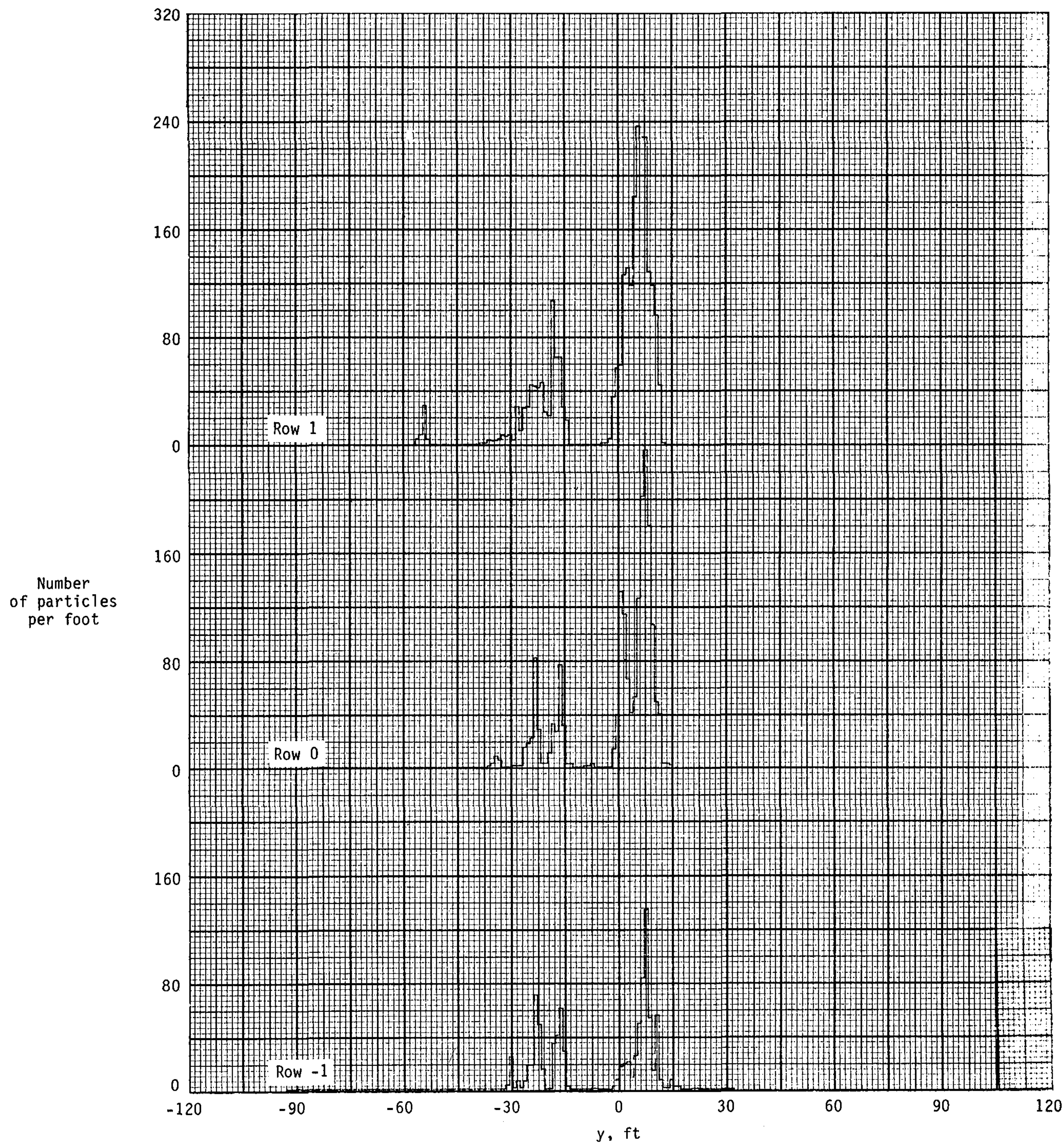

Figure A67.- Ground deposition patterns for flight 60, run 1.6.

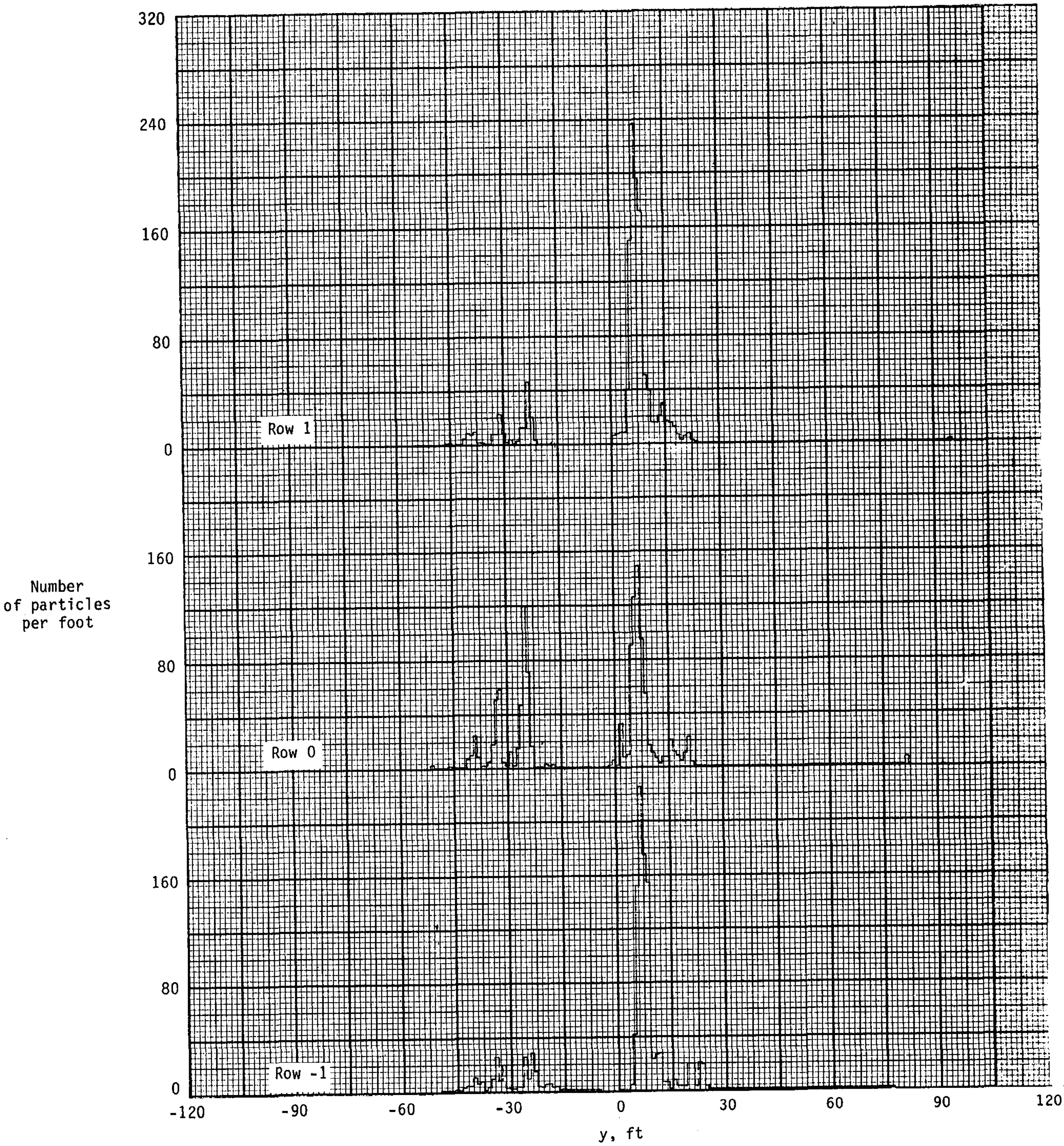

Figure A68.- Ground deposition patterns for flight 60, run 2.1.

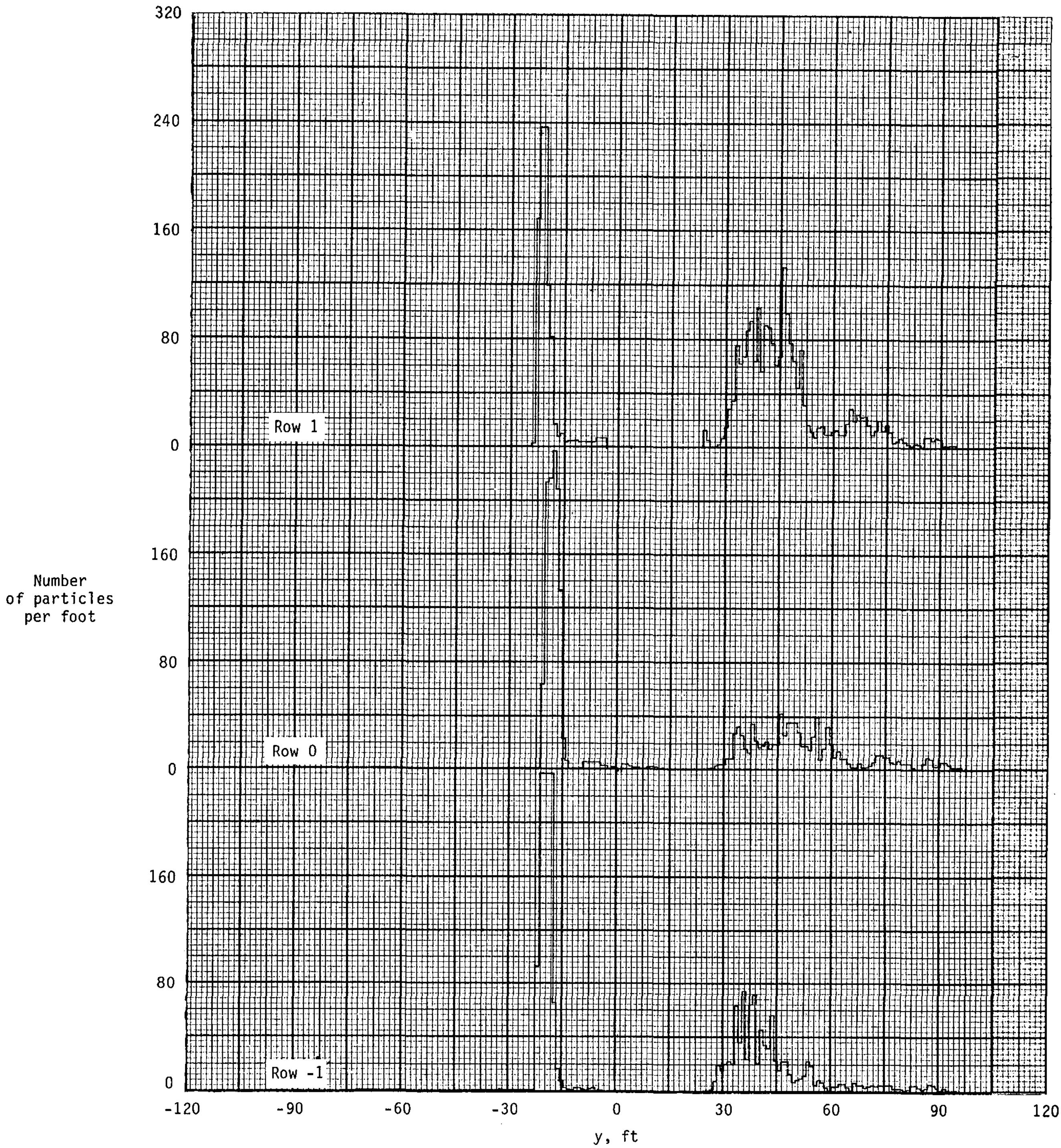

Figure A69.- Ground deposition patterns for flight 67, run 1.1.

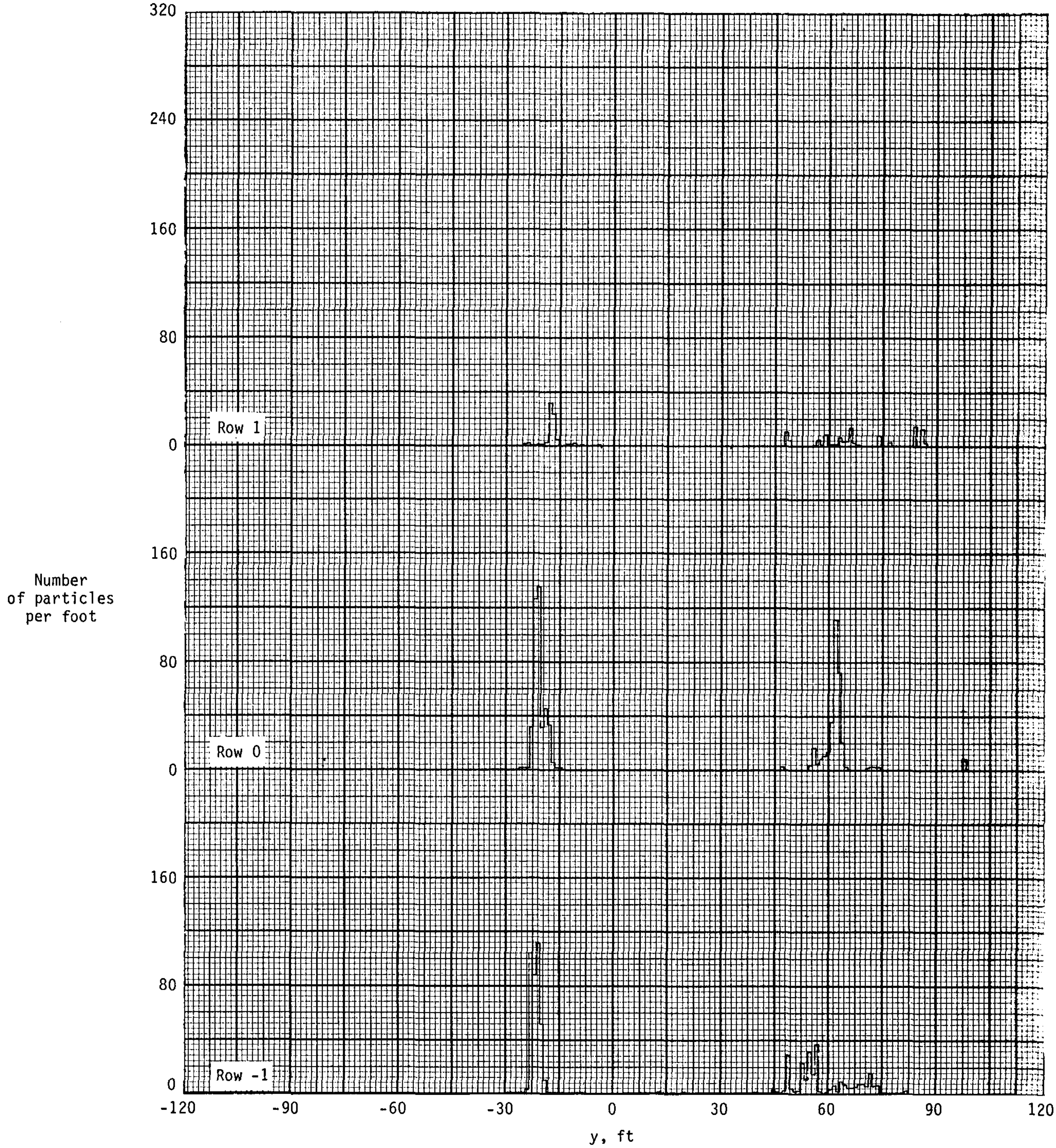

Figure A70.- Ground deposition patterns for flight 67, run 2.1.

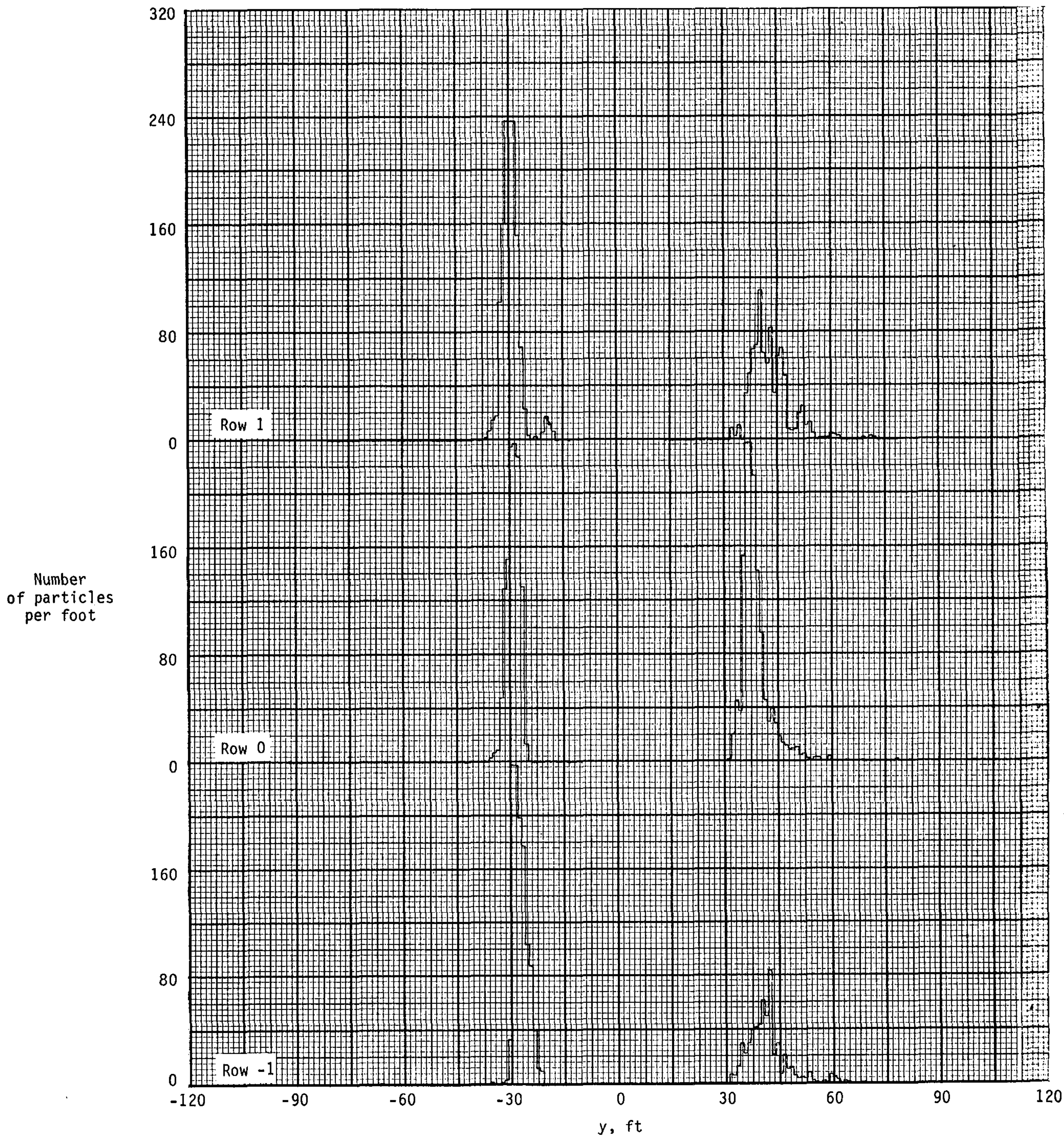

Figure A71.- Ground deposition patterns for flight 74, run 1.0.

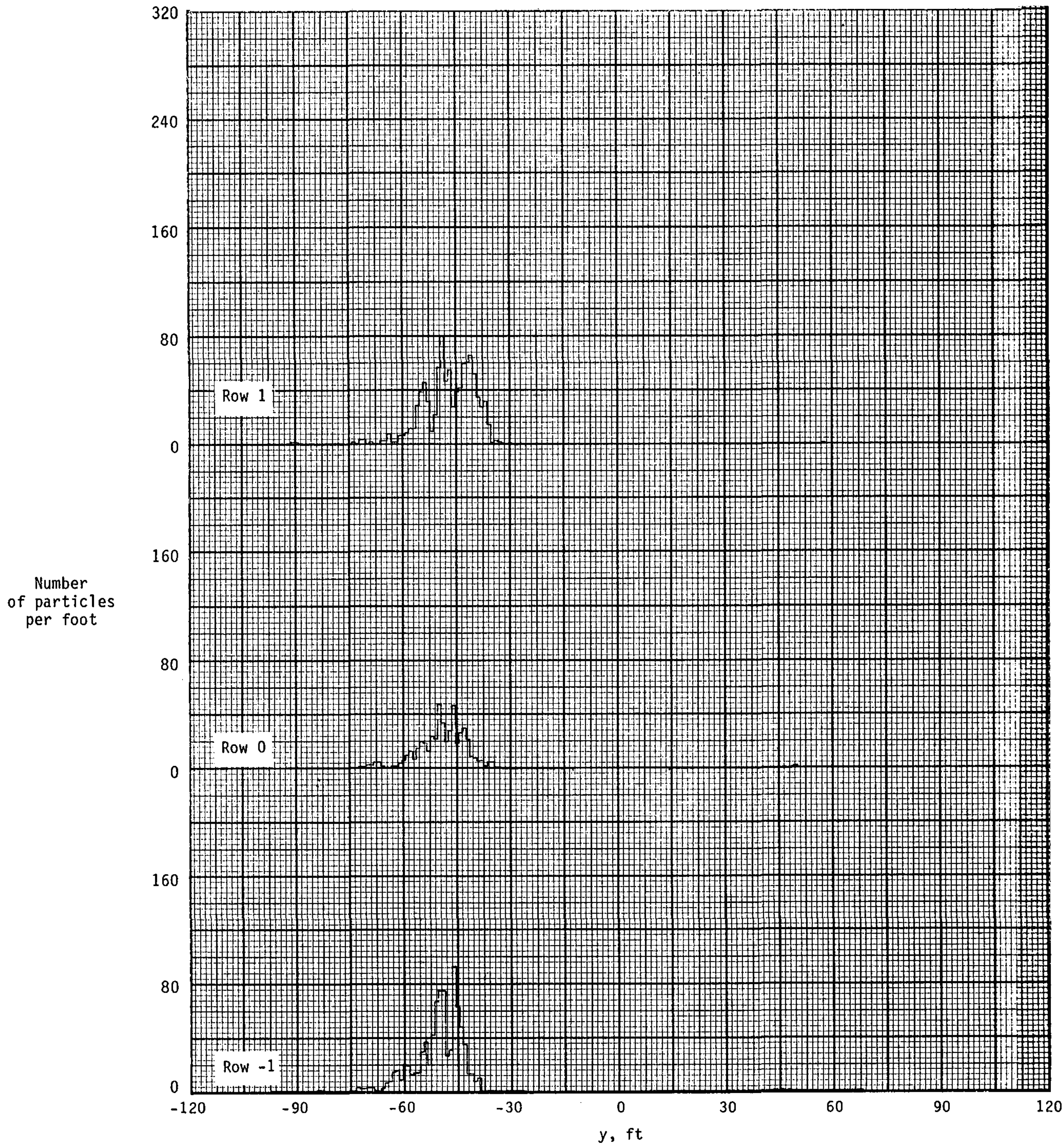

Figure A72.- Ground deposition patterns for flight 74, run 2.4.

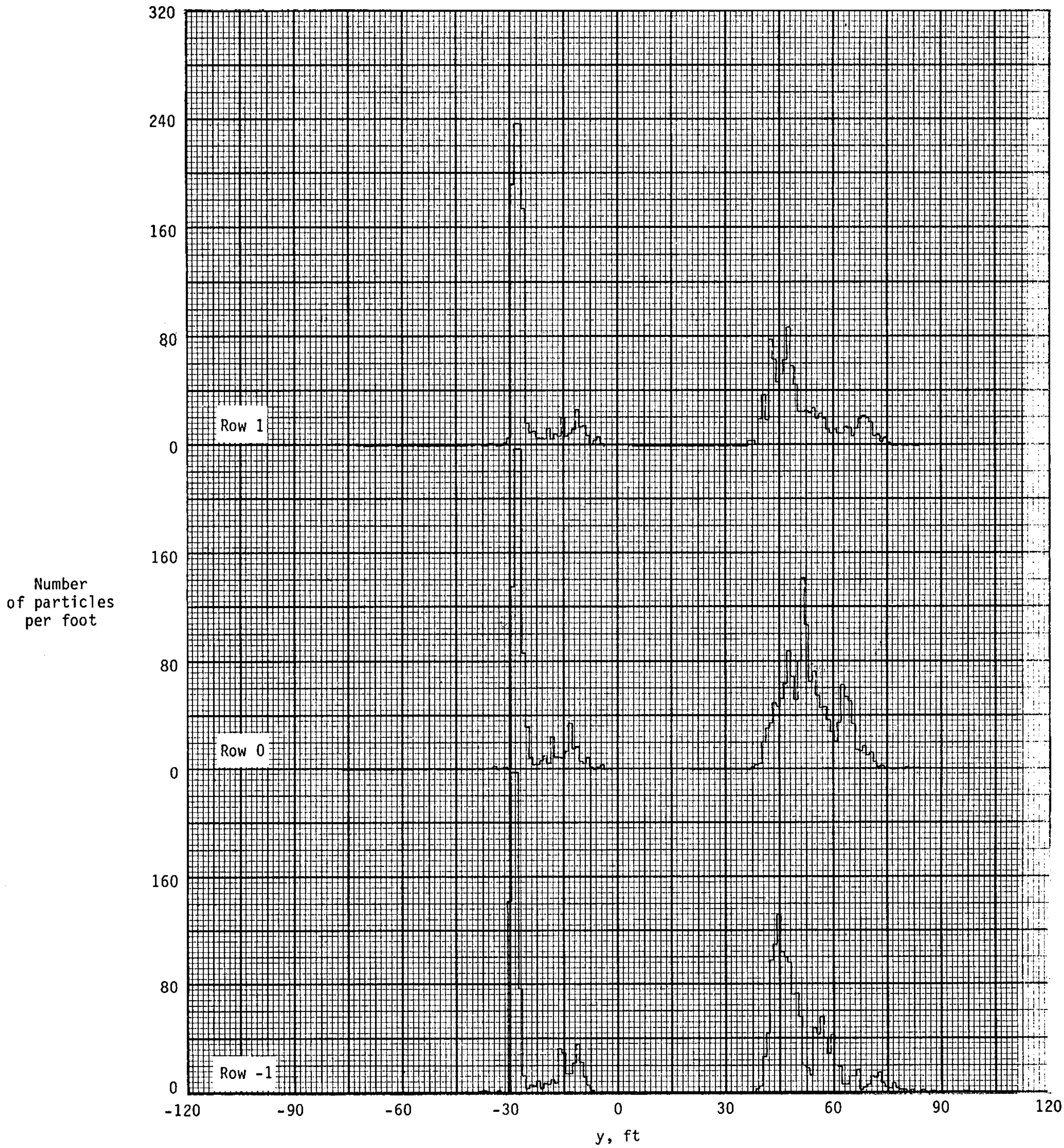

Figure A73.- Ground deposition patterns for flight 74, run 3.2.

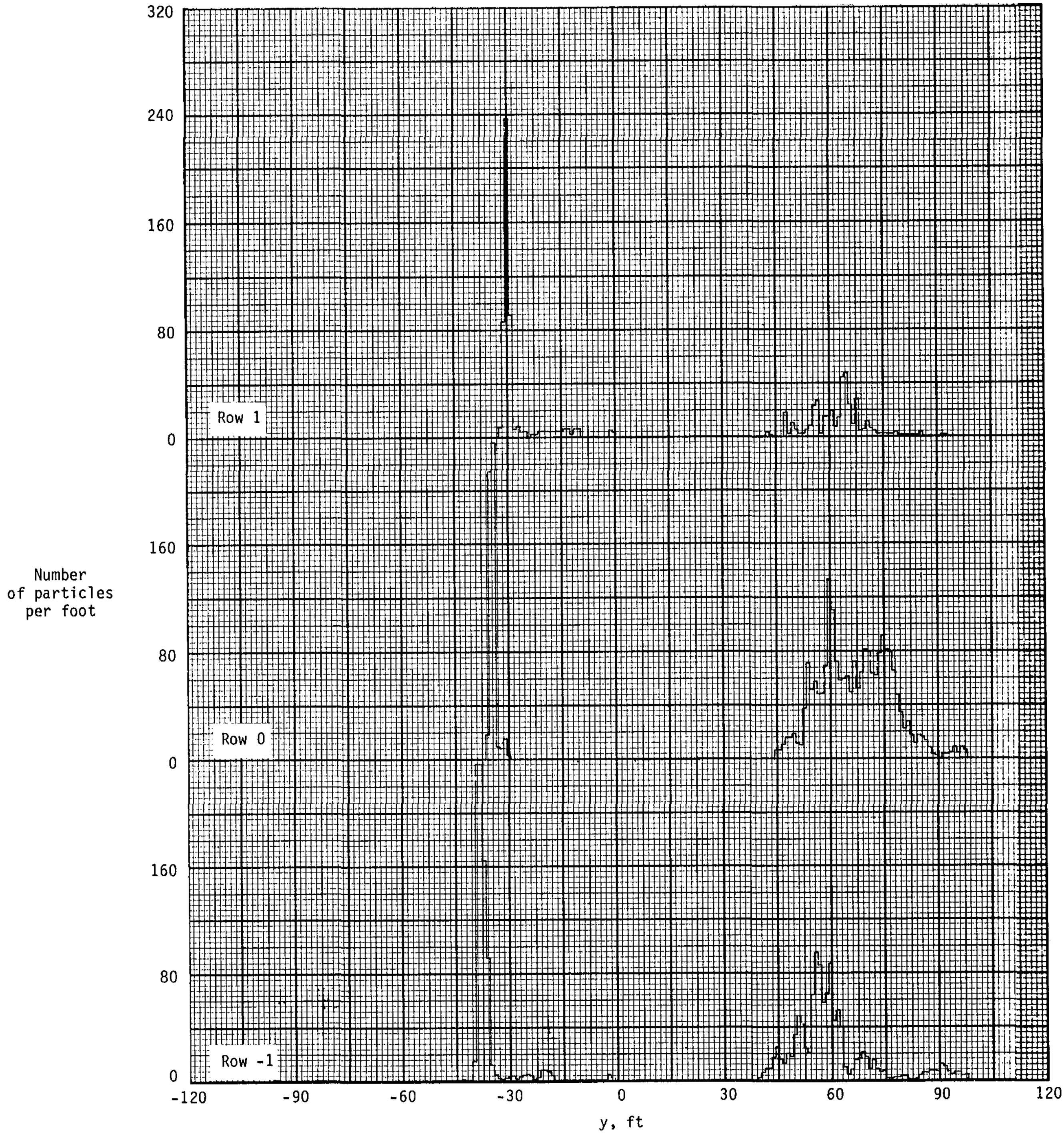

Figure A74.- Ground deposition patterns for flight 74, run 4.0.

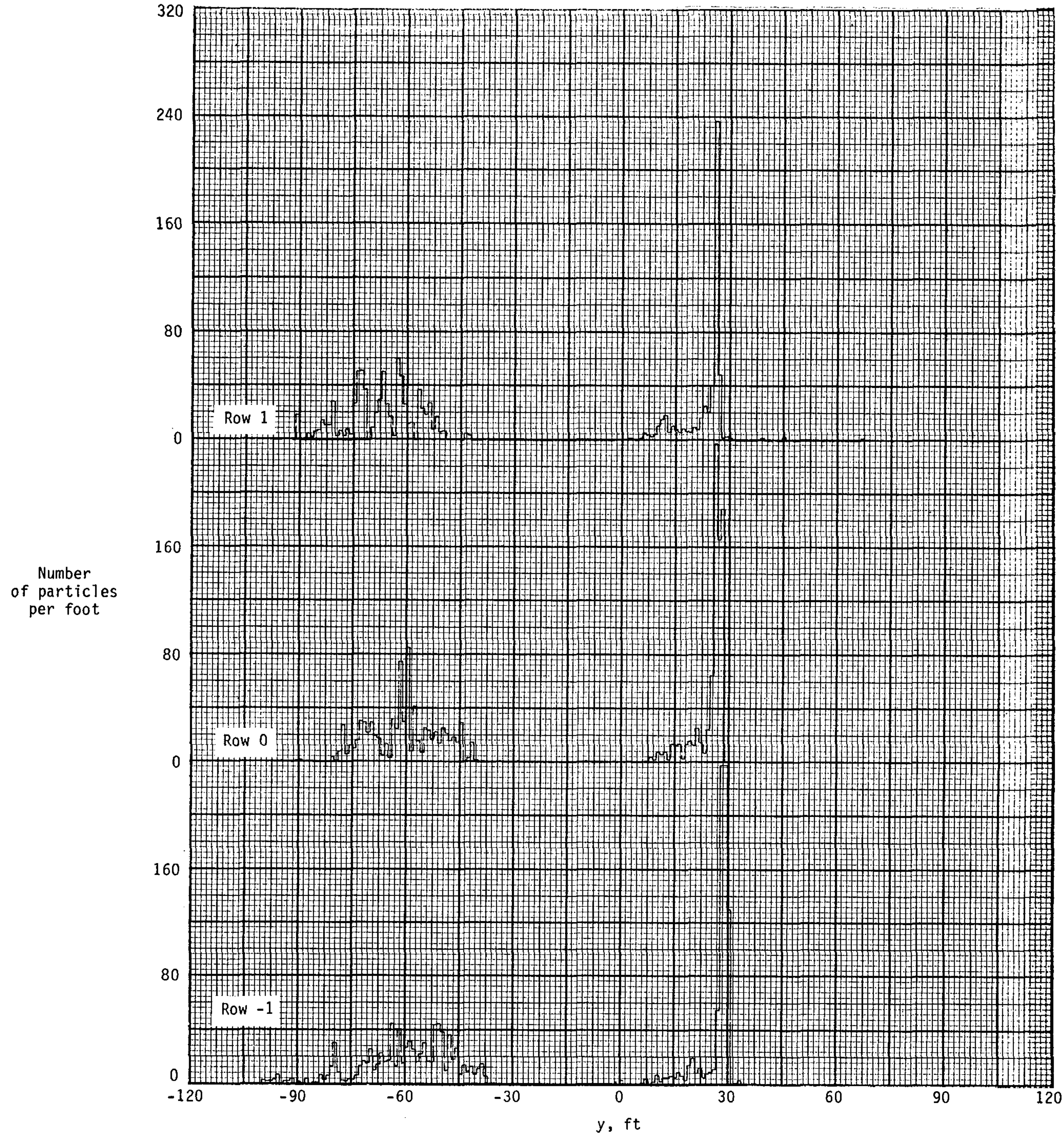

Figure A75.- Ground deposition patterns for flight 76, run 1.0.

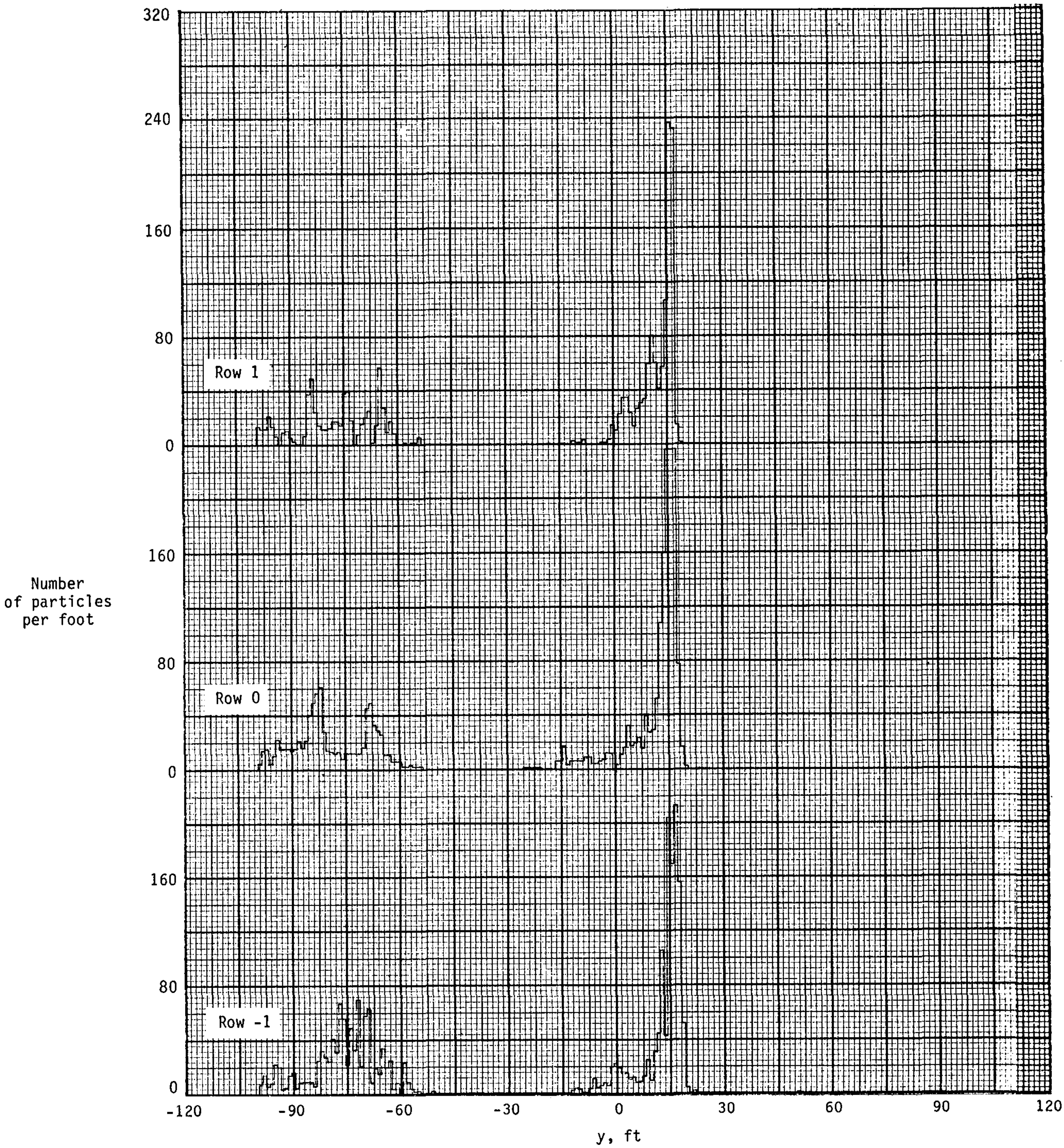

Figure A76.- Ground deposition patterns for flight 76, run 1.1.

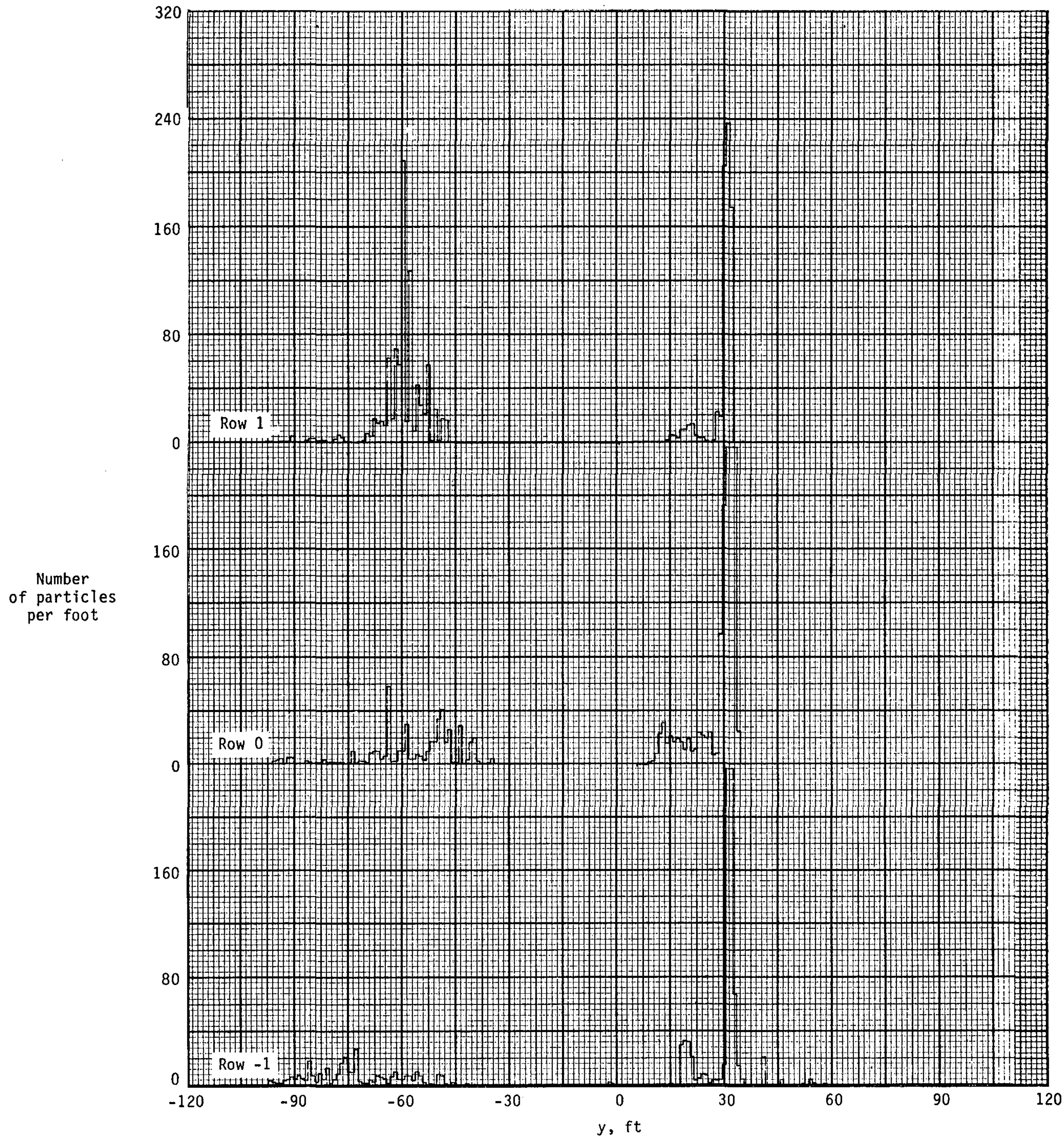

Figure A77.- Ground deposition patterns for flight 76, run 2.0.

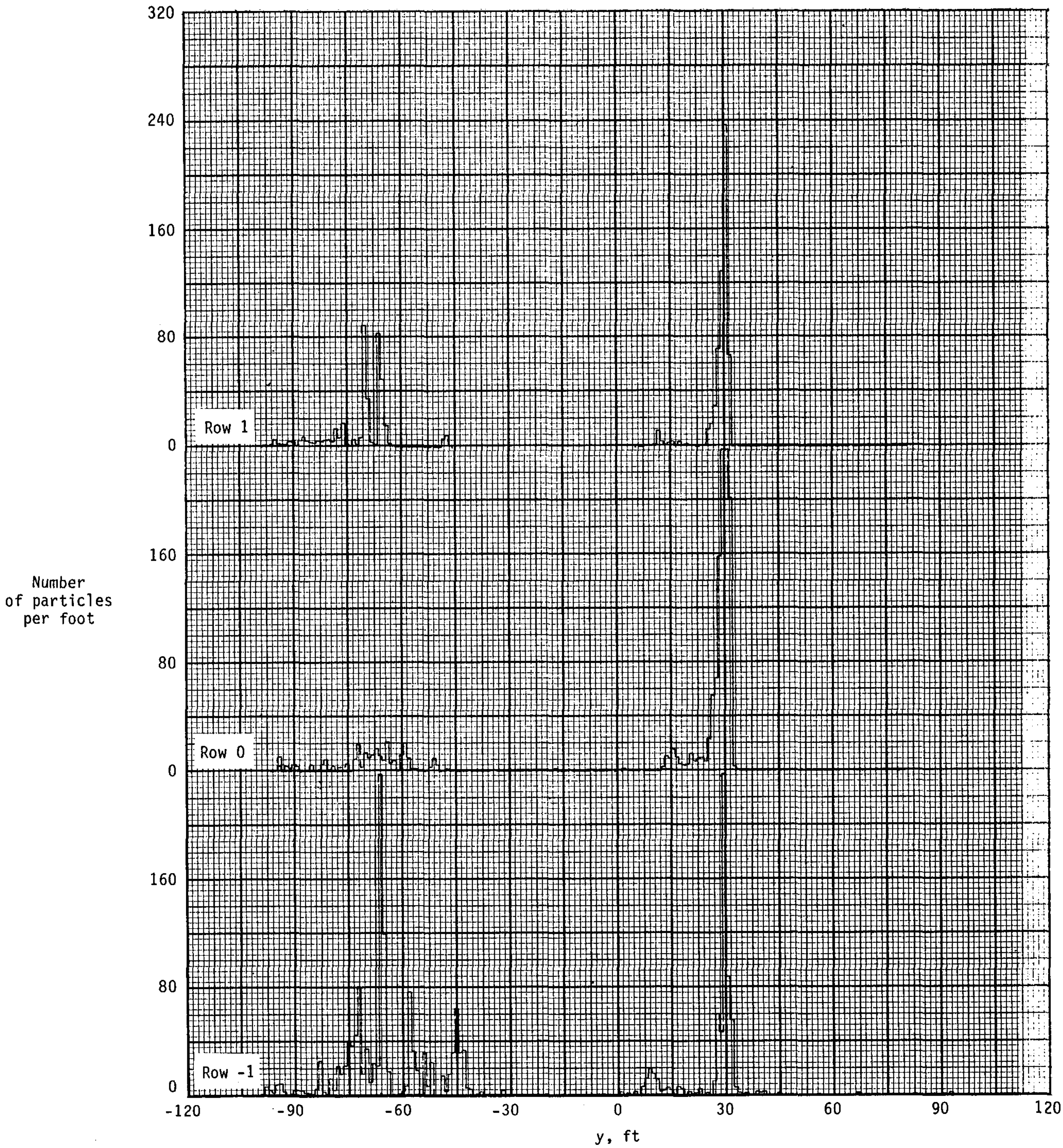

Figure A78.- Ground deposition patterns for flight 76, run 2.1.

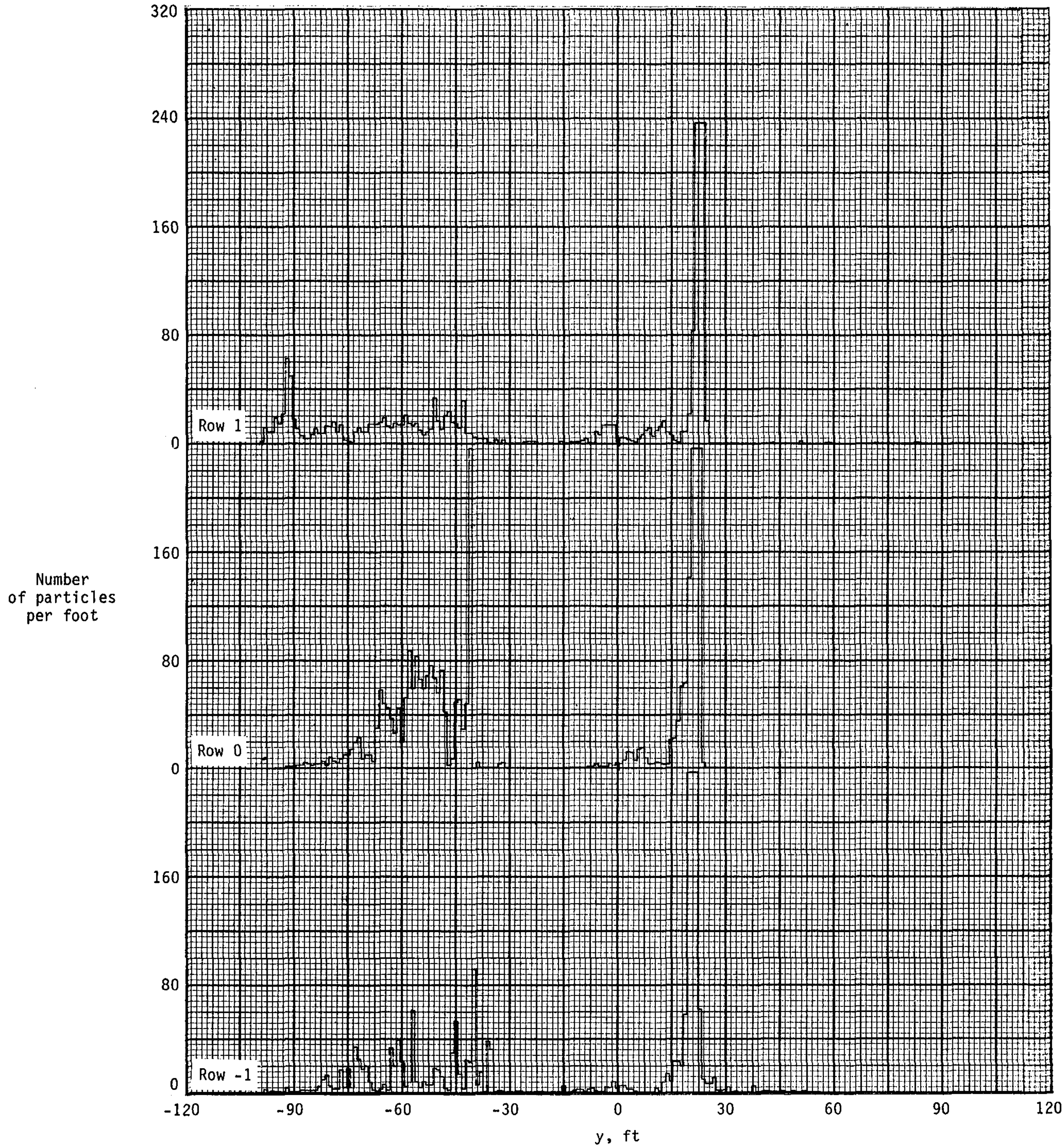

Figure A79.- Ground deposition patterns for flight 76, run 3.0.

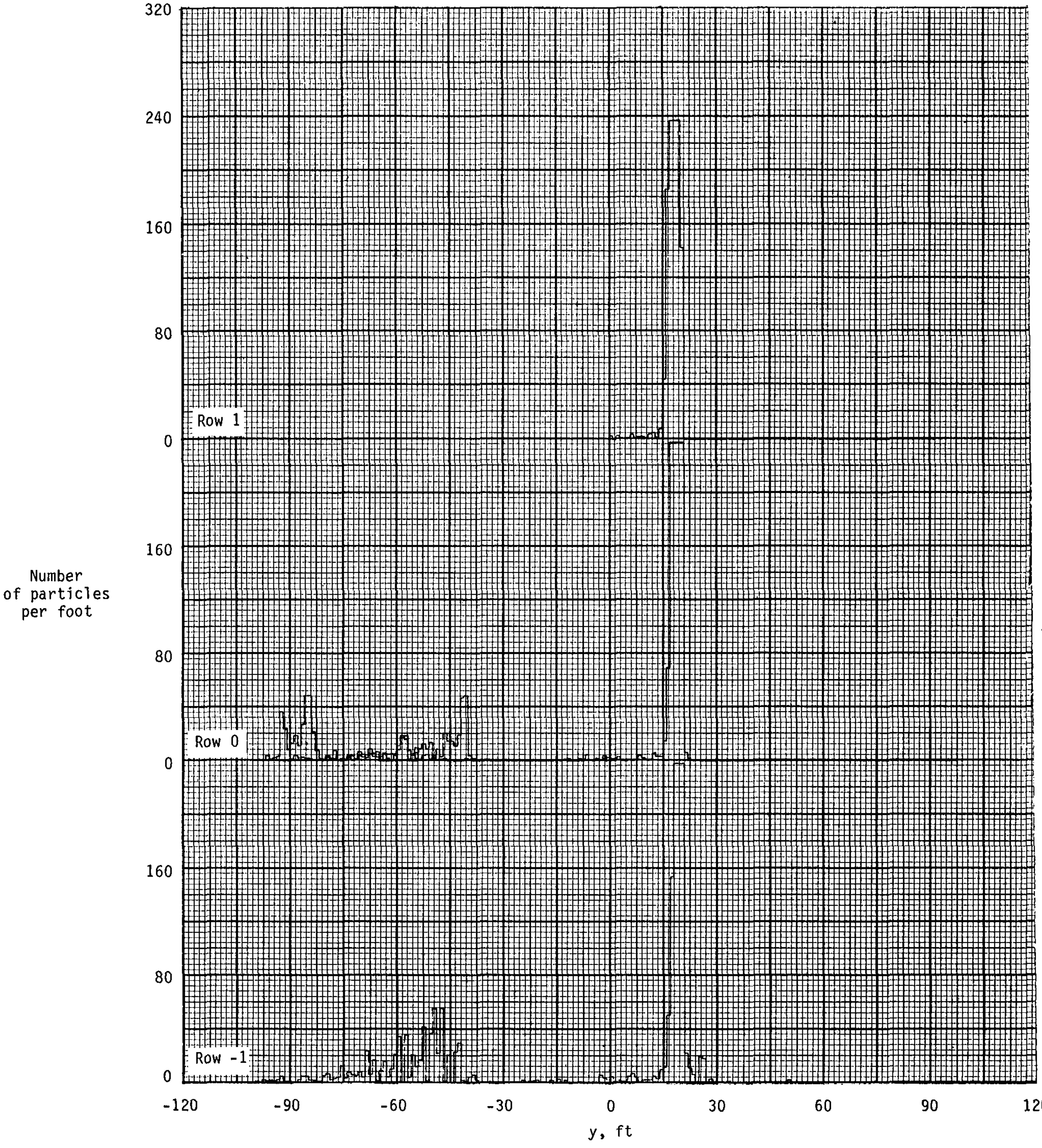

Figure A80.- Ground deposition patterns for flight 76, run 3.1.

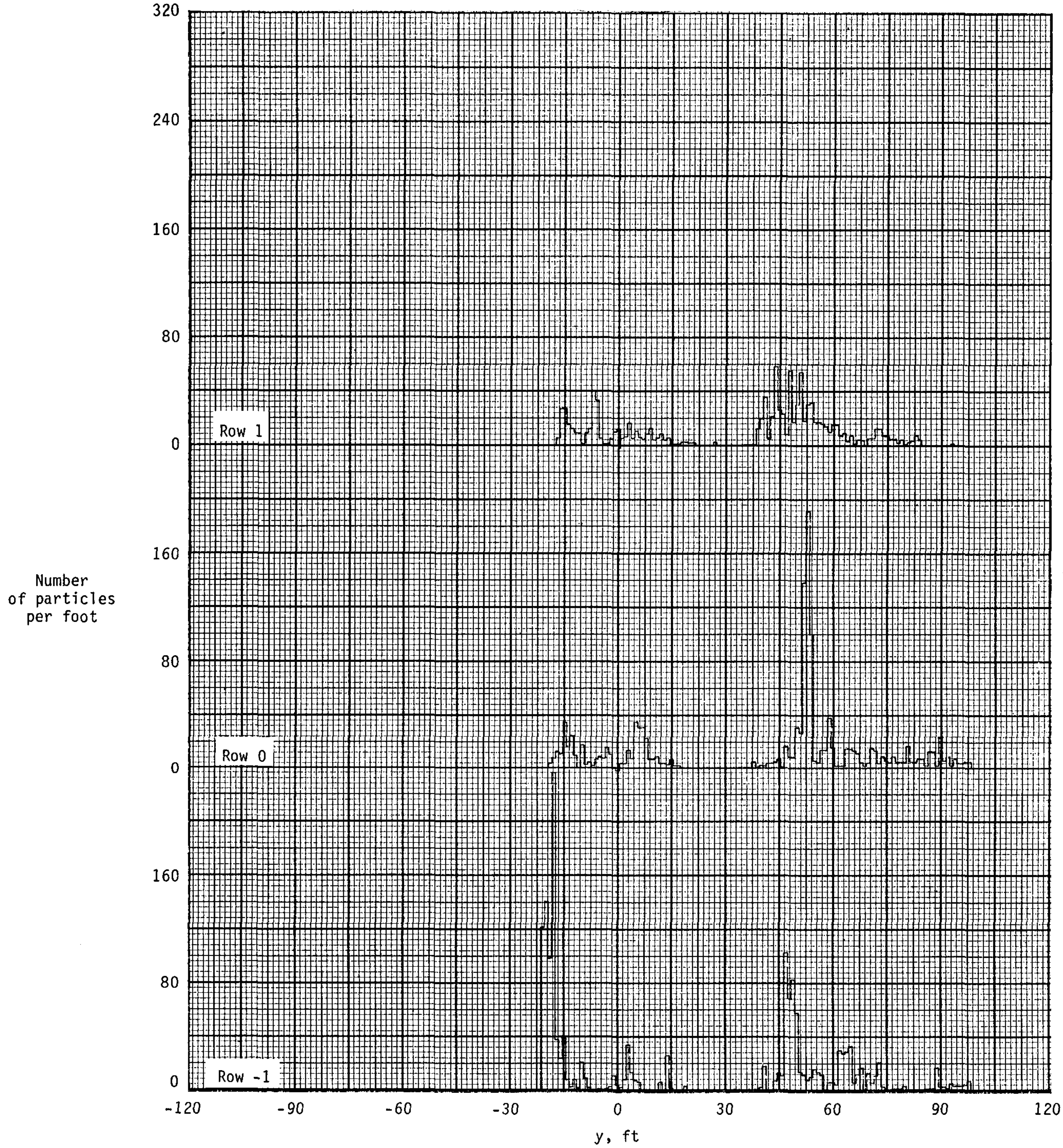

Figure A81.- Ground deposition patterns for flight 77, run 1.5.

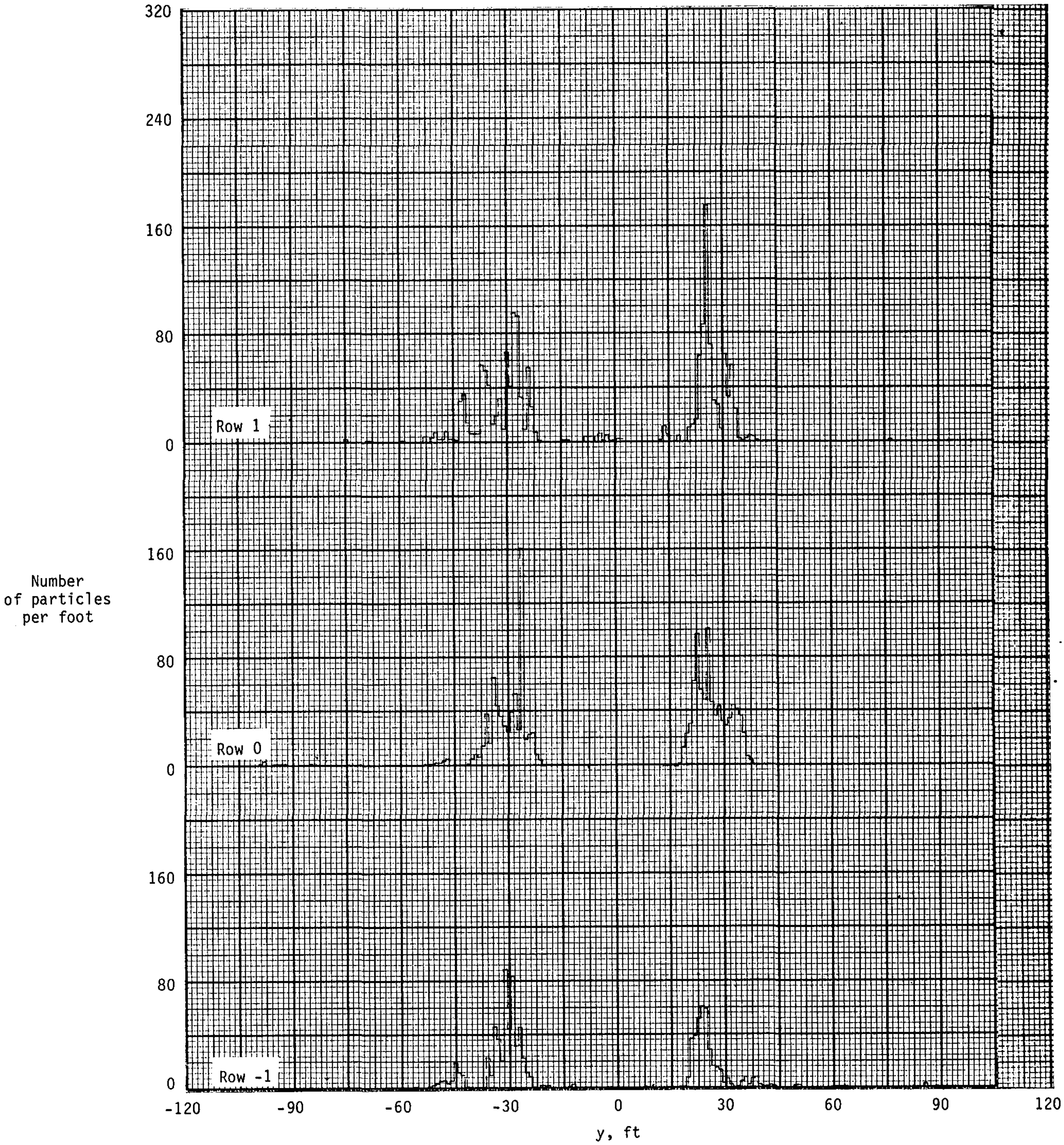

Figure A82.- Ground deposition patterns for flight 78, run 1.5.

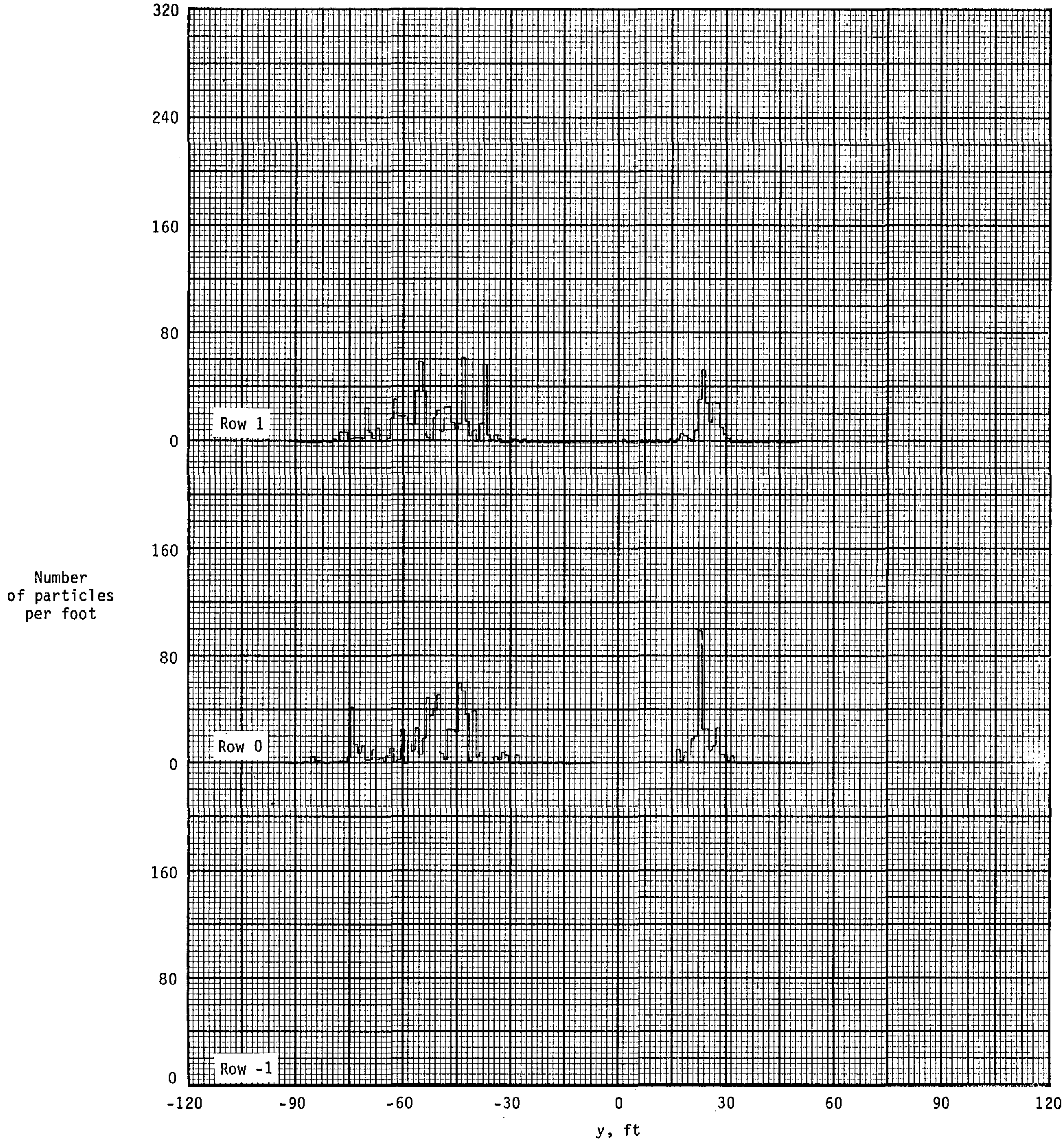

Figure A83.- Ground deposition patterns for flight 78, run 2.0.

REFERENCES

1. Holmes, Bruce J.: Overview of NASA Aerial Applications Research. Paper No. 78-1505, American Soc. Agric. Eng., Dec. 1978.

2. Jordan, Frank L., Jr.: Development of Test Methods for Scale Model Simulation of Aerial Applications in the NASA Langley Vortex Facility. A Collection of Technical Papers - AIAA 11th Aerodynamic Testing Conference, Mar. 1980, pp. 79-93. (Available as AIAA-80-0427.)

3. Bragg, Michael Bradford: The Trajectory of a Liquid Droplet Injected Into the Wake of an Aircraft in Ground Effect. M.S. Thesis, Univ. of Illinois, May 1977.

4. Bilanin, Alan J.; Teske, Milton E.; and Morris, Dana J.: Predicting Aerially Applied Deposition by Computer. SAE Paper No. 810607, Apr. 1981.

5. Morris, Dana J.: Analytical Prediction of Agricultural Aircraft Wakes. Paper No. 78-1506, American Soc. Agric. Eng., Dec. 1978.

6. Johnson, Joseph L., Jr.; McLemore, H. Clyde; White, Richard; and Jordan, Frank L., Jr.: Full-Scale Wind-Tunnel Investigation of An Ayres S2R-800 Thrush Agricultural Airplane. SAE Paper No. 790618, Apr. 1979.

7. Ogburn, Marilyn E.; and Brown, Philip W.: Exploratory Piloted Simulator Study of the Effects of Winglets on Handling Qualities of a Representative Agricultural Airplane. NASA TM-81817, 1980.

8. van Dam, C. P.: Analysis of Nonplanar Wing-Tip-Mounted Lifting Surfaces on Low-Speed Airplanes. NASA CR-3684, 1983.

9. Lan, C. Edward: Calculation of Lateral-Directional Stability Derivatives of Wings by a Nonplanar Quasi-Vortex-Lattice Method. NASA CR-165659, 1981.

10. West, Niel L.: Aerodynamic Force Predictions. Trans. ASAE, vol. 15, no 3, May-June 1972, pp. 584-587.

11. Law, S. Edward; and Collier, John A.: Aerodynamic Resistance Coefficients of Agricultural Particulates Determined by Elutriation. Trans. ASAE, vol. 16, no. 5, Sept.-Oct. 1973, pp. 918-921.

12. Jindal, V. K.; Mohsenin, N.; and Husted, J. V.: Surface Area of Selected Agricultural Seeds and Grains. Trans. ASAE, vol. 17, no. 4, July-Aug. 1974, pp. 720-725, 728.

13. Ormsbee, Allen I.; and Bragg, Michael B.: Trajectory Scaling Laws for a Particle Injected Into the Wake of an Aircraft. ARL 78-1, Aviation Research Lab., Inst. Aviation, Univ. Illinois at Urbana-Champaign, June 1978.

14. Langmuir, Irving; and Blodgett, Katherine B.: A Mathematical Investigation of Water Droplet Trajectories. AAF TR No. 5418 (Contract No. W-33-038-ac-9151), Air Technical Service Command, Army Air Forces, Feb. 19, 1946.

15. Bilanin, A. J.; Teske, M. E.; and Hirsh, J. E.: Neutral Atmospheric Effects on the Dissipation of Aircraft Vortex Wakes. AIAA J., vol. 16, no. 9, Sept. 1978, pp. 956-961.

1. Report No. NASA TP-2348	2. Government Accession No.	3. Recipient's Catalog No.

4. Title and Subtitle
AN EXPERIMENTAL AND THEORETICAL INVESTIGATION OF DEPOSITION PATTERNS FROM AN AGRICULTURAL AIRPLANE

5. Report Date
September 1984

6. Performing Organization Code
505-45-43-02

7. Author(s)
Dana J. Morris, Cynthia C. Croom, Cornelis P. van Dam, and Bruce J. Holmes

8. Performing Organization Report No.
L-15718

9. Performing Organization Name and Address
NASA Langley Research Center
Hampton, VA 23665

10. Work Unit No.

11. Contract or Grant No.

12. Sponsoring Agency Name and Address
National Aeronautics and Space Administration
Washington, DC 20546

13. Type of Report and Period Covered
Technical Paper

14. Sponsoring Agency Code

15. Supplementary Notes
Dana J. Morris, Cynthia C. Croom, and Bruce J. Holmes: Langley Research Center, Hampton, Virginia.
Cornelis P. van Dam: University of Kansas, Lawrence, Kansas, now at Vigyan Research Associates, Inc., Hampton, Virginia.

16. Abstract

A flight test program has been conducted with a representative agricultural airplane to provide data for validating a computer program model which predicts aerially applied particle deposition. Test procedures and the data from this test are presented and discussed. The computer program features are summarized, and comparisons of predicted and measured particle deposition are presented. Applications of the computer program for spray pattern improvement are illustrated.

17. Key Words (Suggested by Author(s))
Agricultural airplane
Particle trajectories
Particle dispersal
Aerial application

18. Distribution Statement
Unclassified - Unlimited

Subject Category 02

19. Security Classif. (of this report)	20. Security Classif. (of this page)	21. No. of Pages	22. Price
Unclassified	Unclassified	155	A08

For sale by the National Technical Information Service, Springfield, Virginia 22161

NASA-Langley, 1984

National Aeronautics and
Space Administration

Washington, D.C.
20546

Official Business
Penalty for Private Use, $300

THIRD-CLASS BULK RATE

Postage and Fees Paid
National Aeronautics and
Space Administration
NASA-451

U.S.MAIL

NASA

POSTMASTER: If Undeliverable (Section 158 Postal Manual) Do Not Return